Purines and 9-deazapurines as Modulators of Multidrug Resistance-associated Protein 1 (MRP1/ABCC1)-mediated Transport

Dissertation

zur

Erlangung des Doktorgrades (Dr. rer. nat.)

der

Mathematisch-Naturwissenschaftlichen Fakultät

der

Rheinischen Friedrich-Wilhelms-Universität Bonn

vorgelegt von

Sven Marcel Schmitt

aus

Mainz

Bonn 2017

Angefertigt mit der Genehmigung der Mathematischen-Naturwissenschaftlichen Fakultät der Rheinischen Friedrich-Wilhelms-Universität Bonn.

1. Gutachter: Prof. Dr. Michael Wiese
2. Gutachter: Prof. Dr. Gerd Bendas
3. Gutachter: Prof. Dr. Ulrich Jaehde
4. Gutachter: Prof. Dr. Arne Lützen

Tag der Promotion: 12.09.2017
Erscheinungsjahr: 2017

This work was proudly produced using Windows XP and Microsoft Word.

Danksagung

Die hier vorliegende Arbeit wurde unter der Leitung von Herrn Prof. Dr. Michael Wiese im Pharmazeutischen Institut der Rheinischen Friedrich-Wilhelms-Universität Bonn angefertigt. Ich danke ihm für die Vergabe dieses interessanten Themas und die Betreuung während meiner Promotion. Neben seinem Fachwissen und seiner konstruktiven Kritik gilt mein besonderer Dank seiner immensen Geduld. Für viele der von mir als vermeintlich „kurz“ angekündigten Gespräche hat er sich stundenlang unter Aufopferung seiner Zeit intensiv für die Erarbeitung von Lösungsansätzen eingesetzt, welche als Fundament dieser Arbeit gesehen werden können.

Herrn Prof. Dr. Gerd Bendas möchte ich hier nicht nur für die Übernahme des Koreferates danken, sondern auch für die reibungslose und gute Zusammenarbeit im Rahmen der Betreuung der Studenten des ersten Semesters.

Herrn Prof. Dr. Ulrich Jaehde sowie Herrn Prof. Dr. Arne Lützen danke ich für die Mitwirkung in der Prüfungskommission.

Auch meinen Kollegen des Arbeitskreises möchte ich meinen Dank aussprechen. Herrn Markus Hanl danke ich, weil er mir den Weg in die biologische Testung bereitete und mich die Erarbeitung von Lösungsansätzen sowie die Entwicklung alternativer Strategien lehrte. Ein Großteil meiner Fähigkeiten verdanke ich seinem Einsatz und seiner Geduld. Diesbezüglich danke ich auch unseren technischen Angestellten, Iris Jusen und Dieter Baumert. Dr. Mathias Weigt danke ich für seine administrative Hilfe. Er war es, der mir meinen Computer zusammenbastelte, der mich bis heute mit Windows XP beglückt und treu an meiner Seite steht. Unserer Sekretärin Tatjana Müller danke ich auch, da sie mit größter Geduld alle meine Anliegen anstandslos erledigte. Auch danke ich allen weiteren Kollegen, mit denen ich an Abstracts und Postern arbeitete, die mir Rat gaben bezüglich Versuchen, Papern oder meiner Dissertation, aber auch jenen, die einfach nur ein Bier mit mir tranken, um das im Labor erlebte zu prozessieren.

Ich danke meinen Freunden und Kollegen aus meinem Büro und der Umgebung, Katja Silbermann, Fabian Baltes und Alexander Neumann. Ohne die tagtägliche „Motivation“ wäre die Arbeit vermutlich schneller fertig geworden. Des weiteren danke ich den Kollegen des ersten Semesters für die gute Zusammenarbeit.

Mein größter Dank gilt drei Menschen in meinem Leben: meiner Mutter, Denise Schmitt, die mich entgegen vieler Widerstände dorthin brachte, wo ich heute bin; meinem besten Freund und Trauzeugen, Stefan Weinz, für sein Ohr, seine Geduld und Lebensweisheiten, und dafür, dass er mich immer wieder auf den Boden der Tatsachen zurückgeholt hat; und meiner Ehefrau, Katja Stefan, für die zeitweise intensive Zusammenarbeit, gerade auch im Hinblick auf unsere Publikationen und die Fertigstellung dieser Arbeit. Ihre Mitwirkung an meinem Projekt hat maßgeblich zum Gelingen dieser Arbeit beigetragen. Мы наши Слатюша, мы нас очень, очень любим!

Für Juli.

Contents

Abbreviations Used ..... **vii**

1. Introduction **1**

1.1. Cancer, Chemotherapy and Multidrug Resistance **1**

1.2. ABC-Transport Proteins **2**

1.2.1. Multidrug Resistance-associated Protein 1 (MRP1, ABCC1) 2

1.2.2. Permeability-Glycoprotein (P-gp, ABCB1) 4

1.2.3. Breast Cancer Resistance Protein (BCRP, ABCG2) 5

1.3. Modulators of ABC-Transport Proteins **6**

1.3.1. Inhibitors of MRP1 7

1.3.1.1. Pharmacological Drugs and Corresponding Synthetic Analogs 7

1.3.1.2. Natural Product Drugs and Synthetic Analogs 10

1.3.1.3. Intrinsic Substrates and Metabolism-related Drugs 12

1.3.1.4. Macromolecules that Influence MRP1 Expression or Function 15

1.3.1.5. HTS Results and Synthetic Approaches 15

1.3.2. Activators of ABC-Transport Proteins 17

1.3.2.1. General Information 17

1.3.2.2. Activators of MRP1 18

1.3.3. Dual Inhibitors of MRP1 and P-gp 20

1.3.4. Dual Inhibitors of MRP1 and BCRP 22

1.3.5. Dual Inhibitors of P-gp and BCRP 23

1.3.6. Triple Inhibitors of MRP1, P-gp and BCRP 24

1.3.7. Partial Inhibitors of ABC-transport proteins 25

2. Aim of the Thesis **27**

3. Synthesis **29**

3.1. Synthesis of Intermediates **29**

3.1.1. Synthesis of 9-deazapurine Precursors 29

3.1.1.1. Synthesis of the 7,8-alicyclic-9-deazapurine Scaffold 29
3.1.1.2. Synthesis of the 7-*N*-substituted-9-deazapurine Scaffold 31
3.1.1.3. Synthesis of the 8,9-annulated-9-deazapurine Scaffold 32
3.1.2. Synthesis of the Piperazine Derivative No. 73 33
3.2. Synthesis of Purine and 9-deazapurine Compounds 33
3.2.1. Synthesis of Piperazine-containing Derivatives 33
3.2.2. Synthesis of Amine Derivatives 36
4. Biological Investigation 39
4.1. Evaluation of 7,8-alicyclic and 7-*N*-alkyl-, -aryl- or -arylalkyl-9-deazapurines 39
4.1.1. Inhibition of MRP1-mediated Transport of Calcein AM and Daunorubicin 39
4.1.2. Analysis of Inhibition Type 46
4.1.3. Inhibition of P-gp-mediated Transport of Calcein AM 47
4.1.4. Inhibition of BCRP-mediated Transport of Pheophorbide A 50
4.1.5. Determination of Intrinsic Toxicity of Selected Compounds 53
4.1.6. MDR Reversal-efficacy of Selected Compounds 54
4.1.7. Summary of Evaluation of 7,8-alicyclic-, 7-*N*-alkyl-, -aryl- or -arylalky-9-deazapurines 59
4.2. Evaluation of 7-*N*-alkyl, -aryl- or -arylalkyl- and 6-aminoarylalkyl-9-deazapurines as well as 6-piperazinyl-purine Analogs 61
4.2.1. Inhibition of MRP1-mediated Transport of Calcein AM and Daunorubicin 61
4.2.1.1. 9-Deazapurine Derivatives 61
4.2.1.2. Purine Analogs 62
4.2.2. Activation of MRP1-mediated Transport of Calcein AM and Daunorubicin 64
4.2.3. Screening with Respect to P-gp Activation and Inhibition 70
4.2.4. Screening with Respect to BCRP Activation and Inhibition 70
4.2.5. Determination of Intrinsic Toxicity 71
4.2.6. MDR Reversal-efficacy of MRP1 Activators 75
4.2.7. Analysis of Activation Type 76
4.2.8. Summary of Evaluation of 7-*N*-alkyl, -aryl or -arylalkyl and 6-aminoarylalkyl-9-deazapurines as well as 6-piperazinyl-purine Analogs 78
4.3. Evaluation of 7,8-alicyclic-, 7-*N*-alkyl-, -aryl- or -arylalkyl-, and 8,9-annulated-9-deazapurines with Heteroaromatic Variations 80
4.3.1. Evaluation of 7,8-alicyclic-9-deazapurines with a Nitrogen Heterocycle at Position 6 80
4.3.2. Evaluation of 9-deazapurines with 4-(2-(1*H*-indole-3-yl)ethyl)piperazine-1-yl Residue at Position 6 and Alkyl or Arylalkyl Variations at Position 7 82

4.3.3. Evaluation of 9-deazapurines with Oxygen Heterocycle at Position 6 or Oxygen Containing Residue at Position 7 85
4.3.4. Evaluation of 8,9-annulated-9-deazapurines with Variations at Position 6 87
4.3.5. Investigation of the Interaction Type of Triple Inhibitor No. 125 89
4.3.6. Determination of Intrinsic Toxicity 90
4.3.7. MDR Reversal-efficacy of Triple Inhibitor No. 125 93
4.3.8. Summary of Evaluation of 7,8-alicyclic-, 7-*N*-alkyl-, -aryl- or -arylalkyl-, and 8,9-annulated-9-deazapurines with Heteroaromatic Variations 96
5. Summary 97
6. Experimental Section 101
6.1. Materials and Methods for Chemical Synthesis 101
6.1.1. Chemicals and Solvents 101
6.1.2. Standard Operation Procedures for Chemical Synthesis 103
6.1.2.1. Appliances Used for Chemical Synthesis 103
6.1.2.2. Microwave-assisted Synthesis 104
6.1.2.3. Thin Layer Chromatography (TLC) 104
6.1.2.4. Column Chromatography (CC) 105
6.1.2.5. Nuclear Magnetic Resonance (NMR) 106
6.1.2.6. Liquid Chromatography-Mass Spectrometry (LC-MS) 107
6.1.3. Synthesis and Characterization of Intermediates 107
6.1.3.1. *O*-methylation of Starting Compounds 107
6.1.3.2. Synthesis of Malononitrile Derivatives 108
6.1.3.3. *N*-acylation of 2-aminobenzonitrile 110
6.1.3.4. Nucleophilic Substitution of Primary Amines to Form Malononitrile Derivatives 110
6.1.3.5. Nucleophilic Substitution of Secondary Amines to Form Pyrrole Derivatives 116
6.1.3.6. Chain Elongation to Form the Formimidamid Derivatives. 124
6.1.3.7. Cyclization to Pyrrimidinon Ring System 133
6.1.3.8. Chlorination and Aromatization to Pyrimidine Ring System 141
6.1.3.9. Alkylation of Piperazine 148
6.1.4. Synthesis and Characterization of Target Compounds via Nucleophilic Substitution at the Aromatic Ring System 149
6.2. Materials and Methods for Biological Investigation 196
6.2.1. Materials 196
6.2.1.1. Chemicals for Biological Testing 196
6.2.1.2. Buffers for Biological Testing 197

6.2.1.3. Solutions for Cell Culture 198
6.2.1.4. Materials for Biological Testing 199
6.2.1.5. Instruments for Basic Operations 200
6.2.1.6. Instruments for Biological Investigations 201
6.2.2. Cell lines 201
6.2.2.1. H69AR and H69 201
6.2.2.2. MDCK II MRP1 and MDCK II 201
6.2.2.3. 2008/MRP1 and 2008 202
6.2.2.4. A2780/ADR and A2780 202
6.2.2.5. MDCK II BCRP 202
6.2.3. Cell Culture 202
6.2.3.1. Cell Line Back-Ups 202
6.2.3.2. Trypsination 203
6.2.3.3. Subculturing 204
6.2.3.4. Cell Counting 204
6.2.4. Cell-based Fluorescence Assays 205
6.2.4.1. Preparation of Serial Dilution and 96 Well Plate 205
6.2.4.2. Calcein AM Assay 206
6.2.4.3. Daunorubicin Assay 219
6.2.4.4. Pheophorbide A Assay 221
6.2.4.5. MTT-viability Assay 223
6.2.4.6. MDR reversal-efficacy Assay 226
6.3. Mathematical Operations 228
6.3.1. Statistical Values 228
6.3.1.1. Average (x) 228
6.3.1.2. Standard Error of the Mean (SEM) 228
6.3.1.3. One-sample t-Test 228
6.3.2. Regression 229
6.3.2.1. Linear Regression 229
6.3.2.2. Nonlinear Regression of Concentration-Effect curves 229
6.3.2.3. Logit Transformation 229
6.3.3. Calculation of the Maximal Inhibition Level (I_{max}) 230
6.3.4. Calculation of Transport Velocity-related Values 230
6.3.4.1. Calculation of the Flux Ratio (Pump Rate) 230
6.3.4.2. Calculation of the Activation Ratio (A_r) 232
6.3.5. Calculation of the Selectivity Ratio (sr) 232
6.3.6. Calculation of the Therapeutic Ratio (tr) 233

6.3.7. Calculation of the Resistance Factor (rf)....233
6.3.8. Calculation of the Potentiation Factor (pf)....233
6.3.9. Calcullation of the Degree of Sensitization (°s)....234
6.3.10. Kinetic Evaluations....234
6.3.10.1. Lineweaver-Burk....234
6.3.10.2. Hanes-Woolf....235
6.3.10.3. Cornish-Bowden....235
7. References....237
8. Publications....257
9. Verfassererklärung....259
10. Lebenslauf....261

Abbreviations Used

A

ABC transporter	ATP-binding cassette transporter
ABCB1	*synonymous for* P-gp
ABCC1	*synonymous for* MRP1
ABCG2	*synonymous for* BCRP
AC_{50}	half-maximal activation concentration
A_{max}	maximal activation level
APT	attached proton test
A_r	activation ratio
ATP	adenosine-5‘-triphosphate

B

BCECF	2',7'-bis-(2-carboxyethyl)-5(6)-carboxyfluorescein
BCPCF	2′,7′-bis-(3-carboxypropyl)-5(6)-carboxyfluorescein
BCRP	Breast Cancer Resistance Protein
BSO	buthionine sulfoximine

C

calcein AM	calcein acetoxymethyl ester
CFDA	carboxyfluorescein diacetate

D

δ	chemical shift
DEPT	distortionless enhancement by polarization transfer
DMF-DMA	dimethylformamide dimethyl acetale
DMS	dimethyl sulfate
DMSO	dimethyl sulfoxide

E

EC_{50}	half-maximal effect concentration

F

F	measured fluorescence (*arbitrary units; a.u.*)
F0	basal fluorescence (*arbitrary unit; a.u.*)

G

GCS	γ-glutamylcystein synthase
GFP	Green Fluorescence Protein
GI_{50}	half-maximal growth inhibition concentration
GPx	glutathione peroxidase
GSH	glutathione, reduced
GSR	glutathione reductase
GSH-S	glutathione synthase
GSSG	glutathione, oxidized (*synonymous for* glutathione disulfide)
GST	glutathione-*S*-transferase
γ-GTP	γ-glutamyl transpeptidase

H

HEPES	*N*-2-hydroxyethylpiperazine-*N*'-2-ethansulfonic acid
HPLC	high performance liquid chromatography
HTS	high throughput screening

I

IC_{50}	half-maximal inhibition concentration
I_{max}	maximal inhibition level

K

KHB	Krebs-HEPES-buffer

L

LC-MS	liquid chromatography-mass spectrometry
logP	calculated partition coefficient of the neutral molecule
LTC_4	leukotriene C_4

M

MDCK	madin-darby canine kidney
MDR	multidrug resistance
miR	micro ribonucleic acid
M_r	molecular weight (*Da*)
mRNA	messenger ribonucleic acid
MRP1	Multidrug Resistance-associated Protein 1
MSD	membrane-spanning domain
MSO	methionine sulfoximine
MTT	3-(4,5-dimethylthiazol-2-yl)-2,5-diphenyltetrazolium

N

NBD	nucleotide-binding domain
NMR	nuclear magnetic resonance
NSAID	non-steroidal antiinflammatory drug

P

pAC_{50}	negative decadic logarithm of half-maximal activation concentration
pEC_{50}	negative decadic logarithm of the half-maximal effect concentration
pf	potentiation factor
pGI_{50}	negative decadic logarithm of the half-maximal growth inhibition concentration
P-gp	Permeability-Glycoprotein
pH	negative decadic logarithm of the hydrogen concentration
pIC_{50}	negative decadic logarithm of half-maximal inhibition concentration
PSO	prothionine sulfoximine

R

rf	resistance factor
RNA	ribonucleic acid

S

°s	degree of sensitization
SAR	structure-activity relationship
SEM	standard error of the mean
shRNA	short hairpin ribonucleic acid
sr	selectivity ratio

T

TEA	triethylamine
TKI	tyrosine kinase inhibitor
TLC	thin layer chromatography
TM	transmembrane α-helices
tr	therapeutic ratio

V

V_{res}	residual cell viability

1. Introduction

1.1. Cancer, Chemotherapy and Multidrug Resistance

Cancer is a malignant tumor characterized by an (i) uncontrollable, (ii) infiltrating, (iii) destructive and (iv) metastasizing growth of cells.[1] The fundamental mechanisms behind these malignancies are diverse. Most important is an (i) enhanced proliferation or (ii) insufficient apoptosis of cells due to multiple defects in the genetic material.[1,2] Besides surgery and radiotherapy, chemotherapy is the main treatment of cancer.[2] Several classes of antineoplastic drugs have been developed during the last decades affecting different stages of cell metabolism. Amongst these are (i) alkylating (e.g. cyclophosphamide) or (ii) intercalating agents (e.g. doxorubicin), (iii) topoisomerase II inhibitors (e.g. etoposide), (iv) antimetabolites (5-fluorouracil), (v) mitosis inhibitors (vincristine) or (vi) tyrosine kinase inhibitors (e.g. gefitinib). A regimen for antineoplastic therapy is often composed of a combination of chemotherapeutic agents.[1,2,3,4]

Multidrug resistance (MDR) is a serious problem in cancer chemotherapy and broadly impairs its outcome. It is defined as cross-resistance toward structurally diverse anticancer drugs.[5] MDR is either (i) acquired after initial chemotherapeutic intervention, or (ii) inherent (already existing). It leads in most cases to an altered accumulation of cytostatics in terms of decreased intracellular concentration.[4] Several mechanisms are causative, such as (i) decreased influx / reduced uptake of the chemotherapeutic agent, (ii) alteration of the cell cycle and thereby reduced apoptosis / changed drug target, (iii) increased repair of DNA damage caused by the antineoplastic agent, (iv) altered metabolism of the drug due to upregulation / mutation of metabolism-related enzymes or (v) increase of energy-dependent efflux.[5,6] The last mechanism is in focus of the present study, since the active efflux of xeno- and endobiotics is mediated by ABC-transport proteins under expense of energy.

1.2. ABC-Transport Proteins

The human ATP-binding cassette transport proteins (ABC-transporters) are a group of integral membrane proteins that recognize and extrude specific substrates against a concentration gradient. Amongst them are representatives that efflux solutes of structural diversity.[5] This process is accompanied by a conformational change of the transporter and release of the solute into the extracellular space. The catalytic cycle is completed by attaining the initial conformation of the ABC-transporter by binding and hydrolyzation of ATP comparable to a mouse trap that has to be re-tensed.[6] There are 48 known expressed drug-transporting ABC-proteins in the human body that are classified in seven subfamilies ABCA-ABCG, based on their sequence homology.[7,8] In this thesis, the focus lies on the three main ABC-transport proteins involved in MDR, namely MRP1, P-gp and BCRP, each having distinct biochemical and pharmacological properties.

Attempts to treat ABC-transporter-related cancers include (i) targeting / inhibition by small molecules, peptides or antibodies or (ii) downregulation of overexpressed ABC-transporter genes (mimic microRNAs / short interfering RNA / antisense oligonucleotides / hammerhead ribozymes).[5] The former approach is the main topic of this thesis.

1.2.1. Multidrug Resistance-associated Protein 1 (MRP1, ABCC1)

The central transporter of this thesis, MRP1, consists of 1531 amino acids. It contains three membrane-spanning domains (MSDs) and two nucleotide-binding domains (NBDs; Figure 1.1). The NBDs are responsible for ATP hydrolysis and provide the energy for the transport process. MSD1 and MSD2 consist of six transmembrane (TM) α-helices each and are suggested to build a membrane spanning pore for solute extrusion.[6] The role of the additional MSD0 is still not clarified, but it was found being important for trafficking of the protein to the membrane.[9] Figure 1.1 gives a proposed topology.

The function of structural parts of MRP1 as well as possible binding sites of endo- or xenobiotics[10,11] have extensively been studied, showing tryptophanes,[12,13] cysteines[14,15] and charged amino acids[16,17] being of greater importance. But specific mechanistic aspects like drug recognition, drug binding, drug translocation via expense of energy or drug release are still not yet elucidated.

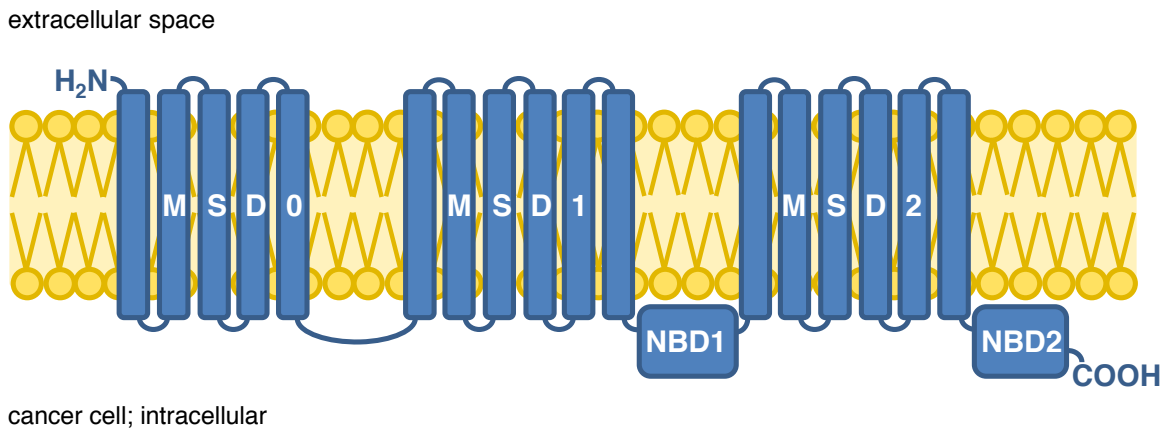

Figure 1.1. Proposed topology of MRP1 (blue). While the MSD1 and MSD2 form a channel for extrusion of xenobiotics, the *N*-terminal MSD0 is supposed to be responsible for correct trafficking of the transport protein to the membrane (yellow).

MRP1 is ubiquitously distributed in the human body,[6,18,19] and its overexpression is connected to several cancers like lung cancer,[20,21] especially non-small cell lung cancer,[22] colon carcinomas and certain leukemias.[6,23,24,25] It extrudes xenobiotics out of cells as phase II drug metabolites, such as glucuronate, glutathione (Figure 1.2) or sulfate conjugates.[26,27,28,29] Since MRP1 has affinity toward mediators of oxidative stress and cell apoptosis like LTC_4,[27,30] or oxidized glutathione (GSSG; Figure 1.2),[31] it is suggested to participate in the regulation of cellular distress.[22,32,33]

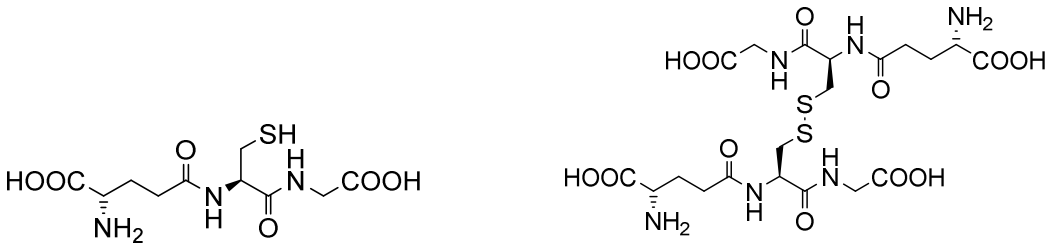

Figure 1.2. Molecular formulas of reduced (left) and oxidized (right) glutathione. GSH is a tripeptide consisting of the amino acids glutamine (Glu), cysteine (Cys) and glycine (Gly). GSSG consists of two GSH units connected by a disulfide bound, which gives it also the name glutathione disulfide.

In 1992, the 190-kDa protein MRP1 was firstly described by *Cole* et al. in the human small cell lung cancer cell line NCI-H69. It conferred resistance toward several structurally unrelated cytotoxic agents, such as anthracyclines, e.g. doxorubicin (adriamycin), daunorubicin (daunomycin; Figure 1.3), epirubicin or menogaril, but also etoposide, mitoxantrone, *Vinca* alkaloids like vincristine (Figure 1.3) or vinblastine, colchicine, acivicin

and gramicidin D.[34] The same resistance pattern was also observed using different MRP1 cDNA transfected HeLa cells, giving the direct connection between MRP1 overexpression and MDR.[35,36] Additionally, resistance toward the antiandrogene flutamide[37] and the antifolates methotrexate, raltitrexed (ZD1694) and GW1843[38] have been observed in MRP1 transfected cells. Recently, the human lung cancer cell line A549 and the human leukemia cell line HL60/ADR were shown to be resistant toward geldanamycin. This natural compound is an inhibitor of the heat shock protein 90 (Hsp90), a protein involved in cancer.[39]

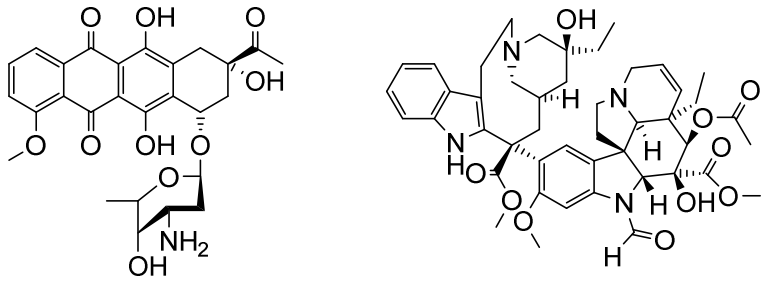

daunorubicin vincristine

Figure 1.3. Molecular formulas of selected anticancer agents that are substrates of MRP1: daunorubicin (left) and vincristine (right).

The structural diversity is explained by a polymorphous drug-binding domain within the MSDs.[6] Many of these cytostatics are effluxed in co-transportation with reduced glutathione (GSH; Figure 1.2),[40,41,42,43,44,45,46] and some are coupled to GSH via glutathione-*S*-transferase (GST)[47,48] before extrusion.[49,50,51] Besides GST, several enzymes related to GSH metabolism are critical in chemotherapy,[52] such as the γ-glutamylcystein synthase (GCS), glutathione synthase (GSH-S), glutathione reductase (GSR), glutathione peroxidase (GPx)[47] as well as γ-glutamyl transpeptidase (γ-GTP).[53] Simultaneous expression of these enzymes and MRP1 has been reported in MDR cell lines.[54]

1.2.2. Permeability-Glycoprotein (P-gp, ABCB1)

Since its discovery by *Juliano* and *Ling* at the end of the 70's of the last century,[55] the 170-kDa P-gp became the most studied ABC-transporter. The 1280 amino acid protein has a similar topology to MRP1, but does not feature the additional MSD0. A topology model is seen in Figure 1.4.

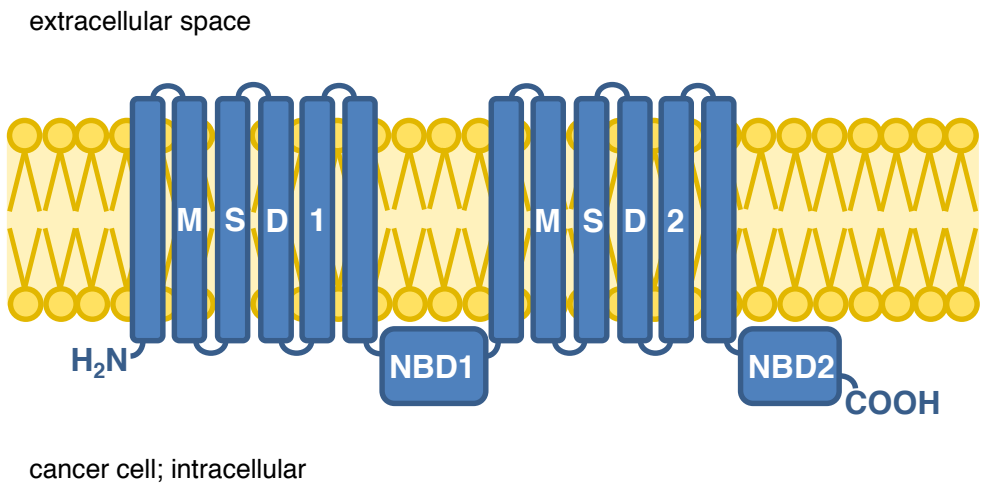

Figure 1.4. Proposed topology of P-gp (blue). The MSD1 and MSD2 form a channel through the membrane region (yellow) while the energy necessary for the conformational change comes from binding and hydrolyzation of ATP at the NBDs.

P-gp was found to be expressed in several cancers such as acute myeloid leukemia, bladder cancer, breast cancer or myeloma.[56] It confers resistance to many structurally unrelated anticancer agents, like camptotecins (topotecan), epipodophyllotoxins (etoposid, teniposid), intercalators (doxorubicin, daunorubicin), taxanes (paclitaxel, docetaxel) and *Vinca* alkaloids (vinblastine, vincristine). Although P-gp and MRP1 share only 15% sequence identity,[32] the substrate pattern of these two transporters is very similar with only few differences (e.g. camptotecins and taxanes). Inhibitors of this transport protein are discussed in detail below. Amongst these are the cardiovascular drug verapamil, the immunosuppressant cyclosporine A or the estrogen receptor modulator tamoxifene.[57,58]

1.2.3. Breast Cancer Resistance Protein (BCRP, ABCG2)

BCRP was discovered most recently by *Doyle* et al. in 1998 in the breast cancer cell line MCF-7.[59] It consists of 655 amino acids and has a structure different from the other two ABC-transporters consisting only of one MSD and one NBD, which gave it the name 'half transporter' (Figure 1.5). Polymerization has been discussed since its discovery, most likely is dimerization, although tetramerization[60,61,62] and polymerization up to 12 units was also observed.[60,63] Interestingly, although a function as monomer of both transporters is highly likely, several reports showed MRP1[64,65] and P-gp[66,67,68] also to occur as dimers under specific circumstances.

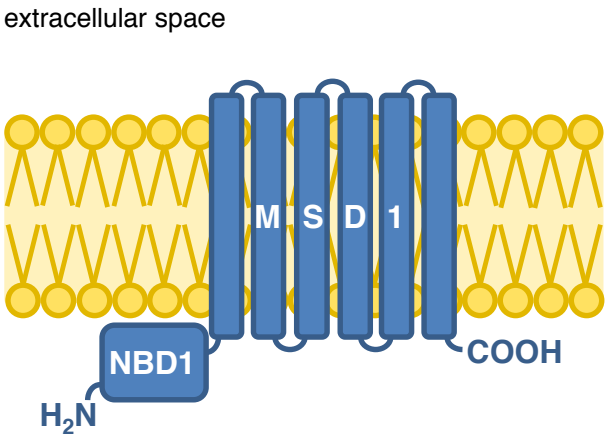

Figure 1.5. Proposed topology model of BCRP. Consisting only of one NBD and one MSD, it is considered to be a half-transporter which agglomerates to polymers, most likely a tetramer.

BCRP confers resistance to mitoxantrone, several camptotecins, like irinotecan and its active metabolite SN-38, or epipodophyllotoxins (like etoposide and teniposide). Although with a smaller substrate spectrum than MRP1 or P-gp, it is still an important mediator of MDR in certain cancers, like acute myeloid leukemia or breast cancer,[56] but also colorectal, ovarian and small cell lung cancer.[69] As a matter of fact, single-amino acid mutants of BCRP (R482S and R482G) were able to transport different anthracyclines (doxorubicin, daunorubicin and epirubicin), although these anticancer drugs are not substrates of the wild-type BCRP.[70] Though, marginal changes in the amino acid sequence of the protein can lead to an additional substrate profile. Inhibitors of BCRP are discussed in detail below, most famous representatives are fumitremorgin C as well as its synthetic analog Ko143 and several tyrosine kinase inhibitors (e.g. gefitinib and imatinib).

1.3. Modulators of ABC-Transport Proteins

The word ‘modulators’ is used in the sense of influencing the ABC transporter-mediated function and is differentiated between (i) inhibition and (ii) activation of transport function. Both processes are characterized by a difference to the basal transport activity which is omnipresent in living cells.

1.3.1. Inhibitors of MRP1

Since its role in MDR was evident, many structurally diverse compounds have been found to inhibit MRP1-mediated transport. [71,72,] Generally, one can differentiate between five classes: (i) pharmacological drugs and corresponding synthetic analogs; (ii) natural product drugs and synthetic analogs; (iii) intrinsic substrates and metabolism-related drugs; (iv) macromolecules that influence MRP1 expression or function, and (v) HTS compounds and synthetic approaches. Of course there are overlaps between these groups, but the categorization makes it easy to classify inhibitors of this transport protein and highlights the importance of certain discoveries. In this section, a detailed overview of found compounds is given that inhibit MRP1 and intervene with the MRP1-related metabolism.

1.3.1.1. Pharmacological Drugs and Corresponding Synthetic Analogs

Already known for its P-gp inhibition,[73,74] the cardiovascular drug verapamil, especially the (*R*)-enantiomer (Figure 1.6), [75] was found to restore sensitivity of small cell lung cancer cells.[76] Several analogs of verapamil were synthesized, with moderate success.[77] The P-gp inhibitors[78,79,80,81] and dihydropyridine derivatives NIK-250 (Figure 1.6) and PAK-104-P (Figure 1.21) restored sensitivity of MRP1 overexpressing glioma,[82] leukemia and sarcoma cells.[83,84] The immunosuppressant cyclosporine A, a calcineurin antagonists and P-gp inhibitor, was also found to sensitize MRP1 overexpressing human lung cancer COR-L23/R cells,[85,86,87] as well as its non-immunosuppressant derivative valspodar (PSC-833).[88] The clinically evaluated biricodar (VX-710; Figure 1.6)[89,90] and its derivative V-104 inhibited not only P-gp,[91] but also MRP1 in transfected Madin-Darby canine kidney (MDCK) II MRP1 and transfected human ovarian carcinoma 2008/MRP1 cells.[92,93] The P-gp inhibitor MS-209 (dofequidar; Figure 1.6)[94,95,96] could also restore sensitivity of human leukemia cells HL60/ADR and human small cell lung cancer cells UMCC-1/VP.[97,98] The protein kinase C inhibitor GF 109203X (Figure 1.6), a bisindoylmaleimide derivative, was shown to restore sensitivity in MRP1 expressing GLC_4/ADR and HL60/ADR cells.[99]

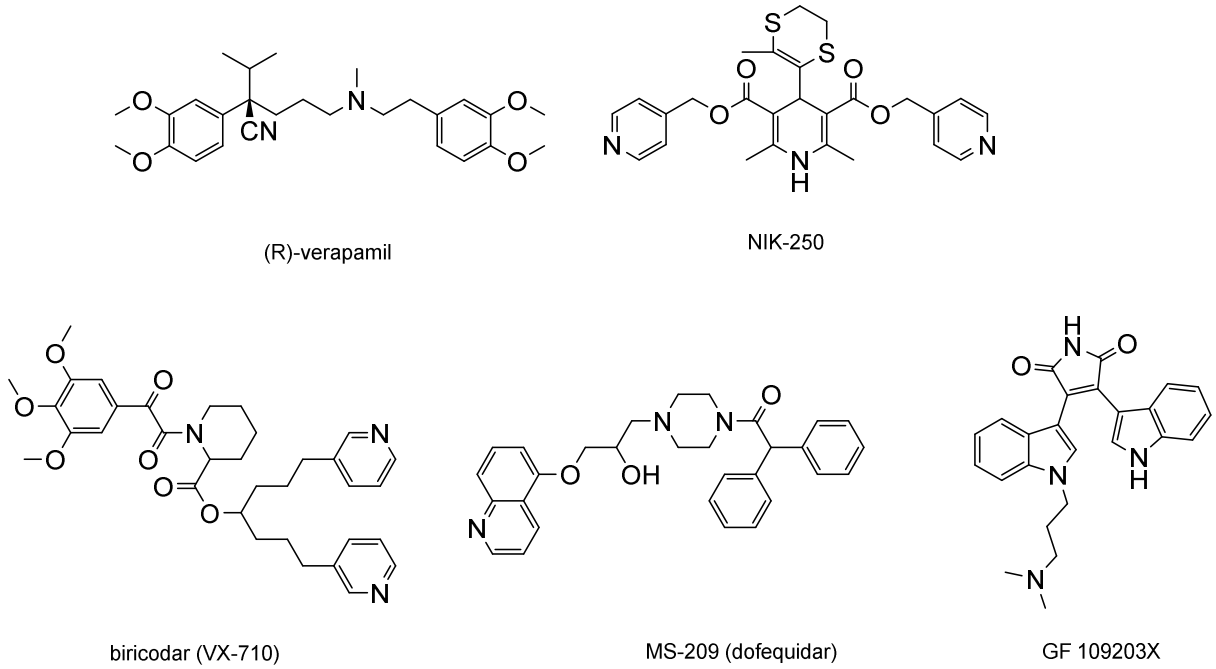

Figure 1.6. Molecular formulas of unspecific MRP1 inhibitors: verapamil (upper left), the dihydropyridine analog NIK-250 (upper right), the pipecolinate derivative biricodar (VX-710; lower left) and the quinoline derivative MS-209 (lower middle). Lower right: the bisindoylmaleimide derivative GF 109203X.

More specific MRP1 inhibitors are the uricosuric drugs probenecid (Figure 1.7), sulfinpyrazone,[100] or benzbromarone (Figure 1.7).[101] Several non-steroidal antiinflammatory drugs (NSAIDs), already known for their antiproliferative properties,[102] have also been shown to be specific MRP1 inhibitors, like acemetacin,[103] ibuprofen,[104] indomethacin (Figure 1.7),[105,106] mefenamic acid[104] sulindac, tolmetin and zomepirac.[103] The active metabolite of sulindac, sulindac sulfone, was extensively evaluated as chemosensitizer *in vitro.*[107,108,109,110] Indomethacin analogs have been synthesized and evaluated with respect to their structure-activity relationship (SAR).[111,112,113]

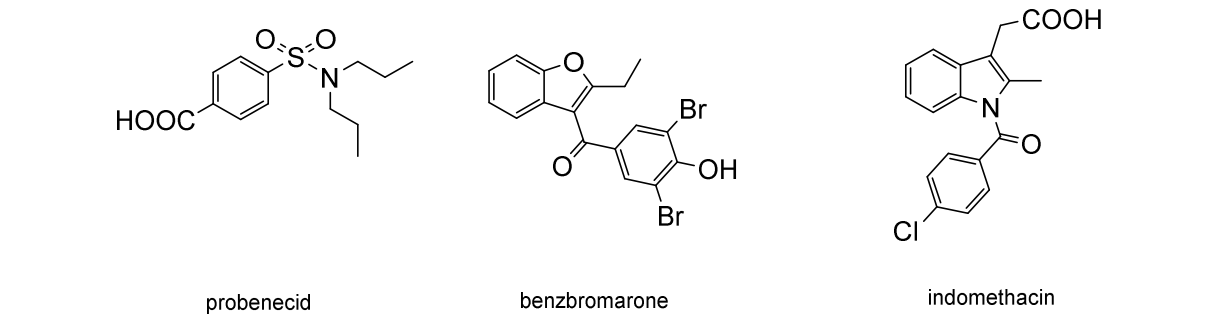

Figure 1.7. Molecular formulas of specific MRP1 inhibitors: the uricosuric drugs probenecid (left) and benzbromarone (middle) as well as the NSAID indomethacin (right).

The already as P-gp and BCRP inhibitors known tyrosine kinase inhibitors (TKIs)[114,115,116,117,118] were also shown to affect MRP1, e.g. AG-1393, OBF-1834, EKI-785, OL-57 and imatinib (STI-571).[119] Lapatinib, clinically evaluated against breast cancer,[120,121,122] was able to sensitize MRP1 overexpressing human epidermoid carcinoma C-A120 cells toward doxorubicin and vincristine.[123] The TKI and pyrazolopyrimidine derivative ibrutinib sensitized human leukemia HL60/ADR as well as MRP1 transfected HEK293 MRP1 cells against vincristine, vinblastine and doxorubicin.[124]

The HIV therapeutic emtricitabine[125] as many other reverse transcriptase inhibitors block MRP1 function.[126] This was also observed for several antibacterial agents like ciprofloxacin,[127] norfloxacin,[128,129] grepafloxacin,[130] penicillin G,[129] rifampicin, rifamycin and rifamycin B.[131] The antidiabetic drug glibenclamide,[132] the anti-abuse drug disulfiram[133] and the abortion-inducer mifepristone (RU486)[134] are also MRP1 inhibitors, the latter is also known to affect P-gp.[135,136]

Several compounds have only rarely been reported as MRP1 inhbitors. The farnesyl protein transferase inhibitor lonafarnib (SCH66336; Figure 1.8) led to accumulation of calcein AM in MDCK MRP1 cells.[137] The p53 activator and clinic aspirant nutilin-3 (Figure 1.8) was shown not only to affect P-gp, but also MRP1.[138] Several pyrazolopyrimidine compounds showed inhibitory power toward MRP1, especially reversan (CBLC4H10; Figure 1.8).[139] Finally, the experimental drug CBT-1, developed as P-gp inhibitor, showed also to enhance intracellular calcein concentration in MRP1-transfected HEK293 cells.[140]

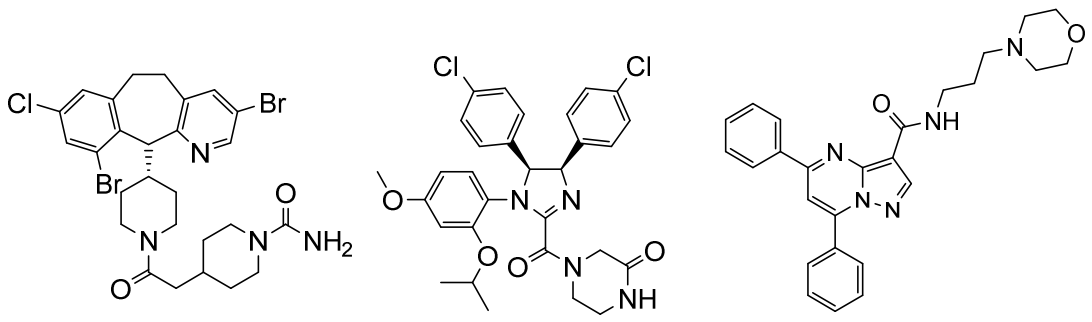

lonafarnib (SCH66336) nutilin-3 reversan (CBLC4H10)

Figure 1.8. Molecular formulas of drugs that have rarely been reported as MRP1 inhibitors. Left: the farnesyl protein transferase inhibitor lonafarnib (SCH66336); middle: The p53 activator nutilin-3; right: the pyrazolopyrimidine derivative reversan (CBLC4H10).

1.3.1.2. Natural Product Drugs and Synthetic Analogs

Besides many cytostatics, like anthracyclines, *Vinca* alkaloids, or podophyllotoxins, many natural drugs were found to be substrates of ABC-transport proteins. Flavonoids for example are known for their anticancer properties,[141,142,143,144] and affection of ABC-transporters like P-gp,[145,146] BCRP,[147,148] and MRP1 as well.[149] Table 1.1 shows selected flavonoids reported to inhibit MRP1. Figure 1.9 gives the molecular structure of selected flavonoids.

Table 1.1. List of flavonoids known to interact with MRP1.

flavonoid	**cell line**	**reported by**
apigenin	GLC_4/ADR	*Versantvoort* et al. 1993 [150]
biochanin A	GLC_4/ADR	*Versantvoort* et al. 1993 [150]
	Panc-1	*Nguyen* et al. 2003 [151]
chrysin	Panc-1	*Nguyen* et al. 2003 [151]
daidzein	COR-L23/R, MOR/R	*Versantvoort* et al. 1996 [152]
euchrestaflavanone A	erythrocytes	*Bombrowska-Hägerstrand* et al. [101]
genistein	GLC_4/ADR	*Versantvoort* et al. 1993 [150]
	Panc-1	*Nguyen* et al. 2003 [151]
genistin	COR-L23/R, MOR/R	*Versantvoort* et al. 1996 [152]
hesperetin	HEK293 MRP1	*Wu* et al. 2005 [153]
kaempferol	GLC_4/ADR	*Hooijberg* et al. 1999 [154]
	HeLa T5 vesicles	*Leslie* et al. 2001 [155]
	Panc-1	*Nguyen* et al. 2003 [151]
morin	Panc-1	*Nguyen* et al. 2003 [151]
myricetin	HeLa T5 vesicles	*Leslie* et al. 2001 [155]
	MDCK II MRP1	*van Zanden* et al. 2005 [156]
naringenin	HEK293 MRP1	*Wu* et al. 2005 [153]
quercetin	GLC_4/ADR	*Versantvoort* et al. 1993 [150]
	HeLa T5 vesicles	*Leslie* et al. 2001 [155]
	Panc-1	*Nguyen* et al. 2003 [151]
	MDCK II MRP1	*van Zanden* et al. 2005 [156]
robinetin	MDCK II MRP1	*van Zanden* et al. 2005 [156]
sophoraflavanone B	erythrocytes	*Wesolowska* et al. 2010 [157]
sophoraflavanone H	erythrocytes	*Bombrowska-Hägerstrand* et al. 2003 [101]

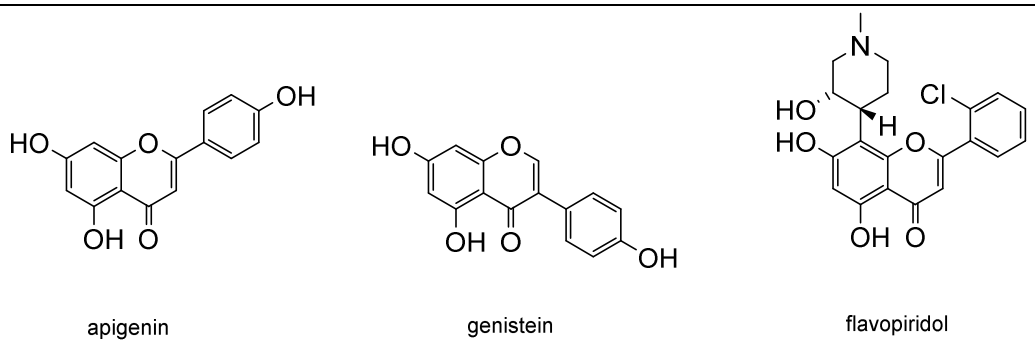

Figure 1.9. Molecular formulas of the naturally occurring flavonoids apigenin (left) and genistein (middle) as well as the synthetic flavonoid flavopiridol (right).

Besides flavonoids, flavolignans (e.g. silybinin[151,153] and dehydrosilybinin[158]) or chalcones (e.g. chalcone and phloretin),[151] some stilbenoids were found to inhibit MRP1 like piceatannol[159] or resveratrol (Fig 1.10)[153,160] and its oligomers (+)-*α*-viniferin, sophorastilbene A and (-)-ε-viniferin.[161] Synthetical flavonoid derivatives were also developed, like flavopiridol (Figure 1.9),[162] or apigenin derivatives.[163,164] Some compounds found the way into the clinic,[165,166,167,168] and had properties like inhibition of angiogenesis,[169] cancer cell proliferation,[170] and expression of MDR-related proteins.[171]

Besides flavonoids and flavonoid-related molecules, many diverse natural compounds were found to modulate MRP1, like diterpenes (e.g. latilagascene B),[159] dietary sterols (guggulsterone, Figure 1.10)[172] dibenzocyclooctadiene lignans (schisandrin B (Figure 1.10) schisandin A, schisandrol A, schisandrol B) [173,174] or synthetic norlignans.[175]

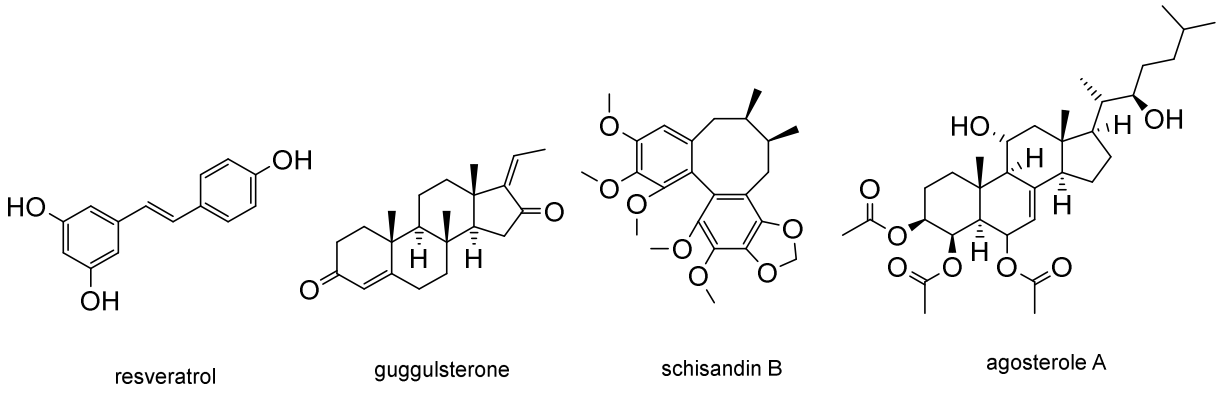

Figure 1.10. Molecular formulas of selected natural compounds that are not flavonoids: the stilbenoid resveratrol (left), the sterole guggulsterone (half left), the dibenzooctadiene lignan schisandin B (half right) and the sterole agosterole A (right).

Furthermore, curcumin, already evaluated in clinical trials with respect to malignancies,[176,177] and known to inhibit P-gp,[178] was found as MRP1 inhibitor.[179] Derivatives like demethoxycurcumin, bisdemethoxycurcumin, and caffeic acid phenethyl ester showed also

inhibitory activity.[180] The lacton antibiotic brefeldin A and the macrolide antibiotic bafilomycin A_1 proved to sensitize COR-L23/R cells overexpressing MRP1.[181] The known P-gp inhibitor[182] dendroamide A also inhibited MRP1.[183] Finally, agosterol A (Figure 1.10),[184,185,186,187] and its derivative 4-deacetoxyagosterol A were shown to have affinity toward P-gp and MRP1, respectively.[188]

1.3.1.3. Intrinsic Substrates and Metabolism-related Drugs

In general, the impact of intrinsic substrates with respect to MRP1 overexpressing cells can be categorized in four subclasses: (i) GSH extrusion via stimulation of MRP1-mediated transport; (ii) inhibition of the GSH coupling enzyme GST; (iii) reduction of intracellular GSH via its chemical elimination or inhibition of its synthesis (GSH depletion); (iv) analogs of intrinsic substrates as MRP1 inhibitors.

1.3.1.3.1. GSH Extrusion

As mentioned before, GSH is an important co-substrate of MRP1.[40,41,42,43,44,45,46] The lack of GSH due to enhanced extrusion or depletion can also sensitize MRP1 overexpressing cells. Table 1.2 shows pharmacological drugs and natural compounds that are also connected to GSH extrusion.

Table 1.2. Survey of pharmacological drugs and natural compounds that were found to stimulate GSH extrusion out of cells.

calcium channel blocker	**cell line**	**reported by**
diltiazeme	CCRF-CEM/E1000	*Cullen* et al. 2001 [189]
nifedipine	CCRF-CEM/E1000	*Cullen* et al. 2001 [189]
verapamil	CCRF-CEM/E1000	*Cullen* et al. 2001 [189]
	BHK-21 MRP1	*Trompier* et al. 2004 [190]
	BHK-21 MRP1	*Barattin* et al. 2010 [191]
flavonoids and chalcones		
biochanin A	Panc-1	*Nguyen* et al. 2003 [151]
chalcone	Panc-1	*Nguyen* et al. 2003 [151]
genistein	Panc-1	*Nguyen* et al. 2003 [151]
phloretin	Panc-1	*Nguyen* et al. 2003 [151]
quercetin	Panc-1	*Nguyen* et al. 2003 [151]

HIV protease inhibitors	cell line	reported by
indinavir	brain astrocytes	*Brandmann* et al. 2012 [192]
nelfinavir	brain astrocytes	*Brandmann* et al. 2012 [192]

1.3.1.3.2. GST Inhibition

GSH is sometimes needed to be coupled with some anticancer drugs like melphalan[50] or chlorambucil[51] before extrusion. Table 1.3 gives an overview of pharmacological drugs and natural compounds that are known to inhibit GST.

Table 1.3. Survey of pharmacological drugs and natural products that were reported to be GST inhibitors.

flavonoids and chalcones	cell line	reported by
butein	COLO 320HSR	*Zhang* et al. 1997[193]
eriodictyol	MCF-7	*van Zanden* et al. 2004 [194]
galangin	MCF-7	*van Zanden* et al. 2004 [194]
kaempferol	MCF-7	*van Zanden* et al. 2004 [194]
morin	COLO 320HSR	*Zhang* et al. 1997[193]
quercetin	COLO 320HSR	*Zhang* et al. 1997 [193]
	MCF-7	*van Zanden* et al. 2004 [194]
NSAIDs		
indomethacin	CHO	*Hall* et al. 1989 [195]
zomepirac	CHO	*Hall* et al. 1989 [195]
polyphenols		
tannic acid	COLO 320HSR	*Zhang* et al. 1997 [193]
steroles		
gossypol	MCF-7/ADR	*Fort* et al. 1991 [196]

High throughput screenings (HTS) gave GST inhibitors of structural diversity.[197] Among them were *α*,*β*-unsaturated carbonyl compounds,[198,199,200] the loop diuretics indacrynic acid, tienilic acid[201,202] and ethacrynic acid (Figure 1.11)[201,202,203,204] and derivatives,[205,206] or the phenol derivative caffeic acid.[207] Ethacrynic acid is by far the most studied compound. It is a MRP1 substrate,[208] and some derivatives are inhibitors of this transport protein.[209] This perspective also led to a clinical trial in combination with thiotepa.[210] But also diethyl maleate,[211,212] *p*-aminohippurate and probenecid,[212,213] clofibrate,[214] misonidazol,[215] piriprost,[216] GSH

conjugates of tetrachloro-1,4-benzoquinone,[217,218] sulfasalazin,[219,220] and the GSH analog TER286[221] amongst other TER compounds[222,223] were found to be GST inhibitors.

ethacrynic acid

buthionine sulfoximine (BSO)

Figure 1.11. Molecular formulas of the loop diuretic ethacrynic acid (left) as a GST inhibitor and buthionine sulfoximine as inhibitor of the γ-glutamylcystein synthase (right).

1.3.1.3.3. GSH Depletion

Acrolein and chloroacetaldehyde are GSH depleters[224,225] and can sensitize MRP1 overexpressing cells.[226] Agosterol A is also suspected to deplete intracellular GSH.[187] The role of GSH in MDR was in focus of several studies before MRP1 was known.[227,228] *Griffith* et al. reported already in 1979 on methionine sulfoximine (MSO), prothionine sulfoximine (PSO) and buthionin sulfoximine (BSO; Figure 1.11) as potent inhibitors of the γ-glutamylcystein synthase, an enzyme crucial for GSH synthesis.[229,230]

1.3.1.3.4. Analogs of Intrinsic Substrates as MRP1 Inhibitors

Since leukotriene C_4 (LTC_4) is a natural substrate of MRP1,[27] it was found that the leukotriene receptor antagonists like MK571 (verlukast; Figure 1.12),[231] ONO-1078 (pranlukast; Figure 1.12),[232] montelukast, LY171883, HAMI 3379, BayCysLT$_2$ and BAY-u9773,[233] inhibit MRP1 function.

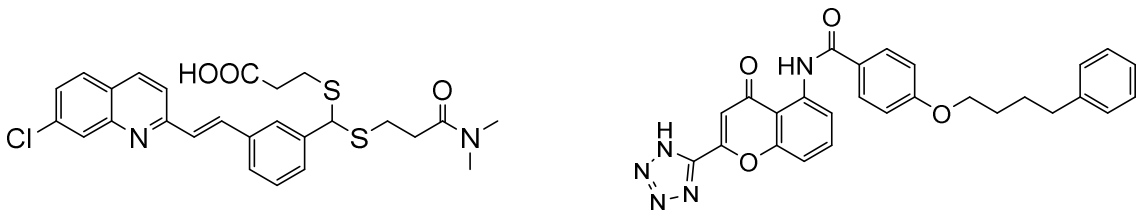

MK571 (verlukast)

ONO-1078 (pranlukast)

Figure 1.12. Molecular formulas of the leukotriene receptor antagonists MK571 (verlukast; left) and ONO-1078 (pranlukast; right).

Glutathione is important part in cell detoxification.[234,235] Especially as a co-substrate of MRP1 it helps to remove several anticancer agents from cells.[40,41,42,43,44,47,48,49,236,237] Analogs of GSH were generated to modulate MRP1-mediated transport. TER199 (ezatiostat) is not only a good inhibitor of GST[238] but also of MRP1.[239] Long-chain *S*-alkylated GSH analogs were found to inhibit MRP1-mediated transport of LTC_4, especially *S*-octyl-GSH, [240] *S*-nonyl-GSH[241] and *S*-decyl-GSH,[240] but also *S*-*p*-nitrobenzyl-GSH and *S*-*p*-chlorphenacyl-GSH.[242] The GSH analogs GIF-0017, GIF-0019, GIF-0068, GIF-0069, GIF-0071 and GIF-0072 were also shown to be potent MRP1 inhibitors.[243] Even analogs of the tripeptide GSH with exchanged amino acids were evaluated as MRP1 inhibitors.[244]

1.3.1.4. Macromolecules that Influence MRP1 Expression or Function

Downregulation of MRP1 is a possible mechanism to sensitize MDR cells. This was shown by introducing oligonucleotides into cancer cell lines. ISIS 7597 for example, a phosphorothioate oligonucleotide, could reduce intracellular MRP1 mRNA about 90% by an incubation time of four hours using H69AR cells.[245] Another phosphorothioate oligonucleotide, PS-TMR10, was able to reduce mRNA MRP1 levels in HL60/ADR cells down to 24% of control.[246] In both cases, the absolute protein amount of MRP1 was significantly reduced. This was also observed with the same group of oligonucleotides in MRP1-overexpressing glioma cells T98G-VP and Gli26-VP.[247] Similar results were obtained using the oligonucleotide named MRP1-ASO, which increased sensitivity of neuroblastoma cells toward etoposide.[248]

Selected cell lines that overexpress MRP1 were shown via micro array hybridization to have elevated levels of microRNAs (miRs). *Liang* et al. showed that miR-326 is down-regulated in MCF-7/VP cells and mimics of this nucleotide can cause sensitivity toward doxorubicin and etoposide.[249] In the human small cell lung cancer cell line H69AR, miR-7 was shown to decline MRP1 expression.[250] Up to now, other miRs have been found via micro array analysis to intervene with MRP1 expression, especially miR-134,[251,252] miR-145.[253,254] Short hairpin RNAs (shRNAs), such as shAbcc17, were also proven to down-regulate MRP1.[255]

Another approach is targeting MRP1 itself via antibodies. Since most of them are known to bind intracellularly,[256,257] and diffusion of such big proteins is difficult, this field of MRP1 inhibition is still in its infancy.

1.3.1.5. HTS Results and Synthetic Approaches

Many working groups and pharmaceutical companies carried out HTS of huge compound libraries to find hits for further synthetic improvement. This approach led to compounds that

were further optimized with respect to inhibition of MRP1, like aromatic 2-(thio)ureidocarboxylic acids (Figure 1.13),[258,259] 4-aminobenzoic acid derivatives (Figure 1.13),[260] or chalcogen pyrylium compounds (Figure 1.13),[261,262] as well as galloyl-based small molecules (Figure 1.17).[263]

The Eli Lilly company reported on many different structures affecting MRP1, such as the raloxifene derivatives LY117018 and LY329146,[264] the PI3K inhibitor LY294002[265] as well as tricyclic isoxazoles (Figure 1.13; e.g. LY475776[266]) as selective and very potent MRP1 inhibitors.[267,268,269]

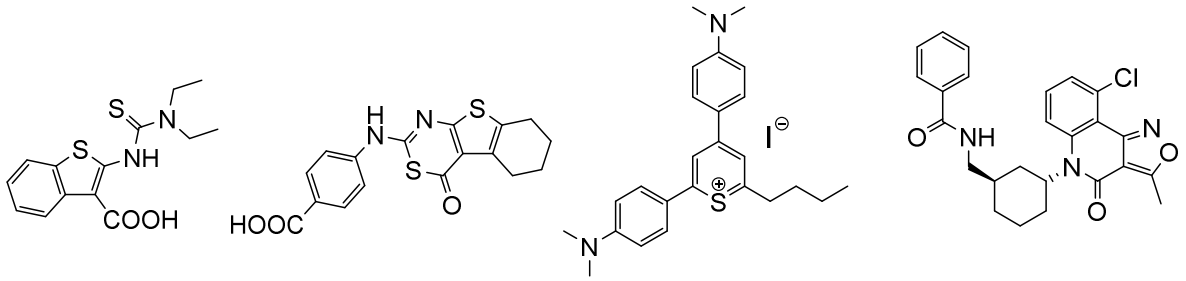

Figure 1.13. Molecular formulas of HTS-derived compounds: the thioureidothiophene derivative no. 48 (left), the 4-aminobenzoic acid derivative 1 (half left), the chalcogen pyrylium compound no. 2 (half right) and the tricyclic oxazole no. 21b (right).

Xenova Ltd. reported on quinazolinones (Figure 1.14),[270] pyrrolo- (Fig 1.14),[271] and indolopyrimdines (Figure 1.14)[272] as inhibitors of MRP1 and P-gp. These compounds are the most potent inhibitors of MRP1-mediated transport and represent the objective of this thesis.

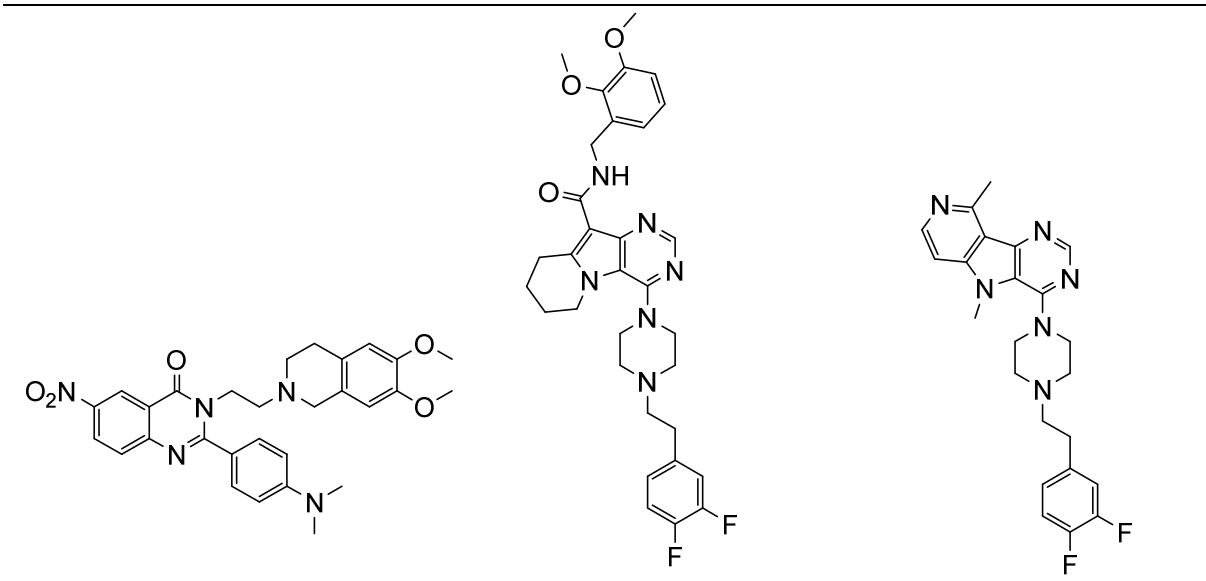

quinazolinone derivative no. 40 | pyrrolopyrimidine derivative no. 57 | indolopyrimidine derivative no. 78

Figure 1.14. Molecular formulas reported by *Wang* et al.: The quinazolinone derivative no. 40, the pyrrolopyrimidine no. 57 as well as the indolopyrimidine no. 78. The latter two substance classes are in focus of this thesis and are members of the compound class of 9-deazapurines as expressed in the title.

1.3.2. Activators of ABC-Transport Proteins

1.3.2.1. General Information

There is only few information about transport activation of ABC-transport proteins. Prazosine and progesterone were reported to stimulate P-gp-mediated transport,[273,274] but also (-)epicatechin,[275] aged garlic extracts,[276] the tyrosine kinase inhibitor erlotinib,[277] the imidazothioazole-derivative QB102[278] and other benzimidazole and benzthiazole derivatives.[279,280,281,282] Furthermore, certain thiophenopyrimidines showed to activate P-gp-mediated efflux of daunorubicin in A2780/ADR cells.[283284] Certain flavonoids were shown to stimulate P-gp-mediated transport.[285,286,287] Several of these compounds were also firstly known as inhibitors of P-gp.[288] Activators of the P-gp ATPase have also been described, such as synthetic hydrophobic peptides,[289] several flavonoids[290,291] or pharmacological drugs like verapamil.[292]

With respect to MRP2, another MDR-conferring efflux pump, the leukotriene receptor antagonists MK571, ONO-1978, montelukast and LY171883 stimulated the transport of $E_2$17βG, a substrate of MRP2. The latter compound also stimulated MRP3-mediated transport of this intrinsic substrate.[233] The benzothiophene derivative Gü658 was also shown to stimulate MRP2-mediated transport of $E_2$17βG.[293]

1.3.2.2. Activators of MRP1

Different mechanisms are conceivable leading to a decreased intracellular concentration of an anticancer drug or fluorescence dye, such as (i) enhanced expression / reduced downregulation of the transporter, (ii) modulation of processes influencing protein trafficking or integration into the membrane or (iii) increased transport activity of the transport protein itself. Table 1.4. gives an overview of compounds that are connected to activation of MRP1 mediated transport.

Table 1.4. Survey of pharmacological drugs, natural compounds, intrinsic substrates and their derivatives that are considered to activate MRP1-mediated transport. [a] = ATPase activation.

calcium channel blockers	**cell line**	**reported by**
verapamil and derivatives	HeLa T14 MRP1 vesicles	*Loe* et al. 2000 [294]
	HeLa T14 MRP1 vesicles	*Loe* et al. 2000 [77]
	CCRF-CEM/E1000	*Cullen* et al. 2001 [189]
	BHK-21 MRP1	*Trompier* et al. 2004 [190]
	BHK-21 MRP1	*Barattin* et al. 2010 [191]
curcuminoids		
curcumin I-III	HEK293 MRP1[a]	*Chearwae* et al. 2006 [295]
GSH analogs		
GSH	2008/MRP1, GLC_4/ADR	*Hooijberg* et al. 2000 [296]
methyl-*S*-GSH	H69AR	*Leslie* et al. 2003 [244]
ethyl-*S*-GSH	H69AR	*Leslie* et al. 2003 [244]
γ-Glu-Leu-Gly	H69AR	*Leslie* et al. 2003 [244]
γ-Glu-Phe-Gly	H69AR	*Leslie* et al. 2003 [244]
GSSG	H69AR	*Mao* et al. 1999 [297]
flavonoids and chalcones		
apigenin	GLC_4/ADR[a]	*Hooijberg* et al. 1999 [154]
	HeLa T5 vesicles	*Leslie* et al. 2001 [155]
	HeLa MRP1, H69AR	*Leslie* et al 2002 [298]
biochanin A	Panc-1	*Nguyen* et al. 2003 [151]
chalcone	Panc-1	*Nguyen* et al. 2003 [151]
daidzein	HEK293 MRP1	*Wu* et al. 2005 [153]
flavopiridol	GLC_4/ADR[a]	*Hooijberg* et al. 1997 [299]
genistein	GLC_4/ADR[a]	*Hooijberg* et al. 1997 [299]
	HeLa MRP1, H69AR	*Leslie* et al. 2002 [298]
	Panc-1	*Nguyen* et al. 2003 [151]
hesperetin	HEK293 MRP1	*Wu* et al. 2005 [153]

flavonoids and chalcones	cell line	reported by
kaempferol	GLC_4/ADR[a]	*Hooijberg* et al. 1997 [299]
myricetin	HeLa T5 vesicles	*Leslie* et al. 2001 [155]
naringenin	HeLa T5 vesicles	*Leslie* et al. 2001 [155]
	HeLa MRP1, H69AR	*Leslie* et al 2002 [298]
	HEK293 MRP1	*Wu* et al. 2005 [153]
phloretin	Panc-1	*Nguyen* et al. 2003 [151]
quercetin	COR-L23/R, MOR/R,	*Versantvoort* et al. 1996 [152]
	HeLa T5 vesicles	*Leslie* et al. 2001 [155]
	HeLa MRP1, H69AR	*Leslie* et al. 2002 [298]
	Panc-1	*Nguyen* et al. 2003 [151]
HIV protease inhibitors		
indinavir	brain astrocytes	*Brandmann* et al. 2012 [192]
nelfinavir	brain astrocytes	*Brandmann* et al. 2012 [192]
	LS-180V	*Perloff* et al. 2001 [300]
stilbenoids		
resveratrol	HEK293 MRP1[a]	*Wu* et al. 2005 [153]

The reverse transcriptase inhibitor ritonavir (Figure 1.15) was reported by *Perloff* et al. to enhance expression of MRP1 in the human colon adenocarcinoma cell line LS-180V. More recently in 2011, *Park* et al. found that α-tocopherol (vitamin E; Figure 1.15) can prevent MRP1 downregulation targeting intracellular microRNA (miR-199a-5p) that is a known regulator of MPR1 expression.[301] The authors also used glutamine to cause intracellular oxidative stress (GSSG overload), which was also a trigger for MRP1 upregulation. One year later the collagen/β-1-integrin was reported to prevent chemosensitivity toward doxorubicin in HSB2 leukemic T-cells by MRP1 upregulation.[302]

With respect to transport activation, the phenothiazine maleates (Figure 1.15), a known class of MRP1 and P-gp inhibitors,[303] were shown to stimulate MRP1-mediated transport of the MRP1 substrates BCPCF and BCECF.[304] Other phenothiazines were found to stimulate MRP1 in MRP1-expressing erythrocytes[305].

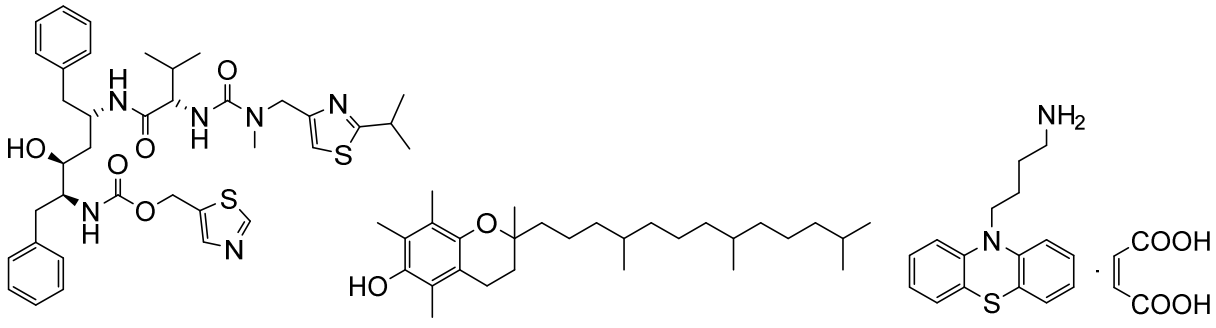

Figure 1.15. Molecular formulas of compounds that enhance MDR in cancer cells that overexpress MRP1. Left: the reverse transcriptase inhibitor ritonavir enhances MRP1 expression; middle: vitamin E (α-tocopherol) affects the microRNA miR-199a-5p, a known regulator of MPR1 expression; right: the phenothiazine maleate derivative 4HPhM as the most potent activator of MRP1-mediated transport.

Hummel et al. showed in 2011, that MRP1-mediated efflux was dependent on actin polymerization of the cytoskeleton.[306] This was also found by *El Azreq* et al.[302] While the disrupter latrunculin B (Figure 1.16) lowered MRP1 function, the actin polymerization enhancer jasplakinolide (Figure 1.16) enhanced the transport of the fluorescence dye and MRP1 substrate CFDA.

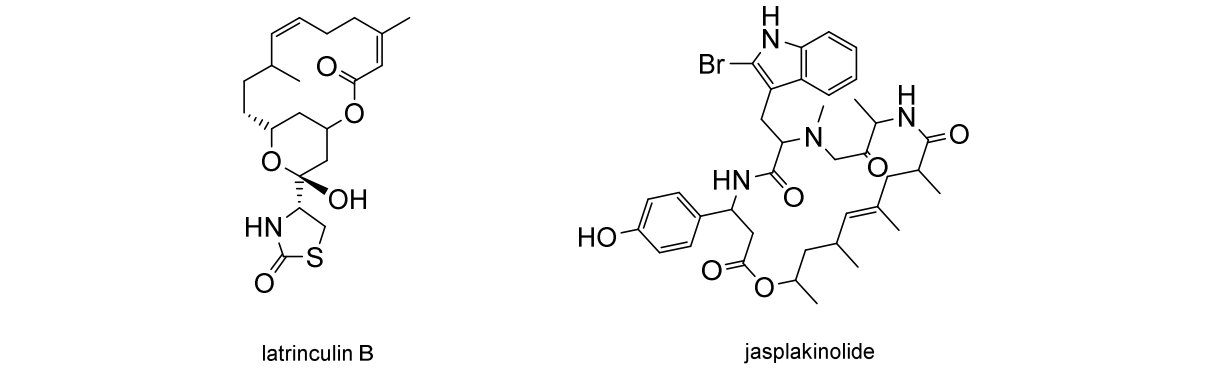

Figure 1.16. Molecular formulas of compounds that influence the polymerization of the intracellular actin skeleton, latrunculin B (left) and jasplakinolide (right). The latter compound enhanced polymerization and therefore MRP1 function, while the former did vice versa.

1.3.3. Dual Inhibitors of MRP1 and P-gp

Several of the pharmacological drugs, natural compounds and synthetic HTS-derived compounds have been reported to affect both, MRP1 and P-gp. Table 1.5 summarizes the known compounds.

Table 1.5. Survey of pharmacological drugs, natural products and HTS-derived compounds that are known to affect both, MRP1 and P-gp.

pharmacological drug	**reference**
CBT-1	[140]
cyclosporine A	[85],[86],[87],[88]
disulfiram	[133]
mifepristone	[134],[135],[136],[307]
MS-209	[94],[95],[96],[97]
NIK-250	[82],[308]
nutilin-3	[138]
verapamil	[73],[74],[76],[309],[310]
natural compounds	
agosterol A	[184],[185],[186],[187]
curcumin	[178],[179]
4-deacetoxyagosterol A	[188]
dendroamide	[182],[183]
genistin	[152]
8-prenylnaringenin	[157]
schisandrin B	[173],[311],[312]
synthetic HTS-derived compounds	
galloyl-based derivative 11f	[263]
LY117018	[264]
LY329146	[264]
LY335979	[267],[268]
LY465803	[267],[268]
LY475776	[267],[268]

The tricyclic isoxazole derivatives published by *Norman* et al. as well as the quinazolinones and 9-deazapurine derivatives reported by *Wang* et al. were very potent dual inhibitors with IC_{50} values in the low micromolar range or even better. Galloyl-based compounds reported by *Pellicani* et al. showed also dual inhibitory activity toward MRP1 and P-gp. Figure 1.17 gives an overview of the best dual inhibitors.

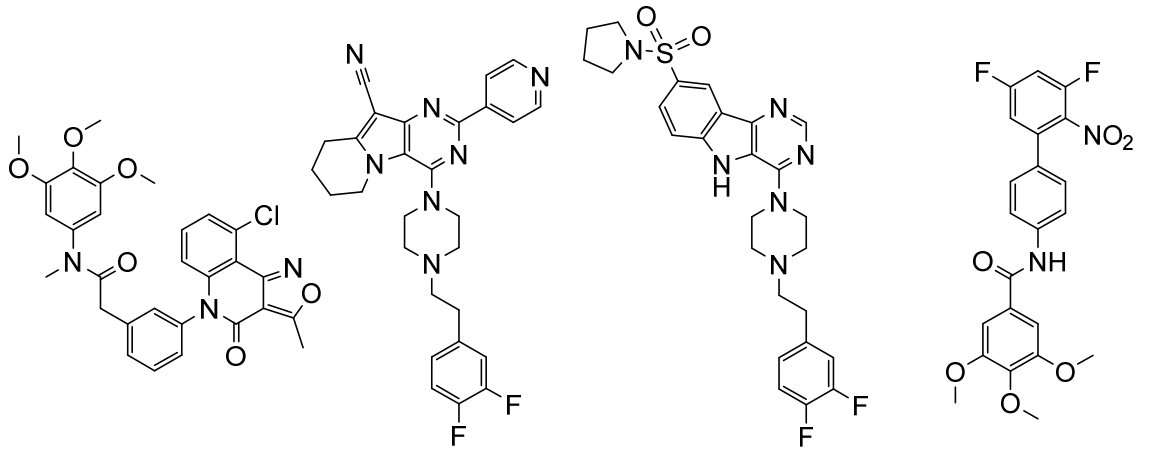

Figure 1.17. Molecular formulas of most recently published dual inhibitors of MRP1 and P-gp: the tricyclic isoxazole derivative no. 13 (left), the pyrrolopyrimidine derivative no. 47 (half left) and the indolopyrimidine derivative no. 49 (half right). The most recent report has been made for galloyl-based compounds, where derivative no. 11f (right) showed best inhibitory activities toward MRP1 and P-gp.

1.3.4. Dual Inhibitors of MRP1 and BCRP

Dual inhibition of MRP1 and BCRP has rarely been reported in the literature. The (thio)ureidocarboxylic acids by *Häcker* et al.[258] affected besides MRP1 also BCRP, but only at high concentrations. Specific dual flavonoids were shown to inhibit both transporters (Figure 1.18).[313,314]

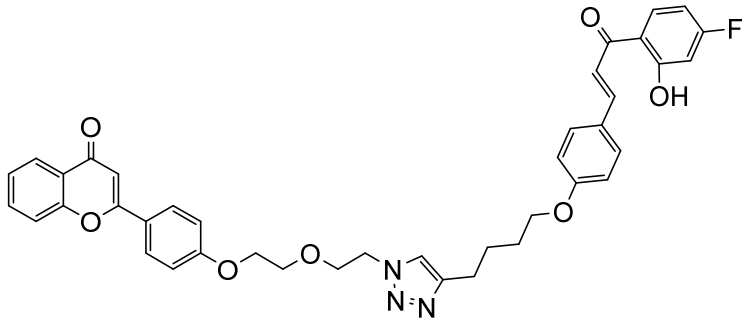

Figure 1.18. Molecular formula of a rare dual inhibitor of MRP1 and BCRP: the triazole containing flavonoid named 'AclOAzl'.

1.3.5. Dual Inhibitors of P-gp and BCRP

Many compounds were reported as dual inhibitors of P-gp and BCRP, such as elacridar (GF120918)[315] or tariquidar (XR9567).[316] Also several synthesized analogs of these reversers showed to be dual inhibitors (Figure 1.19).[317,318] BCRP inhibitors derived from known P-gp inhibitors were also reported to affect both transport proteins, like tetrazolic HM30181 derivatives (Figure 1.19) by *Köhler* et al.,[319] or tetrahydro-*β*-carboline analogs reported by *Spindler* et al. (Figure 1.19).[320] And since flavonoids were already discussed as inhibitors of MRP1, P-gp and BCRP,[145,146,147,148,149] many flavonoids (Figure 1.19),[321] as well as their precursors, the chalcones and derivatives (Figure 1.19),[322,323,324,325] proved to be dual inhibitors of P-gp and BCRP. Quinazoline moieties (Figure 1.19) were also shown to be effective in blocking P-gp- and BCRP-mediated transport of fluorescence probes.[326,327,328,329] Analogs of the antiarrhythmic drug propafenone were found to affect both transport proteins using human myeloid leukemia cells PLB985 transfected with BCRP as well as the human T-lymphoblast cell line CCRF VCR1000 overexpressing P-gp.[330] Most recently, acryloylphenylcarboxamides (Figure 1.19)[331] and acryloylphenylcarboxylates (Figure 1.19)[332] were shown to inhibit both, P-gp and BCRP, using in A2780/ADR and MDCK II BCRP cells overexpressing P-gp and BCRP, respectively.

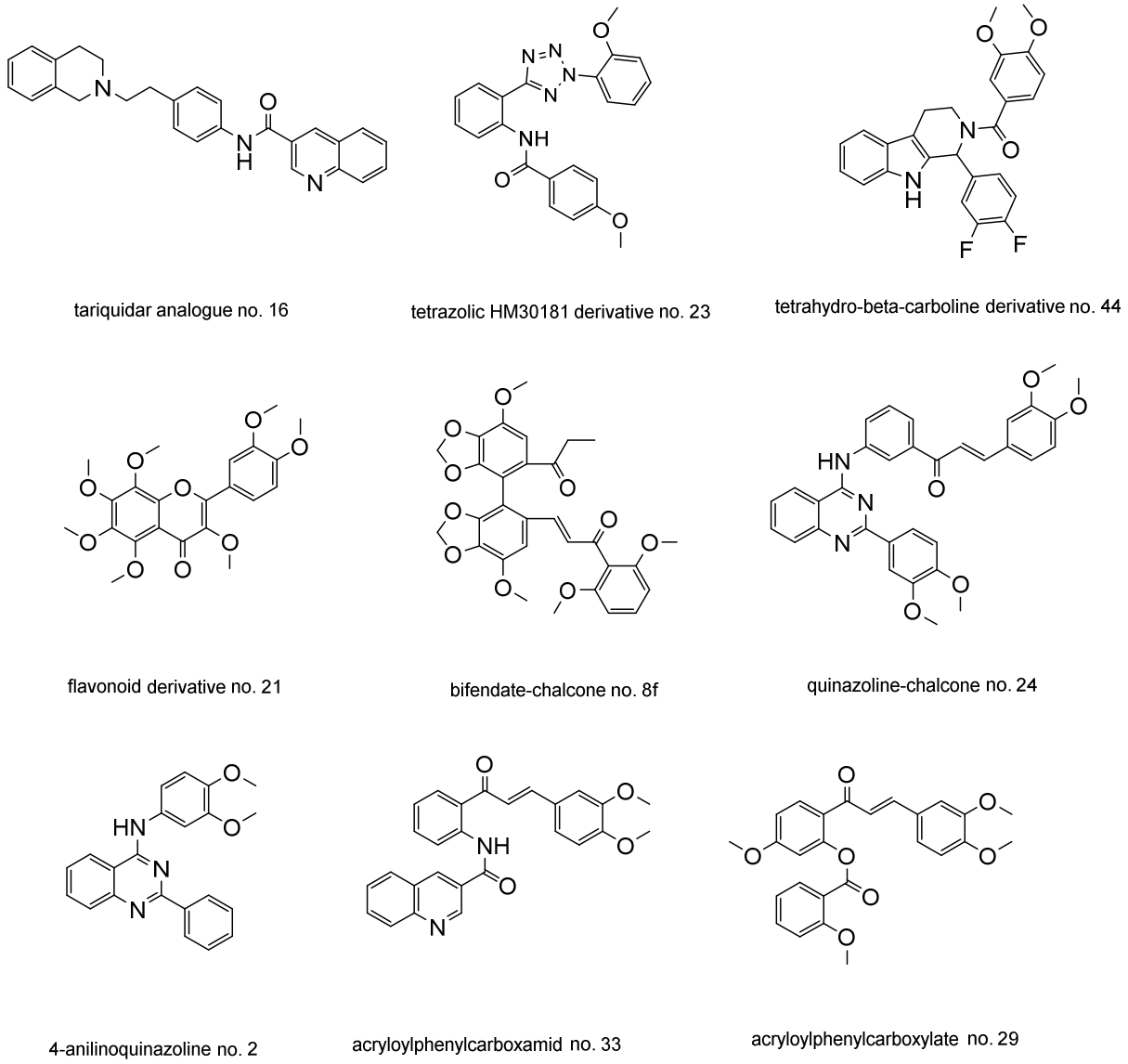

Figure 1.19. Molecular formulas of potent dual inhibitors of P-gp and BCRP.

1.3.6. Triple Inhibitors of MRP1, P-gp and BCRP

An exciting field of transporter science is multiple inhibition of transport proteins. The natural compound piperine (Figure 1.20) was found to cause accumulation of specific MRP1, P-gp and BCRP substrates in the corresponding overexpressing cell lines.[333] The clinical trial candidate biricodar[89,90,91,92] is nowadays considered to affect all three transporters.[334] The same applies for the standard inhibitor of BCRP, Ko143 (Figure 1.20), although the concentration needed to affect MRP1 is rather high.[335] A tariquidar analog (no. 14; Figure 1.20), a compound class providing some dual inhibitors, was investigated by *Pick* et al. using 2008/MRP1, A2780/ADR and MCF-7/MX cells, respectively. Although all three major

transporters were affected,[317] the effect on MRP1 was in low magnitude.[336] Some quinazoline (Figure 1.20)[337] and quinoline (Figure 1.20)[338] derivatives were also shown to be triple inhibitors.

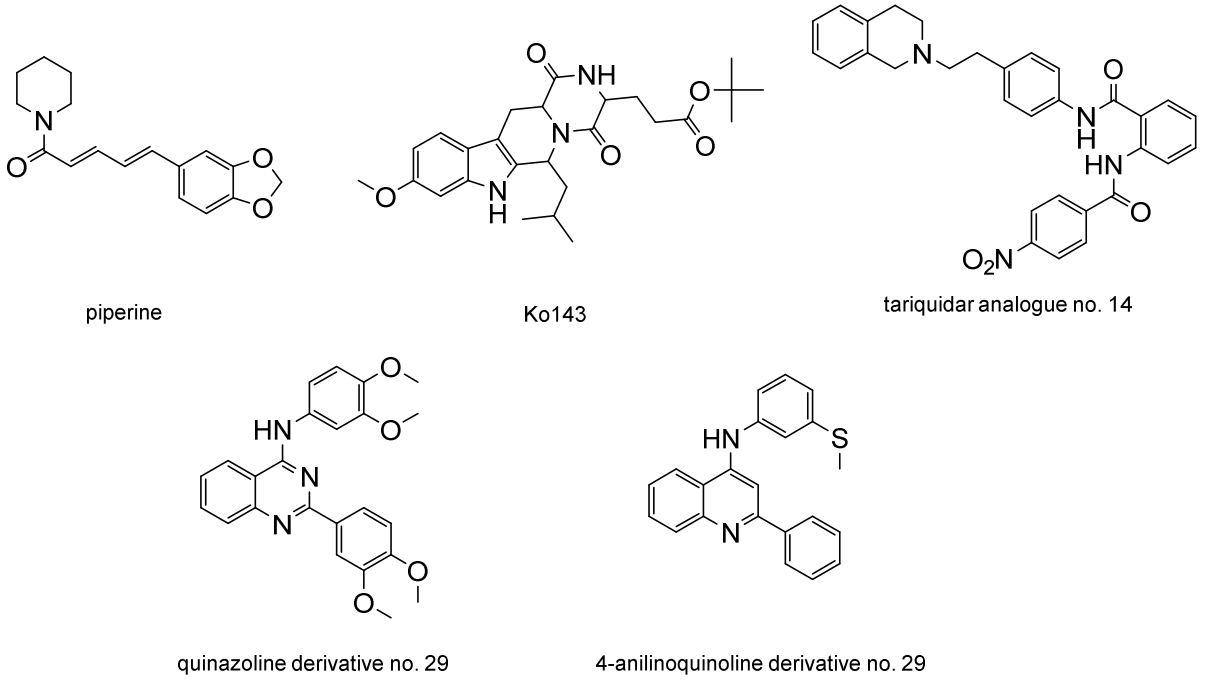

Figure 1.20. Molecular formulas of compounds known to affect all three ABC-transport proteins, MRP1, P-gp and BCRP.

1.3.7. Partial Inhibitors of ABC-transport proteins

Partial inhibition can be defined differently. It can refer to the ratio of the current effect and the maximal achievable effect of a standard compound expressed as percentage of control. For example the natural drug cepharanthine (Figure 1.21), known to reverse MRP7-mediated MDR,[339] was only partially able to reverse vincristine, etoposide and doxorubicin resistance in the glioma cell lines IN500 and T98G, both overexpressing MRP1.[82] Another example is the pyridine analog PAK-104 P (Figure 1.21), which could reverse doxorubicin resistance in HL60/ADR cells only partially.[83] Also MK571 (Figure 1.11), the most widely used standard inhibitor of MRP1, was shown to reverse doxorubicin-related MDR only partially in GLC_4/ADR cells.[231] The authors speculated that an altered topoisomerase II activity or co-expression of the lung resistance protein (LRP) might be responsible.

In screening experiments, as also performed in this work, a fixed compound concentration (e.g. 10 μmol · L^{-1}) is compared to a reference compound. The result is expressed as

percentage inhibition compared to the standard, and if less than 100% one can consider this effect being partial.

Different from this point of view, partial inhibition can also be defined as the maximal effect of a compound (e.g. measured plateau of its concentration-effect curve) which is distinct from the maximal effect of the standard compound. This was reported in 2000 with respect to many known P-gp inhibitors,[340,341] and was also observed for the quinazoline-chalcones in case of P-gp inhibition.[326] The tetrazolic HM30181 derivatives (Figure 1.21)[319] and their analogs,[342] but also some quinazolines (Figure 1.21)[338] result in maximum inhibition levels distinct from the used standard inhibitors.

The reasons for partial inhibition are diverse: (i) solubility can limit effectiveness of a drug if precipitation occurs;[343] (ii) fluorescence quenching of the substrate caused by the inhibitor might lead to reduced measured effects; (iii) protein binding could lead to a reduced fraction of inhibitor which is free to act, which is rather unlikely in cell-based *in vitro* assays; (iv) the transport function can be blocked only partially, that would result in a residual efflux.

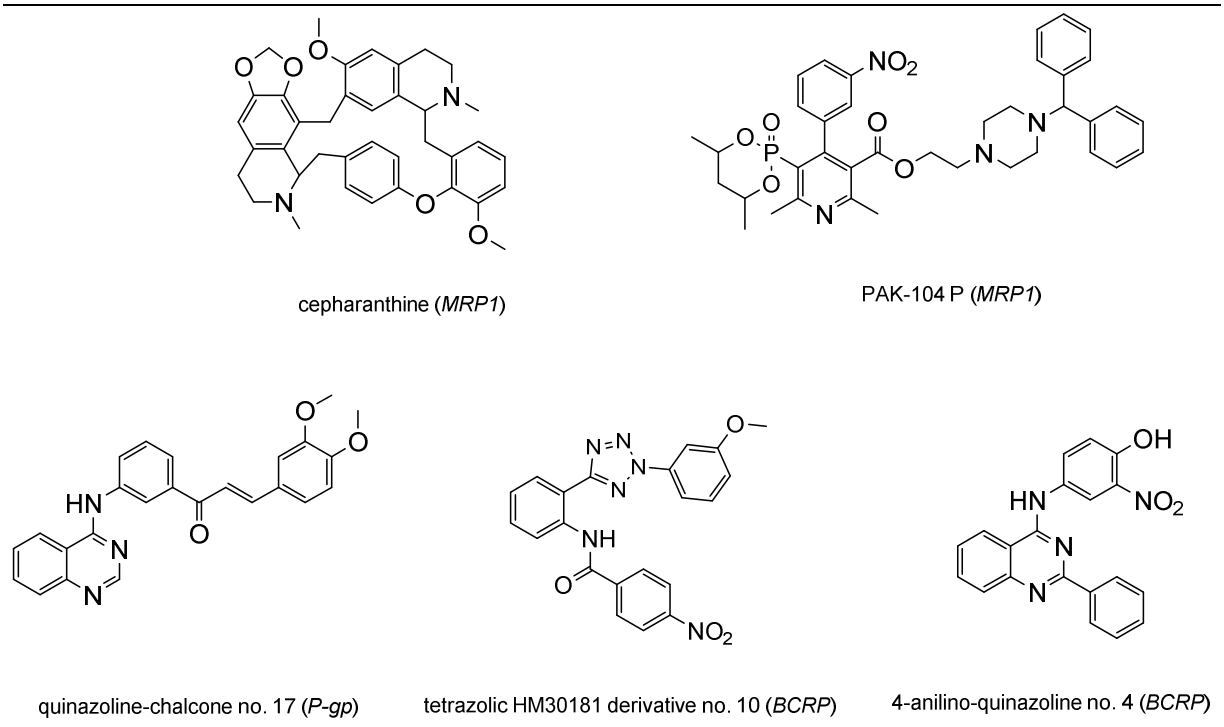

Figure 1.21 Molecular formulas of reported partial inhibitors of ABC-transport proteins. The tetrazolic HM30181 derivative reported by *Köhler* et al. possessed an IC_{50} value of 78.9 nmol · L^{-1} but with only 58% inhibition as compared to the standard compound Ko143. The quinazoline-chalcone no. 17 had good affinity toward P-gp with an IC_{50} of 0.42 μmol · L^{-1}, but with a maximum inhibition level of only 66%. The aniline-quinazoline no. 4 possessed an IC_{50} value of 80 nmol · L^{-1} but with 79% inhibition.

2. Aim of the Thesis

Chemotherapy still fails due to resistant cancers. Upregulation of ABC-transport proteins is one major mechanism behind this phenomenon. Colon carcinomas, lung or breast cancer are the most common malignancies in Germany,[344] mostly involved with the expression of MRP1, P-gp and BCRP.[56] This makes these proteins important targets in cancer chemotherapy. Unfortunately, clinical trials with the purpose to overcome MDR by inhibition of ABC-transporters failed due to severe side effects amongst other reasons.[74,345,346,347]

Hence, the development of new, potent, selective, but also broad-spectrum inhibitors is desirable to overcome ABC-transporter-mediated MDR. Furthermore, critical key points of the function of ABC-transport proteins are still unknown as useful tools like modulators / activators are missing. The aim of this thesis is (i) the synthesis and biological evaluation of new purines and 9-deazapurines as inhibitors of MRP1 based on the previous reports on pyrrolo- and indolopyrimidines;[270,271,348] (ii) investigation of the selectivity of the compounds toward P-gp and BCRP, and evaluation of selected compounds with respect to dual and triple inhibition; (iii) elucidation of structure-activity relationships of the compounds; (iv) characterization of the toxicity of the compounds toward different cancer cell lines; (v) evaluation of their MDR-reversing property; (vi) evaluation of the type of inhibition regarding the three herein presented ABC-transport proteins; (vii) analysis of the activating property of the compounds, their MDR-enhancing feature and activation type; (viii) establishment of the calcein AM and daunorubicin assay using the small-cell lung cancer cell line H69AR; (ix) development of new, potent and reliable standard inhibitors of MRP1 for further biological investigations.

3. Synthesis

3.1. Synthesis of Intermediates

3.1.1. Synthesis of 9-deazapurine Precursors

3.1.1.1. Synthesis of the 7,8-alicyclic-9-deazapurine Scaffold

The alicyclic educts **59** and **60** for the target compounds **74**-**87**, **111**-**117**, **126**-**127** and **130**-**131** were prepared as already described in the literature[271,348] with minor modifications.[349] Methylation of the lactam oxygen of the educts δ-valerolactam and ε-caprolactam was performed with dimethyl sulfate (DMS; Scheme 3.1) as described in detail in section 6.1.3.1.

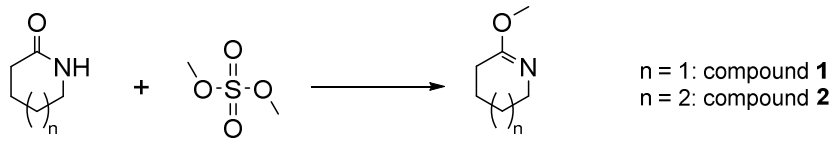

Scheme 3.1. Methylation of δ-valerolactam or ε-caprolactam with dimethyl sulfate to yield compounds **1** and **2**.

The obtained *O*-methylated intermediates **1** and **2** were treated with *CH*-acidic malononitrile resulting in spontaneous formation of the malononitrile derivatives **3** and **4** through nucleophilic substitution (Scheme 3.2; see section 6.1.3.2).

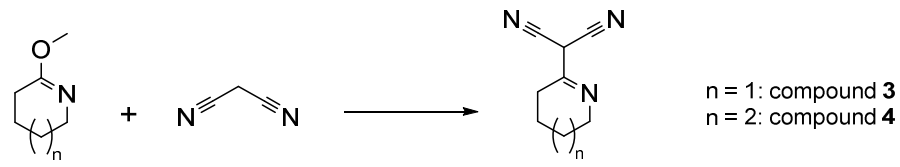

Scheme 3.2. Depiction of nucleophilic substitution of *O*-methylated derivatives **1** and **2** with *CH*-acidic malononitrile to yield compounds **3** and **4**.

The malononitrile derivatives **3** and **4** were exposed to ethyl bromoacetate and excess potassium carbonate to yield the pyrrole derivatives **17** and **18** as described in section 6.1.3.5. Scheme 3.3 gives an overview of the reaction.

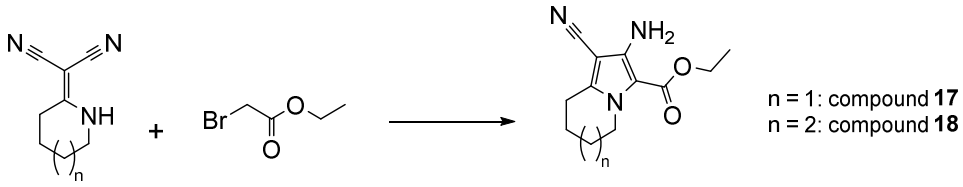

Scheme 3.3. Alkylation of the alicyclic secondary amine and formation of the pyrrole derivatives **17** and **18**.

Dimethylformamide dimethyl acetale (DMF-DMA) as a one-carbon synthon was added to the pyrrole derivatives **17** and **18** to give the formimidamides **31** and **32** (Scheme 3.4). The complete synthesis is presented in section 6.1.3.6.

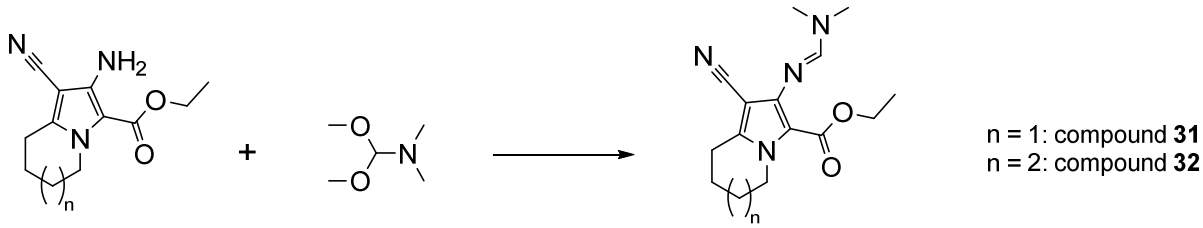

Scheme 3.4. The one-carbon synthon dimethylformamide dimethyl acetale introduces a carbon at the primary amine of compound **17** and **18** leading to the formimidamide derivatives **31** and **32**.

Gaseous ammonia was streamed through the reaction mixture containing the intermediates **31** and **32** leading to the pyrimidinon **45** and **46** as depicted in Scheme 3.5 and described in section 6.1.3.7.

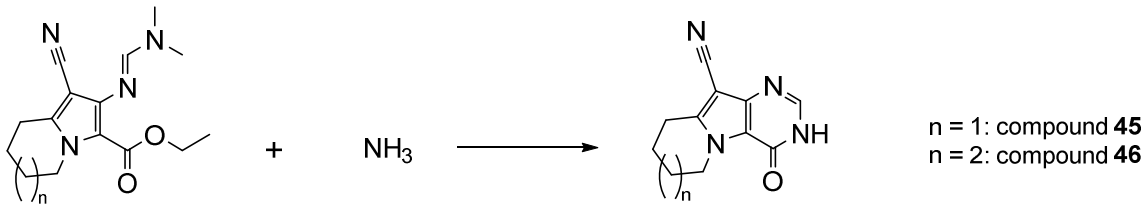

Scheme 3.5. Formation of the pyrimidinone derivatives **45** and **46** by exposure of intermediates **31** or **32** to gaseous ammonia.

Finally, the lactam intermediates **45** and **46** were aromatized using phosphoryl chloride as discussed in detail in section 6.1.3.8, resulting in the chlorinated precursors **59** and **60** (Scheme 3.6) of the target compounds **74-87**, **111-117**, **126-127** and **130-131**.

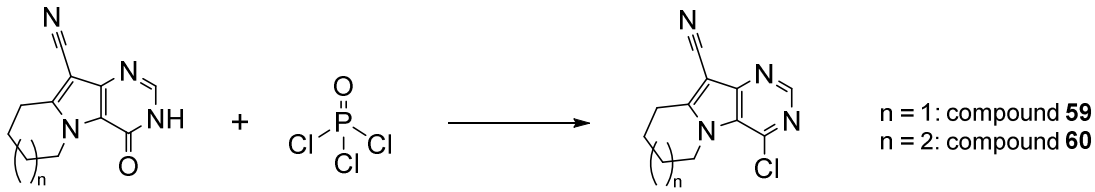

Scheme 3.6. Formation of the pyrimidine derivatives **59** and **60** as chlorinated precursors of the target compounds **74-87**, **111-117**, **126-127**, **130-131**.

3.1.1.2. Synthesis of the 7-*N*-substituted-9-deazapurine Scaffold

The synthesis of the chlorinated precursors with aliphatic (**61-65**), aromatic (**66-68**) and arylaliphatic (**69-71**) residues of the target compounds **88-106**, **118-125**, **128-129** and **132-135** started from (ethoxymethylene)malononitrile and different commercially available primary amines (see section 6.1.3.4) resulting in the malononitrile derivatives **6-16** (Scheme 3.7).[349,350]

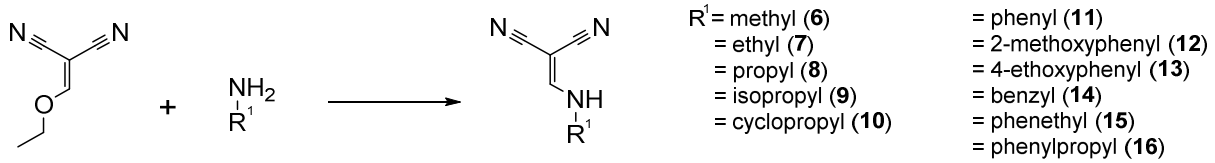

Scheme 3.7. Nucleophilic substitution of (ethoxymethylene)malononitrile by different primary amines resulting in the malononitrile derivatives **6-16**.

The reactions to form the chlorinated precursors **61**-**71** are similar to the above described synthesis (see section 6.1.3.5-8). In short, the malononitrile derivatives **6**-**16** were treated with ethyl bromoacetate to form the pyrrole analogs **19**-**29**. Exposure to dimethylformamide dimethyl acetale gave the formimidamide derivatives **33**-**43**. Ring closure was achieved using gaseous ammonia giving the pyrimidinones **47**-**57**. Finally, treatment with phosphoryl chloride yielded the aromatic, chlorinated 9-deazapurine precursors **61**-**71**. These reactions are summarized in Scheme 3.8.

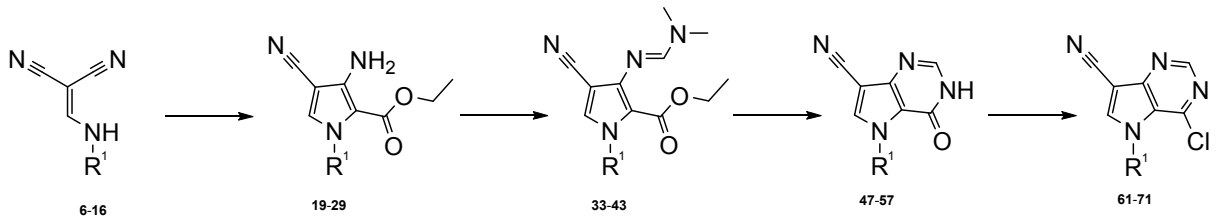

Scheme 3.8. Summary of the synthesis of chlorinated precursors **61**-**71** for synthesis of target compounds **88**-**106**, **118**-**125**, **128**-**129** and **132**-**135**.

3.1.1.3. Synthesis of the 8,9-annulated-9-deazapurine Scaffold

Since the yield of the reaction between 2-aminobenzonitrile and ethyl bromoacetate was not satisfactory, the educt was acylated using acetic anhydride (Scheme 3.9; see section 6.1.3.3) forming compound **5**.

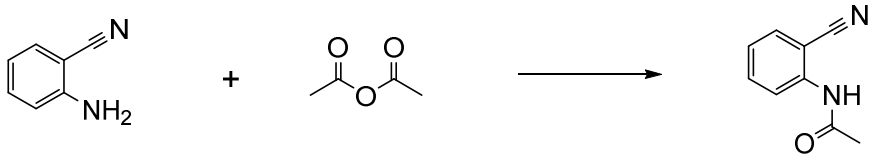

Scheme 3.9. Formation of the acylated benzonitrile derivative **5** with acetic anhydride.

The following reactions to form the chlorinated precursor **72** are similar to the above described synthesis (see section 6.1.3.5-7). In short, the acylated benzonitrile derivative **5** was exposed to ethyl bromoacetate to form the pyrrole derivative **30**. Treatment with dimethylformamide dimethyl acetale resulted in intermediate **44**. Exposure to gaseous ammonia yielded the ring-closed analog **58**. Treatment with excess phosphoryl chloride gave the chlorinated precursor **72**. Scheme 3.10 summarizes the described synthesis steps.

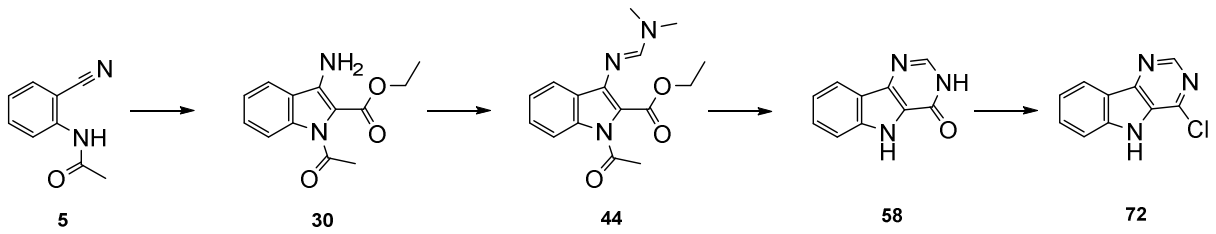

Scheme 3.10. Summary of the synthesis of chlorinated precursor **72** for synthesis of target compounds **136**-**144**.

3.1.2. Synthesis of the Piperazine Derivative No. 73

The 1*H*-indole-containing compound **73** was not commercially available and had to be synthesized.[351] Excess piperazine (4 eq.) was alkylated with 3-(2-bromoethyl)-1*H*-indole in the presence of Hünig's base (diisopropylethylamine; 6 eq.) yielding compound **73** as depicted in Scheme 3.11. Further information is provided in section 6.1.3.9.

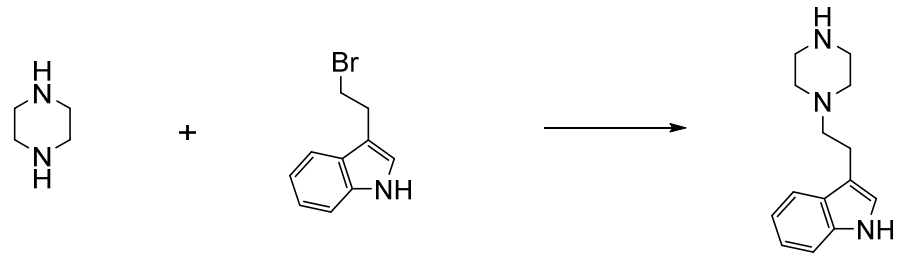

Scheme 3.11. Synthesis of piperazine derivative **73** via nucleophilic substitution of 3-(2-bromoethyl)-1*H*-indole by piperazine.

3.2. Synthesis of Purine and 9-deazapurine Compounds

3.2.1. Synthesis of Piperazine-containing Derivatives

In general, this work presents purines or 9-deazapurines with piperazine substituent at position 6 (**74**-**79**, **84**-**100**, **107**-**112**, **114**-**144**), or 9-deazapurines with amino residues at position 6 (**80**-**83**, **101**-**106** and **113**). The piperazine-bearing compounds were synthesized by nucleophilic substitution using either 6-chloropurine, the chlorinated precursors with 7,8-alicyclic variations (**59**-**60**), 7-*N*-aliphatic (**61**-**65**), -aromatic (**66**-**68**) or -arylaliphatic (**69**-**71**) variations or the 8,9-annulated-9-deazapurine precursor **72** (see also section 6.1.4).[349,350] Employing microwave-assisted synthesis at fixed parameters (200 W, 110 °C), equimolar amounts of the chlorinated precursors and piperazine derivatives solved in 1.5 mL

dimethylformamide in the presence of 1.5 eq. trimethylamine yielded the target compounds (Schemes 3.12-14). Tables 3.1-3 summarize the synthesized purines with variations at position 6 as well as 9-deazapurines with variations at positions 7, 8 and 9 with piperazine substituents.

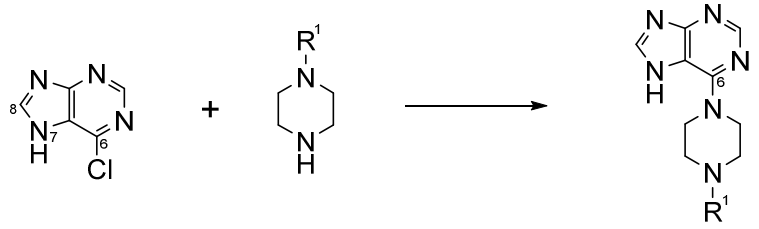

Scheme 3.12. Nucleophilic substitution of 6-chloropurine with a piperazine derivative resulting in the purine analogs **107**-**110**.

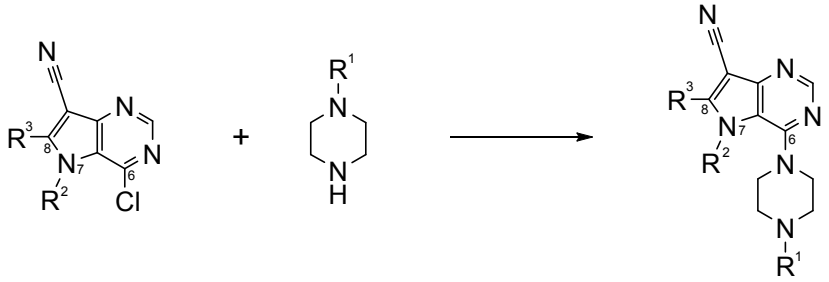

Scheme 3.13. Nucleophilic substitution of the chlorinated precursors **59**-**71** for synthesis of target compounds **74**-**79**, **84**-**100**, **111**-**112**, **114**-**135**.

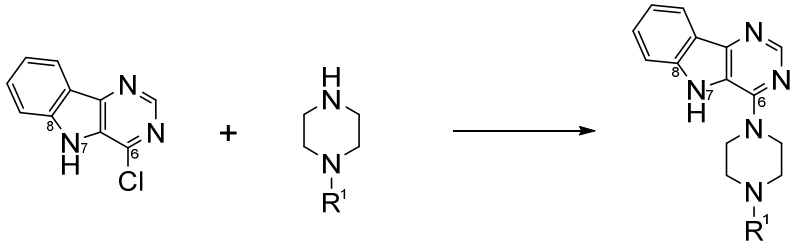

Scheme 3.14. Synthesis of 8,9-annulated-9-deazapurines with variations at position 6 using the chlorinated precursor **72** resulting in compounds **136**-**144**.

Table 3.1. Summary of synthesized purine analogs **107**-**110**.

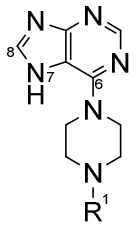

no.	R^1	no.	R^1
107	phenethyl	**109**	benzhydryl
108	benzyl	**110**	phenyl

Table 3.2. Summary of synthesized 9-deazapurines with variations at positions 7 and 8 with piperazine-bearing structure at position 6 (**74**-**79**, **84**-**100**, **111**-**112**, **114**-**135**).

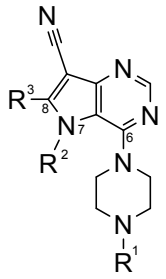

no.	R^1	R^2	R^3	no.	R^1	R^2	R^3
74	phenethyl	cyclohexyl		**111**	2-(1*H*-indole-3-yl)ethyl	cyclohexyl	
75	benzyl	cyclohexyl		**112**	2-(1*H*-indole-3-yl)ethyl	cycloheptyl	
76	benzhydryl	cyclohexyl		**114**	2-(pyridin-4-yl)ethyl	cyclohexyl	
77	phenyl	cyclohexyl		**115**	2-(pyridin-4-yl)ethyl	cycloheptyl	
78	methyl	cyclohexyl		**116**	pyridin-2-yl	cyclohexyl	
79	H	cyclohexyl		**117**	pyridin-2-yl	cycloheptyl	
84	phenethyl	cycloheptyl		**118**	2-(1*H*-indole-3-yl)ethyl	methyl	H
85	benzyl	cycloheptyl		**119**	2-(1*H*-indole-3-yl)ethyl	ethyl	H
86	benzhydryl	cycloheptyl		**120**	2-(1*H*-indole-3-yl)ethyl	propyl	H
87	phenyl	cycloheptyl		**121**	2-(1*H*-indole-3-yl)ethyl	cyclopropyl	H
88	phenethyl	methyl	H	**122**	2-(1*H*-indole-3-yl)ethyl	phenyl	H
89	phenethyl	ethyl	H	**123**	2-(1*H*-indole-3-yl)ethyl	benzyl	H
90	phenethyl	propyl	H	**124**	2-(1*H*-indole-3-yl)ethyl	phenethyl	H
91	phenethyl	isopropyl	H	**125**	2-(1*H*-indole-3-yl)ethyl	phenylpropyl	H
92	phenethyl	cyclopropyl	H	**126**	piperonyl	cyclohexyl	
93	phenethyl	phenyl	H	**127**	piperonyl	cycloheptyl	
94	benzyl	phenyl	H	**128**	piperonyl	phenyl	H
95	phenethyl	benzyl	H	**129**	piperonyl	phenethyl	H
96	benzyl	benzyl	H	**130**	2-furoyl	cyclohexyl	
97	phenethyl	phenethyl	H	**131**	2-furoyl	cycloheptyl	
98	benzyl	phenethyl	H	**132**	phenethyl	2-methoxyphenyl	H
99	phenethyl	phenylpropyl	H	**133**	benzyl	2-methoxyphenyl	H
100	benzyl	phenylpropyl	H	**134**	phenethyl	4-ethoxyphenyl	H
				135	benzyl	4-ethoxyphenyl	H

Table 3.3. Summary of synthesized 8,9-annulated-9-deazapurines **136**-**144**.

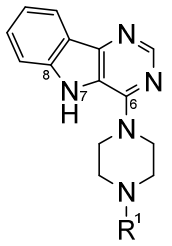

no.	R^1	no.	R^1
136	phenethyl	**141**	2-(pyridin-2-yl)ethyl
137	benzyl	**142**	pyridin-2-yl
138	benzhydryl	**143**	piperonyl
139	phenyl	**144**	2-furoyl
140	2-(1*H*-indole-3-yl)ethyl		

3.2.2. Synthesis of Amine Derivatives

Additionally, 9-deazapurines were synthesized via nucleophilic substitution of the chlorinated precursors **59**, **61** and **66**-**68** using a primary amine resulting in the target compounds **80**-**83**, **101**-**106** and **113**.[349,350] The procedure is similar to the above described synthesis of the piperazine derivatives and is summarized in Scheme 3.15 and section 6.1.4. Table 3.4 summarizes the synthesized compounds.

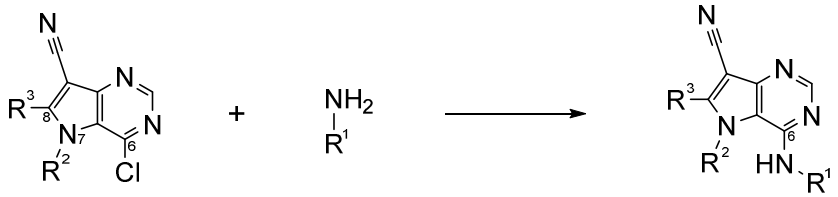

Scheme 3.15. Nucleophilic substitution of the chlorinated precursors **59**, **61** and **66**-**68** giving the amino-derivatives **80**-**83**, **101**-**106** and **113**.

Table 3.4. Summary of synthesized compounds **80**-**83**, **101**-**106** and **113**.

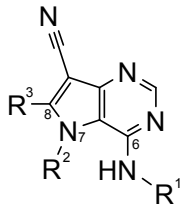

no.	R^1	R^2	R^3	no.	R^1	R^2	R^3
80	phenethyl	cyclohexyl		**103**	benzyl	benzyl	H
81	benzyl	cyclohexyl		**104**	phenylpropyl	benzyl	H
82	benzhydryl	cyclohexyl		**105**	phenethyl	phenethyl	H
83	phenyl	cyclohexyl		**106**	phenylpropyl	phenethyl	H
101	benzyl	methyl	H	**113**	2-(1*H*-indol3-yl)ethyl	cyclohexyl	
102	benzyl	phenyl	H				

4. Biological Investigation

4.1. Evaluation of 7,8-alicyclic and 7-*N*-alkyl-, -aryl- or -arylalkyl-9-deazapurines

4.1.1. Inhibition of MRP1-mediated Transport of Calcein AM and Daunorubicin

The calcein AM and daunorubicin assays were used to evaluate the synthesized compounds with respect to MRP1 inhibition. The exact procedures are described in the experimental sections 6.2.4.2 and 6.2.4.3. In brief, the non-fluorescent calcein acetoxymethyl (AM) is a high-affinity substrate of MRP1. It easily diffuses through the cell membrane into the cell. During membrane passage, it is recognized and extruded by MRP1. Intracellularly, the ester is cleaved by unspecific esterases giving the fluorescent calcein. Inhibition of MRP1 transport function leads to an increased intracellular concentration of calcein AM which is then cleaved by these esterases. Therefore, fluorescence increases with inhibition of MRP1. Plotting of the fluorescence values against the logarithmic concentration of the used inhibitor gives a sigmoidal relation from which the half-maximal inhibitory concentration (IC_{50}) can be deduced.

In principle, the same applies for the antineoplastic drug daunorubicin, although no intracellular esterases are involved. Daunorubicin diffuses passively through the cell membrane into the cell, and gets extruded via MRP1-mediated transport. Inhibition of MRP1 leads to increased intracellular concentrations of daunorubicin, which can be determined fluorometrically. Again, the measured fluorescence increases with the degree of MRP1 inhibition. This assay was established and performed by Katja Stefan. The compounds and activities presented in this subchapter have already been published.[349]

Starting point of this series was compound **74**, which was already described by *Wang* et al. (compound 30 in reference [271]). This compound was established as standard inhibitor (together with compound **126**) as described in section 6.2.4.2.3. While the 7,8-cyclohexyl moiety was kept, the side chain at position 6 was changed to elucidate structural preferences with respect to MRP1 inhibition. Table 4.1 summarizes half-maximal inhibition concentrations (IC_{50}) determined in both performed assays. Additionally, the molecular weight as well as the calculated partition coefficient of the neutral molecule (logP) of the compounds is listed.

Table 4.1. Summary of calcein and daunorubicin assay results of 7,8-cyclohexyl-9-deazapurines with variations at position 6 (compounds **74**-**83**). Additionally, the molecular weight as well as the calculated logP value is depicted. Given is IC_{50} value of at least three independent experiments with duplicate measurements ± standard error of the mean (SEM) as described in section 6.3.1.2. Furthermore, the negative decadic logarithm of the IC_{50} value (pIC_{50}) ± SEM is listed; [a] = compound **81** has already been published (compound 25 in ref. [271]).

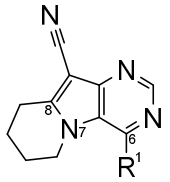

no.	R^1	M_r [Da]	logP (calc.)	calcein AM IC_{50} ± SEM [μmol · L^{-1}]	calcein AM pIC_{50} ± SEM	daunorubicin IC_{50} ± SEM [μmol · L^{-1}]	daunorubicin pIC_{50} ± SEM
74	4-phenethyl-piperazine-1-yl	386.50	2.81	0.369 ± 0.007	6.433 ± 0.012	0.195 ± 0.012	6.710 ± 0.041
75	4-benzyl-piperazine-1-yl	372.48	2.36	0.672 ± 0.041	6.173 ± 0.040	0.634 ± 0.028	6.198 ± 0.029
76	4-benzhydryl-piperazine-1-yl	448.57	3.82	1.62 ± 0.07	5.791 ± 0.027	1.07 ± 0.03	5.971 ± 0.020
77	4-phenyl-piperazine-1-yl	358.45	2.02	2.54 ± 0.23	5.598 ± 0.059	2.90 ± 0.07	5.538 ± 0.015
78	4-methyl-piperazine-1-yl	296.38	0.86	5.06 ± 0.15	5.296 ± 0.020	2.85 ± 0.19	5.546 ± 0.043
79	piperazine-1-yl	282.35	0.17	26.6 ± 3.0	4.578 ± 0.075	10.8 ± 0.2	4.966 ± 0.015
80	phenylpropyl-amino	331.42	3.92	2.46 ± 0.28	5.611 ± 0.076	2.82 ± 0.18	5.550 ± 0.042
81	phenethyl-amino[a]	317.40	3.45	8.22 ± 0.90	5.088 ± 0.072	4.97 ± 0.27	5.305 ± 0.036
82	benzyl-amino	303.37	2.89	14.2 ± 1.2	4.851 ± 0.054	8.72 ± 0.66	5.061 ± 0.050
83	aniline	289.34	2.73	14.1 ± 0.8	4.850 ± 0.037	9.40 ± 0.30	5.027 ± 0.021

Figure 4.1 shows a scatter plot of the pIC_{50} values determined in both assays. As indicated by the slope of 0.90 ± 0.07 and a R^2 value of 0.94, the data is highly correlated. While for the whole compound set no obvious correlation could be observed between pIC_{50} and the

calculated logP values, this could be achieved by classification into (i) piperazine-bearing and (ii) amine-bearing compounds. This applied for the calcein AM (Figure 4.1 B) and the daunorubicin (Figure 4.1. C) assay, respectively. Compound **76** constituted an outlier, which could be explained by its bulky and sterically demanding benzhydryl residue at position 6. Compared to compounds **80**-**83** (ii), it is obvious that the piperazine linker of compounds **74**-**79** (i) at the same position is more beneficial for MRP1 inhibition than the secondary amine of compounds **80**-**83**. But taken together, high lipophilicity seemed to be preferred with regard to MRP1 inhibition. This was shown before for thioureidothiophenes.[352]

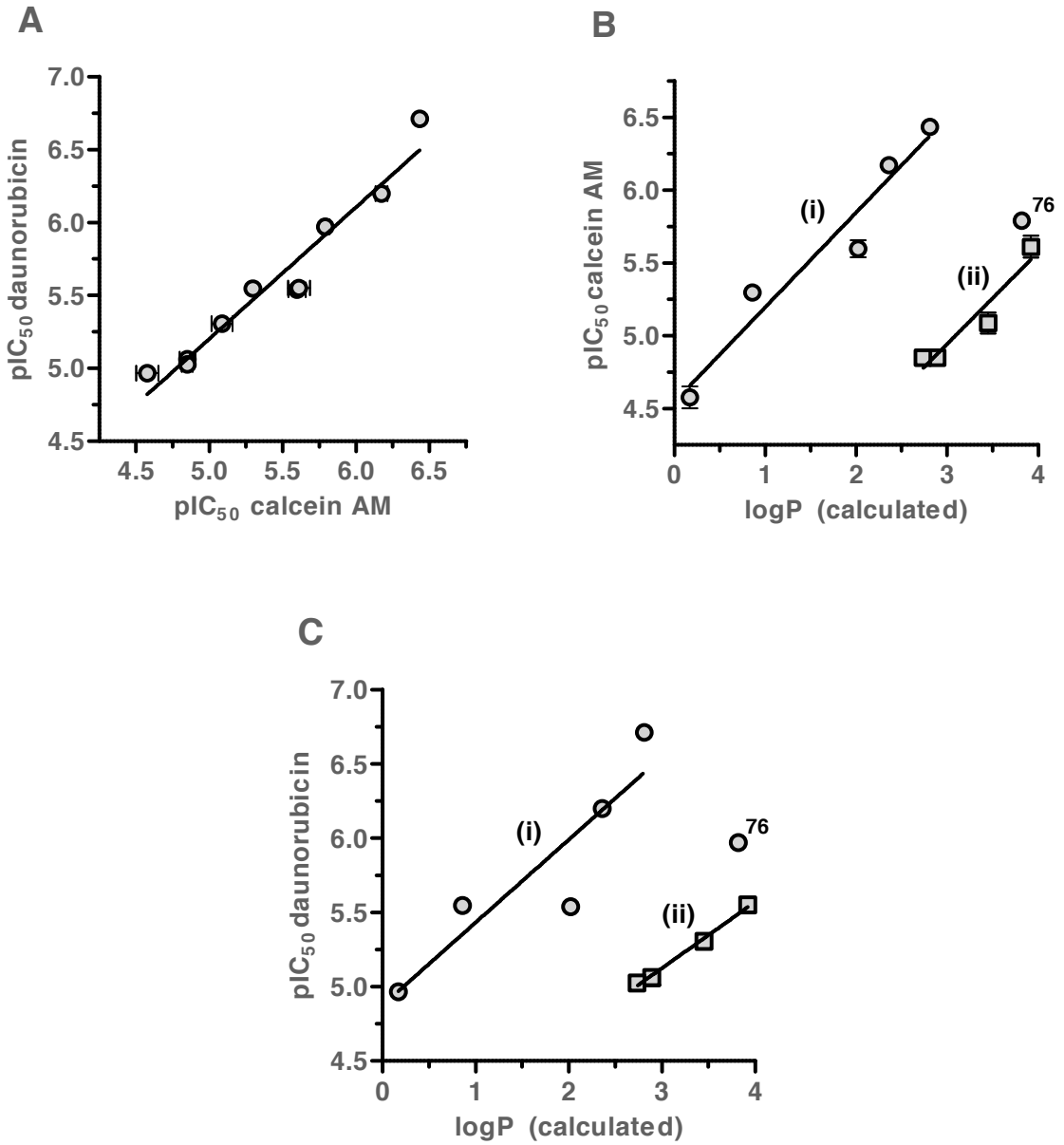

Figure 4.1. (A): Correlation of calcein AM and daunorubicin assay results for compounds **74**-**83**. (B): Correlation between inhibitory activity obtained in the calcein AM assay and the calculated logP values of tested compounds. (C): Correlation between inhibitory activity obtained in the daunorubicin assay and the calculated logP values of tested compounds; open circles: piperazine-bearing derivatives (i); open squares: secondary amine-bearing structures (ii).

The interrelationship between inhibitory activity and calculated logP value can also be seen in the corresponding concentration-effect curves. Figure 4.2 compares compound **74** to compounds **75** and **77** (calcein AM assay; A) and to compounds **78** and **79** (daunorubicin assay; B). The selected compounds are 7,8-cyclohexyl-9-deazapurine derivatives with reduced linker length at position 6. The decreased inhibitory power of these compounds is indicated by a shift of the corresponding concentration-effect curves to the right. Hence, the phenethylpiperazinyl residue at position 6 is most preferred with respect to MRP1 inhibition.

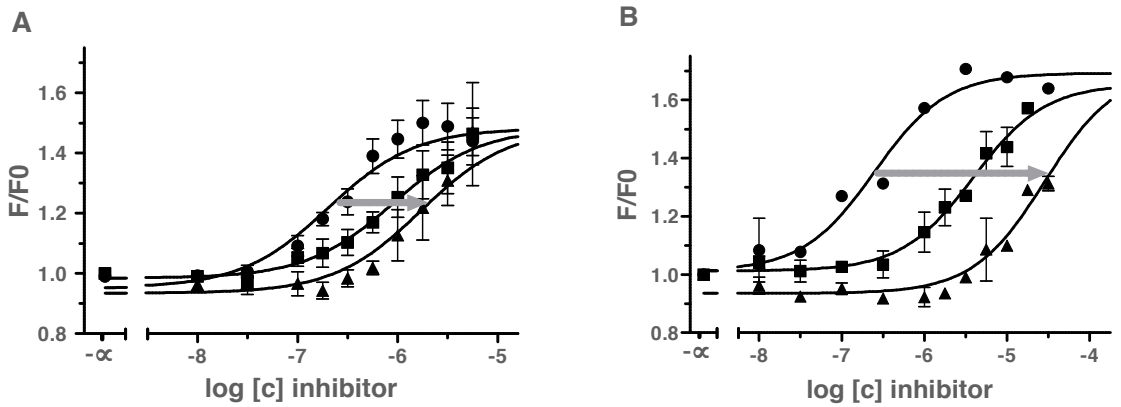

Figure 4.2. (A): Concentration-effect curve of compound **74** (closed circles) in comparison to compounds **75** (closed squares) and **76** (closed upward triangles) evaluated in the calcein AM assay. (B): Concentration-effect curve of compound **74** (closed circles) in comparison to compound **78** (closed squares) and **79** (closed upward triangles) evaluated in the daunorubicin assay as determined by Katja Stefan. Depicted are representative experiments of at least three independent experiments with duplicate measurements. Ordinate (F/F0): quotient of measured fluorescence at different compound concentration and basal fluorescence without compound supplementation (-∝). Data points are expressed as mean ± SEM. The grey arrow indicates the decrease of inhibitory activity accompanied by change of the phenethylpiperazinyl side chain at position 6.

Enlargement of the alicyclic ring system to a cycloheptyl residue at positions 7 and 8 gave compounds with inferior inhibitory activity in comparison to their 7,8-cyclohexyl counterparts (**74**-**77**). Figures 4.3 A-B show the plots between inhibitory property of the 7,8-cycloheptyl-9-deazapurines **84**-**87** and calculated logP values. Compound **86** resulted in a decreased inhibitory activity toward MRP1 in spite of its high logP value. This was already shown for its 7,8-cyclohexyl counterpart no. **76**. Though, the bulky benzhydryl residue was not beneficial for MRP1 inhibition. Table 4.2 summarizes the determined biological data. In summary, the increase of lipophilicity due to the enlarged alicyclic ring system at positions 7 and 8 resulted not in the expected enhanced inhibitory power. This might – in analogy to the benzhydryl residue of compound **76** and **86** – caused by the steric demands of the binding pocket(s).

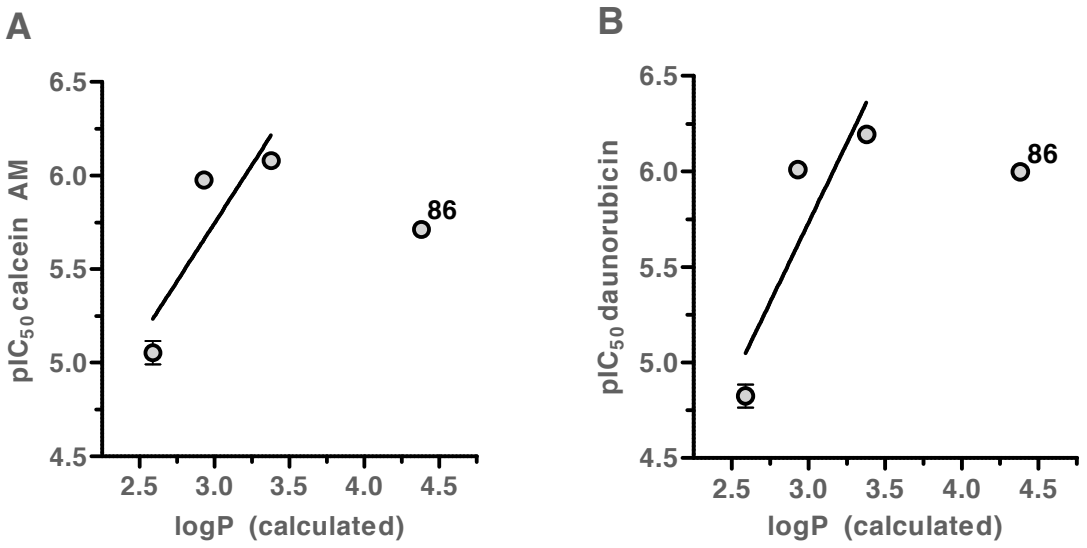

Figure 4.3. Correlation between inhibitory activity obtained in the calcein AM assay (A) and daunorubicin assay (B) and calculated logP values of compounds **84**-**87**.

Table 4.2. Inhibitory activity data of 7,8-cycloheptyl-9-deazapurines with variations at position 6 (compounds **74**-**83**) as well as their molecular weight and calculated logP value.

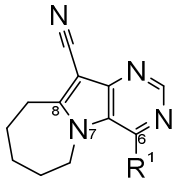

no.	R^1	M_r [Da]	logP (calc.)	calcein AM IC_{50} ± SEM [µmol · L^{-1}]	calcein AM pIC_{50} ± SEM	daunorubicin IC_{50} ± SEM [µmol · L^{-1}]	daunorubicin pIC_{50} ± SEM
84	4-phenethyl-piperazine-1-yl	400.53	3.38	0.833 ± 0.022	6.080 ± 0.022	0.641 ± 0.037	6.194 ± 0.038
85	4-benzyl-piperazine-1-yl	386.50	2.93	1.06 ± 0.02	5.976 ± 0.013	0.980 ± 0.041	6.009 ± 0.028
86	4-benzhydryl-piperazine-1-yl	462.60	4.38	1.94 ± 0.08	5.712 ± 0.026	1.01 ± 0.02	5.998 ± 0.016
87	4-phenyl-piperazine-1-yl	372.48	2.59	8.90 ± 0.84	5.053 ± 0.062	15.1 ± 1.4	4.824 ± 0.060

Since the phenethyl- and benzylpiperazine residues of the 7,8-alicyclic-9-deazapurines (**74**-**77** and **84**-**87**) seemed to be most accepted by MRP1, these structural elements were adopted for the 9-deazapurines with variations at the pyrrole nitrogen at position 7. The 7,8-alicyclic substituent was removed and different *N*-alkyl- or -alkylaryl linker were introduced to elucidate the preference with respect to MRP1 inhibition. Table 4.3 gives the determined biological data.

Table 4.3. Inhibitory activity data of 7-*N*-substituted-9-deazapurines. Aliphatic, aromatic or arylaliphatic variations were introduced at position 7. Position 6 contained either a phenethylpiperazine or benzylpiperazine residue. Additionally, the molecular weight and the calculated logP value are depicted.

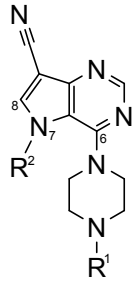

no.	R^1	R^2	M_r [Da]	logP (calc.)	calcein AM IC_{50} ± SEM [μmol · L^{-1}]	calcein AM pIC_{50} ± SEM	daunorubicin IC_{50} ± SEM [μmol · L^{-1}]	daunorubicin pIC_{50} ± SEM
88	phen-ethyl	methyl	346.44	1.75	0.712 ± 0.032	6.148 ± 0.029	0.695 ± 0.049	6.159 ± 0.046
89	phen-ethyl	ethyl	360.47	2.28	1.05 ± 0.05	5.977 ± 0.031	0.785 ± 0.053	6.106 ± 0.045
90	phen-ethyl	propyl	374.49	2.81	0.540 ± 0.035	6.269 ± 0.043	0.417 ± 0.016	6.380 ± 0.025
91	phen-ethyl	iso-propyl	374.49	2.63	0.813 ± 0.064	6.091 ± 0.052	1.23 ± 0.07	5.909 ± 0.036
92	phen-ethyl	cyclo-propyl	372.48	1.76	0.243 ± 0.018	6.615 ± 0.049	0.199 ± 0.014	6.703 ± 0.047
93	phen-ethyl	phenyl	408.51	3.97	0.752 ± 0.052	6.130 ± 0.046	0.340 ± 0.004	6.469 ± 0.008
94	benzyl	phenyl	394.48	3.52	1.20 ± 0.14	5.923 ± 0.079	0.863 ± 0.042	6.064 ± 0.032
95	phen-ethyl	benzyl	422.54	3.46	1.00 ± 0.05	6.002 ± 0.031	0.619 ± 0.052	6.210 ± 0.055
96	benzyl	benzyl	408.51	3.01	2.74 ± 0.21	5.563 ± 0.051	0.876 ± 0.019	6.058 ± 0.015
97	phen-ethyl	phen-ethyl	436.56	3.90	0.920 ± 0.067	6.037 ± 0.048	1.11 ± 0.08	5.955 ± 0.046
98	benzyl	phen-ethyl	422.54	3.44	0.891 ± 0.131	6.055 ± 0.096	0.973 ± 0.097	6.014 ± 0.066
99	phen-ethyl	phenyl-propyl	450.59	4.34	0.947 ± 0.066	6.025 ± 0.046	0.585 ± 0.015	6.233 ± 0.017
100	benzyl	phenyl-propyl	436.56	3.89	3.15 ± 0.11	5.502 ± 0.024	2.36 ± 0.07	5.628 ± 0.020

These compounds were found to be very active, most possessing IC_{50} values of 1 μmol · L^{-1} or less. Interestingly, no correlation could be observed with respect to calculated logP values. Categorization of the tested compounds **88**-**100** into the subclasses (i) 7-*N*-alkyl-substituted-9-deazapurines (**88**-**92**), (ii) 7-*N*-aryl- or -arylalkyl-substituted-9-deazapurines with phenethylpiperazine moiety at position 6 (**93**,**95**,**97** and **99**) and (iii) 7-*N*-aryl- or -arylalkyl-substituted-9-deazapurines with benzylpiperazine moiety at position 6 (**94**,**96**,**98** and **100**)

showed that that molecular weight is a moderately good descriptor for prediction of inhibitory activity (see Figures 4.4 A-B). Compound **91** is an outlier, giving less inhibition than could be expected with respect to its molecular weight.

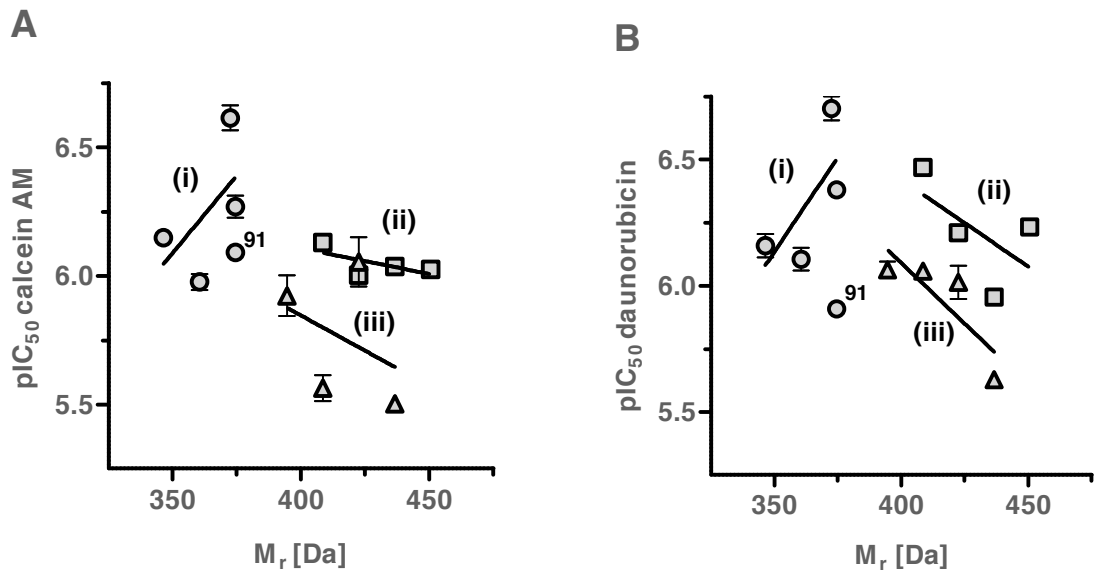

Figure 4.4. Plot of biological data and molecular weight for evaluated compounds **88**-**100**. Depicted are (i) 7-*N*-alkyl-substituted-9-deazapurines (open circles), (ii) 7-*N*-aryl- or -arylalkyl-substituted-9-deazapurines with phenethylpiperazine moiety at position 6 (open squares) and (iii) 7-*N*-aryl- or -arylalkyl-substituted-9-deazapurines with benzylpiperazine moiety at position 6 (open upward triangles) evaluated in the calcein AM assay (A) and daunorubicin assay (as determined by Katja Stefan; B).

Except for compound **91**, the inhibitory activity increases with length of the side chain of compound subset (i). The alicyclic cyclopropyl substituent of compound **92** was mostly preferred and represents the best compound of this thesis. Vice-versa, compound **93** represents the best compound of subset (ii), while the increase of the aliphatic side chain lowered MRP1 inhibition. Finally, the compounds of subset (iii) with the benzylpiperazine residue at position 6 (**94**, **96**, **98** and **100**) were all inferior compared to their phenethylpiperazine counterparts (**93**,**95**,**97** and **99**). Thus, the extended side chain at position 7 cannot be compensated by a shorter side chain at position 6. But as can be seen from Figures 4.4 A-B, the inhibitory activities of subsets (ii) and (iii) showed only a low correlation to molecular weight.

4.1.2. Analysis of Inhibition Type

The type of inhibition is important with respect to comparability of biological data. In case of competitive inhibition, the IC_{50} depends on the used concentration of the fluorescence dye. This does not apply to noncompetitive inhibitors. Table 4.4 gives representatives of known MRP1 inhibitors and their inhibition type with regard to selected MRP1 substrates.

Table 4.4. List of common MRP1 inhibitors and their mode of action with respect to selected MRP1 substrates.

inhibitor	MRP1 substrate	type of inhibition
benzbromarone	BCPCF	competitive [353]
cyclosporine A	BCPCF	noncompetitive [353]
genistein	daunorubicin	competitive [354]
PAK-104 P	daunorubicin	noncompetitive [84]

Compound **74** is a noncompetitive inhibitor of MRP1-mediated calcein AM (Figure 4.5 A) as well as daunorubicin (Figure 4.5 B) transport as indicated by the intersection at the abscissa. The interpretation and evaluation of the obtained data was in collaboration with Katja Stefan. The basic mathematical equations behind this can be drawn from reference [355]. Experimental section 6.3.10.1 gives a short summary.

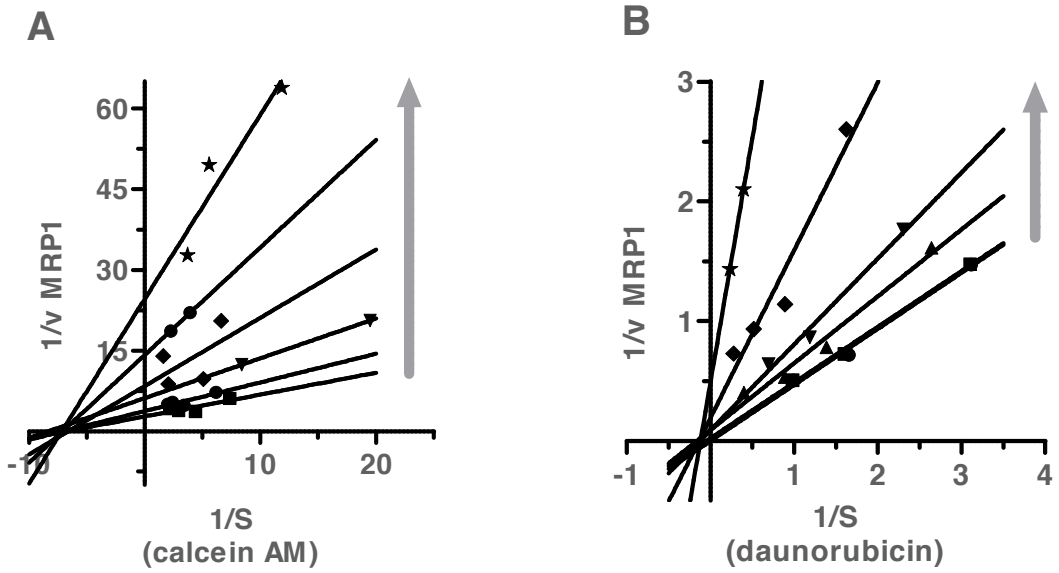

Figure 4.5. Evaluation of the type of inhibition of standard inhibitor **74** with respect to MRP1-mediated transport of calcein AM (A) and daunorubicin (B). Left graphic: calcein AM was used at concentrations of 0.2, 0.3, 0.5, 0.6 and 0.7 μmol · L^{-1}; compound **74** was used at concentrations of 31.6 (closed squares), 100 (closed upward triangles), 177 (closed downward triangles) 316 (closed rhombs) and 562 (closed stars) nmol · L^{-1}. Right graphic: daunorubicin was used at concentrations of 1, 2, 3 and 5 μmol · L^{-1}; compound **74** was used at concentrations of 3.16 (closed squares), 10.0 (closed upward triangles), 32.6 (closed downward triangles), 100 (closed rhombs) and 316 (closed stars) nmol · L^{-1}; the control is depicted as closed circles in both assay; the grey upward oriented arrow indicates the inhibitory manner. The latter assay was performed by Katja Stefan.

4.1.3. Inhibition of P-gp-mediated Transport of Calcein AM

The synthesized compounds were also evaluated with regard to inhibition of P-gp and BCRP. Figure 4.6 summarizes the screening results for inhibition of P-gp-mediated calcein AM transport. The assay was performed as described in section 6.2.4.2. Table 4.5 gives the obtained biological results. Compounds showing more than 25% inhibition compared to the standard inhibitor were further characterized with respect to their inhibitory power (IC_{50}; Table 4.5). Compounds below 25% were not further characterized since their estimated IC_{50} equals 25 μmol · L^{-1} or higher.

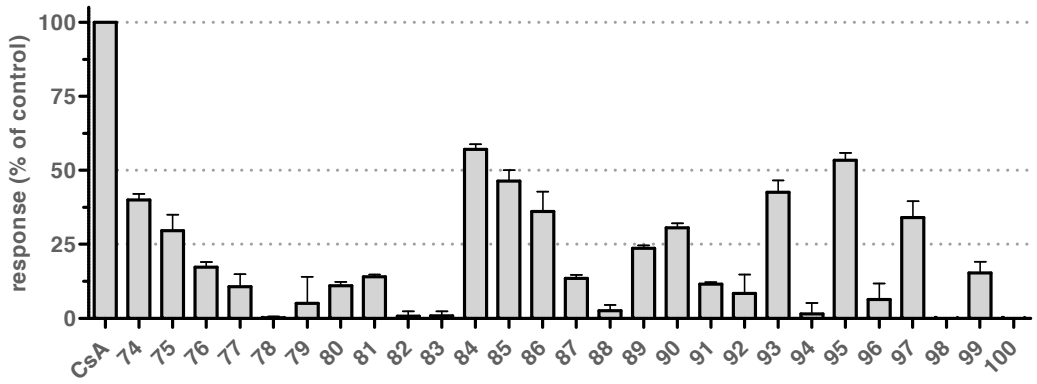

Figure 4.6. Summary of P-gp screening data obtained in the calcein AM assay using A2780/ADR cells. The I_{max} values of the compounds at 10 μmol · L^{-1} is compared to full inhibition caused by the standard inhibitor cyclosporine A (CsA) at 10 μmol · L^{-1}. The dashed lines represent the 25, 50 and 100% boundaries. Shown are at least three independent experiments with duplicate measurements.

As one can see, the obtained IC_{50} values ranged mostly in double-digit micromolar range. The most potent P-gp inhibitors were compounds **74**, **84**-**85**, **93** and **95**, all reaching around 40-70% inhibition at 10 μmol · L^{-1} compared to cyclosporine A at the same concentration. Though, these compounds were still 50- (**74**), 23- (**84**), 20- (**85**), 9.1- (**93**) and 11-fold (**95**) more potent toward MRP1 than P-gp (see Tables 4.1-3 and 4.5 as well as section 6.3.5). The other evaluated compounds can be considered as rather selective. In contrast to the standard inhibitor **74**, the equally potent MRP1 inhibitor **92** had no affinity toward P-gp.

Table 4.5. Summary of P-gp screening results (I_{max} at 10 μmol · L^{-1}, IC_{50} and pIC_{50}) obtained in the calcein AM assay using A2780/ADR cells; n.d. = not determined due to lack of inhibitory activity ($I_{max} \leq 25\%$). The IC_{50} values were determined by fitting the resultant concentration-effect curve to the top value of the standard inhibitor cyclosporine A using the statistically preferred parameter model (see section 6.3.2.2). The compounds were constrained to the top value resulting from the concentration-effect curve of cyclosporine A.

no.	calcein AM I_{max} [%] ± SEM	calcein AM IC_{50} ± SEM [μmol · L^{-1}]	calcein AM pIC_{50} ± SEM	no.	calcein AM I_{max} [%] ± SEM	calcein AM IC_{50} ± SEM [μmol · L^{-1}]	calcein AM pIC_{50} ± SEM
74	40.0 ± 1.2	18.6 ± 1.5	4.733 ± 0.053	**88**	2.6 ± 1.1	n.d.	n.d.
75	29.7 ± 3.0	32.0 ± 2.1	4.496 ± 0.043	**89**	23.7 ± 0.6	n.d.	n.d.
76	17.3 ± 1.0	n.d.	n.d.	**90**	30.5 ± 0.9	39.2 ± 6.4	4.412 ± 0.213
77	10.7 ± 2.5	n.d.	n.d.	**91**	11.6 ± 0.3	n.d.	n.d.
78	0.2 ± 0.3	n.d.	n.d.	**92**	8.4 ± 3.7	n.d.	n.d.
79	5.1 ± 5.2	n.d.	n.d.	**93**	42.6 ± 2.3	6.81 ± 0.20	5.167 ± 0.020
80	11.0 ± 0.7	n.d.	n.d.	**94**	1.56 ± 2.1	n.d.	n.d.
81	14.0 ± 0.5	n.d.	n.d.	**95**	53.4 ± 1.4	10.6 ± 0.4	4.977 ± 0.054
82	0.8 ± 0.9	n.d.	n.d.	**96**	9.5 ± 0.1	n.d.	n.d.
83	0.8 ± 0.9	n.d.	n.d.	**97**	34.1 ± 3.1	32.2 ± 1.9	4.493 ± 0.069
84	57.1 ± 1.0	19.1 ± 1.0	4.719 ± 0.035	**98**	-1.4 ± 2.4	n.d.	n.d.
85	46.4 ± 2.1	21.6 ± 1.0	4.667 ± 0.030	**99**	15.3 ± 2.2	n.d.	n.d.
86	36.1 ± 3.9	28.0 ± 2.7	4.555 ± 0.063	**100**	-3.2 ± 0.1	n.d.	n.d.
87	13.5 ± 0.7	n.d.	n.d.				

Figure 4.7 A shows that the determined I_{max} of the screening is coherent with the determined pIC_{50} value of the compounds that reached over 25% inhibition compared to the standard inhibitor of P-gp, cyclosporine A, except for compound **93**. This makes this method valid for initial compound evaluation. Concomitant to MRP1, the inhibitory property of the compounds correlated strongly with the calculated logP value (Figure 4.7 B) and molecular weight (Figure 4.7 C).

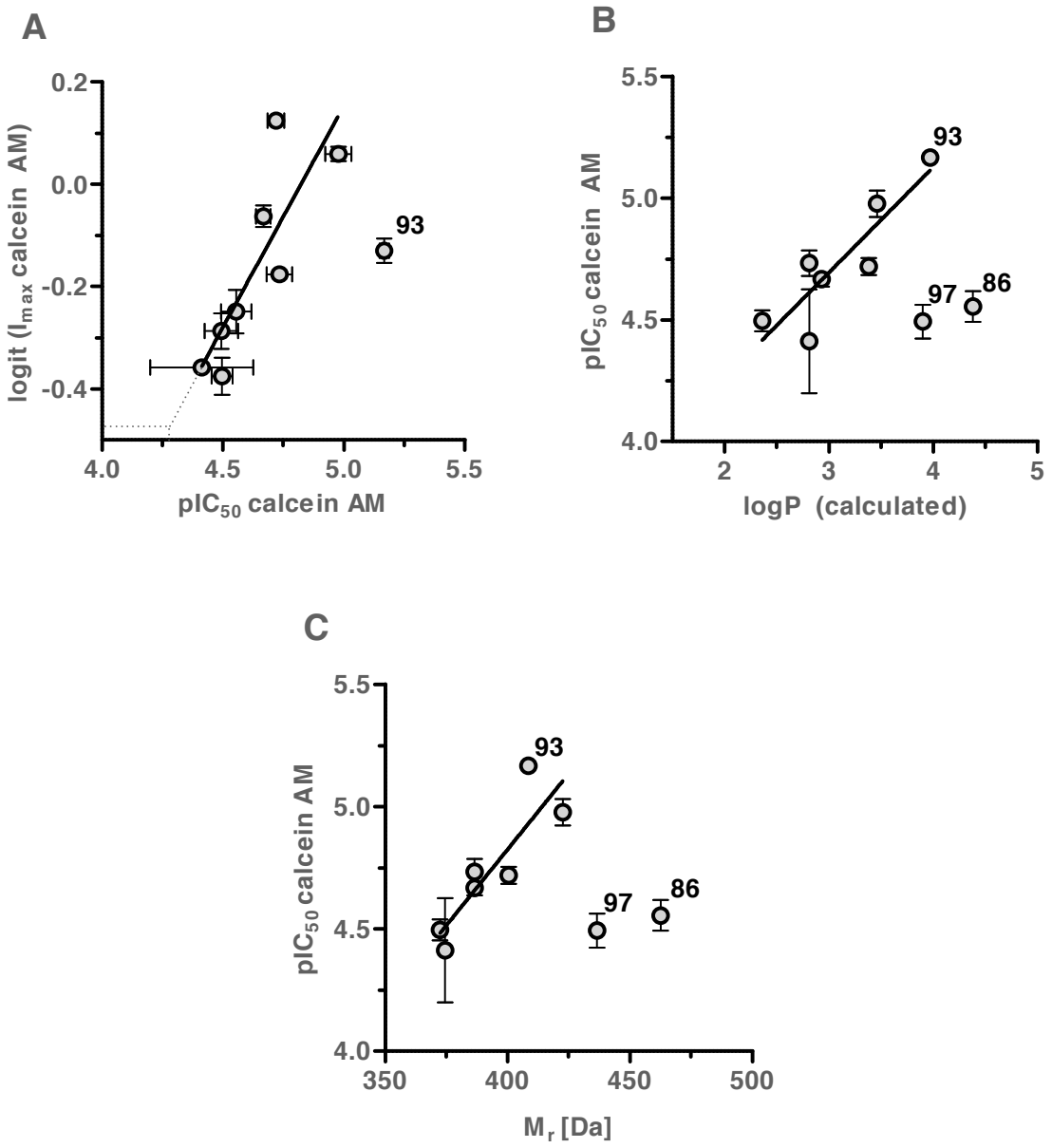

Figure 4.7. (A): Correlation of inhibitory activity obtained in the calcein AM assay (pIC_{50}) and the logit (see section 6.3.2.3) of the maximal inhibition level (I_{max}) of the screening of compounds at 10 μmol · L^{-1} that reached more than 25% maximal inhibition (**74**-**75**, **84**-**86**, **90**, **93**, **95**, **97**); the dashed lines indicate the extrapolated pIC_{50} value of compounds with a maximum inhibition level of 25% or less ($pIC_{50} \leq 4.3$). (B): Plot of the determined pIC_{50} and calculated logP values. (C): Correlation of the determined pIC_{50} value and molecular weight.

Compound **93** with its phenyl substituent at position 7 represents an outlier, since its determined inhibitory activity toward P-gp was better than the maximum inhibition at 10 μmol · L^{-1} suggested. As already found for MRP1, an increase of the logP (3.5-4) as well as molecular weight (400-420 Da) is also beneficial for P-gp inhibition. This was shown before for specific P-gp inhibitors.[282] But as compounds **86** and **97** indicate, this relationship is limited as these two compounds do not fit into this pattern. The reason might be less

related to the partition coefficient but more to the binding pocket(s) and its steric demands. Another possibility is that a logP of 4 and a molecular weight of 400 conform a local maximum. Another uncertainty of this postulation is the small range of the values: since there was only one order of magnitude difference in the activity data and the inhibitory activity was generally low (between 10-40 μmol · L^{-1}), the interpretation should be handled with care.

4.1.4. Inhibition of BCRP-mediated Transport of Pheophorbide A

The synthesized compounds were also evaluated with respect to BCRP inhibition, as described in the experimental section (6.2.4.4). This assay was performed by Katja Stefan. Figure 4.8 visualizes the screening results of the compound at 10 μmol · L^{-1}. Table 4.6 shows the obtained biological data.

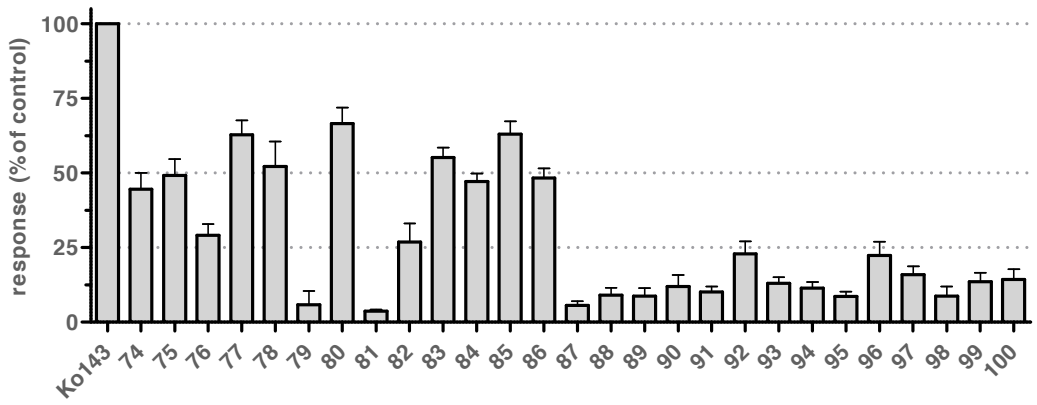

Figure 4.8. Summary of BCRP screening results obtained in the pheophorbide A assay using MDCK II BCRP cells. The I_{max} value of the compounds at 10 μmol · L^{-1} is compared to full inhibition caused by the standard compound Ko143 at 10 μmol · L^{-1}. The dashed lines represent the 25, 50 and 100% boundaries. Shown are at least three independent experiments with duplicate measurements.

Generally, the 7,8-alicyclic-9-deazapurines had moderately good affinity to BCRP. Compounds **74**-**75**, **77**-**78**, **80**, and **83**-**86** reached around 50% or more in the screening at 10 μmol · L^{-1} and showed all inhibitory activity in the single-digit micromolar range. The best MRP1 inhibitors of this set, compounds **74**-**75** and **84**, were still 22-, 12-, and 12-fold more potent against MRP1 than BCRP (see Tables 4.1-2 and 4.6 as well as section 6.3.5). Two compounds, **78** and **83** had more affinity to BCRP than MRP1 (1.2-fold and 1.8-fold, respectively). They represent two moderately good dual inhibitors. The 7-*N*-alkyl, -aryl-, or -arylalkyl-9-deazapurines had no noteworthy affinity to BCRP. The best compound of this thesis, **92**, showed to be a very selective MRP1 inhibitor.

Table 4.6. Summary of BCRP screening results (I_{max} at 10 μmol · L^{-1}, IC_{50} and pIC_{50}) obtained in the pheophorbide A assay using MDCK II BCRP cells; n.d. = not determined due to lack of inhibitory activity ($I_{max} \leq 25\%$). The IC_{50} values were determined by fitting the resultant concentration-effect curve to the top value of the standard inhibitor Ko143 using the statistically preferred parameter model (see section 6.3.2.2).

no.	pheophorbide A I_{max} [%] ± SEM	pheophorbide A IC_{50} ± SEM [μmol · L^{-1}]	pheophorbide A pIC_{50} ± SEM	no.	pheophorbide A I_{max} [%] ± SEM	pheophorbide A IC_{50} ± SEM [μmol · L^{-1}]
74	44.6 ± 5.4	8.06 ± 0.84	5.096 ± 0.069	**88**	9.0 ± 2.5	n.d.
75	49.1 ± 5.5	8.11 ± 0.74	5.093 ± 0.060	**89**	8.7 ± 2.6	n.d.
76	29.1 ± 3.8	14.3 ± 0.7	4.846 ± 0.031	**90**	11.9 ± 3.9	n.d.
77	62.8 ± 4.8	5.80 ± 0.56	5.238 ± 0.063	**91**	10.1 ± 1.8	n.d.
78	52.2 ± 8.3	4.24 ± 0.21	5.374 ± 0.033	**92**	22.8 ± 4.2	n.d.
79	5.8 ± 4.6	n.d.	n.d.	**93**	13.0 ± 2.1	n.d.
80	66.6 ± 5.3	6.01 ± 0.49	5.223 ± 0.053	**94**	11.4 ± 2.0	n.d.
81	3.6 ± 0.5	n.d.	n.d.	**95**	8.6 ± 1.5	n.d.
82	26.9 ± 6.2	15.6 ± 1.3	4.808 ± 0.057	**96**	22.3 ± 4.8	n.d.
83	55.2 ± 3.4	7.66 ± 0.65	5.118 ± 0.056	**97**	15.9 ± 2.8	n.d.
84	47.2 ± 2.7	9.91 ± 0.45	5.005 ± 0.030	**98**	8.7 ± 3.2	n.d.
85	63.0 ± 4.3	4.66 ± 0.33	5.333 ± 0.046	**99**	13.4 ± 3.1	n.d.
86	48.4 ± 3.2	8.70 ± 0.32	5.061 ± 0.024	**100**	14.3 ± 3.6	n.d.
87	5.6 ± 1.4	n.d	n.d			

As for P-gp, the biological data of the pheophorbide A assay was plotted against the I_{max} of the screening data (Figure 4.9 A). This data correlated strongly. Compound **78** seems to be an outlier, but still fits into the correlation line (with **78**: $R^2 = 0.75$; without **78**: $R^2 = 0.91$). Furthermore, the data was correlated with respect to the calculated logP value (Figure 4.9 B) and molecular weight of the compounds (Figure 4.9 C).

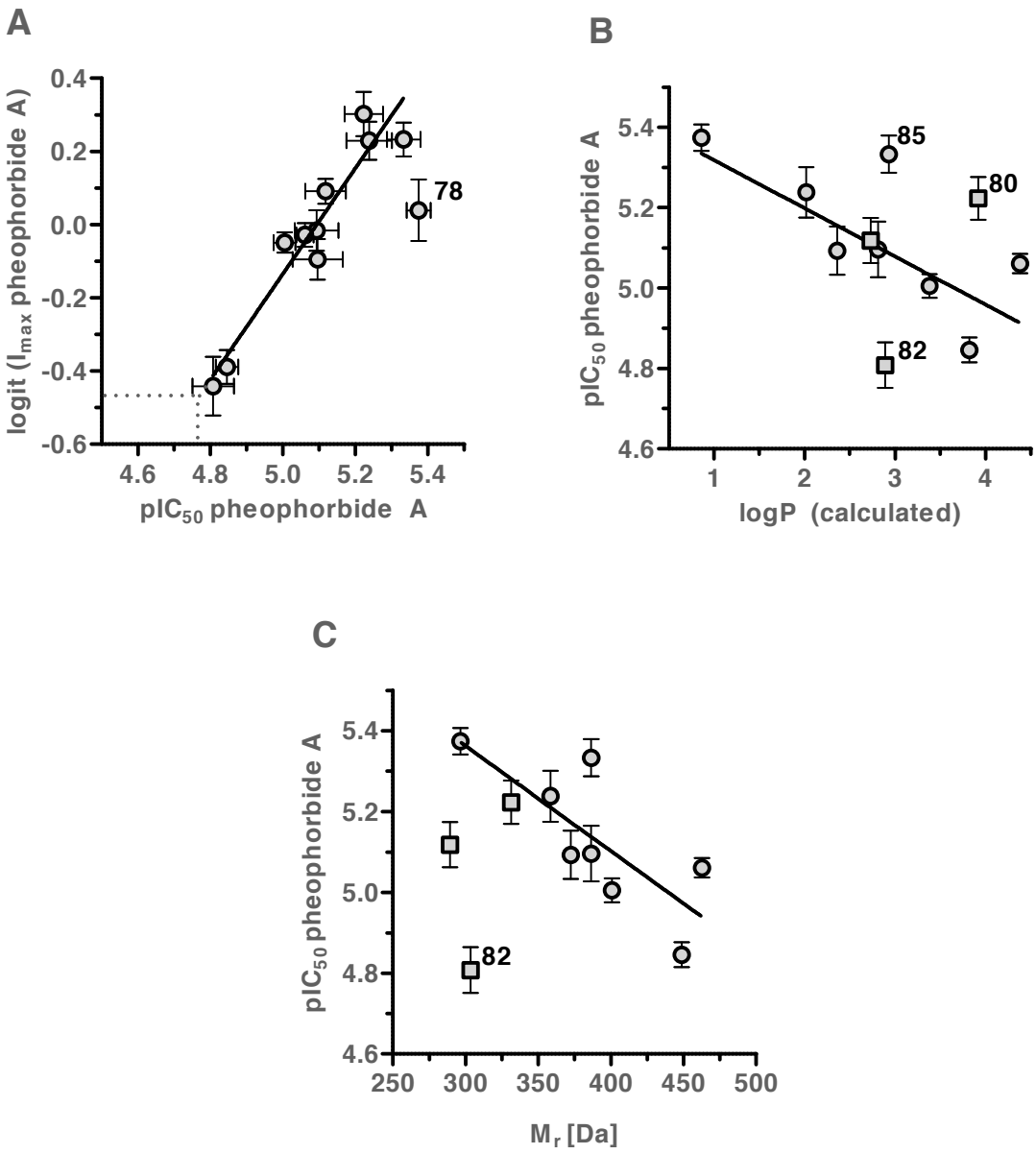

Figure 4.9. (A): Correlation of inhibitory data obtained in the pheophorbide A assay (pIC_{50}) and the logit (see section 6.3.2.3) of the maximal inhibition level (I_{max}) of the screening of compounds showing more than 25% maximal inhibition (**74-78**, **80**, **82-86**); the dashed lines indicate the extrapolated pIC_{50} value of compounds with a maximum inhibition level of 25% or less ($pIC_{50} \leq 4.8$). (B): Correlation between the pIC_{50} and calculated logP values of piperazine-bearing compounds (open circles) or non-piperazine-bearing compounds (open squares). (C): Plot of the pIC_{50} values and their molecular weight.

While no correlation could be observed with respect to pIC_{50} versus logP for the non-piperazine-bearing structures (**80**, **82-83**), the piperazine derivatives **74-78** and **84-86** showed correlations between pIC_{50} values and calculated logP or molecular weight. In constrast to P-gp, the data is inversely proportional to these descriptors. The bigger the molecules and the higher their logP, the less active are the compounds referred to BCRP

inhibition. But as already stated for P-gp, the range of the data set with respect to inhibitory activity is rather limited.

4.1.5. Determination of Intrinsic Toxicity of Selected Compounds

A MTT-based viability assay was employed for compound evaluation as described in section 6.2.4.5. This was performed by Katja Stefan. Representatives from each structural class – (i) 6-piperazinyl-7,8-cyclohexyl- (**74, 79**), (ii) 6-amino-7,8-cyclohexyl- (**80**), (iii) 6-piperazinyl-7-*N*-alkyl- (**92**) and (iv) 6-piperazinyl-7-*N*-aryl-9-deazapurines (**93**) - were evaluated with respect to their intrinsic toxicity. The impact of the compounds at 10 μmol · L^{-1} on H69AR cells over 72 hours was measured (Figure 4.10). Table 4.7 shows the half-maximal growth inhibition concentration (GI_{50}) as well as the residual viability (V_{res}) at 10 μmol · L^{-1} compound concentration and the therapeutic ratio calculated using the data obtained in the daunorubicin assay (see Tables 4.1 and 4.3)

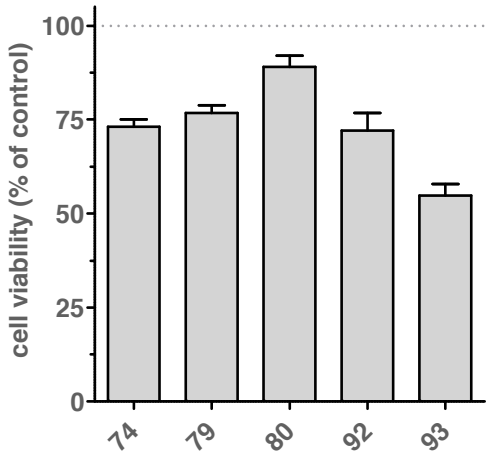

Figure 4.10. Evaluation of the toxicity of compounds **74**, **79**-**80** and **92**-**93** using a MTT-viability assay. The negative control was regular cell growth in pure cell culture medium without further supplementation and was defined as 100% (grey dashed line). The positive control was DMSO at 10%, defining 0% cell viability. The compounds were used at 10 μmol · L^{-1}. Shown are at least three independent experiments with duplicate measurements.

Table 4.7. Summary of the cell viability data using H69AR cells conformed by the value of residual viability (V_{res} at 10 μmol · L^{-1}) after 72 hours of exposure, half-maximal growth inhibition concentration (GI_{50}) as well as the negative decadic logarithm of the GI_{50} (pGI_{50}) and the therapeutic ratio (tr) calculated from the IC_{50} value obtained in the daunorubicin assay which is also depicted in the Table (see section 6.3.6).

no.	V_{res} [%] ± SEM	GI_{50} ± SEM [μmol · L^{-1}]	pGI_{50} ± SEM	IC_{50} ± SEM [µmol · L^{-1}] daunorubicin	tr
74	73.1 ± 1.9	37.7 ± 5.0	4.428 ± 0.087	0.195 ± 0.012	193
79	76.8 ± 2.1	42.9 ± 5.5	4.370 ± 0.069	10.8 ± 0.2	3.97
80	89.1 ± 2.9	127 ± 14	3.898 ± 0.074	2.82 ± 0.18	45.0
92	72.1 ± 4.7	35.8 ± 2.1	4.447 ± 0.038	0.199 ± 0.014	180
93	54.7 ± 3.1	22.4 ± 4.0	4.657 ± 0.116	0.340 ± 0.004	65.9

Except for compound **93**, which resulted in diminished cell growth (V_{res} = 54.7%), the compounds were nontoxic. These results are reflected in the half-maximal growth inhibition values (GI_{50}). Even the most toxic compound **93** had a GI_{50} value of more than 20 μmol · L^{1}. The standard compound **74** and the *N*-alkyl derivative **92** had a therapeutic ratio of nearly 200. This makes them good candidates for *in vivo* evaluation. This applies most notably to compound **92**, which had no significant affinity toward the other two tested transport proteins, P-gp and BCRP.

4.1.6. MDR Reversal-efficacy of Selected Compounds

The most important *in vitro* evaluation of chemosensitizers is their ability to restore sensitivity of MDR-conferring cell lines. Selected compounds – (i) 6-piperazinyl-7,8-cyclohexyl- (**74, 79**), (ii) 6-amino-7,8-cyclohexyl- (**80**), (iii) 6-piperazine-7-*N*-alkyl- (**92**) and (iv) 6-piperazine-7-*N*-aryl-9-deazapurines (**93**) – were tested with respect to their capability to reverse daunorubicin resistance in H69AR cells. The same MTT-viability assay was employed as stated above (see section 6.2.4.6). This was performed by Katja Stefan. Tables 4.8 A-B summarize the results.

Table 4.8 A. MDR reversal-efficacy data obtained for compounds **74**, **79**-**80**, and **92**-**93**. The GI_{50} values of daunorubicin tested in the resistant and the sensitive cell lines H69AR and H69 without compound were compared to the GI_{50} values of daunorubicin in combination with 1, 5 and 10 μmol · L^{-1} of the corresponding compound.

no.	resistant cells GI_{50} ± SEM [μmol · L^{-1}]	1 μM GI_{50} ± SEM [μmol · L^{-1}]	5 μM GI_{50} ± SEM [μmol · L^{-1}]	10 μM GI_{50} ± SEM [μmol · L^{-1}]	sensitive cells GI_{50} ± SEM [μmol · L^{-1}]
74		0.879 ± 0.220	0.611 ± 0.124	0.362 ± 0.068	
79		2.89 ± 0.39	2.44 ± 0.29	1.80 ± 0.24	
80	2.75 ± 0.15	2.33 ± 0.44	0.747 ± 0.055	0.446 ± 0.041	0.361 ± 0.016
92		0.807 ± 0.128	0.566 ± 0.111	0.384 ± 0.065	
93		0.745 ± 0.166	0.508 ± 0.115	0.375 ± 0.075	

Table 4.8 B. Negative decadic logarithm of the GI_{50} values of compounds **74**, **79**-**80**, and **92**-**93** taken from Table 4.8 A.

no.	resistant cells pGI_{50} ± SEM	1 μM pGI_{50} ± SEM	5 μM pGI_{50} ± SEM	10 μM pGI_{50} ± SEM	sensitive cells pGI_{50} ± SEM
74		6.069 ± 0.162	6.223 ± 0.132	6.449 ± 0.123	
79		5.543 ± 0.088	5.615 ± 0.079	5.750 ± 0.087	
80	5.563 ± 0.035	5.641 ± 0.124	6.128 ± 0.049	6.353 ± 0.061	6.444 ± 0.029
92		6.099 ± 0.104	6.255 ± 0.128	6.421 ± 0.111	
93		6.139 ± 0.145	6.305 ± 0.147	6.436 ± 0.131	

As can be seen from Table 4.8 A-B, the resistance against daunorubicin is gradually reversed with increased concentration of the compounds. The potency ranking of the compounds determined in the calcein AM and daunorubicin assay (Tables 4.1 and 4.3) is related to efficacy of reversal (e.g. **74** vs. **79**). The concentration-effect curves of compound **92** as the best, most selective and nontoxic compound are depicted in Figure 4.11. The concentration-effect curve of daunorubicin gets shifted to the left, which is an indicator that the cells get sensitized toward this cytotoxic agent.

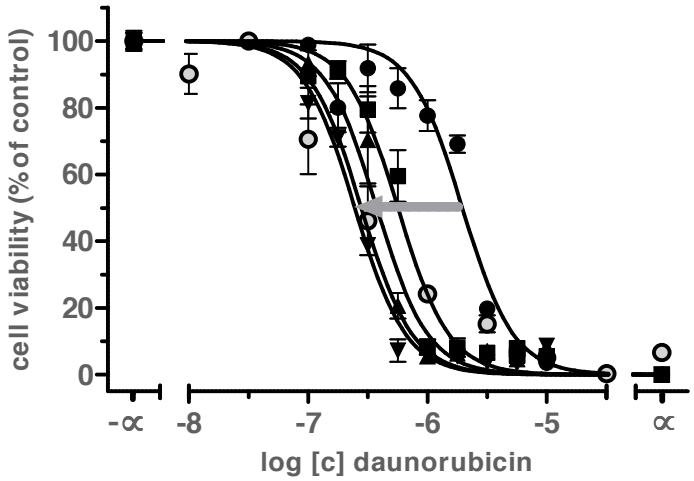

Figure 4.11. Sensitization of H69AR cells by compound **92** determined in the MDR reversal-efficacy assay. The shift of the concentration-effect curve from the resistant (closed circles) to the sensitive (open circles) cells is indicated by the grey arrow. Compound **92** was used at concentrations of 1 (closed square), 5 (closed upward triangle) and 10 μmol · L^{-1} (closed downward triangle).

Plotting of the negative decadic logarithm of the GI_{50} values of daunorubicin with or without compound addition and the logarithmic compound concentration resulted in a sigmoidal relation (Figure 4.12). The top and bottom values were fixed to the values obtained for the sensitive (H69) and resistant (H69AR) cancer cells that are shown in Table 4.8 B. The derived half-maximal effect concentration (EC_{50}) is a measure for the compound efficacy. While the GI_{50} as determined in Table 4.8 is related to the daunorubicin concentration-effect curve, the calculated EC_{50} in the new plot (Figure 4.12) is related to the tested compound. It gives the concentration of the compound at which resistance is reduced by 50% with respect to the used cytostatic agent (daunorubicin). The lower the value, the better the MDR reversing property of the compound. Table 4.9 summarizes the calculated EC_{50} values.

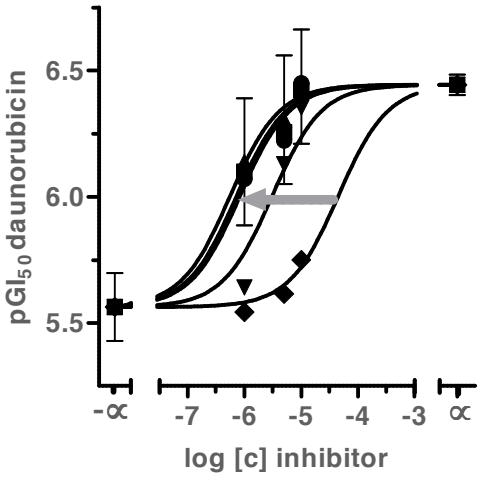

Figure 4.12. Evaluation of the efficacy of compounds **74** (closed circles), **79** (closed rhombs) **80** (closed downward triangles), **92** (closed squares) and **93** (closed upward triangles) using a MTT-based MDR reversal-efficacy assay. On the ordinate the determined pGI_{50} values are plotted. On the abscissa the used compound concentrations are presented. Each resultant curve is calculated from 5 data points and fixed to the data of the resistant (H69AR, -∝, bottom) and sensitive cell line (H69, ∝, top). Shown is EC_{50} of at least three independent experiments with duplicate measurements.

Table 4.9. MDR reversal-efficacy data obtained for compounds **74**, **79**-**80**, and **92**-**93**. Shown is EC_{50} and pEC_{50} of at least three independent experiments with duplicate measurements.

no.	H69 AR EC_{50} ± SEM [μmol · L^{-1}]	H69 AR pEC_{50} ± SEM
74	0.741 ± 0.229	6.150 ± 0.199
79	99.8 ± 74.4	4.097 ± 0.759
80	3.01 ± 0.65	5.531 ± 0.141
92	0.831 ± 0.445	6.135 ± 0.331
93	0.575 ± 0.419	6.333 ± 0.430

Although the relationship should be interpreted with caution due to the number of data points, one can see the difference between a less potent compound (**79**), a moderately potent compound (**80**) and very potent compounds (**74**, **92** and **93**). The obtained EC_{50} values and the IC_{50} values of the calcein AM and daunorubicin assay correlated strongly, making the latter two assays very good surrogates for the real effectiveness of a compound with respect to reversal of MDR (Figures 4.13 A-B). The slope of the linear regression line is 0.79 ± 0.18 in Figure 4.13 A. Taking the deviation into account, it can be concluded that the calcein AM assay gives an adequate evaluation with respect to MRP1 inhibition and MDR reversal. Furthermore, not only the efficacy is correctly mirrored in the results, but also the direct connection of MRP1 inhibition and MDR reversal. Figure 4.13 B shows the same for the

daunorubicin assay (slope = 0.85 ± 0.16). The R^2 values of the data sets are 0.86 and 0.90, respectively.

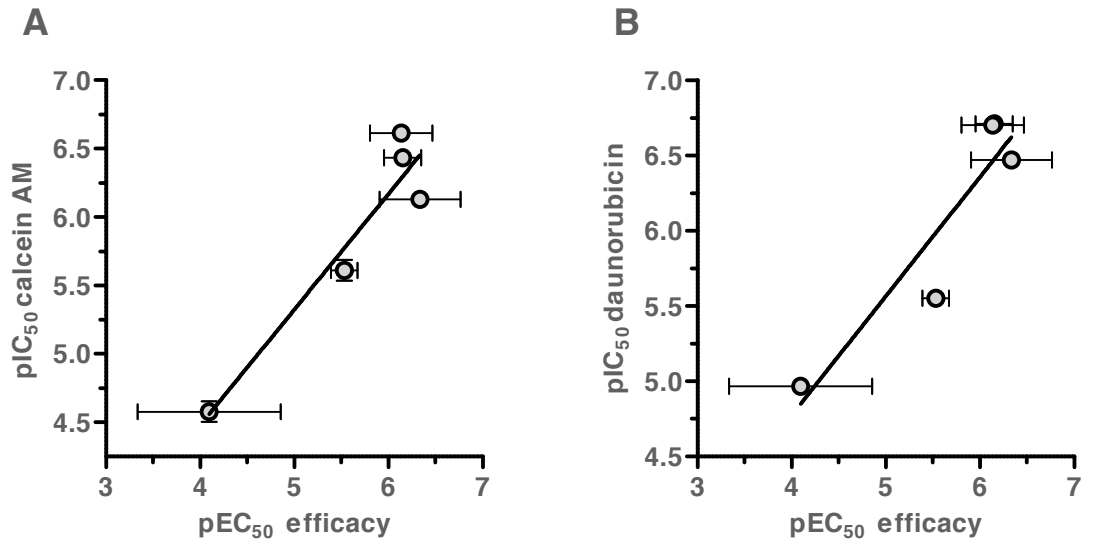

Figure 4.13. Correlation between the pEC_{50} values of compounds **74**, **79**-**80**, **92**-**93** as shown in Table 4.9 and the pIC_{50} values obtained in the calcein AM (A) and daunorubicin assay (B). Left graphic: slope = 0.79 ± 0.18, R^2 = 0.86. Right graphic: slope = 0.85 ± 0.16, R^2 = 0.90.

4.1.7. Summary of Evaluation of 7,8-alicyclic-, 7-*N*-alkyl-, -aryl- or -arylalky-9-deazapurines

In this subchapter a variety of 9-deazapurines with variations at positions 6, 7 and 8 have been synthesized and biologically evaluated in two different cell-based fluorescence assays, the calcein AM and daunorubicin assay. With respect to MRP1 inhibition, it was shown that the phenethylpiperazine residue at position 6 is superior to other side chains, and that shortening of the side chain is not beneficial for activity against MRP1. Piperazine-bearing compounds were superior in comparison to their amine-bearing counterparts. Additionally, it could be shown that the cyclohexyl residue at position 7 and 8 of the starting compound **74**, which was used as standard inhibitor of MRP1, could be replaced by other aliphatic side chains. Especially the cyclopropyl residue at position 7 of compound **92** seemed equally beneficial compared to the cyclohexyl residue, while position 8 has not to be occupied by a substituent for potent MRP1 inhibition.

In different subsets, a correlation could be observed between the inhibitory activity and the calculated logP values of the compounds as well as their molecular weight. Obviously bigger (molecular weight around 370 Da) and more lipophilic molecules (logP around 3 for piperazine-bearing compounds) are preferred with respect to MRP1 inhibition.

Some compounds had affinity toward P-gp (**74**, **84**-**85**, **93** and **95**), which is clear since this compound class was already reported to provide dual inhibitors of MRP1 and P-gp.[271] Their IC_{50} ranged from about 7-21 μmol · L^{-1}. The same tendency as for MRP1 could be observed with regard to logP and molecular weight.

Furthermore, some compounds were also BCRP inhibitors (**74**-**75**, **77**-**78**, **79**, and **83**-**86**), with IC_{50} values ranging from about 8-16 μmol · L^{-1}. This is a new fact, since this compound class has never been reported before to inhibit BCRP. In contrast to MRP1 and P-gp, inhibitory activities were better with decreased logP and molecular weight.

While the standard inhibitor **74** is a rather unselective MRP1 inhibitor, the equally potent compound **92** had no noteworthy affinity toward the other two transport proteins, P-gp and BCRP.

Representative compounds of the first compound set were shown to have only a slight influence on cell viability. Standard inhibitor **74** and the best compound in this set, no. **92**, had therapeutic ratios of 180 and more. The same compound set was analyzed with respect to MDR reversal. Here, the two best compounds, **74** and **92**, were shown to completely reverse MDR in H69AR lung cancer cells.

Compound **74** as a representative of the first compound set was analyzed with regard to its inhibition type and showed to be a noncompetitive inhibitor of calcein AM and daunorubicin

transport. Furthermore, it could be proved that the inhibitory activities obtained in both assay equal with nearly a slope of 1. Additionally, the same applied for the MDR reversal-efficacy and the calcein AM as well as the daunorubicin assay. Since these assays give comparable results, the latter a two are good surrogates for the former.

4.2. Evaluation of 7-*N*-alkyl, -aryl- or -arylalkyl- and 6-aminoarylalkyl-9-deazapurines as well as 6-piperazinyl-purine Analogs

4.2.1. Inhibition of MRP1-mediated Transport of Calcein AM and Daunorubicin

4.2.1.1. 9-Deazapurine Derivatives

In order to generate more new, potent and selective inhibitors of MRP1, 6-aminoarylalkyl-9-deazapurines with variations at position 7 and 6-piperazinyl-purine analogs were synthesized and evaluated with respect to their inhibitory power against MRP1, but also P-gp and BCRP. The compounds and activities presented in this subchapter have already been published.[350] Table 4.10 summarizes the molecular formula of the compounds and the inhibitory power in the daunorubicin assay, which was performed by Katja Stefan. Additionally, the calculated logP value as well as the molecular weight of the compounds is listed. These descriptors were plotted against the obtained inhibitory activities (Figures 4.14 A-B).

Table 4.10. Inhibitory activity of 7-*N*-alkyl, -aryl- or -arylalkyl- and 6-aminoarylalkyl-9-deazapurines obtained in the daunorubicin assay (IC_{50} ± SEM and pIC_{50} ± SEM) using H69AR cells. Additionally, the molecular weight as well as the calculated logP value of each compound is depicted.

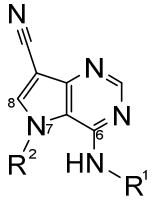

no.	R^1	R^2	M_r [Da]	logP (calc.)	daunorubicin IC_{50} ± SEM [μmol · L^{-1}]	daunorubicin pIC_{50} ± SEM
101	benzyl	methyl	263.30	1.82	16.7 ± 2.5	4.781 ± 0.097
102	benzyl	phenyl	325.38	4.04	3.96 ± 0.40	5.404 ± 0.066
103	benzyl	benzyl	339.40	3.53	7.28 ± 0.85	5.141 ± 0.077
104	phenylpropyl	benzyl	367.46	4.56	0.782 ± 0.081	6.109 ± 0.068
105	phenethyl	phenethyl	367.46	4.53	1.42 ± 0.22	5.852 ± 0.099
106	phenylpropyl	phenethyl	381.48	5.00	0.822 ± 0.051	6.086 ± 0.041

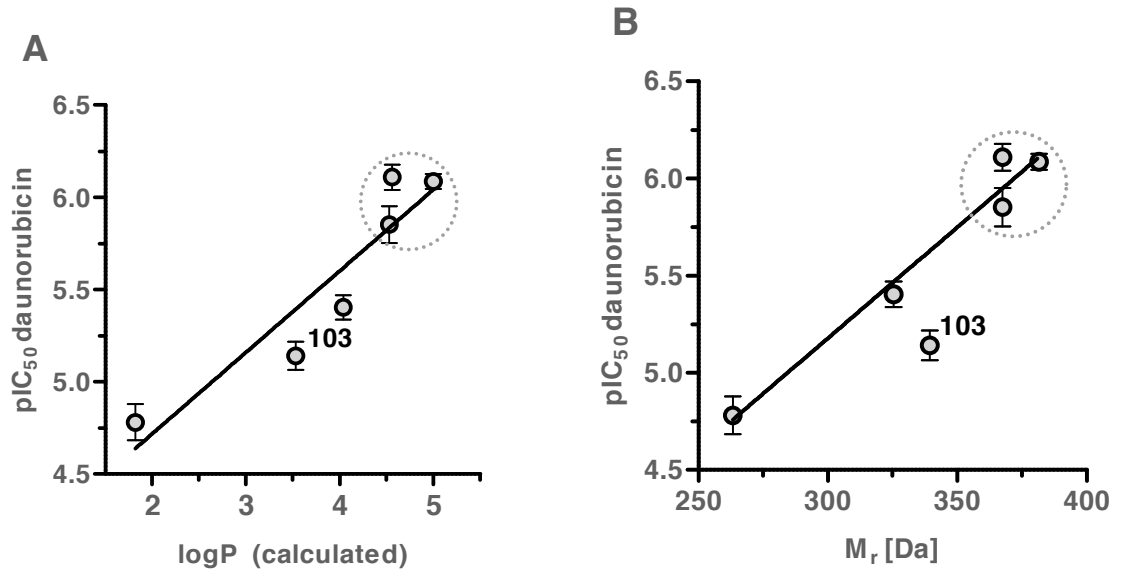

Figure 4.14. Correlation between the inhibitory activity of compounds **101**-**106** toward MRP1 determined in the daunorubicin assay and the calculated logP value (A) and the molecular weight (B) of the compounds. The most potent compounds (**104**-**106**) are characterized by a calculated logP of at least 4.5 and a molecular weight of approximately 370 Da as indicated by the grey dashed circles.

The inhibitory power of the compounds is strongly dependent on the partition coefficient, as this was already found for their 6-piperazinyl-7,8-alicyclic-9-deazapurine counterparts (see subchapter 4.1). The same applies for the correlation to molecular weight, although compound **103** represented an outlier. The inhibitory power of the compounds is rather poor, only compounds over 370 Da or a logP value above 4.5 had an IC_{50} around 1 μmol · L^{-1} (**104**-**106**). But compared to 6-piperazinyl-7,8-alicyclic-9-deazapurines (e.g. compound **74**; logP = 2.81; M_r = 386.50 Da) or 6-piperazinyl-7-*N*-alkyl-9-deazapurines (compound **92**; logP = 1.76; M_r = 372.48 Da), the non-piperazine-bearing structures proved to be inferior with respect to MRP1 inhibition. Their activity is more comparable to the above described non-piperazine-bearing compounds **80**-**83**. Here again, the piperazine plays a crucial role concerning MRP1 inhibition, as already found before (see subchapter 4.1).

4.2.1.2. Purine Analogs

Purine analogs of the 6-piperazinyl-9-deazapurines **74**-**77** were generated to evaluate the inhibitory potential of this compound class. Table 4.11 gives the obtained biological data. As done before for compounds **84**-**87** (see Figures 4.3 A-B), the calculated logP value and the molecular weight of the compounds were correlated. But due to the low inhibitory power and therefore low accuracy of the measurements, the plot is rather inconclusive (Figures 4.15 A-

B). The parabola suggests a logP of more than 2 and a molecular weight of approximately 320-350 Da to be the optimum. These values are lower than the optima of other 9-deazapurines (except for compounds **88**-**92**). This might occur because purines form an own class of MRP1 inhibitors and behave differently with respect to membrane partition, binding pocket(s) or intracellular accumulation.

Table 4.11. Inhibitory activity of 6-piperazinyl-purine derivatives. The data (IC_{50} ± SEM and pIC_{50} ± SEM) was obtained in the daunorubicin assay by Katja Stefan using the H69AR cells. Additionally, the molecular weight as well as the calculated logP value of each compound is depicted. The compounds were constrained to the top value resulting from the concentration-effect curve of compound **74**.

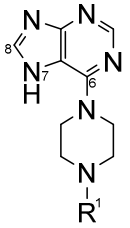

no.	R^1	M_r [Da]	logP (calc.)	daunorubicin IC_{50} ± SEM [μmol · L^{-1}]	daunorubicin pIC_{50} ± SEM
107	phenethyl	308.39	1.97	20.0 ± 0.6	4.699 ± 0.019
108	benzyl	294.36	1.52	22.7 ± 5.2	4.655 ± 0.149
109	benzhydryl	370.46	2.97	18.0 ± 4.5	4.758 ± 0.162
110	phenyl	280.34	1.17	30.5 ± 7.7	4.529 ± 0.164

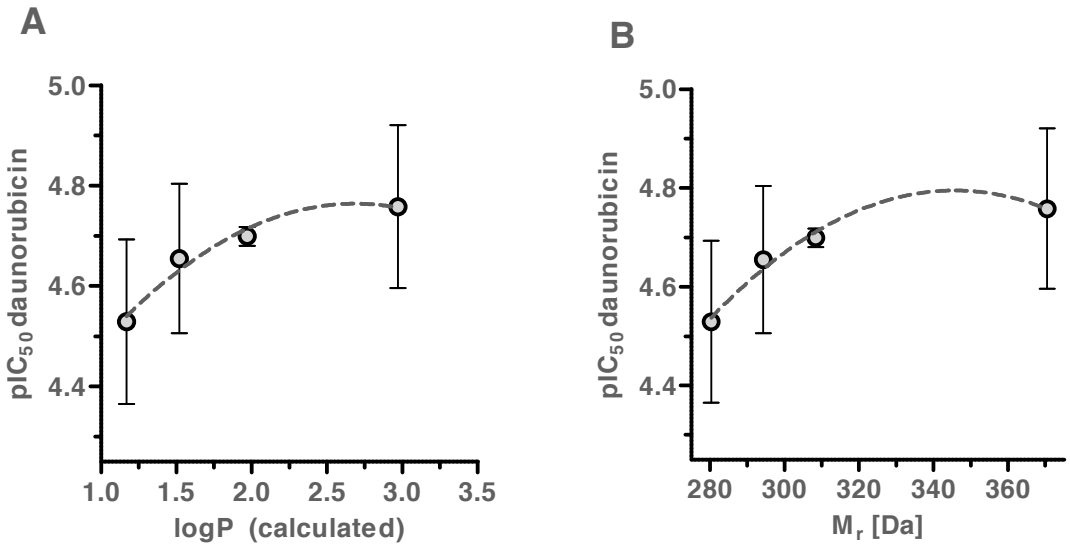

Figure 4.15. Correlation between the inhibitory activity of compounds **107**-**110** obtained in the daunorubicin assay and the calculated logP value (A) as well as molecular weight (B) of the compounds. A dashed grey line is used to underline the high deviation due to the lack of effective inhibitory power.

4.2.2. Activation of MRP1-mediated Transport of Calcein AM and Daunorubicin

A specialty of these 9-deazapurines and purine analogs is their capability to accelerate the transport velocity of calcein AM and daunorubicin mediated by MRP1. This effect was firstly observed for the 6-aminoaryl- and 6-aminoarylalkyl-7,8-cyclohexyl-9-deazapurine analogs **80**-**83** as well as for the 4*H*-piperazine-bearing compound **79** (see Figures 4.16 A-E). The concentration-effect curves show a two-phase progression. First, at low concentrations, calcein AM transport is accelerated (approx. 10 nmol · L^{-1}). Second, the substrate efflux is inhibited at concentrations of 1 μmol · L^{-1} or more. Table 4.12 gives the half-maximal activation concentration (AC_{50}) and the maximal activation level (A_{max}; percentage of basal fluorescence F0) of these compounds in correlation to their IC_{50} and pIC_{50} value as stated in Table 4.1.

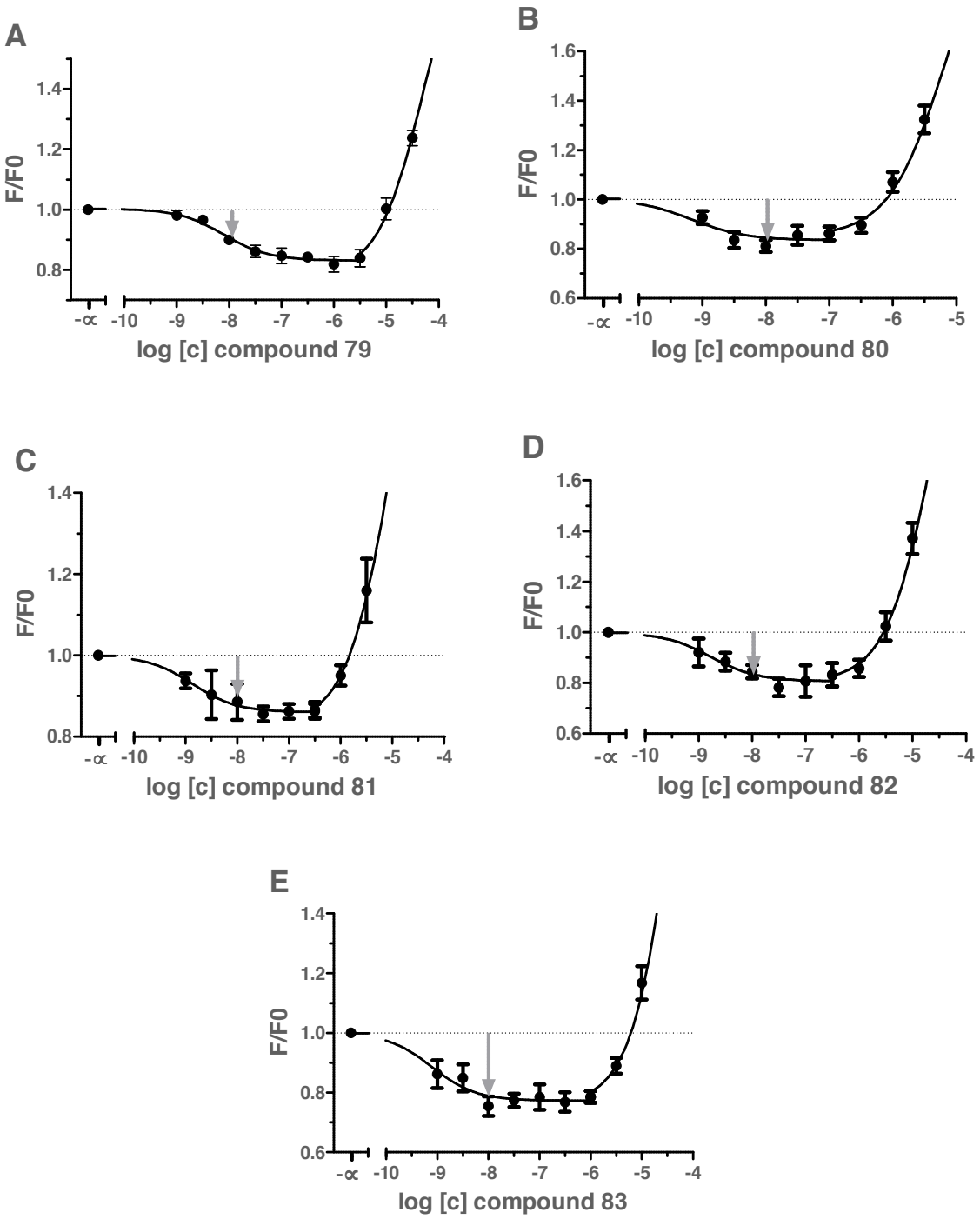

Figure 4.16. Biphasic concentration-effect curves of compounds **79** (A), **80** (B), **81** (C), **82** (D), and **83** (E) determined in the calcein AM assay using H69AR cells. The grey arrow indicates the concentration of 10 nmol · L^{-1} which was used for further evaluation of the compounds **101**-**110**.

Table 4.12. Summary of half-maximal activation concentration (AC_{50}), maximal activation (A_{max}) of compounds **79**-**83** as determined in the calcein AM assay using H69AR cells. Additionally, the IC_{50} values obtained in the calcein AM and daunorubicin assays are depicted as already stated in Table 4.1. The latter assay was performed by Katja Stefan.

no.	calcein AM AC_{50} ± SEM [nmol · L^{-1}]	calcein AM pAC_{50} ± SEM	calcein AM A_{max} [%] of F0	calcein AM IC_{50} ± SEM [μmol · L^{-1}]	calcein AM pIC_{50} ± SEM	daunorubicin IC_{50} ± SEM [μmol · L^{-1}]	daunorubicin pIC_{50} ± SEM
79	9.25 ± 3.19	8.058 ± 0.221	82.7 ± 2.2	26.6 ± 3.0	4.578 ± 0.075	10.8 ± 0.2	4.966 ± 0.015
80	0.479 ± 0.320	9.401 ± 0.401	83.0 ± 2.7	2.46 ± 0.28	5.611 ± 0.076	2.82 ± 0.18	5.550 ± 0.042
81	2.04 ± 1.33	8.768 ± 0.393	84.8 ± 2.3	8.22 ± 0.90	5.088 ± 0.072	4.97 ± 0.27	5.305 ± 0.036
82	1.57 ± 0.36	8.816 ± 0.149	81.0 ± 4.2	14.2 ± 1.2	4.851 ± 0.054	8.72 ± 0.66	5.061 ± 0.050
83	0.772 ± 0.283	9.140 ± 0.234	77.2 ± 2.4	14.1 ± 0.8	4.850 ± 0.037	9.40 ± 0.30	5.027 ± 0.021

Since inhibition and activation are opposing effects, a suitable concentration is needed for a proper evaluation of the activating property of the compounds. A concentration of 10 nmol · L^{-1} was chosen to compare the compounds to each other because it is around 100 times lower than the IC_{50} of the best compound (**104**, ~ 0.8 μmol · L^{-1}.). Figure 4.17 gives the activation ratio (see section 6.3.4.2) of compounds **79**-**83** at 10 nmol · L^{-1}. The value of the ordinate gives the multiple of the basal transport velocity of calcein AM by MRP1 in presence of the corresponding compound. The same mathematical procedure was used for compounds **101**-**110** (Figures 4.18 A-B). The daunorubicin assay data was determined by Katja Stefan.

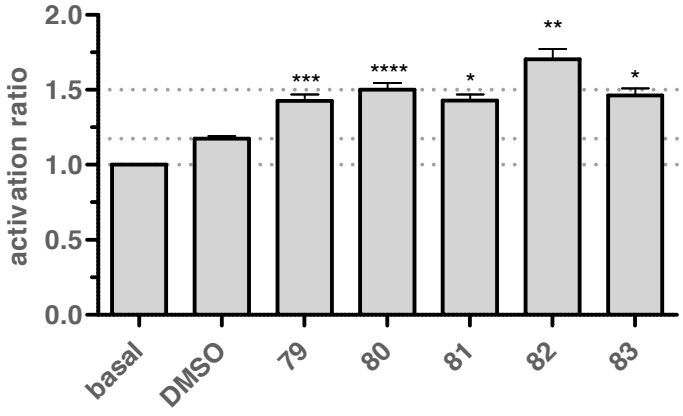

Figure 4.17. Activation ratio (see section 6.3.4.2) of compounds **79**-**83** at 10 nmol · L^{-1} determined in the calcein AM assay using H69 AR cells. The lower grey dashed line indicates the basal pump velocity, which is defined as 1.0; the upper grey dashed line indicates the average accelerating power of the compounds of approximately 1.5. Significance was calculated using one sample *t*-tests (see section 6.3.1.3) and is given as *: $p \leq 0.05$, **: $p \leq 0.01$, ***: $p \leq 0.001$, ****: $p \leq 0.0001$, hypothetical value = effect of DMSO (0.0001%; 1.175; middle grey dashed line).

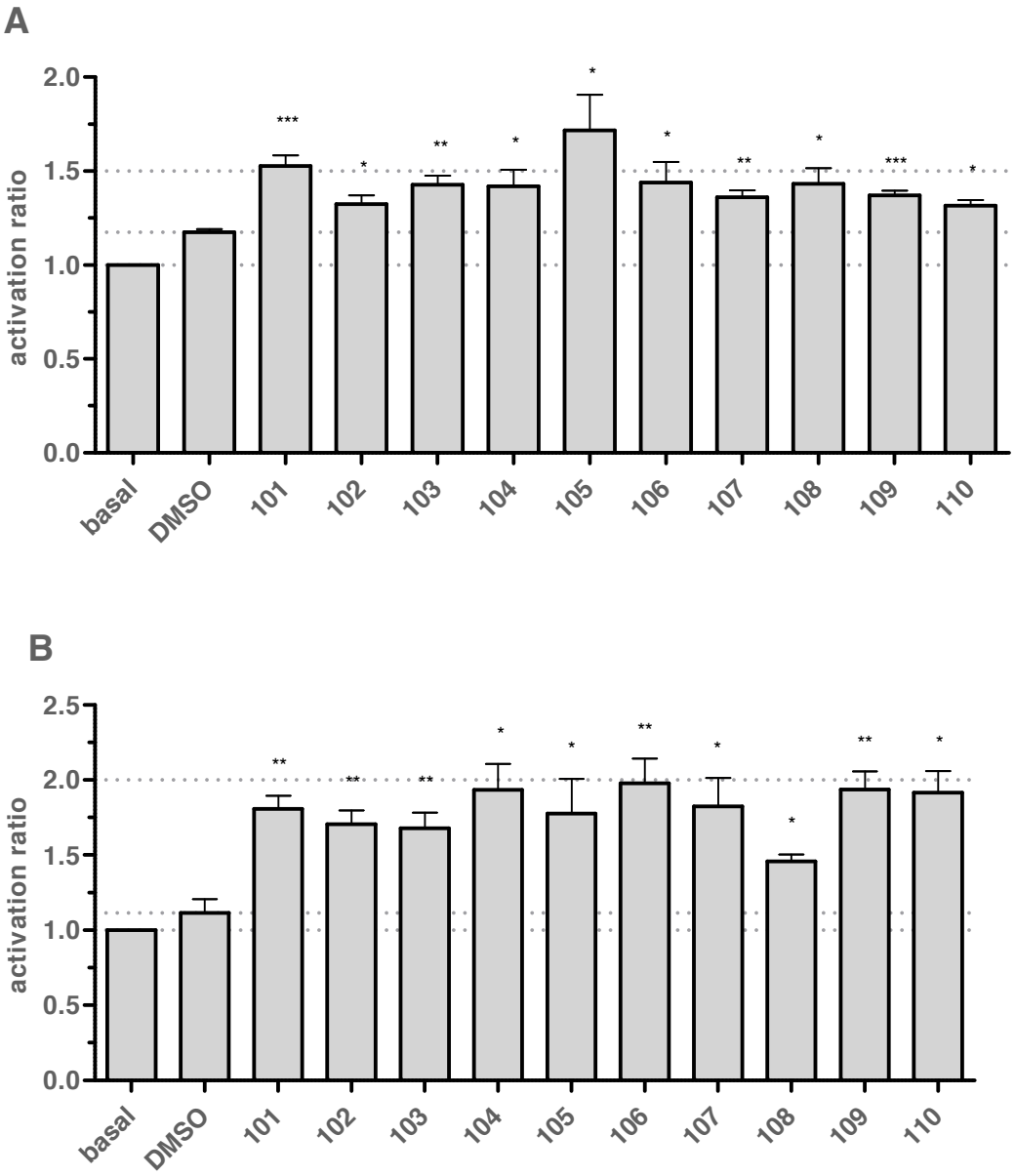

Figures 4.18. Activation ratio (see section 6.3.4.2) of compounds **101**-**110** at 10 nmol · L^{-1}. Basal activity is defined as 1.0 (lower grey dashed line). Shown is mean ± SEM of at least three independent experiments with duplicate measurements. (A): calcein AM assay using the MRP1 overexpressing cell line H69AR. (B): daunorubicin assay using the MRP1 overexpressing cell line MDCK II MRP1. Significance was calculated using one sample *t*-tests (see section 6.1.3.1) and is given as *: $p \leq 0.05$, **: $p \leq 0.01$, ***: $p \leq 0.001$, ****: $p \leq 0.0001$, hypothetical value = effect of DMSO (A: 1.175; B: 1.115), in each case indicated by the middle grey dashed line; upper dashed line indicates the approximate accelerating character of the corresponding compounds.

The calcein AM assay was performed using H69AR cells, while the daunorubicin assay was accomplished with MDCK II MRP1 cells. Since activation was observed in both cell lines, the observed effect is not cell line specific and occurs in selected (H69AR) as well as transfected (MDCK II MRP1) cells. Furthermore, no effect was seen in sensitive cell lines (Figure 14.19 A). The significance of the effect is confirmed by one-sample *t*-test (see section

6.3.1.3), which gave p values of less than 0.05 for all compounds. Tables 4.13 A-B give the activation ratio (A_r) as well as the half-maximal activation concentration (AC_{50}). The latter was determined on the basis of (i) the measured concentration-effect curves (see Figure 4.19 A) as well as on the basis of (ii) the concentration-effect curves resulting from the calculated activation ratio (see Figure 4.19 B; see section 6.3.4.2). The values are very similar, and differ in average only by a factor of 1.2 (calcein AM) and 1.3 (daunorubicin).

Table 4.13 A. Activation ratio (A_r) and half-maximal activation concentration (AC_{50}) on the basis of (i) measured concentration-effect curves and on the basis of (ii) concentration-effect curves derived from calculated activation ratio of compounds **101**-**110** obtained in the calcein AM assay using H69AR cells; n. d. = not determined.

no.	A_r (calcein AM) [fold increase]	$AC_{50\ (measured)}$ (i) (calcein AM) [nmol · L^{-1}]	$pAC_{50\ (measured)}$ (i) (calcein AM)	$AC_{50\ (calculated)}$ (ii) (calcein AM) [nmol · L^{-1}]	$pAC_{50\ (calculated)}$ (ii) (calcein AM)
DMSO	1.175 ± 0.017	n. d.	n. d.	n. d.	n. d.
101	1.527 ± 0.057	0.059 ± 0.004	10.23 ± 0.042	0.074 ± 0.006	10.13 ± 0.049
102	1.324 ± 0.047	0.077 ± 0.004	10.12 ± 0.033	0.093 ± 0.005	10.03 ± 0.037
103	1.428 ± 0.048	0.060 ± 0.005	10.23 ± 0.057	0.064 ± 0.008	10.19 ± 0.08
104	1.420 ± 0.088	0.064 ± 0.003	10.20 ± 0.030	0.093 ± 0.004	10.03 ± 0.08
105	1.717 ± 0.190	0.087 ± 0.016	10.07 ± 0.117	0.101 ± 0.021	10.00 ± 0.134
106	1.439 ± 0.110	0.053 ± 0.003	10.28 ± 0.033	0.062 ± 0.003	10.21 ± 0.027
107	1.362 ± 0.036	0.038 ± 0.001	10.42 ± 0.015	0.041 ± 0.001	10.38 ± 0.015
108	1.433 ± 0.083	0.136 ± 0.009	9.869 ± 0.045	0.169 ± 0.011	9.773 ± 0.041
109	1.371 ± 0.025	0.068 ± 0.004	10.17 ± 0.042	0.079 ± 0.006	10.10 ± 0.049
110	1.315 ± 0.031	0.025 ± 0.006	10.61 ± 0.162	0.028 ± 0.007	10.56 ± 0.162

Table 4.13 B. Activation ratio (A_r) and half-maximal activation concentration (AC_{50}) on the basis of (i) measured concentration-effect curves or on the basis of (ii) concentration-effect curves derived from calculated activation ratio of compounds **101**-**110** obtained in the daunorubicin assay using MDCK II MRP1 cells; n.d. = not determined. The assay was conducted by Katja Stefan.

no.	A_r (daunorubicin) [fold increase]	$AC_{50\ (measured)}$ (i) (daunorubicin) [nmol · L^{-1}]	$pAC_{50\ (measured)}$ (i) (daunorubicin)	$AC_{50\ (calculated)}$ (ii) (daunorubicin) [nmol · L^{-1}]	$pAC_{50\ (calculated)}$ (ii) (daunorubicin)
DMSO	1.115 ± 0.092	n. d.	n. d.	n. d.	n. d.
101	1.808 ± 0.086	0.133 ± 0.056	9.910 ± 0.264	0.182 ± 0.082	9.781 ± 0.283
102	1.705 ± 0.090	0.119 ± 0.047	9.955 ± 0.251	0.151 ± 0.065	9.859 ± 0.274
103	1.678 ± 0.103	0.106 ± 0.033	9.994 ± 0.203	0.149 ± 0.052	9.852 ± 0.223
104	1.934 ± 0.173	0.110 ± 0.040	9.986 ± 0.232	0.139 ± 0.060	9.893 ± 0.270
105	1.777 ± 0.231	0.353 ± 0.146	9.486 ± 0.261	0.355 ± 0.218	9.519 ± 0.372
106	1.979 ± 0.164	0.062 ± 0.002	10.21 ± 0.02	0.089 ± 0.002	10.05 ± 0.02
107	1.823 ± 0.191	0.322 ± 0.139	9.529 ± 0.272	0.567 ± 0.264	9.289 ± 0.291
108	1.457 ± 0.046	0.227 ± 0.050	9.654 ± 0.145	0.311 ± 0.083	9.522 ± 0.173
109	1.937 ± 0.120	0.615 ± 0.647	9.373 ± 0.569	0.757 ± 0.814	9.288 ± 0.578
110	1.916 ± 0.142	0.189 ± 0.068	9.750 ± 0.231	0.210 ± 0.063	9.697 ± 0.193

As one can see, the activation ratio calculated in the calcein AM assay is generally lower than in the daunorubicin assay. This can be explained by the lipophilicity of calcein AM and daunorubicin. The former is a highly lipophilic molecule (see Figure 6.1) that diffuses into the cell through the membrane rather fast. In case of an enhanced efflux of calcein AM, which is a good MRP1 substrate, it can easily diffuse back through the membrane into the cell increasing its intracellular concentration. The intracellular concentration of calcein AM is critical for its hydrolysis by unspecific esterases to the fluorescent dye calcein. Hence, the fluorescence increase is a function of time, transport and diffusion velocity of calcein AM. Since the last parameter is higher with respect to calcein AM than to daunorubicin, the activation ratio determined using former must be lower than for using the latter. Because in contrast to calcein AM, daunorubicin is a more hydrophilic molecule (Figure 1.3) which slowly diffuses into the cell. This is reflected in the incubation time needed to perform the assay (3 hours). Due to higher passive diffusion velocity the intracellular clearance of calcein AM by MRP1 is less effective than for daunorubicin. This explains the difference in the activation ratio of the both assays.

Figures 4.19 A-B show compound **104** as a dual modulator (activation and inhibition). Since no effect was observed using the sensitive MDCK II cells (Figure 4.19 A), it is highly likely that the membrane integrity was not affected by the compounds and the difference in the distribution of calcein AM and daunorubicin is due to real activation.

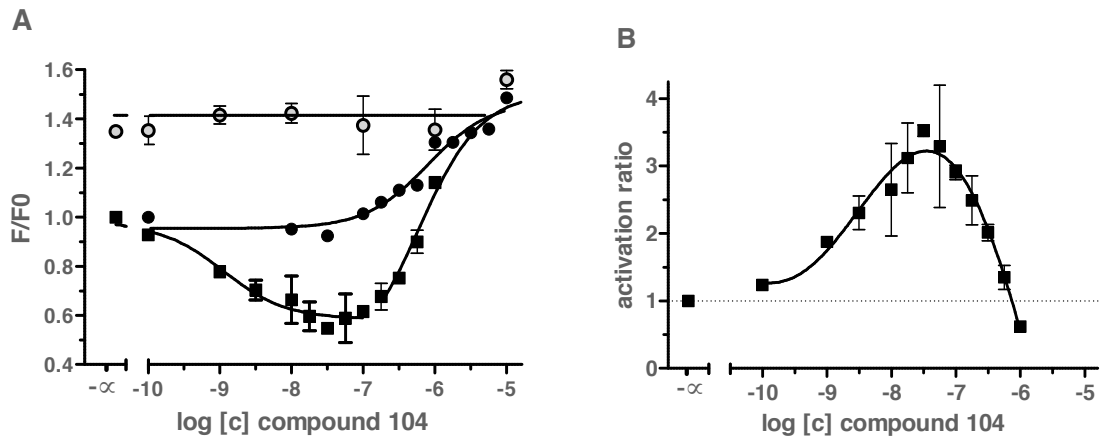

Figure 4.19. (A): compound **104** (closed squares) in comparison to standard inhibitor **74** (closed circles) in the daunorubicin assay using MDCK II MRP1 cells. The sensitive cell line MDCK II is depicted by open circles. (B): Calculation of the activation ratio of compound **104** resulting in a parabola. The assay was performed by Katja Stefan.

4.2.3. Screening with Respect to P-gp Activation and Inhibition

Compounds **101**-**110** were evaluated with respect to their capability to affect P-gp (see also 6.2.4.2). Figure 4.20 summarizes the obtained results of the calcein AM assay using A2780/ADR cells. The lower dashed line marks the -5% boundary. Only compounds at 10 nmol · L^{-1} that resulted in significantly lower response values than -5% were further investigated. The upper dashed line indicates 25% inhibition, which was reached by compound **104** only. It possessed an IC_{50} value of 14.0 ± 0.4 μmol · L^{-1} (pIC_{50} = 4.855 ± 0.018). The whole compound set had no activating properties.

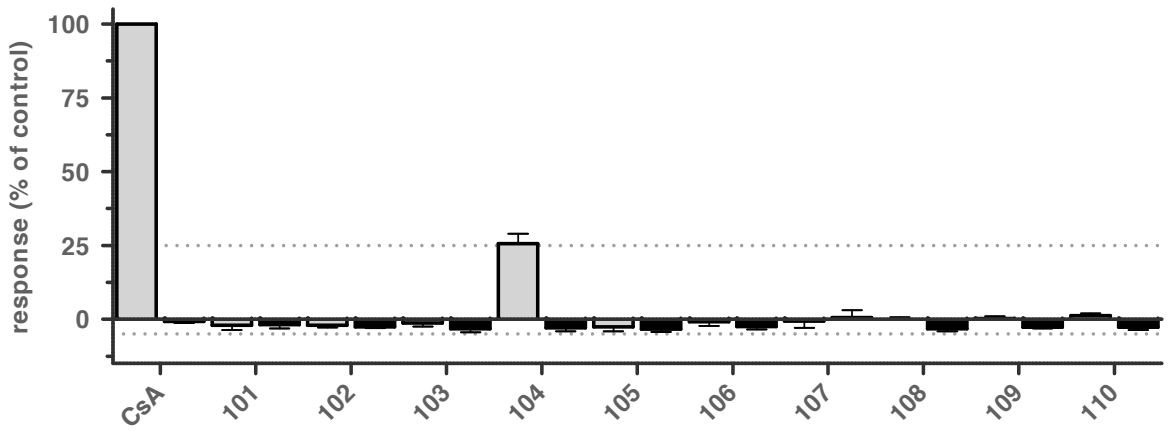

Figure 4.20. P-gp screening of compounds **101**-**110** in the calcein AM assay using A2780/ADR cells. Shown is percentage inhibition compared to the standard inhibitor cyclosporine A (CsA, 10 μmol · L^{-1}) of at least three independent experiments with duplicate measurements; light grey bars: effect at 10 μmol · L^{-1}; black bars: effect at 10 nmol · L^{-1}. The IC_{50} value of compound **104** was determined by fitting the resultant concentration-effect curve to the top value of the standard inhibitor cyclosporine A using the statistically preferred parameter model (see section 6.3.2.2).

4.2.4. Screening with Respect to BCRP Activation and Inhibition

Furthermore, the activating and inhibiting properties of compound **101**-**110** were evaluated using concentrations of 10 nmol · L^{-1} and 10 μmol · L^{-1} (see also 6.2.4.4). This was performed by Katja Stefan. Figure 4.21 gives the obtained results. Since the black bars were not significantly different to -5%, none of these marginal effects have been evaluated in detail. Compound **101** and **104** showed more than 25% inhibition compared to the standard inhibitor Ko143 at 10 μmol · L^{-1}. They possessed an IC_{50} value of 19.9 ± 2.7 μmol · L^{-1} and 19.5 ± 3.0 μmol · L^{-1}, respectively (pIC_{50} value = 4.705 ± 0.088 μmol · L^{-1} and 4.715 ± 0.100 μmol · L^{-1}, respectively). Although their inhibitory power against BCRP is poor, compound

101 represents a rare example of a dual inhibitor of MRP1 and BCRP. The other compounds showed only a slight increase of fluorescence below 25% compared to Ko143 and were not further investigated.

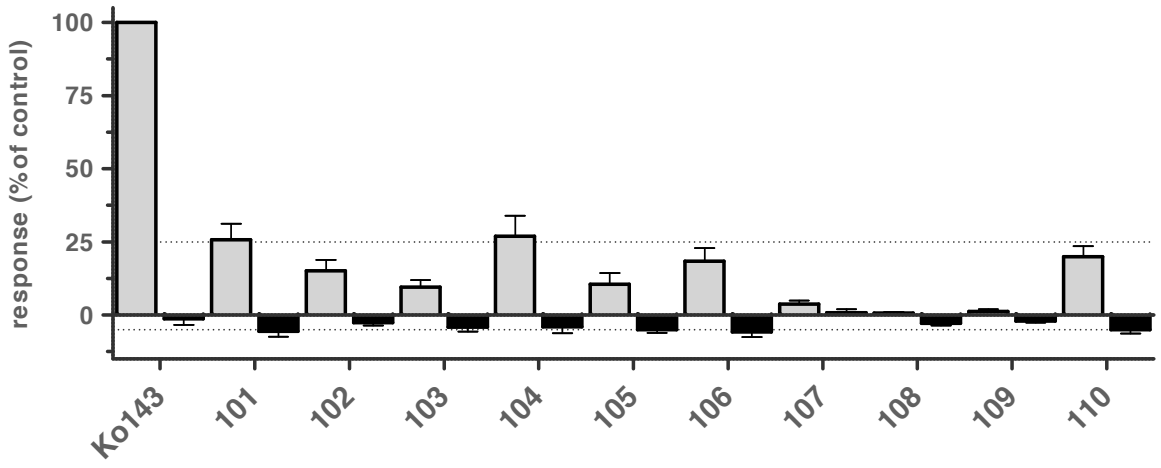

Figure 4.21. BCRP screening of compounds **101-110** in the pheophorbide A assay using MDCK II BCRP cells. Shown is percentage inhibition compared to the standard inhibitor Ko143 (10 μmol · L^{-}1) of at least three independent experiments with duplicate measurements; light grey bars: effect at 10 μmol · L^{-1}; black bars: effect at 10 nmol · L^{-1} The IC_{50} values of compounds **101** and **104** were determined by fitting the resultant concentration-effect curve to the top value of the standard inhibitor Ko143 using the statistically preferred parameter model (see section 6.3.2.2).

4.2.5. Determination of Intrinsic Toxicity

The intrinsic toxicity of compounds **101-110** was investigated using the MTT-viability assay (see also 6.2.4.5) and was performed by Katja Stefan. Tables 4.14 A-B give the obtained GI_{50} values using different MDR cell lines. Although the values differ between the cell lines, it can be said that the compounds are generally nontoxic. The most toxic compound was **104**, which possessed in the tested cell lines GI_{50} values of around 20-30 μmol · L^{-1}. With respect to MRP1 inhibition as stated in Table 4.10, its therapeutic ratio was about 40 (MDCK II MRP1; see section 6.3.6). Compared to activation, the compounds are over 10.000-fold more activating than toxic. Figures 4.22 A-F visualize the obtained biological data.

Table 4.14 A. GI_{50} and pGI_{50} values of compounds **101-110** obtained in the MTT-viability assay using H69AR, MDCK II MRP1 and MDCK II cells.

no.	H69AR GI_{50} ± SEM [μmol · L^{-1}]	H69AR pGI_{50} ± SEM	MDCK II MRP1 GI_{50} ± SEM [μmol · L^{-1}]	MDCK II MRP1 pGI_{50} ± SEM	MDCK II GI_{50} ± SEM [μmol · L^{-1}]	MDCK II pGI_{50} ± SEM
101	> 100	> 4.000	> 100	> 4.000	> 100	> 4.000
102	62.1 ± 15.4	4.220 ± 0.161	> 100	> 4.000	66.9 ± 8.0	4.178 ± 0.079
103	> 100	> 4.000	> 100	> 4.000	> 100	> 4.000
104	34.0 ± 3.6	4.471 ± 0.069	31.7 ± 1.1	4.499 ± 0.024	30.9 ± 0.3	4.510 ± 0.006
105	> 100	> 4.000	> 100	> 4.000	> 100	> 4.000
106	> 100	> 4.000	> 100	> 4.000	> 100	> 4.000
107	> 100	> 4.000	> 100	> 4.000	> 100	> 4.000
108	> 100	> 4.000	> 100	> 4.000	> 100	> 4.000
109	> 100	> 4.000	> 100	> 4.000	> 100	> 4.000
110	> 100	> 4.000	> 100	> 4.000	> 100	> 4.000

Table 4.14 B. GI_{50} and pGI_{50} values of compounds **101-110** obtained in the MTT-viability assay using 2008/MRP1, A2780/ADR and MDCK II BCRP cells.

no.	2008/MRP1 GI_{50} ± SEM [μmol · L^{-1}]	2008/MRP1 pGI_{50} ± SEM	A2780/ADR GI_{50} ± SEM [μmol · L^{-1}]	A2780/ADR pGI_{50} ± SEM	MDCK II BCRP GI_{50} ± SEM [μmol · L^{-1}]	MDCK II BCRP pGI_{50} ± SEM
101	83.8 ± 5.7	4.078 ± 0.045	85.5 ± 0.6	4.068 ± 0.05	82.6 ± 5.1	4.084 ± 0.041
102	70.2 ± 9.7	4.158 ± 0.091	65.2 ± 11.0	4.192 ± 0.111	36.6 ± 7.0	4.445 ± 0.125
103	> 100	> 4.000	85.1 ± 4.2	4.071 ± 0.033	> 100	> 4.000
104	35.4 ± 0.2	4.451 ± 0.005	32.5 ± 4.0	4.492 ± 0.082	18.2 ± 3.1	4.747 ± 0.112
105	> 100	> 4.000	66.0 ± 4.1	4.182 ± 0.041	> 100	> 4.000
106	> 100	> 4.000	> 100	> 4.000	> 100	> 4.000
107	> 100	> 4.000	79.1 ± 6.7	4.104 ± 0.056	> 100	> 4.000
108	> 100	> 4.000	63.6 ± 2.6	4.197 ± 0.027	84.5 ± 5.5	4.074 ± 0.074
109	> 100	> 4.000	74.0 ± 8.7	4.134 ± 0.077	77.3 ± 7.7	4.114 ± 0.114
110	> 100	> 4.000	36.8 ± 0.5	4.434 ± 0.009	> 100	> 4.000

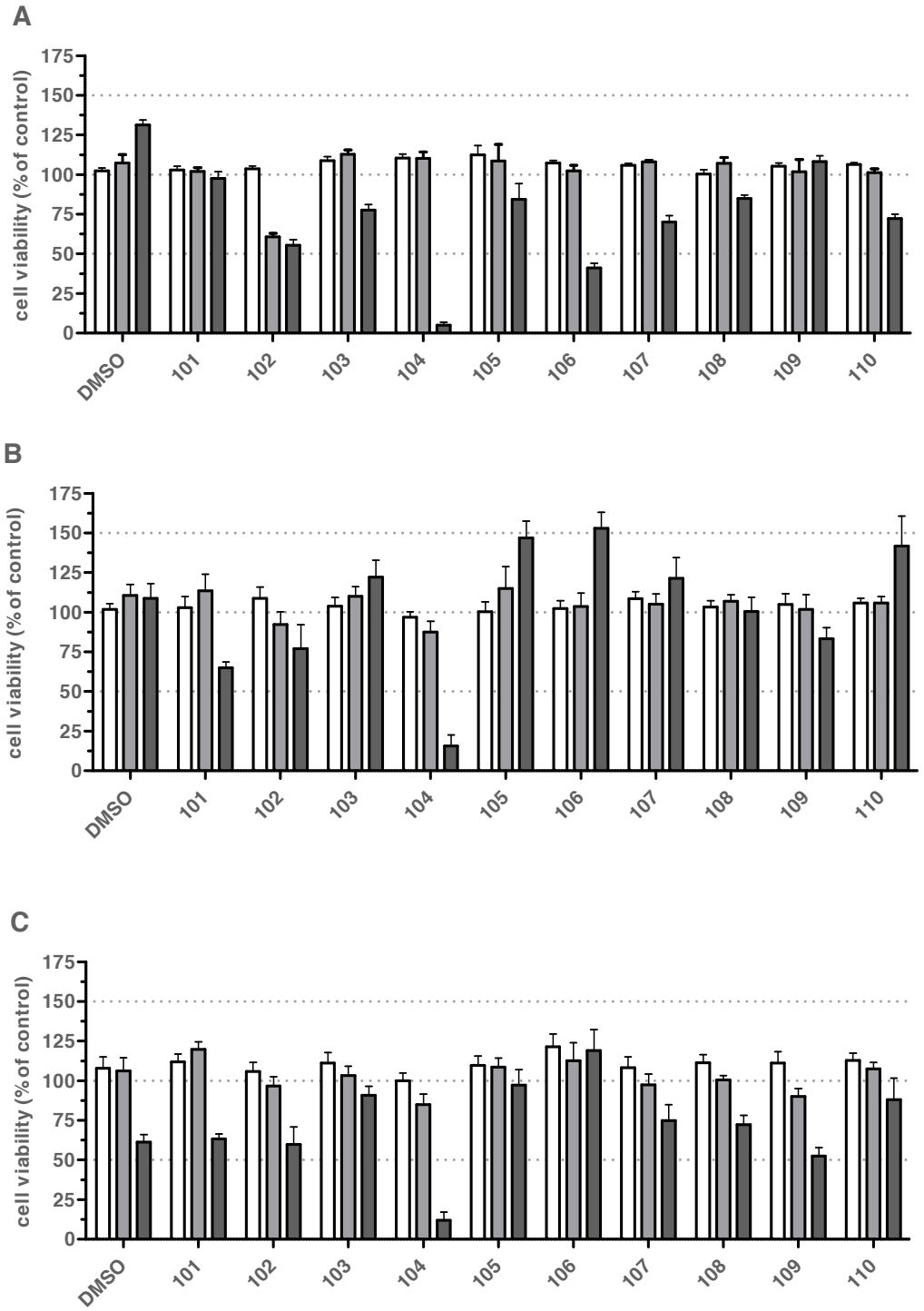

Figures 4.22. MTT-viability assay of compounds **101**-**110** at concentrations of 1 (white bar), 10 (light grey bar) and 100 μmol · L^{-1} (dark grey bar) compared to DMSO content of these dilutions (0.01, 0.1 and 1%); 100% cell viability is defined as pure cell culture medium without further supplements; 0% cell viability is caused by 10% DMSO. (A): H69AR. (B): MDCK II MRP1. (C): MDCK II. The dashed lines indicate 50 (lower), 100 (middle) and 150% (upper) cell viability.

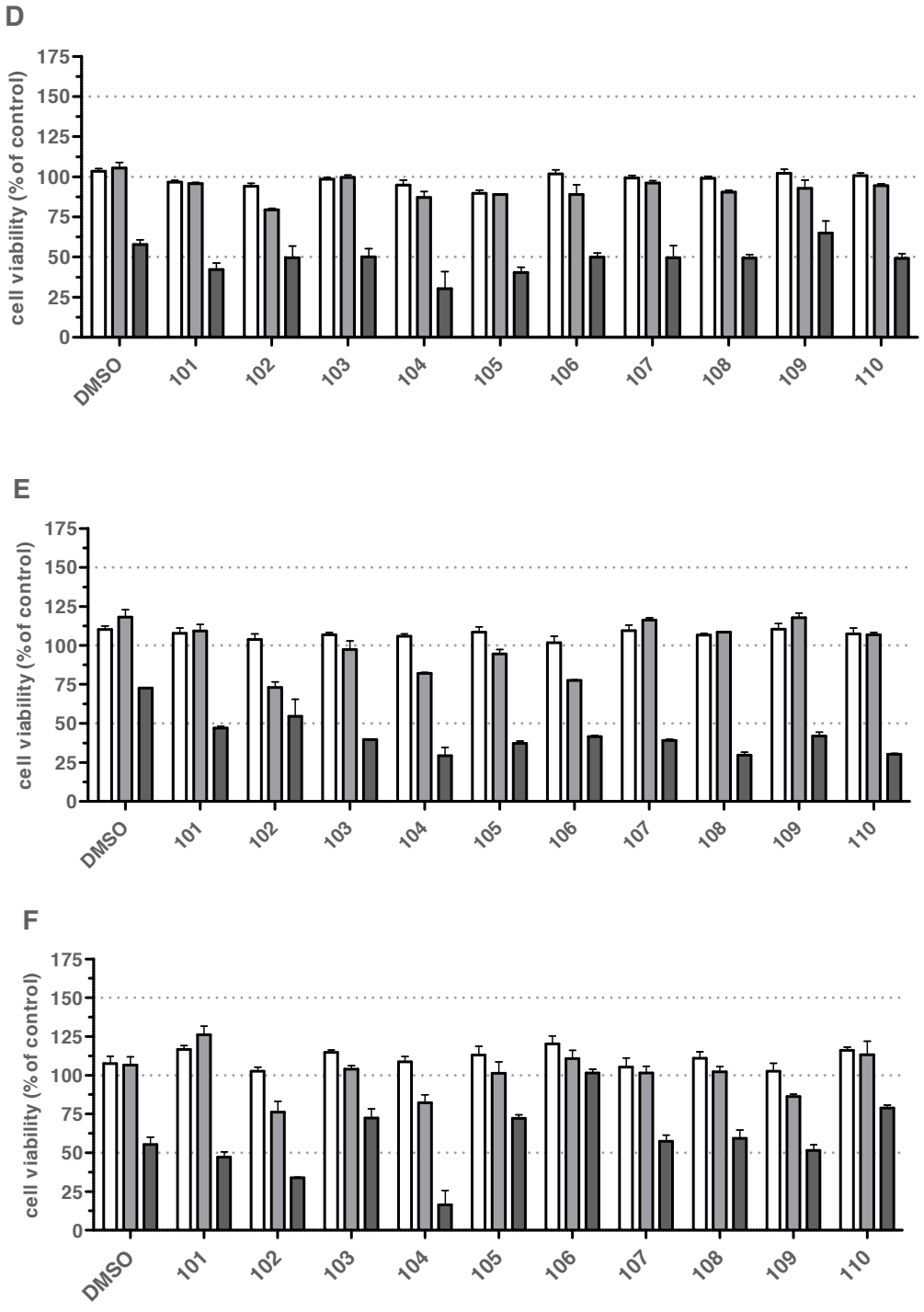

Figures 4.22. MTT-viability assay of compounds **101**-**110** at concentrations of 1 (white bar), 10 (light grey bar) and 100 μmol · L^{-1} (dark grey bar) compared to DMSO content of these dilutions (0.01, 0.1 and 1%); 100% cell viability is defined as pure cell culture medium without further supplements; 0% cell viability is caused by 10% DMSO (D): 2008/MRP1. (E): A2780/ADR. (F): MDCK II BCRP. The dashed lines indicate 50 (lower), 100 (middle) and 150% (upper) cell viability.

In most cases, DMSO had either no or a negative effect on cell viability. Interestingly, the data of the MRP1 transfected MDCK II cell line indicated that the compounds enhance cell

viability. But this could neither be confirmed by the biological data of the H69AR or 2008/MRP1 cells. Compound **104** is the only compound that had in every cell line a negative influence on the cell viability. Except for the 2008/MRP1 cells, the compounds were well tolerated by MRP1 overexpressing cells. The differences between these cells might be explained by the different expression level of MRP1.

4.2.6. MDR Reversal-efficacy of MRP1 Activators

In contrast to the before stated MDR reversal-efficacy assay conducted for the already mentioned MRP1 inhibitors (see section 4.1.6), the MRP1 activators **101**-**110** were evaluated with respect to an enhanced resistance of MRP1 overexpressing cells toward daunorubicin. This was conducted by Katja Stefan. In theory, an activator should be able to reduce the intracellular concentration of the cytotoxic compound and therefore enhance the resistance. Unfortunately, this could only be observed for compound **110** at a much higher concentration than expected (1 and 10 μmol · L^{-1}; Figure 4.23 A). Most compounds had either no influence on cell viability or reversed MDR in MDCK II MRP1 cells, as shown for compound **104** in Figure 4.23 B. The latter fact could be explained by the partially inhibiting feature of the compounds, especially 9-deazapurines. Compound **110** has the least inhibitory power toward MRP1 (see Tables 4.10-11) and increased cell viability over a period of 72 hours (Figure 4.23 A).

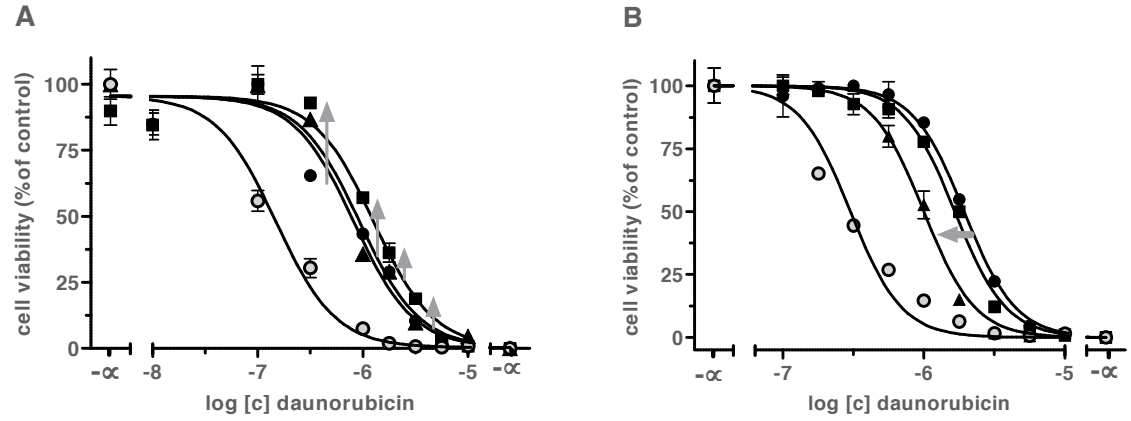

Figure 4.23. (A): 1 μmol · L^{-1} (closed triangles) and 10 μmol · L^{-1} (closed squares) of compound **110** as activator of daunorubicin efflux enhancing resistance toward this cytotoxic agent, in comparison to control (closed circles) and the sensitive cell line MDCK II (open circles). Resistance could be increased about 50%, as indicated by the grey arrows. (B): 0.1 μmol · L^{-1} (closed squares) and 1 μmol · L^{-1} (closed triangles) of compound **104** sensitized MDCK II MRP1 cells (closed circles) to the left toward the sensitive cell line (open circles) as indicated by the grey arrow.

4.2.7. Analysis of Activation Type

Compound **101** was used as representative of the MRP1 activators to analyze the type of activation. This was performed by Katja Stefan. Different concentrations of compound **101** were combined with different concentrations of daunorubicin and analyzed according to Lineweaver-Burk, Hanes-Woolf and Cornish-Bowden. The basic mathematical equations can be found in reference [355]. A summary can be found in section 6.3.10.

According to *Segel's* "Enzyme Kinetics", the compounds can be considered as nonessential activators.[355] Regarding the double reciprocal plot of Lineweaver-Burk, activators are characterized by downward oriented lines. Although the tendency of the intersection of the lines in Figure 4.24 A is toward the ordinate, which would represent a competitive activation, a mixed-type activator as described by *Segel* is more likely. And although the additional plots of Hanes-Woolf and Cornish-Bowden (Figures 4.24 B-C) also indicate a competitive relation of activator and substrate, competitive nonessential activators have never been reported since enzymes cannot be occupied at the active site by an activator while the substrate has to be formed to the product in the same binding pocket. Only mixed-type systems are described, in which the used compound has the feature of an activator (noncompetitive) and inhibitor (competitive) at low and high concentrations, respectively. This is quite conceivable since the herein presented activators have also an inhibitory property.

But one should handle the obtained results with care, since a transporter is not an enzyme. Although specific binding sites for P-gp have been reported,[274] the transport process and its exact procedure is still unknown, so are binding sites for MRP1. And since it it is not known how many participants take part in the transport process of MRP1 (e.g. activator, substrate, GSH, GSSG, etc.), the system can be rather complex and might not be evaluated by basic enzymatic equations.

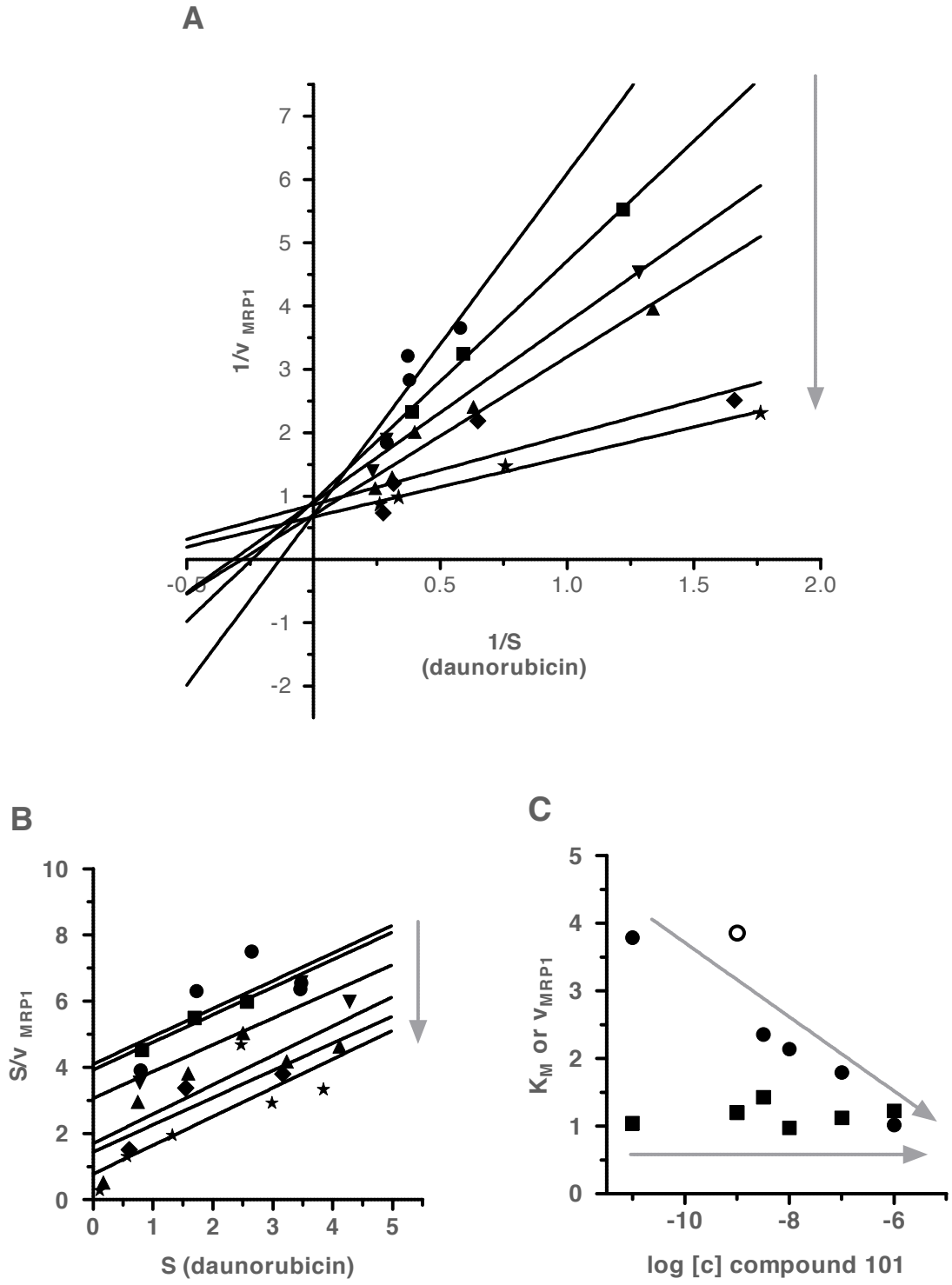

Figure 4.24. Kinetic evaluation of compound **101** with respect to the type of activation of MRP1-mediated transport of daunorubicin using H69AR cells. (A): Lineweaver-Burk plot of control (closed circles) and compound **101** at 1.0 (closed squares), 3.2 (closed downward triangles), 10 (closed upward triangles), 100 (closed rhombs) and 1000 nmol · L^{-1} (closed stars); the intersection at the ordinate indicates a competitive relation; the downward oriented grey arrow indicates the activating character. (B): Corresponding Hanes-Woolf plot; the parallel lines indicate a competitive relation; the downward oriented grey arrow indicates the activating character. (C): Cornish-Bowden plot of K_M (closed circle) and V_{max} (squares); open circle: outlier.

4.2.8. Summary of Evaluation of 7-*N*-alkyl, -aryl or -arylalkyl and 6-aminoarylalkyl-9-deazapurines as well as 6-piperazinyl-purine Analogs

The herein presented 9-deazapurines and purine analogs compounds inhibited MRP1-mediated transport of calcein AM and daunorubicin as could be expected from their logP value. While the compounds with most lipophilicity (logP between 4 and 5; compounds **102** and **104**-**106**) had the best inhibitory activity around 1 μmol · L^{-1}, the other representatives had rather low inhibitory power. Especially the purine derivatives were characterized by almost no inhibition of MRP1, which might be because purines form an own class of compounds and do not fulfill the requirements of the binding pocket(s) completely.

Interestingly, the compounds were able to accelerate calcein AM and daunorubicin transport mediated by MRP1. At low concentrations between 1 and 100 nmol · L^{-1} the compounds led to a significant reduction of intracellular fluorescence of calcein in H69AR cells and daunorubicin in MDCK II MRP1 cells. The use of these two different MRP1 substrates and two different cell lines showed this effect being independent from these two parameters. The magnitude of the effect was different (calcein AM about a factor of 1.5; daunorubicin about a factor of 2). This could be explained by the lipophilicity of the substrates. Since no effects in the sensitive cell lines were observed, other mechanisms like disturbance of the membrane integrity or fluidity are highly unlikely. Additionally, the MTT-viability assay data suggests that the compound have no destructive but rather viability-enhancing influence on the cells. This was not observed for all MRP1 overexpressing cell lines, but this could be related to the different expression level of MRP1. Only compound **104** showed at high concentrations (around 100 μmol · L^{-1}) a negative influence on cell viability.

Unfortunately, the activating effect could not be transferred to an enhancement of MDR. Compound **110** was the only exception that increased the resistance toward daunorubicin, but at much higher concentration than could be expected from the assay data. One explanation why only this compound showed the described effect could be its low inhibitory power against MRP1 function while other compounds like **104** sensitized MDR cells in agreement to their inhibitory activity. Another mechanism which could explain the difference between the activating power in the calcein AM and daunorubicin assay and the lacking capability to enhance MDR could be related to the MRP1 expression. Since the cancer cells were exposed to the acitvators as well as the cytotoxic agent over a period of 72 hours, regulatory mechanisms could have reduced the amount of present MRP1. But this is rather speculative and needs to be clarified in future experiments.

With respect to P-gp, only compound **104** showed inhibitory activity toward this transporter, but only in double-digit micromolar range. Referred to BCRP, only compounds **101** and **104**

showed inhibitory power, but with rather poor effectiveness. No activation could be observed with respect to both transporters.

Compound **104** represents a rare example of a triple inhibitor of MRP1, P-gp and BCRP, which can be a template for ongoing research. Compound **101** represents a dual inhibitor of MRP1 and BCRP. As stated in the introduction, almost nothing is known regarding this kind of inhibitors.

Interestingly, the analysis of the activating part of the concentration-effect curves of compound **101** as representative of the MRP1 transport activators showed these compounds to be nonessential activators.[355] According to Lineweaver-Burk, Cornish-Bowden and Hanes-Woolf a competitive relation between compound **101** and daunorubicin can be deduced, although this interaction has never been reported before. According to *Segel's* "Enzyme Kinetics", a mixed-type nonessential activation is more likely. But the complexitiy of the system regarding reacting agents makes the interpretation rather difficult.

4.3. Evaluation of 7,8-alicyclic-, 7-*N*-alkyl-, -aryl- or -arylalkyl-, and 8,9-annulated-9-deazapurines with Heteroaromatic Variations

Since several structural elements of formerly published MRP1 inhibitors were shown to be beneficial for activity, further 9-deazapurine derivatives with these variations were synthesized. These structural elements include heterocycles like furan (benzbromarone, Figure 1.7), indole (GF109203X, Figure 1.6; indomethacin, Figure 1.7), dioxindanes (bifendate-chalcone, Figure 1.19; piperine, Figure 1.20; cepharanthine, Figure 1.21), pyridine (biricodar, NIK-250, Figure 1.6; lonafarnib, Figure 1.8) or quinoline (MS-209, Figure 1.6; MK571, Figure 1.12), and methoxyphenyl (verapamil, biricodar, Figure 1.6; several flavonoids, Figure 1.9; schisandin B, Figure 1.10). The compounds and activities presented in this subchapter have already been published.[356]

The synthesized compounds can be grouped into four classes, (i) 7,8-alicyclic-9-deazapurines with a nitrogen heterocycle at position 6, (ii) 9-deazapurines with 4-(2-(1*H*-indole-3-yl)ethyl)piperazine-1-yl residue at position 6 and alkyl, aryl or arylalkyl variations at position 7, (iii) 9-deazapurines with oxygen heterocycle at position 6 or oxygen containing residue at position 7 and (iv) 8,9-annulated-9-deazapurines with variations at position 6.

The four classes are separately discussed. The biological evaluation using the daunorubicin assay, the calcein AM assay as well as the pheophorbide A assay was performed by Katja Stefan.

4.3.1. Evaluation of 7,8-alicyclic-9-deazapurines with a Nitrogen Heterocycle at Position 6

The starting point of this compound series was compound 29 (**111**) reported by *Wang* et al. in 2004 (compound 29 in ref. [271]. A variety of different derivatives was synthesized, such as enlargement of the cyclohexyl (**111**, **113**-**114**, **116**) to a cycloheptyl ring system at positions 7 and 8 (**112**, **115**, **117**) as well as change of the 4-(2-(1*H*-indole-3-yl)ethyl)piperazine-1-yl substituent (**111**-**112**) at position 6 to either a (2-(1*H*-indole-3-yl)ethyl)amino residue (**113**) or a pyridine containing substituent (**114**-**117**). Figure 4.25 visualizes the screening of the compounds in all three applied assays. Table 4.15 A summarizes the corresponding biological data for all three tested ABC-transport proteins, MRP1, P-gp and BCRP. Table 4.15 B gives the pIC_{50} values of the compounds.

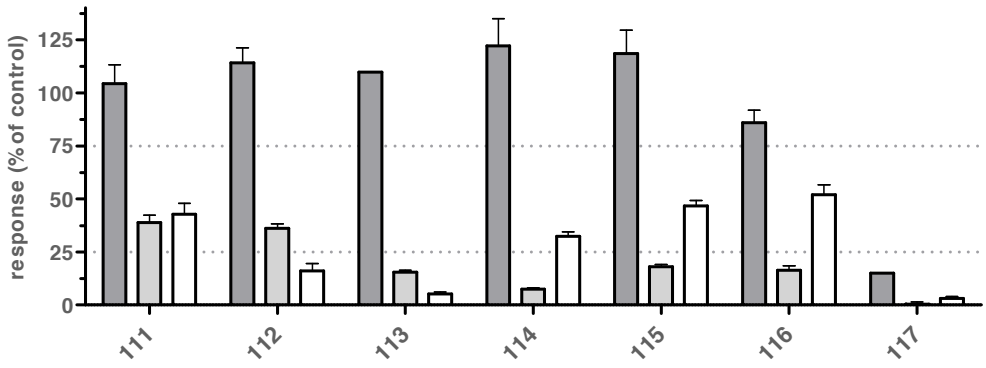

Figure 4.25. Screening of compound class (i) (**111**-**117**; 10 μmol · L^{-1}) in the daunorubicin assay (MRP1, dark grey bark), calcein AM assay (P-gp, light grey bark), and pheophorbide A assay (BCRP, white bark) using H69AR (dark grey bark), A2780/ADR (light grey bark) and MDCK II BCRP (white bark) cells. 100% is defined as the effect of the standard inhibitors **74** (MRP1), cyclosporine A (P-gp) and Ko143 (BCRP) at a concentration of 10 μmol · L^{-1}. Shown are at least three independent experiments with duplicate measurements.

Table 4.15 A. Summary of inhibitory activity of compounds **111**-**117** obtained in the daunorubicin assay (MRP1), calcein AM assay (P-gp) and pheophorbide A assay (BCRP) using H69AR (MRP1), A2780/ADR (P-gp) and MDCK II BCRP (BCRP); n.d. = not determined due to lack of inhibitory activity (I_{max} ≤ 25%). The biological data was determined by Katja Stefan.

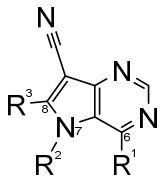

no.	R^1	R^2	R^3	daunorubicin (MRP1) IC_{50} ± SEM [μmol · L^{-1}]	calcein AM (P-gp) IC_{50} ± SEM [μmol · L^{-1}]	pheophorbide A (BCRP) IC_{50} ± SEM [μmol · L^{-1}]
111	4-(2-(1*H*-indole-3-yl)ethyl)piperazin-1-yl	cyclohexyl		0.344 ± 0.018	5.62 ± 0.41	3.41 ± 0.20
112	4-(2-(1*H*-indole-3-yl)ethyl)piperazin-1-yl	cycloheptyl		0.289 ± 0.008	1.71 ± 0.14	n.d.
113	(2-(1*H*-indole-3-yl)ethyl)amino	cyclohexyl		0.957 ± 0.019	n.d.	n.d.
114	4-(2-(pyridin-4-yl)ethyl)piperazin-1-yl	cyclohexyl		0.672 ± 0.034	n.d.	27.8 ± 4.3
115	4-(2-(pyridin-4-yl)ethyl)piperazin-1-yl	cycloheptyl		1.14 ± 0.07	n.d.	12.4 ± 0.4
116	4-(pyridin-2-yl)piperazin-1-yl	cyclohexyl		1.02 ± 0.02	n.d.	4.86 ± 0.36
117	4-(pyridin-2-yl)piperazin-1-yl	cycloheptyl		n.d.	n.d.	n.d.

Table 4.15 B. Negative decadic logarithm of the IC_{50} values of compound **111**-**117** taken from Table 4.15 A.

no.	R^1	R^2	R^3	daunorubicin (MRP1) pIC_{50} ± SEM	calcein AM (P-gp) pIC_{50} ± SEM	pheophorbide A (BCRP) pIC_{50} ± SEM
111	4-(2-(1*H*-indole-3-yl)ethyl)piperazin-1-yl	cyclohexyl		6.464 ± 0.034	5.252 ± 0.048	5.468 ± 0.036
112	4-(2-(1*H*-indole-3-yl)ethyl)piperazin-1-yl	cycloheptyl		6.540 ± 0.018	5.768 ± 0.055	n.d.
113	(2-(1*H*-indole-3-yl)ethyl)amino	cyclohexyl		6.019 ± 0.013	n.d.	n.d.
114	4-(2-(pyridin-4-yl)ethyl)piperazin-1-yl	cyclohexyl		6.173 ± 0.033	n.d.	4.561 ± 0.101
115	4-(2-(pyridin-4-yl)ethyl)piperazin-1-yl	cycloheptyl		5.944 ± 0.040	n.d.	4.906 ± 0.023
116	4-(pyridin-2-yl)piperazin-1-yl	cyclohexyl		5.993 ± 0.010	n.d.	5.313 ± 0.017
117	4-(pyridin-2-yl)piperazin-1-yl	cycloheptyl		n.d.	n.d.	n.d.

Since compound **104** inhibited all three transport proteins, the possibility of multiple inhibition was in focus of these investigations. Compound **111**, which had already been reported to be a dual inhibitor of MRP1 and P-gp,[271] inhibited also BCRP. The 7,8-alicyclic compounds **111** and **112** had great inhibitory power toward MRP1, the latter represented a good dual inhibitor of MRP1 and P-gp. Compound **113,** lacking the piperazine partial structure, was inferior compared to its piperazine-bearing counterparts **111** and **112**. This underlines the fact that the piperazine structure is necessary, as already shown before (see subchapters 4.1-2).
The pyridine derivatives **114** and **115** were good inhibitors with IC_{50} values around 1 μmol· L^{-1} or less. The same applied for compound **116**, which contained no ethylene linker between the pyridine and piperazine substructures. Similar compounds already presented above (**77** and **87**) were inferior compared to compound **116**. This compound is a rare example of a good dual inhibitor of MRP1 and BCRP. Unfortunately compound **117** could not be evaluated due to solubility issues.

4.3.2. Evaluation of 9-deazapurines with 4-(2-(1*H*-indole-3-yl)ethyl)piperazine-1-yl Residue at Position 6 and Alkyl or Arylalkyl Variations at Position 7

Compound **92** was the most active representative of the subchapter (see Table 4.3) and compound **111** of subclass (i) (see Table 4.15 A-B) was a very good inhibitor as well. Therefore, the synthesis of a combination of structural features from both subclasses with specific variations at position 7 was performed (compared to compounds **88**-**99**). Figure 4.26 gives the screening results of the compounds. Table 4.16 A and B give a summary of the corresponding biological data. All synthesized compounds (**118**-**125**) were very good inhibitors of MRP1 with a concentration range of about 300-500 nmol · L^{-1}, except for

compound **119**. As was already found in section 4.1.3, higher molecular weight seemed to be preferred with respect to P-gp inhibition. This could also be seen in this subset of compounds in the screening data (Figure 4.26). Compounds **124** and **125** are both very effective P-gp inhibitors, although the former reached only 34% of the standard compound cyclosporine A at 10 μmol · L^{-1}. With respect to BCRP both compounds were good inhibitors of this transporter with IC_{50} values in low single-digit micromolar concentration range. This contradicts the above stated finding that small molecules with low logP and low molecular weight are preferred regarding BCRP inhibition (see section 4.1.4). Hence, these compounds seem to have other attributes of greater importance, e.g. a more suitable residue for the binding pocket(s).

As compound **125** reached in all three assays 75% inhibition in comparison to the corresponding standard compounds, it was further investigated with respect to its type of inhibition (see section 4.3.5) and MDR reversal (see section 4.3.7) toward MRP1, P-gp and BCRP.

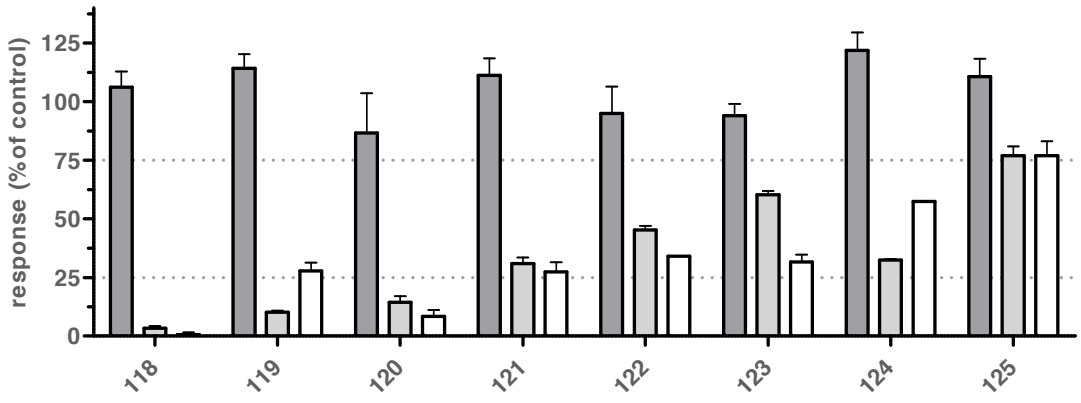

Figure 4.26. Screening of compound class (ii) (**118**-**125**; 10 μmol · L^{-1}) in the daunorubicin assay (MRP1, dark grey bark), calcein AM assay (P-gp, light grey bark), and pheophorbide A assay (BCRP, white bark) using H69AR (dark grey bark), A2780/ADR (light grey bark) and MDCK II BCRP (white bark) cells. 100% is defined as the effect of the standard compounds **74** (MRP1), cyclosporine A (P-gp) and Ko143 (BCRP) at a concentration of 10 μmol · L^{-1}. Shown are at least three independent experiments with duplicate measurements.

Table 4.16 A. Summary of inhibitory activity data of compounds **118**-**125** obtained in the daunorubicin assay (MRP1), calcein AM assay (P-gp) and pheophorbide A assay (BCRP) using H69AR (MRP1), A2780/ADR (P-gp) and MDCK II BCRP cells (BCRP); n.d. = not determined due to lack of inhibitory activity (I_{max} ≤ 25%). The biological data was determined by Katja Stefan.

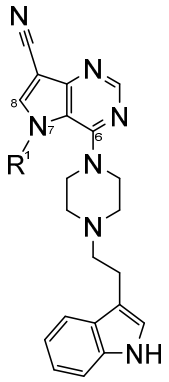

no.	R^1	daunorubicin (MRP1) IC_{50} ± SEM [μmol · L^{-1}]	calcein AM (P-gp) IC_{50} ± SEM [μmol · L^{-1}]	pheophorbide A (BCRP) IC_{50} ± SEM [μmol · L^{-1}]
118	methyl	0.337 ± 0.020	n.d.	n.d.
119	ethyl	0.855 ± 0.063	n.d.	13.8 ± 1.0
120	propyl	0.468 ± 0.012	n.d.	n.d.
121	cyclopropyl	0.316 ± 0.009	3.85 ± 0.36	18.9 ± 1.7
122	phenyl	0.328 ± 0.022	1.28 ± 0.14	n.d.
123	benzyl	0.405 ± 0.028	4.48 ± 0.25	4.07 ± 0.36
124	phenethyl	0.524 ± 0.013	1.64 ± 0.04	1.39 ± 0.08
125	phenylpropyl	0.501 ± 0.025	1.46 ± 0.10	1.69 ± 0.07

Table 4.16 B. Negative decadic logarithm of the IC_{50} values of compounds **118**-**125** taken from Table 4.16 A.

no.	R^1	daunorubicin (MRP1) pIC_{50} ± SEM	calcein AM (P-gp) pIC_{50} ± SEM	pheophorbide A (BCRP) pIC_{50} ± SEM
118	methyl	6.473 ± 0.039	n.d.	n.d.
119	ethyl	6.069 ± 0.048	n.d.	4.861 ± 0.048
120	propyl	6.330 ± 0.017	n.d.	n.d.
121	cyclopropyl	6.501 ± 0.019	5.417 ± 0.062	4.725 ± 0.060
122	phenyl	6.485 ± 0.045	5.896 ± 0.074	n.d.
123	benzyl	6.394 ± 0.046	5.459 ± 0.047	5.392 ± 0.058
124	phenethyl	6.281 ± 0.016	5.784 ± 0.047	5.859 ± 0.037
125	phenylpropyl	6.301 ± 0.033	5.836 ± 0.043	5.772 ± 0.028

4.3.3. Evaluation of 9-deazapurines with Oxygen Heterocycle at Position 6 or Oxygen Containing Residue at Position 7

Since several known inhibitors of MRP1 contain oxygen substituents or oxygen heterocylces like verapamil (Figure 1.6), biricodar (Figure 1.6) and piperine (Figure 1.20), derivatives with piperonyl and furanoyl substituents as well as alkoxy residues were synthesized. Figure 4.27 shows the obtained screening data. Tables 4.17 A and B summarize the corresponding biological results.

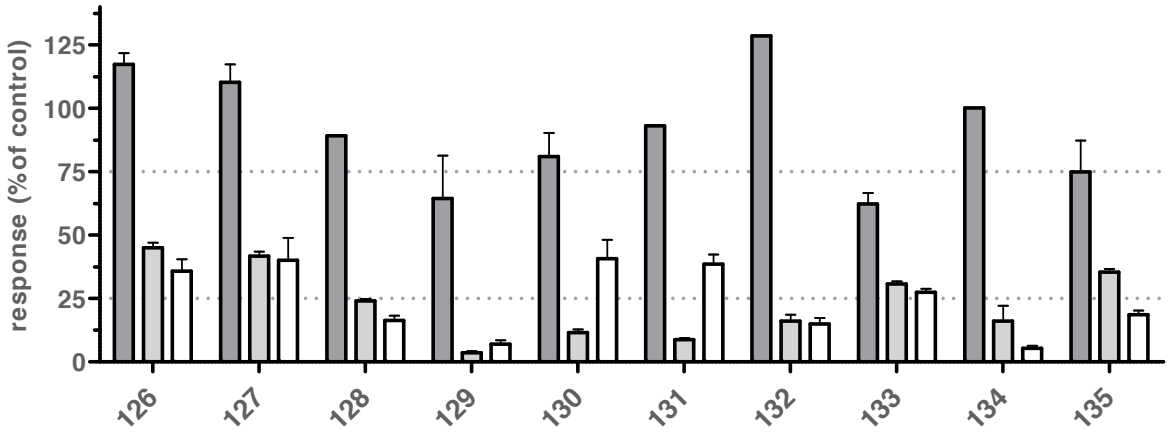

Figure 4.27. Screening of compound class (iii) (**126**-**135**; 10 μmol · L^{-1}) in the daunorubicin assay (MRP1, dark grey bark), calcein AM assay (P-gp, light grey bark), and pheophorbide A assay (BCRP, white bark) using H69AR (dark grey bark), A2780/ADR (light grey bark) and MDCK II BCRP (white bark) cells. 100% is defined as the effect of the standard compounds **74** (MRP1), cyclosporine A (P-gp) and Ko143 (BCRP) at a concentration of 10 μmol · L^{-1}. Shown are at least three independent experiments with duplicate measurements.

Table 4.17 A. Summary of inhibitory activity data of compounds **126**-**135** obtained in the daunorubicin assay (MRP1), calcein AM assay (P-gp) and pheophorbide A assay (BCRP) using H69AR (MRP1), A2780/ADR (P-gp) and MDCK II BCRP cells (BCRP); n.d. = not determined due to lack of inhibitory activity (I_{max} ≤ 25%). The biological data was determined by Katja Stefan.

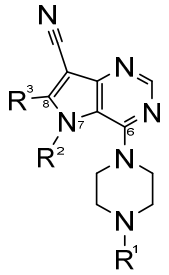

no.	R^1	R^2	R^3	daunorubicin (MRP1) IC_{50} ± SEM [μmol · L^{-1}]	calcein AM (P-gp) IC_{50} ± SEM [μmol · L^{-1}]	pheophorbide A (BCRP) IC_{50} ± SEM [μmol · L^{-1}]
126	piperonyl	cyclohexyl		0.322 ± 0.019	13.9 ± 1.4	14.6 ± 1.8
127	piperonyl	cycloheptyl		1.02 ± 0.04	5.71 ± 0.60	23.7 ± 4.0
128	piperonyl	phenyl	H	0.751 ± 0.126	n.d.	n.d.
129	piperonyl	phenethyl	H	1.80 ± 0.16	n.d.	n.d.
130	furanoyl	cyclohexyl		0.883 ± 0.060	n.d.	29.5 ± 1.4
131	furanoyl	cycloheptyl		1.01 ± 0.04	n.d.	12.9 ± 0.8
132	phenethyl	2-methoxyphenyl	H	0.638 ± 0.026	n.d.	n.d.
133	benzyl	2-methoxyphenyl	H	0.327 ± 0.028	19.1 ± 0.7	37.9 ± 3.6
134	phenethyl	4-ethoxyphenyl	H	1.32 ± 0.10	n.d.	n.d.
135	benzyl	4-ethoxyphenyl	H	0.859 ± 0.067	7.29 ± 0.44	n.d.

Table 4.17 B. Negative decadic logarithm of IC_{50} values of compounds **126**-**135** taken from Table 4.17 A.

no.	R^1	R^2	R^3	daunorubicin (MRP1) pIC_{50} ± SEM	calcein AM (P-gp) pIC_{50} ± SEM	pheophorbide A (BCRP) pIC_{50} ± SEM
126	piperonyl	cyclohexyl		6.493 ± 0.040	4.858 ± 0.064	4.837 ± 0.079
127	piperonyl	cycloheptyl		5.991 ± 0.028	5.246 ± 0.069	4.632 ± 0.110
128	piperonyl	phenyl	H	6.130 ± 0.110	n.d.	n.d.
129	piperonyl	phenethyl	H	5.746 ± 0.057	n.d.	n.d.
130	furanoyl	cyclohexyl		6.055 ± 0.044	n.d.	4.531 ± 0.031
131	furanoyl	cycloheptyl		5.994 ± 0.027	n.d.	4.892 ± 0.043
132	phenethyl	2-methoxyphenyl	H	6.195 ± 0.027	n.d.	n.d.
133	benzyl	2-methoxyphenyl	H	6.487 ± 0.056	4.719 ± 0.025	4.423 ± 0.063
134	phenethyl	4-ethoxyphenyl	H	5.882 ± 0.050	n.d.	n.d.
135	benzyl	4-ethoxyphenyl	H	6.067 ± 0.051	5.138 ± 0.039	n.d.

Referred to MRP1, the compounds showed to be moderately good inhibitors with IC_{50} values around 1 μmol · L^{-1}, while the inhibitory power against P-gp as well as BCRP was negligible. The best compounds are **126** and **133**. Both compounds are comparable to no. **104**,

inhibiting all three transport proteins, but P-gp and BCRP with much less potency. Although the alkoxy partial structure has often been seen in P-gp inhibitors, the outcome of these results is rather poor. The same holds for BCRP inhibition, where activities were only in double-digit micromolar range.

4.3.4. Evaluation of 8,9-annulated-9-deazapurines with Variations at Position 6

The 8,9-annulated deazapurines had already been shown to be very effective MRP1 inhibitors by *Wang* et al. in 2004.[272] Therefore, the basic 5*H*-pyrimido[5,4-*b*]indole structure was combined with beneficial residues at position 6 as discussed in subchapter 4.1, 4.3.1 and 4.3.3. The resultant 8,9-annulated-9-deazapurines contained either (a) aryl- or arylalkyl variations (**136**-**139**), (b) nitrogen containing residues (**140**-**142**) or (c) oxygen containing substituents (**143**-**144**). Figure 4.28 gives the obtained screening results. Tables 4.18 A and B summarize the biological data.

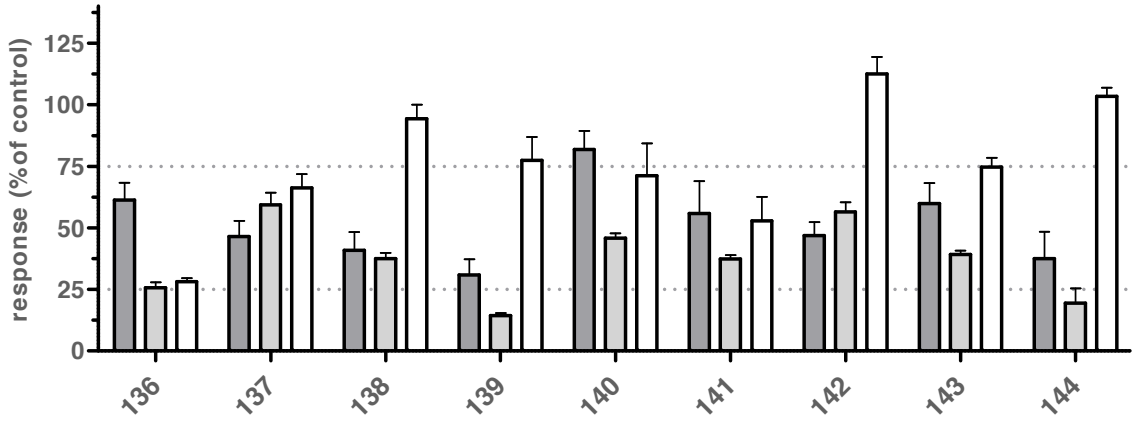

Figure 4.28. Screening of compound class (iv) (**136**-**144**; 10 μmol · L^{-1}) in the daunorubicin assay (MRP1, dark grey bark), calcein AM assay (P-gp, light grey bark), and pheophorbide A assay (BCRP, white bark) using H69AR (dark grey bark), A2780/ADR (light grey bark) and MDCK II BCRP (white bark) cells. 100% is defined as the effect of the standard compounds **74** (MRP1), cyclosporine A (P-gp) and Ko143 (BCRP) at a concentration of 10 μmol · L^{-1}. Shown are at least three independent experiments with duplicate measurements.

This class of compounds was not very effective with respect to inhibition of MRP1 or P-gp at a concentration of 10 μmol · L^{-1}. They reached only 30-60% inhibition compared to the corresponding standard inhibitors. In contrast, 8,9-annulated-9-deazapurines potently inhibited BCRP. This has been shown for this compound class before.[320]

The first subset (a) (**136**-**139**) contained very good dual (**139**) and triple (**136**) inhibitors, with IC_{50} values ranging from 0.15 to 0.45 μmol · L^{-1}. But with respect to MRP1 inhibition, one must take the insufficient I_{max} values into account (**136** = 61%; **139** = 31%). The same holds for P-gp inhibition ($I_{max\ (136)}$ = 26%; $I_{max\ (139)}$ = 14%). The reason for this partial inhibition has not been elucidated until now. Solely BCRP inhibition was convincing, except for compound **136** (I_{max} = 28%).

The same applies for subset (b) (**140**-**142**). Most compounds had a maximum inhibition level of MRP1 and P-gp around 47-82% and 37-56%, respectively. Compound **140** was in this regard the most effective one in this subset (MRP1 = 82%; P-gp = 46%; BCRP = 71%). This applied also for its IC_{50} values, which ranged all in the single-digit micromolar concentration range. But it was not further investigated since the compound did not reach the necessary level of 75% inhibition in all three transporter assays.

Subset (c) consisted only of compounds **143** and **144**. For further investigations both compounds lacked the necessary effectiveness toward MRP1 and BCRP with respect to the chosen I_{max} values of 75%. Compound **143** was comparable to compound **140**, as it turned out to be a moderately good triple inhibitor with IC_{50} values in the single-digit micromolar concentration range and I_{max} values of 60% (MRP1), 39% (P-gp) and 75% (BCRP).

Table 4.18 A. Summary of inhibitory activity data of compounds **136**-**144** obtained in the daunorubicin assay (MRP1), calcein AM assay (P-gp) and pheophorbide A assay (BCRP) using H69AR (MRP1), A2780/ADR (P-gp) and MDCK II BCRP cells (BCRP); n.d. = not determined due to lack of inhibitory activity (I_{max} ≤ 25%). The biological data was determined by Katja Stefan.

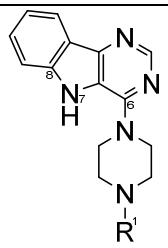

no.	R^1	daunorubicin (MRP1) IC_{50} ± SEM [μmol · L^{-1}]	calcein AM (P-gp) IC_{50} ± SEM [μmol · L^{-1}]	pheophorbide A (BCRP) IC_{50} ± SEM [μmol · L^{-1}]
136	phenethyl	0.405 ± 0.019	1.11 ± 0.04	0.839 ± 0.054
137	benzyl	0.363 ± 0.014	9.49 ± 0.67	6.08 ± 0.39
138	benzhydryl	0.409 ± 0.030	2.33 ± 0.17	1.38 ± 0.12
139	phenyl	0.146 ± 0.004	n.d.	1.10 ± 0.08
140	2-(1*H*-indole-3-yl)ethyl	0.921 ± 0.012	3.50 ± 0.36	6.21 ± 0.30
141	2-(pyridin-2-yl)ethyl	0.345 ± 0.012	10.7 ± 0.7	11.6 ± 0.7
142	pyridin-2-yl	0.495 ± 0.037	5.00 ± 0.40	1.81 ± 0.10
143	piperonyl	0.717 ± 0.030	3.92 ± 0.23	7.93 ± 0.51
144	furanoyl	0.169 ± 0.005	n.d.	6.06 ± 0.30

Table 4.18 B. Negative decadic logarithm of the IC_{50} values of compounds **136**-**144** taken from Table 4.18 A.

no.	R^1	daunorubicin (MRP1) pIC_{50} ± SEM	calcein AM (P-gp) pIC_{50} ± SEM	pheophorbide A (BCRP) pIC_{50} ± SEM
136	phenethyl	6.393 ± 0.031	5.953 ± 0.021	6.077 ± 0.042
137	benzyl	6.440 ± 0.026	5.024 ± 0.046	5.217 ± 0.042
138	benzhydryl	6.390 ± 0.026	5.632 ± 0.048	5.862 ± 0.055
139	phenyl	6.836 ± 0.016	n.d.	5.957 ± 0.045
140	2-(1*H*-indole-3-yl)ethyl	6.036 ± 0.009	5.458 ± 0.067	5.207 ± 0.032
141	2-(pyridin-2-yl)ethyl	6.462 ± 0.022	4.972 ± 0.043	4.935 ± 0.042
142	pyridin-2-yl	6.306 ± 0.050	5.306 ± 0.052	5.743 ± 0.036
143	piperonyl	6.145 ± 0.028	5.407 ± 0.039	5.102 ± 0.042
144	furanoyl	6.772 ± 0.020	n.d.	5.218 ± 0.032

4.3.5. Investigation of the Interaction Type of Triple Inhibitor No. 125

Many of the herein presented compounds inhibited all three tested ABC-transport proteins. But as one can see in Figures 4.29 A-C, not all of these were able to lead to a full inhibition at 10 μmol · L^{-1} compared to the standard compound of the corresponding test system. Only compound **125** reached more than 75% of the corresponding standard compound in all test systems with sufficient potency of around 1 μmol · $L^{-.1}$. Therefore, this compound was further characterized with respect to its interaction with the corresponding substrates of MRP1, P-gp and BCRP. The assays were performed and analyzed by Katja Stefan. Compound **125** is a noncompetitive inhibitor of MRP1-mediated transport of daunorubicin, P-gp-mediated transport of calcein AM and BCRP-mediated transport of pheophorbide A, as indicated by the intersection at the abscissa. The basic mathematical equations behind this can be drawn from reference [355]. Experimental section 6.3.10.1 gives a short summary.

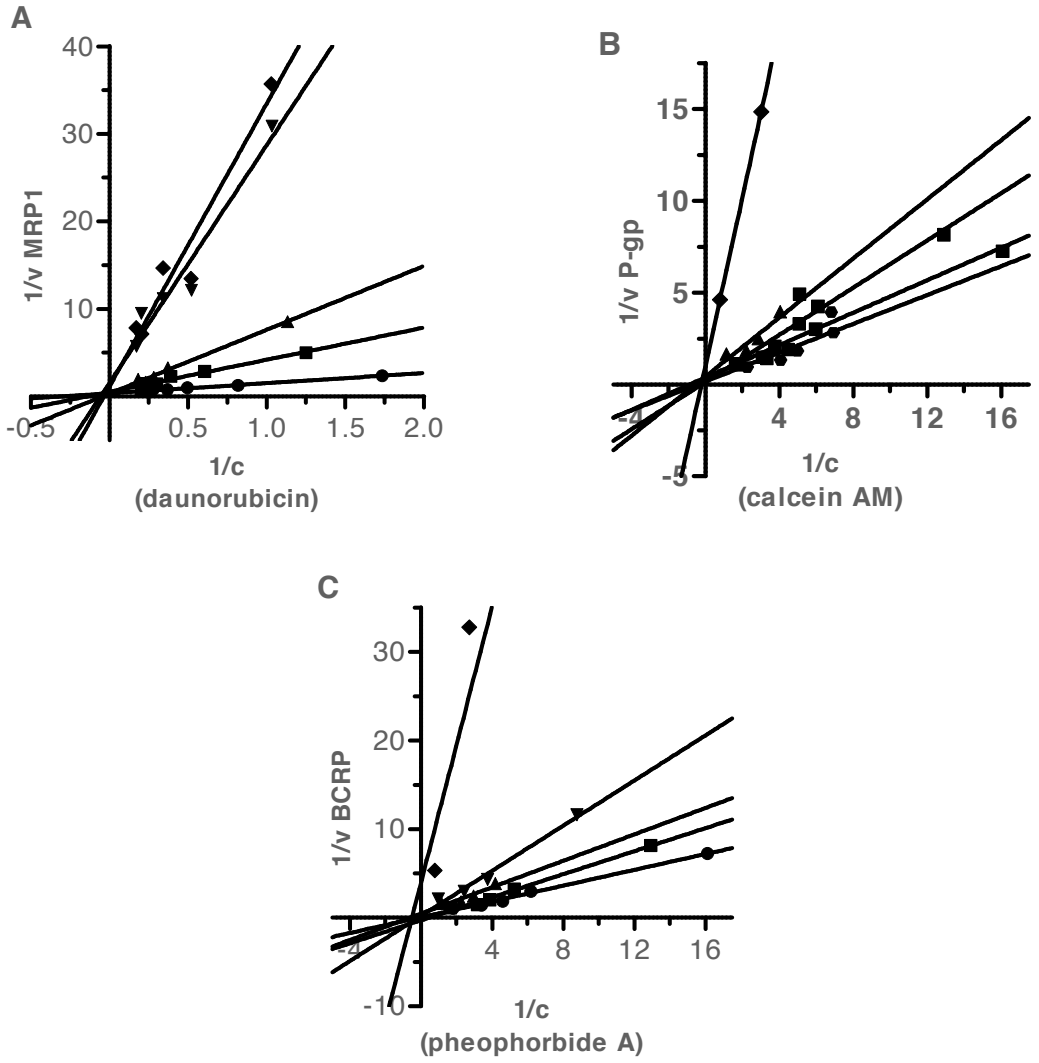

Figure 4.29. Lineweaver-Burk analysis of compound **125** using H69AR (MRP1, A), A2780/ADR (P-gp, B) and MDCK II BCRP cells (BCRP, C). Concentrations of compound **125** were as follows: 0.1 (closed squares), 0.25 (closed upward triangles), 0.5 (closed downward triangles) and 2.5 μmol · L^{-1} (closed rhombs); closed circles: control. (A): Daunorubicin was used at 1.0, 2.0, 3.0, 4.0, 5.0 and 6.0 μmol · L^{-1}; (B): Calcein AM was used at 0.1, 0.2, 0.3, 0.4, 0.5, and 0.6 μmol · L^{-1}; (C): Pheophorbide A was used at 0.2, 0.4, 0.5, 0.75, 1.0 and 1.5 μmol · L^{-1}.

4.3.6. Determination of Intrinsic Toxicity

All synthesized 9-deazapurines of this subchapter were evaluated with respect to their intrinsic toxicity toward the used cell lines (H69AR, A2780/ADR and MDCK II BCRP as well as their sensitive counterparts). As in the screening experiments (see Figures 4.25-28), the compounds were used at 10 μmol · L^{-1}. Figures 4.30 A-C summarize the biological data, which was determined by Katja Stefan.

It can be seen that most compounds were nontoxic with respect to H69AR and H69 cells, except for compounds **118**, **127** and **129**, which possessed slight toxicity. With regard to

A2780/ADR and A2780 cells, the tested compounds reduced the cell viability to a value of approximately 60% except for compound **138**, that was more toxic. Concerning MDCK II BCRP and wild type cells only the four compounds **117-118**, **138** and **140** showed slight to severe toxicity, while all other compounds led to no reduction of cell viability. In summary, except for the stated compounds, the evaluated substances of this subchapter have no noteworthy toxicity up to a concentration of 10 μmol · L^{-1}.

Since compound **125** was the only representative of a very effective triple inhibitor, it was evaluated with respect to its full spectrum of cell toxicity at varying concentrations. Table 4.19 gives the therapeutic ratio calculated for to all used cell lines. Since the values are around 10 or higher, it represents a good candidate for clinical evaluation as MDR reverser in specific cancers that simultaneously overexpress the three herein presented MDR-conferring transport proteins.

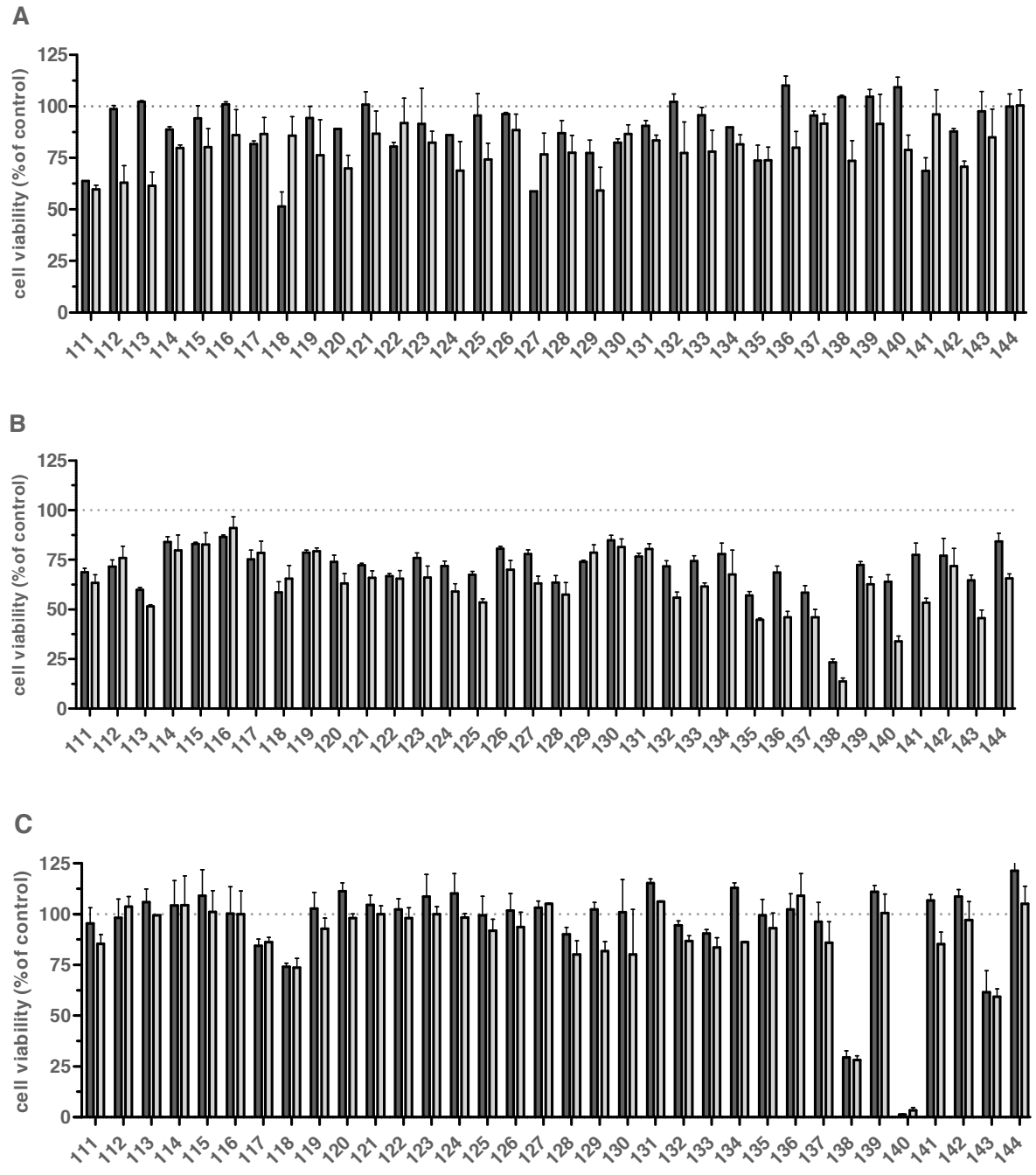

Figure 4.30. MTT-viability assay results of compounds **111**-**144** at 10 μmol · L^{-1} with respect to the corresponding transporter-overexpressing cells (dark grey bar) and the sensitive counterpart (light grey bar). 100% is defined as pure cell culture medium and 0% cell viability by 10% DMSO, respectively. Shown is mean ± SEM of at least three independent experiments with duplicate measurements. (A): H69AR (dark grey bark) and H69 (light grey bark) cells. (B): A2780/ADR (dark grey bark) and A2780 (light grey bark) cells. (C) MDCK II BRCP (dark grey bark) and MDCK II (light grey bark) cells. Shown are at least three independent experiments with duplicate measurements.

Table 4.19. GI_{50} values of compound **125** with respect to the six evaluated cell lines as well as the calculated therapeutic ratio (tr) using the above stated IC_{50} values out of the corresponding test system (see Table 4.16 A and section 6.3.6).

cell line	GI_{50} ± SEM [μmol · L^{-1}]	pGI_{50} ± SEM	IC_{50} ± SEM [μmol · L^{-1}]	tr
H69AR	152 ± 20	3.822 ± 0.085	0.501 ± 0.025	303
H69	55.4 ± 4.8	4.258 ± 0.057		
A2780/ADR	13.7 ± 0.3	4.863 ± 0.014	1.46 ± 0.10	9.38
A2780	6.36 ± 0.11	5.196 ± 0.011		
MDCK II BCRP	23.2 ± 1.0	4.634 ± 0.027	1.69 ± 0.07	13.7
MDCK II	37.2 ± 0.1	4.430 ± 0.001		

4.3.7. MDR Reversal-efficacy of Triple Inhibitor No. 125

Restoration of sensitivity of cancer cells is the most important measure of compound evaluation. Compound **125** as the best and most promising triple inhibitor of the 9-deazapurines was tested using H69AR, A2780/ADR and MDCK II BCRP cells as well as their sensitive counterparts. Figures 4.31 A-C show graphically the obtained concentration-effect curves. Table 4.20 A lists the calculated EC_{50} values of daunorubicin (MRP1, P-gp) and SN-38 (BCRP) in combination with compound **125** as well as the corresponding resistance factor (rf; see section 6.3.7) and potentiation factor (pf; see section 6.3.8). This assay was performed by Katja Stefan.

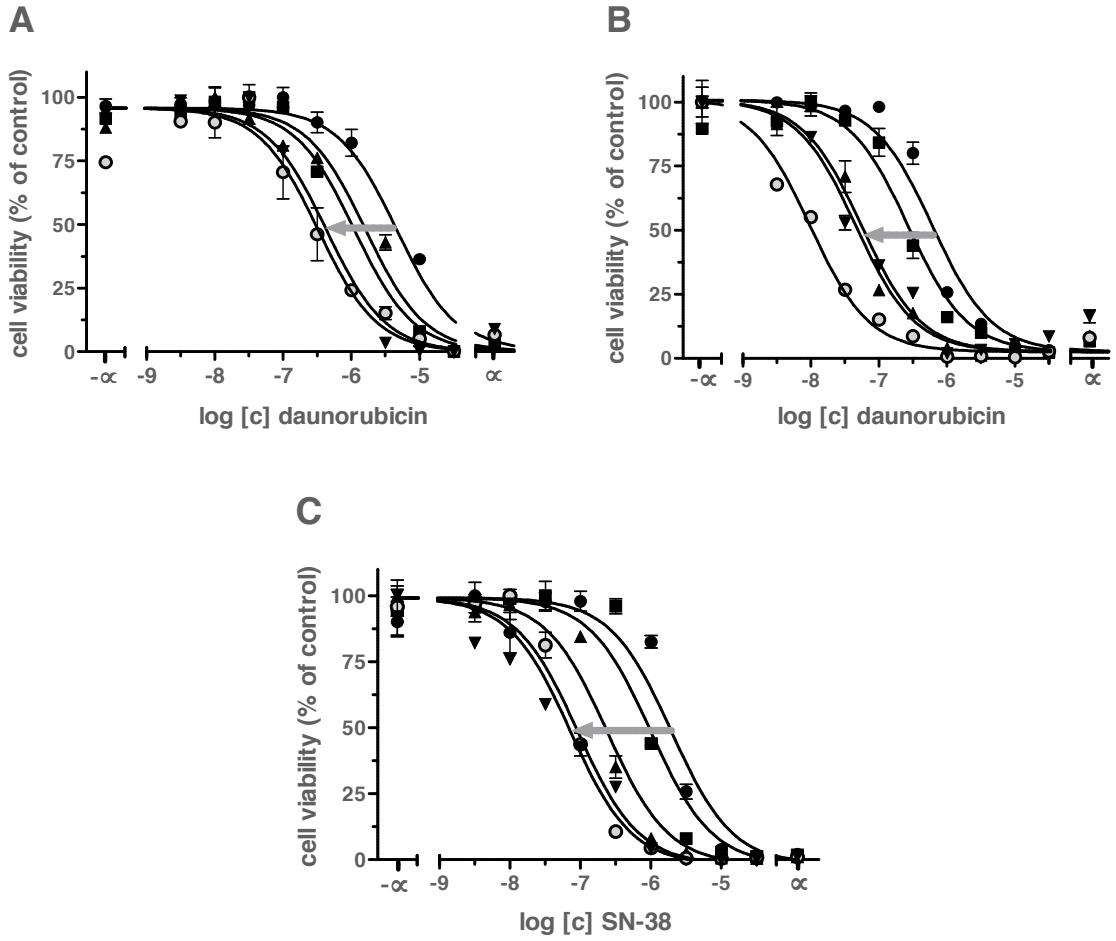

Figure 4.31. Reversal of MRP1- (A), P-gp- (B), and BCRP (C)-mediated MDR using H69AR (A), A2780/ADR (B) and MDCK II BCRP (C) cells (control, closed circles) as well as their sensitive counterparts H69 (A), A2780 (B) and MDCK II (C) (open circles). Compound **125** was used at 0.1 (closed squares), 1 (upward closed triangles) and 10 μmol · L^{-1} (downward closed triangles). Daunorubicin was used for MRP1 and P-gp (A-B) and SN-38 for BCRP (C). Shown are at least three independent experiments with duplicate measurements.

Table 4.20 A. MDR reversal-efficacy data obtained for compound **125** as well as calculated resistance and potentiation factors (see sections 6.3.7-8) with respect to the tested transporters in three different cell lines. Shown is also the degree of sensitization (°s; see section 6.3.9) determined at 10 μmol · L^{-1} compound concentration.

ABC-Transporter	resist. cells GI_{50} ± SEM [μmol · L^{-1}]	0.1 μM GI_{50} ± SEM [μmol · L^{-1}]	1 μM GI_{50} ± SEM [μmol · L^{-1}]	10 μM GI_{50} ± SEM [μmol · L^{-1}]	sens. cells GI_{50} ± SEM [μmol · L^{-1}]	°s [%]
MRP1	3.84 ± 0.60	2.10 ± 0.29	1.17 ± 0.003	0.445 ± 0.003	0.361 ± 0.016	
rf	11	5.8	3.2	1.2	1	81
pf	1	1.8	3.3	8.6	11	
P-gp	0.575 ± 0.005	0.286 ± 0.004	0.058 ± 0.001	0.044 ± 0.002	0.010 ± 0.001	
rf	54	27	5.5	4.1	1	24
pf	1	2.0	9.8	13	54	
BCRP	1.71 ± 0.16	0.916 ± 0.054	0.211 ± 0.002	0.061± 0.007	0.086 ± 0.004	
rf	20	11	2.5	0.7	1	140
pf	1	1.9	8.1	28	20	

Compound **125** has the ability to sensitize all three MDR cell lines (see Tables 4.20 A-B). While the H69AR and MDCK II BCRP cells showed complete reversal of MDR, the A2780/ADR were only partially sensitized (°s = 24%). Although this value seems to be low, one must take the logarithmic scale into account. Compound **125** decreased the resistance of P-gp overexpressing A2780/ADR cells from a factor of 54 to a factor of only 4. This means compound **125** potentiated the toxicity of daunorubicin by a factor of 13. Figure 4.32 shows the pGI_{50} values taken from Table 4.20 A of the corresponding used cytotoxic agents plotted against the used concentrations of compound **125** (log [c]). As already explained in section 4.1.6, the resultant EC_{50} represents the concentration of the inhibitor, at which the resistance of the corresponding cell line is reduced by 50%. These are 0.959 ± 0.126 (MRP1), 0.563 ± 0.060 (P-gp) and 0.478 ± 0.053 (BCRP). This shows that submicromolar concentrations are necessary to reduce the resistance of the tested MDR cell lines by half. Triple inhibitors of this quality and effectiveness have never been described before. Being *de facto* a 'dirty drug', compound **125** is a noticeable aspirant for clinical evaluation.

Table 4.20 B. Negative decadic logarithm of GI_{50} values taken from Table 4.20 A.

ABC-transporter	resist. cells pGI_{50} ± SEM	0.1 μM pGI_{50} ± SEM	1 μM pGI_{50} ± SEM	10 μM pGI_{50} ± SEM	sens. cells pGI_{50} ± SEM	pEC_{50}
MRP1	5.421 ± 0.103	5.683 ± 0.091	5.934 ± 0.002	6.352 ± 0.005	6.444 ± 0.029	6.022 ± 0.086
P-gp	6.240 ± 0.006	6.543 ± 0.010	7.233 ± 0.014	7.353 ± 0.027	7.972 ± 0.067	6.252 ± 0.070
BCRP	5.768 ± 0.060	6.039 ± 0.039	6.676 ± 0.006	7.215 ±0.071	7.068 ± 0.032	6.323 ± 0.073

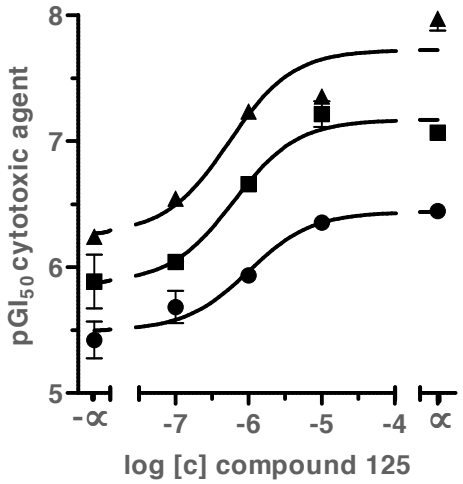

Figure 4.32. Evaluation of the efficacy of compounds **125** with respect to its MDR reversing potency using H69AR (closed circles), A2780/ADR (closed triangles) and MDCK II BCRP (closed upward triangles) cells. On the ordinate the determined pGI_{50} values of Table 4.20 B are plotted. On the abscissa, the used compound concentrations are presented. Each resultant curve is calculated from five data points and constrained to the data of the resistant (-∝, bottom) and sensitive cell line (∝, top).

4.3.8. Summary of Evaluation of 7,8-alicyclic-, 7-*N*-alkyl-, -aryl- or -arylalkyl-, and 8,9-annulated-9-deazapurines with Heteroaromatic Variations

9-deazapurines with heterocyclic elements were synthesized to obtain more new and potent inhibitors of MRP1, but also P-gp and BCRP, since the used structural elements were already known to be part of inhibitors of ABC-transport proteins. Containing compounds of rather poor selectivity, this compound class has promising members with respect to multiple inhibition of ABC transporters. Compounds **112**, **122**, and **135** are representatives of good dual MRP1/P-gp inhibitors, with low single-digit micromolar inhibitory activity, although the latter had an insufficient I_{max} with respect to MRP1 inhibition compared to the standard compound **74**.

Dual Inhibitors of MRP1 and BCRP were also found, which was more interesting due to lack of reports in literature. Compounds **116**, **139** and **144** are promising structures for further experiments.

Although compound **139** yielded the best IC_{50} determined in this work regarding MRP1, the compound failed to inhibit this transporter in comparable magnitude as the standard compound **74**. The same holds for compound **144**.

Compound **125** is the best hit out of this subchapter. It had good inhibitory power toward all the herein tested ABC-transport proteins around 1 μmol · L^{-1}. Additionally, the magnitude of the effect of 10 μmol · L^{-1} of compound **125** was comparable to the effect of the corresponding standard compounds at the same concentration. Furthermore, compound **125** showed to be a noncompetitive inhibitor of daunorubicin (MRP1), calcein AM (P-gp) and pheophorbide A (BCRP) transport. While possessing only slight toxicity toward the corresponding cell lines having a therapeutic ratio of at least around 9, compound **125** was able to reverse resistance of H69AR (MRP1), A2780/ADR (P-gp) and MDCK II BCRP (BCRP) cells. Furthermore, it was found that submicromolar concentrations are sufficient to reduce cancer cell growth by half. A triple inhibitor with these characteristics has never been reported before in the literature and makes this compound a very good candidate for clinical evaluation against cancer cells that simultaneously overexpress the three herein presented MDR-conferring transport proteins.

5. Summary

Expression of ABC-transport proteins is a major obstacle in cancer chemotherapy. Especially MRP1, P-gp and BCRP are expressed in different malignancies like lung cancer, colon carcinomas, leukemias, bladder cancer, myeloma, ovarian carcinomas or breast cancer, often simultaneously. These key proteins extrude a variety of structurally diverse antineoplastic agents out of cells, which results in the phenomenon called multidrug resistance (MDR). Many compounds of different origin were found to inhibit different ABC-transporters, e.g. pharmacological drugs, natural compounds, intrinsic substrates and synthetic compounds derived from screening of huge compound libraries. But most of these inhibitors lacked the necessary potency and selectivity, and often led to severe side effects in clinical evaluations. Especially with respect to MRP1, only rare reports have been made for compounds in the submicromolar concentration range. Hence, the development of new compounds is desirable to obtain more potent inhibitors for this transport protein.

The aim of the thesis was to develop new, potent, nontoxic and selective inhibitors of MRP1, based on earlier reports of pyrrolo- and indolopyrimidines. The compounds have been evaluated in two different assays, the calcein AM and daunorubicin assay.

The substituents of the starting compound **74** were varied to elucidate the preferences with regard to MRP1 inhibition. It was found that the phenethylpiperazine side chain at position 6 was superior in comparison to shortened alkyl linker or abolishing of the piperazine partial structure. Additionally, alkyl, aryl or arylalkyl substituents could be introduced at position 7 leading to potent compounds in submicromolar range. Compound **92** with its cyclopropyl residue was shown to be the best inhibitor of the newly synthesized compounds. It was equally potent in comparison to the standard inhibitor and starting compound **74**. But in contrast to the latter, the former had no inhibitory activity against P-gp and BCRP, which makes this compound a very selective inhibitor of MRP1. Compound **92** was able to reduce MDR of H69AR cells by half in submicromolar concentration range, reversed MRP1-mediated MDR completely at 10 μmol · L^{-1} and possessed no noteworthy toxicity at this

concentration. Compound **92** is only six times less effective than the best known inhibitor of MRP1, and in contrast to the latter, it is absolutely selective, which makes it a great aspirant for clinical evaluation in cancer cell lines that overexpress MRP1.

Purine analogs of 9-deazapurines showed only inhibitory power in upper double-digit concentration range, but were able to stimulate MRP1-mediated transport. This was found for calcein AM and daunorubicin in two different MRP1 expressing cell lines, H69AR and MDCK II MRP1. Several 9-deazapurines also stimulated MRP1-mediated transport, although long side chains at position 6 also gave compounds with moderate to good inhibitory power. These compounds gave biphasic concentration-effect curves. Most of the compounds were selective inhibitors of MRP1, only compound **104** affected all three transporters in an inhibitory way. It was the first herein reported triple inhibitor, although the inhibitory power toward P-gp and BCRP was rather low. The purine and 9-deazapurine activators were biologically evaluated with respect to their half-maximal activating concentration and activation ratio, which could only be observed with respect to MRP1. Analyzation of the type of activation of compound **101** as representative of the MRP1 activators showed that these compounds are nonessential activators, most likely "mixed-type" according to *Segel's* "Enzyme Kinetics". Although the compounds could reduce the intracellular concentration of the cytotoxic agent daunorubicin in the daunorubicin assay, this activating power could not be transferred to the MDR reversal-efficacy assay. Except for compound **110**, none of the compounds enhanced MDR, on the contrary compounds with good inhibitory power rather reversed resistance in MRP1 overexpressing cancer cell lines (e.g. **104**).

Since pyrrolo- und indolopyrimidines were shown before to inhibit P-gp, but also BCRP, some 9-deazapurines were evaluated regarding their capability to inhibit all three transporters reported in this thesis. Besides some dual inhibitors, compound **125** was found as the best triple inhibitor ever reported until now. It was able to inhibit MRP1 in submicromolar range and P-gp as well as BCRP at low micromolar concentrations. It is a noncompetitive inhibitor of daunorubicin, calcein AM and pheophorbide A transport mediated by MRP1, P-gp and BCRP, respectively. Finally, the compound could reduce MDR in several cancer cell lines. The effectiveness of this MDR reversal was in submicromolar range, comparable to the data obtained for the standard inhibitor **74** and the best compound of this thesis, **92**. This makes compound **125** also a great aspirant for clinical evaluation for use in cancers with multiple expression of ABC-transport proteins.

Finally, the H69AR lung cancer cell line could be established as test system and compounds **74** and **126** were established as standard inhibitors for the calcein AM and daunorubicin assay, superseding the former standard inhibitors indomethacin, cyclosporine A, MK571 and ONO-1078, which all lacked either the necessary selectivity, potency or reliability.

The results of this thesis give new insights in the field of MRP1-mediated MDR and the compound classes of purines and 9-deazapurines. These contain compounds that inhibit MRP1 with great potency and selectivity, which has rarely been reported. But also broad-spectrum inhibitors have been found, which is a good starting point for clinical evaluation in oncology. Finally, the activating property of several representatives might be a good tool for further experiments to elucidate the mechanistic aspects of ABC-transport proteins.

6. Experimental Section

6.1. Materials and Methods for Chemical Synthesis

6.1.1. Chemicals and Solvents

All chemicals and solvents were supplied by Acros Organics (Geel, Belgium), Alfa Aesar (Karlsruhe, Germany), Applichem GmbH (Darmstadt, Germany), ChemSolute (a brand of Th. Geyer GmbH & Co. KG, Renningen, Germany), Fisher Scientific GmbH (Waltham, MA, USA), Grüssing GmbH Analytika (Filsum, Germany), Julius Hösch GmbH und Co. KG (Düren, Germany), Merck Millipore (Billerica, MA, USA), Sigma-Aldrich (St. Louis, MO, USA), TCI Deutschland GmbH (Eschborn, Germany), VWR International GmbH (Darmstadt, Germany) and Wacker Chemie (München, Germany) and were used for synthesis without further purification. Demineralized water was generated using a WAT membrantec module (WAT membrantec water services GmbH, Erkrath, Germany) and ultrapure water was gained using PureLab flex purification system (Elga LabWater / Veolia Water Technologies, Celle, Germany). Table 6.1 summarizes used educts and building blocks for the compounds described in this work. Table 6.2 gives a summary of the used solvents.

Table 6.1. List of used chemicals and building blocks for synthesis of intermediates **1**-**73** and compounds **74**-**144**.

name	provider	used for compound no.
acetic anhydryide	Grüssing	**5**
2-aminobenzonitrile	Alfa Aesar	**5**
ammonia solution (25%)	ChemSolute	**45**-**58**
aniline	Alfa Aesar	**11**,**83**
azepan-2-one (syn. ε-caprolactam)	Alfa Aesar	**2**

name	provider	used for compound no.
1-benzhydrylpiperazine	Fluka	**76**,**86**,**109**,**138**
(syn. 1-(diphenylmethyl)piperazine)		
benzylamine	Acros Organics	**14**,**82**,**101-103**
1-benzylpiperazine	Alfa Aesar	**75**,**85**,**94**,**96**,**98**,**100**,**108**,**133**,**135**,**137**
3-(2-bromoethyl)-1*H*-indole	Sigma-Aldrich	**73**
6-chloropurine	Alfa Aesar	**107-110**
cyclopropylamine	Alfa Aesar	**10**
diisopropylethylamine (Hünig's base)	TCI	**73**
N,*N*-dimethylformamide dimethyl acetale	Alfa Aesar	**31-44**
dimethyl sulfate	Sigma-Aldrich	**1-2**
(ethoxymethylene)malononitrile	Sigma-Aldrich	**6-16**
4-ethoxyaniline (syn. *p*-phenethidine)	Merck Millipore	**13**
ethylamine hydrochloride	Alfa Aesar	**7**
ethyl bromoacetate	Acros Organics	**17-30**
1-furanoylpiperazine	Alfa Aesar	**130-131**,**144**
(syn. 1-(2-furoyl)piperazine)		
isopropylamine	Alfa aesar	**9**
magnesium sulfate	VWR Chemicals	**1-2**
malononitrile	Sigma-Aldrich	**3-4**
2-methoxyaniline (syn. *o*-anisidine)	Merck Millipore	**12**
methylamine hydrochloride	Alfa Aesar	**6**
1-methylpiperazine	Fluka	**78**
parrafin oil	Wacker Chemie	**1-2**, **17-72**
phenethylamine	Alfa Aesar	**15**,**81**,**105**
1-phenethylpiperazine	Alfa Aesar	**74**,**84**,**88-93**,**95**,**97**,**99**,**107**,**132**,**134**,**136**
(syn. 1-(2-phenethyl)piperazine)		
1-phenylpiperazine	Acros Organics	**77**,**87**,**110**,**139**
phenylpropylamine	Alfa Aesar	**16**,**80**,**104**,**106**
phosphoryl chloride	Acros Organics	**59-72**
piperazine (anhydrous)	Merck Millipore	**73**
piperidin-2-one (syn. δ-valerolactam)	Alfa Aesar	**1**
1-piperonylpiperazine	Acros Organics	**126-129**,**143**
propylamine	Alfa Aesar	**8**
potassium carbonate	Alfa Aesar	**17-30**
1-(pyridin-2-yl)piperazine	Acros Organics	**116-117**,**142**
4-(2-(pyridin-2-yl)ethyl)piperazine	Sigma-Aldrich	**141**
1-(2-(pyridin-4-yl)ethyl)piperazine	Sigma Aldrich	**114-115**
sodium hydroxide	VWR Chemicals	**1-2**, **45-58**
triethylamine (TEA)	Acros Organics	**6-7**, **74-144**
tryptamine	Sigma Aldrich	**113**
(syn. 2-(1*H*-indole-3-yl)ethan-1-amine)		

Table 6.2. List of used solvents for chemical synthesis, thin layer chromatography (TLC), column chromatography (CC), crystallization (cry.) of compounds **1**-**73** or NMR- or LC-MS analysis.

name	provider	used for
acetic acid	Fisher Chemical	synthesis (no. **45**-**58**)
acetic anhydride	Grüssing	synthesis (no. **5**)
acetone	Julius Hösch	TLC, CC
acetonitrile	Fisher Chemical	synthesis (no. **73**)
ammonia solution (25%)	ChemSolute	synthesis (no. **45**-**58**), TLC, CC
benzene	Applichem	synthesis (no. **1**-**29**
$CDCl_3$	Deutero	NMR
DMSO-d_6	Deutero	NMR
ethanol	Julius Hösch	synthesis (no. **3**-**16**, **45**-**58**), TLC, CC, cry.
methanol	Sigma-Aldrich	TLC, CC
methanol, LC-MS grade	VWR Chemicals	LC-MS
methylene chloride	Julius Hösch	TLC, CC
N,*N*-dimethylformamide	Fisher Chemical	synthesis (no. **17**-**44**)
petroleum ether	Julius Hösch	synthesis (no. **31**-**44**) TLC, CC, cry.
phosphoryl chloride	Acros Organics	synthesis (no. **59**-**72**)
water, demineralized	wat membrantec	synthesis (no. **5**, **17**-**30**, **45**-**72**)
water, ultrapure	Elga PureLab flex	LC-MS

6.1.2. Standard Operation Procedures for Chemical Synthesis

6.1.2.1. Appliances Used for Chemical Synthesis

The standard operation procedures for analogous synthesis were performed using the in Table 6.3 listed appliances.

Table 6.3. List of appliances used for chemical synthesis.

equipment	provider
Braun Injekt 10 mL syringe	B. Braun Melsungen AG (Melsungen, Germany)
diaphragm vacuum pump	Vacuubrand GmbH + Co. KG (Wertheim, Germany)
drying cabinet T 420 S0	Hereus Holding GmbH (Hanau, Germany)
evaporator R-3 HB	Büchi Labortechnik AG (Flawil, Switzerland)
glass Pasteur pipettes (150 mm)	Brand GmbH + Co. KG (Wertheim, Germany)
hot-plate magnetic-stirrer	C. Gerhardt GmbH & Co. KG (Königswinter, Germany)
hot-plate magnetic-stirrer RCT standard	OKA-Werke GmbH Co. KG (Staufen, Germany)
Katrin system towel M 2	Metsä tissue GmbH (Kreuzau, Germany)
magnetic-stirrer MAG	C. Gerhardt GmbH & Co. KG (Königswinter, Germany)
micro scale MC1 Analytic AC 210 S	Sartorius AG (Göttingen, Germany)

equipment	provider
Microflex xceed powder-free nitrile examination gloves (M)	Microflex (Reno, Nevada, United States of America)
NORM-JECT tuberculin 1 mL syringe	Henke Sass Wolf (Tuttlingen, Germany)
Sterican 0.80 x 120 mm cannula	B. Braun Melsungen AG (Melsungen, Germany)
ultrasonic cleaner	VWR International GmbH (Darmstadt, Germany)
UV cabinet II	Camag (Muttent, Switzerland)
UV lamp	Camag (Muttent, Switzerland)

6.1.2.2. Microwave-assisted Synthesis

Microwave-assisted synthesis was performed using a CEM Discover Microwave (CEM GmbH, Kamp-Lintfort, Germany). The reaction mixture in acetic anhydride (**5**) or *N*,*N*-dimethylformamide (**74-144**) was heated to 100 °C (**5**) or 110 °C (**74-144**) at 200 W for 20-60 minutes.

6.1.2.3. Thin Layer Chromatography (TLC)

Reaction progress was monitored by thin layer chromatography (TLC) using silica gel F_{254} coated aluminum plates. A solution of compounds in methanol or methylene chloride was applied using glass capillaries (approx. 10 μL) about 1 cm above the edge of the plate. After the spots had dried, the plate was put into a glass TLC developing chamber and rested for the time of eluation until the solvent front moved about 1 cm distance to the top edge of the plate. The eluent was allowed to dry followed by detection of the spots via fluorescence quenching using an UV cabinet equipped with an UV lamp at 254 nm. Table 6.4 shows all used materials for TLC and Table 6.5 gives an overview of the used eluents.

Table 6.4. Summary of used materials for thin layer chromatography (TLC).

equipment	provider
glass capillaries	Hilgenberg GmbH (Malsfeld, Germany; distributed by OMNILAB GmbH & Co. KG, Bremen, Germany)
silica gel F_{254} coated aluminum plate	Merck Millipore, Billerica, MA, USA

Table 6.5. Summary of used eluents for thin layer chromatography (TLC).

eluent	solvent mixture
methylene chloride / acetone	18:1
methylene chloride / acetone	9:1
methylene chloride / acetone / methanol	18:1:1
methylene chloride / acetone / methanol	9:1:1
methylene chloride / acetone / ethanol / ammonia (25%) solution	1:1:1:0.5

6.1.2.4. Column Chromatography (CC)

Individual intermediates and all compounds were purified by column chromatography (CC). The glass column was packed with a slurry of silica gel 60 (43-60 μm; stationary phase) and the first solvent mixture (mobile phase) of the gradient elution, mostly petroleum ether or petroleum ether / methylene chloride (1:1). The viscous suspension of silica gel was poured into the glass column after a wad of glass wool had been put in the base of the CC tube. An aquarium pump was used to compress the gel and increase the throughput of solvent generating a constant flowing stream. When the gel surface was reached, the solved or suspended compound (solute) in methylene chloride was put on the silica gel using a glass Pasteur pipette. The elevated solvent level was reduced using the pump until the compound was fully transferred into the adsorbent resulting in a narrow transverse band. Finally, employing gradient elution (200 mL each step), the compounds were purified and the eluent solution was collected in small glass fraction tubes (10 mL). The collected fractions were spotted on a TLC plate and the relevant fractions combined, evaporated and the resulting compound crystallized from methanol / petroleum ether 1:10. Table 6.6 shows all used materials for column chromatography, while Table 6.7 gives an overview of the used eluents for CC.

Table 6.6. Summary of used materials for column chromatography.

equipment	provider
aquarium pump	Optima (Hagen, Germany)
glass fraction tubes (10 mL)	Brand GmbH + Co. KG (Wertheim, Germany)
glass Pasteur pipettes (230 mm)	Brand GmbH + Co. KG (Wertheim, Germany)
silica gel 60 (43-60 μm)	Merck Millipore, Billerica, MA, USA

Table 6.7. Summary of used eluents for column chromatography.

eluent	solvent mixture
pretroleum ether	1
petroleum ether / methylene chloride	1:1
methylene chloride	1
methylene chloride / acetone	18:1
methylene chloride / acetone	9:1
methylene chloride / acetone / methanol	18:1:1
methylene chloride / acetone / methanol	9:1:1
methylene chloride / acetone / ethanol / ammonia (25%) solution	1:1:1:0.5
methylene chloride / acetone / ethanol / ammonia (25%) solution	1:1:1:1

6.1.2.5. Nuclear Magnetic Resonance (NMR)

^{1}H NMR spectroscopy was generally used to identify the intermediates **1-73** in case crystallization or solidification was possible. Additionally, the purified compounds **74-144** were characterized with respect to identity and purity by ^{1}H as well as ^{13}C NMR spectroscopy. The NMR spectra were recorded in DMSO-d_6 or $CDCl_3$ employing a Bruker Avance 500 MHz (500/126 MHz). The chemical shifts (δ) are expressed as ppm calibrated to the solvent signal of DMSO (^{1}H NMR δ 2.50; ^{13}C NMR δ 39.5) or $CDCl_3$ (^{1}H NMR δ 7.26; ^{13}C NMR δ 77.1). Distortionless enhancement by polarization transfer (DEPT) and attached proton test (APT) techniques were used to assign ^{13}C signals. Spin multiplicities of the compounds **1-144** are depicted as singulet (s), doublet (d), doublet of doublets (dd), doublet of doublet of doublets (ddd), triplet of doublets (td), triplet (t), doublet of triplets (dt), quartet (q), quintet (quint), heptet (hept) and multiplet (m). The resulting raw data was analyzed using MestReNova. Table 6.8 gives a summary of the used materials and software with respect to NMR spectroscopy. This work was kindly performed by the technical assistants Sabine Terhart-Krabbe, Annette Reiner and Marion Schneider.

Table 6.8. Summary of used materials and software for nuclear magnetic resonance.

equipment	provider
Bruker Avance 500 MHz NMR spectrometer	Bruker (Billerica, Massachusetts, United States of America)
$CDCl_3$	Deutero GmbH (Kastellaun, Germany)
DMSO-d_6	Deutero GmbH (Kastellaun, Germany)
MestReNova (Version 6.0.2-5475)	Mestrelab Research (Santiago de Compostella, Spain)

6.1.2.6. Liquid Chromatography-Mass Spectrometry (LC-MS)

All target compounds were analyzed with regard to their molecular weight to determine their identity and purity. An Agilent 1100 series with photo diode array (DAD) detector with a Nucleodur column C18 was used to analyze the target compounds, followed by ESI mass spectrometry with an API 200 Triple Quadrupole mass spectrometer. 0.1-0.3 mg of the compound was solved in 8 μL of LC-MS grade methanol. Starting with 90% water and 10% methanol, gradient elution was performed with a constant flow of 300 $\mu L \cdot min^{-1}$. Compound detection was performed via photo diode array (DAD). Analysis was conducted using the Sciex Analyst Software. The purity of all investigated compounds in biological testing in this work was determined as ≥ 90%. Table 6.9 gives a summary of the used equipment and software in LC-MS analysis. This work was kindly performed by Marion Schneider.

Table 6.9. Summary of used materials and softwares used for LC-MS.

equipment	provider
Agilent 1100 HPLC system	Agilent (Böblingen, Germany)
API 2000 Triple Quadrupole mass spectrometer	Applied Biosystems (Darmstadt, Germany)
methanol, LC-MS grade	VWR International GmbH (Darmstadt, Germany)
Nucleodur column EC50 C18 Gravity 3 μm	Macherey-Nagel (Düren, Germany)
Sciex Analyst Software version 1.5.1	AB Sciex Germany GmbH

6.1.3. Synthesis and Characterization of Intermediates

6.1.3.1. *O*-methylation of Starting Compounds

The corresponding lactam solved in an adequate volume of benzene was heated to reflux before dropwise addition of an equimolar amount of dimethyl sulfate. After 3-6 hours a 4 $mol \cdot L^{-1}$ solution of sodium hydroxide was added to eliminate excess dimethyl sulfate, stirring for further 30 minutes. The benzene phase reaction was separated and the water phase was extracted three times with 50 mL benzene. The organic phases were combined and dried over magnesium sulfate. Filtration and evaporation resulted in an oil containing the methylated product that was used without further characterization and purification.

6.1.3.1.1. Synthesis of **6-methoxy-2,3,4,5-tetrahydropyridine (1)**

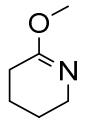

synonyms:	SMS-**A-1** compound **1a** (*J. Med. Chem.* **2016**, *59*, 3018–3033)
educts:	piperidin-2-one (syn. δ-valerolactam) and dimethyl sulfate (1 eq.)
yield:	not determined
visual appearance:	yellowish oil
chemical formula:	$C_6H_{11}NO$
molecular weight:	113.16 Da
LC-MS analysis:	calculated: 113.08 Da; found: not determined
purity:	not determined
^{1}H NMR:	not determined
^{13}C NMR:	not determined

6.1.3.1.2. Synthesis of **7-methoxy-3,4,5,6-tetrahydro-2*H*-azepine (2)**

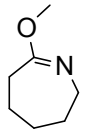

synonyms:	SMS-**A-28** compound **1b** (*J. Med. Chem.* **2016**, *59*, 3018–3033)
educts:	azepan-2-one (syn. ε-caprolactam) and dimethyl sulfate (1 eq.)
yield:	not determined
visual appearance:	yellowish oil
chemical formula:	$C_7H_{13}NO$
molecular weight:	127.19 Da
LC-MS analysis:	calculated: 127.10 Da; found: not determined
purity:	not determined
^{1}H NMR:	not determined
^{13}C NMR:	not determined

6.1.3.2. Synthesis of Malononitrile Derivatives

To compounds **1** or **2** a saturated, equimolar solution of malononitrile in ethanol was added under stirring. The reaction progress was followed visibly as the resultant malononitrile

derivative precipitated after a reaction time of 5 to 30 minutes. The precipitate was rinsed with ethanol and diethyl ether and dried in a hot-air cabinet.

6.1.3.2.1. Synthesis of **2-(piperidin-2-ylidene)malononitrile (3)**

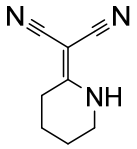

synonyms:	SMS-**A**-**2** compound **2a** (*J. Med. Chem.* **2016**, *59*, 3018–3033)
educts:	6-methoxy-2,3,4,5-tetrahydropyridine (**1**) and malononitrile (1 eq.)
yield:	77%
visual appearance:	white needles
chemical formula:	$C_8H_9N_3$
molecular weight:	147.18 Da
LC-MS analysis:	calculated: 147.08 Da; found: not determined
purity:	not determined
^{1}H NMR:	500 MHz, DMSO-d_6, δ 9.01 (s, 1H), 3.23 (t, J = 6.0 Hz, 2H), 2.55 (t, J = 6.0 Hz, 2H), 1.74-159 (m, 4H)
^{13}C NMR:	126 MHz, DMSO-d_6, δ 171.5, 117.2, 116.0, 45.3, 42.3, 26.8, 20.7, 18.0

6.1.3.2.2. Synthesis of **2-(azepan-2-ylidene)malononitrile (4)**

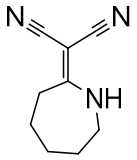

synonyms:	SMS-**A**-**29** compound **2b** (*J. Med. Chem.* **2016**, *59*, 3018–3033)
educts:	7-methoxy-3,4,5,6-tetrahydro-2*H*-azepine (**2**) and malononitrile (1 eq.)
yield:	55%
visual appearance:	white needles
chemical formula:	$C_9H_{11}N_3$
molecular weight:	161.21 Da
LC-MS analysis:	calculated: 161.10 Da; found: not determined
purity:	not determined
^{1}H NMR:	500 MHz, DMSO-d_6, δ 8.93 (s, 1H), 3.41-3.38 (m, 2H), 2.67-2.64 (m, 2H), 1.70-1.64 (m, 2H), 1.58-1.55 (m, 2H), 1.52-1.46 (m, 2H)
^{13}C NMR:	126 MHz, DMSO-d_6, δ 177.1, 117.4, 115.9, 46.9, 44.8, 30.9, 29.2, 27.8, 24.2

6.1.3.3. *N*-acylation of 2-aminobenzonitrile

2-aminobenzonitrile was dissolved in excess acetic anhydride and heated at 100 °C using microwave-assisted synthesis at 200 W and 2 hours. The reaction mixture was poured into water and the precipitate was rinsed with fresh water and filtered, giving the acylated intermediate.

6.1.3.3.1. Synthesis of **N-(2-cyanophenyl)acetamide (5)**

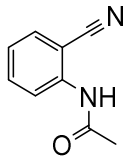

synonyms:	SMS-**A-163** compound **36** (*J. Med. Chem.* **2017**, *accepted 10th of October, 2017*)
educts:	2-aminobenzonitrile and acetic anhydride (excess)
yield:	70%
visual appearance:	white needles
chemical formula:	$C_9H_8N_2O$
molecular weight:	160.18 Da
LC-MS analysis:	calculated: 160.06 Da; found: not determined
purity:	not determined
^{1}H NMR:	500 MHz, DMSO-d_6, δ 10.11 (s, 1H), 7.78 (dd, J = 7.6, 1.4 Hz, 1H), (ddd, J = 8.3, 7.5, 1.6 Hz, 1H), 7.57 (dd, J = 8.4, 0.9 Hz, 1H), 7.32 (td, J = 7.6, 1.2 Hz, 1H), 2.09 (s, 3H)
^{13}C NMR:	126 MHz, DMSO-d_6, δ 168.8, 140.5, 133.9, 133.3, 125.7, 125.6, 117.0, 107.4, 23.3

6.1.3.4. Nucleophilic Substitution of Primary Amines to Form Malononitrile Derivatives

To the corresponding amine a saturated solution of (ethoxymethylene)malononitrile (1.2 eq.) in ethanol was added under stirring. In case of amine hydrochlorides 1.5 eq. of triethylamine (TEA) were additionally added. The reaction progress was followed visibly as the product precipitated after a reaction time of 5-60 minutes of stirring. The precipitate was rinsed with ethanol and diethyl ether and dried.

6.1.3.4.1. Synthesis of **2-((methylamino)methylene)malononitrile (6)**

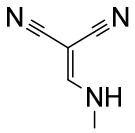

synonyms:	SMS-**A-227** compound **7a** (*J. Med. Chem.* **2016**, *59*, 3018–3033) compound **1a** (*Biochim. Biophys. Acta* **2017**, *1859*, 69–79)
educts:	(ethoxymethylene)malononitrile, methylamine hydrochloride (1.2 eq.) and TEA (2 eq.)
yield:	63%
visual appearance:	yellow needles
chemical formula:	$C_5H_5N_3$
molecular weight:	107.12 Da
LC-MS analysis:	calculated: 107.05 Da; found: not determined
purity:	not determined
^{1}H NMR:	500 MHz, DMSO-d_6, δ 8.91 (s, 1H), 7.86 (s, 1H), 2.96 (s, 3H)
^{13}C NMR:	not determined

6.1.3.4.2. Synthesis of **2-((ethylamino)methylene)malononitrile (7)**

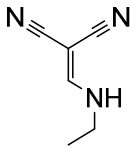

synonyms:	SMS-**A-472** compound **7b** (*J. Med. Chem.* **2016**, *59*, 3018–3033)
educts:	(ethoxymethylene)malononitrile, ethylamine hydrochloride (1.2 eq.) and TEA (2 eq.)
yield:	63%
visual appearance:	yellow needles
chemical formula:	$C_6H_7N_3$
molecular weight:	121.14 Da
LC-MS analysis:	calculated: 121.06 Da; found: not determined
purity:	not determined
^{1}H NMR:	500 MHz, DMSO-d_6, δ 8.91 (s, 1H), 7.86 (s, 1H), 2.96 (s, 3H)
^{13}C NMR:	not determined

6.1.3.4.3. Synthesis of **2-((propylamino)methylene)malononitrile (8)**

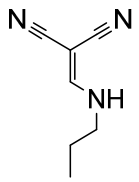

synonyms:	SMS-**A-479** compound **7c** (*J. Med. Chem.* **2016**, *59*, 3018–3033)
educts:	(ethoxymethylene)malononitrile and propylamine (1.2 eq.)
yield:	quantitative
visual appearance:	yellow needles
chemical formula:	$C_7H_9N_3$
molecular weight:	135.17 Da
LC-MS analysis:	calculated: 135.08 Da; found: not determined
purity:	not determined
^{1}H NMR:	500 MHz, DMSO-d_6, δ 9.12 (s, 1H), 7.89 (d, J = 14.8 Hz, 1H), 3.28-3.24 (m, 2H), 1.11 (t, J = 7.2 Hz, 3H)
^{13}C NMR:	not determined

6.1.3.4.4. Synthesis of **2-((isopropylamino)methylene)malononitrile (9)**

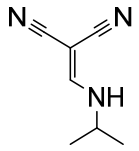

synonyms:	SMS-**A-486** compound **7d** (*J. Med. Chem.* **2016**, *59*, 3018–3033)
educts:	(ethoxymethylene)malononitrile and isopropylamine (1.2 eq.)
yield:	quantitative
visual appearance:	orange needles
chemical formula:	$C_7H_9N_3$
molecular weight:	135.17 Da
LC-MS analysis:	calculated: 135.08 Da; found: not determined
purity:	not determined
^{1}H NMR:	500 MHz, DMSO-d_6, δ 9.12 (s, 1H), 7.89 (d, J = 14.8 Hz, 1H), 3.28-3.24 (m, 2H), 1.11 (t, J = 7.2 Hz, 3H)
^{13}C NMR:	not determined

6.1.3.4.5. Synthesis of **2-((cyclopropylamino)methylene)malononitrile (10)**

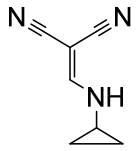

synonyms:	SMS-**A-493**
	compound **7e** (*J. Med. Chem.* **2016**, *59*, 3018–3033)
educts:	(ethoxymethylene)malononitrile and cyclopropylamine (1.2 eq.)
yield:	quantitative
visual appearance:	yellow needles
chemical formula:	$C_7H_7N_3$
molecular weight:	133.15 Da
LC-MS analysis:	calculated: 133.06 Da; found: not determined
purity:	not determined
^{1}H NMR:	not determined
^{13}C NMR:	not determined

6.1.3.4.6. Synthesis of **2-((phenylamino)methylene)malononitrile (11)**

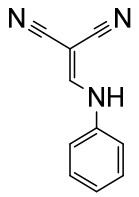

synonyms:	SMS-**A-184**
	compound **7f** (*J. Med. Chem.* **2016**, *59*, 3018–3033)
	compound **1b** (*Biochim. Biophys. Acta* **2017**, *1859*, 69–79)
educts:	(ethoxymethylene)malononitrile and aniline (1.2 eq.)
yield:	78%
visual appearance:	yellow needles
chemical formula:	$C_{10}H_7N_3$
molecular weight:	169.19 Da
LC-MS analysis:	calculated: 169.06 Da; found: not determined
purity:	not determined
^{1}H NMR:	500 MHz, DMSO-d_6, δ 11.09 (s, 1H), 8.49 (s, 1H), 7.42 (d, J = 7.7 Hz, 2H), 7.37 (t, J = 7.4 Hz, 2H), 7.17 (t, J = 7.3 Hz, 1H)
^{13}C NMR:	not determined

6.1.3.4.7. Synthesis of **2-(((2-methoxyphenyl)amino)methylene)malononitrile (12)**

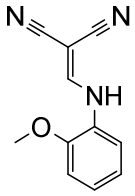

synonyms:	SMS-**A-292**
	compound **31a** (*J. Med. Chem.* **2017**, *accepted 10th of October, 2017*)
educts:	(ethoxymethylene)malononitrile and 2-methoxyaniline (1.2 eq.)
yield:	46%
visual appearance:	yellow needles
chemical formula:	$C_{11}H_9N_3O$
molecular weight:	199.21 Da
LC-MS analysis:	calculated: 199.07 Da; found: not determined
purity:	not determined
^{1}H NMR:	not determined
^{13}C NMR:	not determined

6.1.3.4.8. Synthesis of **2-(((4-ethoxyphenyl)amino)methylene)malononitrile (13)**

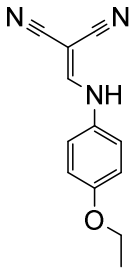

synonyms:	SMS-**A-277**
	compound **31b** (*J. Med. Chem.* **2017**, *accepted 10th of October, 2017*)
educts:	(ethoxymethylene)malononitrile and 4-ethoxyaniline (1.2 eq.)
yield:	73%
visual appearance:	yellowish powder
chemical formula:	$C_{12}H_{11}N_3O$
molecular weight:	213.24 Da
LC-MS analysis:	calculated: 213.09 Da; found: not determined
purity:	not determined
^{1}H NMR:	500 MHz, DMSO-d_6, δ 10.98 (s, 1H), 8.34 (s, 1H), 7.33 (d, J = 9.1 Hz, 2H), 6.91 (d, J = 9.1 Hz, 2H), 4.00 (q, J = 7.0 Hz, 1H), 1.30 (t, J = 7.0 Hz, 3H)
^{13}C NMR:	not determined

6.1.3.4.9. Synthesis of **2-((benzylamino)methylene)malononitrile (14)**

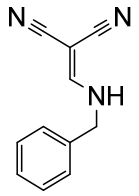

synonyms:	SMS-**A-197** compound **7g** (*J. Med. Chem.* **2016**, *59*, 3018–3033) compound **1c** (*Biochim. Biophys. Acta* **2017**, *1859*, 69–79)
educts:	(ethoxymethylene)malononitrile and benzylamine (1.2 eq.)
yield:	61%
visual appearance:	yellow needles
chemical formula:	$C_{11}H_9N_3$
molecular weight:	183.21 Da
LC-MS analysis:	calculated: 183.08 Da; found: not determined
purity:	not determined
^{1}H NMR:	500 MHz, DMSO-d_6, δ 9.58 (s, 1H), 8.08 (s, 1H), 7.40-7.35 (m, 2H), 7.34-7.28 (m, 3H), 4.44 (s, 2H)
^{13}C NMR:	not determined

6.1.3.4.10. Synthesis of **2-((phenethylamino)methylene)malononitrile (15)**

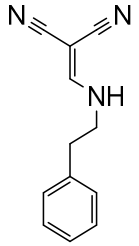

synonyms:	SMS-**A-202** compound **7h** (*J. Med. Chem.* **2016**, *59*, 3018–3033) compound **1d** (*Biochim. Biophys. Acta* **2017**, *1859*, 69–79)
educts:	(ethoxymethylene)malononitrile and phenethylamine (1.2 eq.)
yield:	61%
visual appearance:	white needles
chemical formula:	$C_{12}H_{11}N_3$
molecular weight:	197.24 Da
LC-MS analysis:	calculated: 197.10 Da; found: not determined
purity:	not determined

^{1}H NMR:	500 MHz, DMSO-d_6, δ 9.16 (s, 1H), 7.76 (s, 1H), 7.33-7.29 (m, 2H), 7.24-7.21 (m, 1H), 7.21-7.18 (m, 2H), 3.49 (t, J = 7.1 Hz, 2H), 2.82 (t, J = 7.3 Hz, 2H)
^{13}C NMR:	not determined

6.1.3.4.11. Synthesis of **2-(((3-phenylpropyl)amino)methylene)malononitrile (16)**

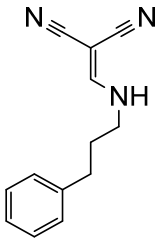

synonyms:	SMS-**A-207** compound **7i** (*J. Med. Chem.* **2016**, *59*, 3018–3033)
educts:	(ethoxymethylene)malononitrile and phenylpropylamine (1.2 eq.)
yield:	70%
visual appearance:	white needles
chemical formula:	$C_{13}H_{13}N_3$
molecular weight:	211.27 Da
LC-MS analysis:	calculated: 211.11 Da; found: not determined
purity:	not determined
^{1}H NMR:	500 MHz, DMSO-d_6, δ 9.10 (s, 1H), 7.88 (s, 1H), 7.30-7.25 (m, 2H), 7.21-7.16 (m, 3H), 3.26 (t, J = 7.1 Hz, 2H), 2.56 (t, J = 7.5 Hz, 2H), 1.86-1.79 (m, 2H)
^{13}C NMR:	not determined

6.1.3.5. Nucleophilic Substitution of Secondary Amines to Form Pyrrole Derivatives

A solution of the corresponding malononitrile derivative in 20 mL *N*,*N*-dimethylformamide was heated to 100 °C in the presence of excess potassium carbonate followed by dropwise addition of an equimolar amount of ethyl bromoacetate. After a reaction duration 3 to 6 hours, the reaction mixture was poured into ice-cold water and stirred for 1 hour. The resultant precipitate was filtered, rinsed with fresh water and dried, yielding the pyrrole derivative.

6.1.3.5.1. Synthesis of **ethyl 2-amino-1-cyano-5,6,7,8-tetrahydroindolizine-3-carboxylate (17)**

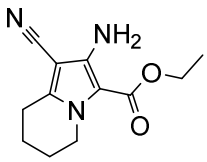

synonyms:	SMS-**A-3** compound **3a** (*J. Med. Chem.* **2016**, *59*, 3018–3033)
educts:	2-(piperidin-2-ylidene)malononitrile (**3**) and ethyl bromoacetate (1 eq.)
yield:	quantitative
visual appearance:	white powder
chemical formula:	$C_{12}H_{15}N_3O_2$
molecular weight:	233.27 Da
LC-MS analysis:	calculated: 233.12 Da; found: not determined
purity:	not determined
^{1}H NMR:	500 MHz, DMSO-d_6, δ 5.75 (s, 2H), 4.19 (q, J = 7.1 Hz, 2H), 4.05 (t, J = 6.1 Hz, 2H), 2.70 (t, J = 6.4 Hz, 2H), 1.88-1.83 (m, 2H), 1.74-1.69 (m, 2H), 1.25 (t, J = 7.1 Hz, 3H)
^{13}C NMR:	126 MHz, DMSO-d_6, δ 160.7, 146.0, 142.5, 115.2, 104.0, 79.3, 59.0, 45.7, 22.4, 22.3, 18.3, 14.6

6.1.3.5.2. Synthesis of **ethyl 2-amino-1-cyano-6,7,8,9-tetrahydro-5*H*-pyrrolo[1,2-*a*]azepine-3-carboxylate (18)**

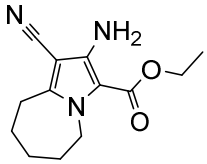

synonyms:	SMS-**A-30** compound **3b** (*J. Med. Chem.* **2016**, *59*, 3018–3033)
educts:	2-(azepan-2-ylidene)malononitrile (**4**) and ethyl bromoacetate (1 eq.)
yield:	55%
visual appearance:	pale yellow powder
chemical formula:	$C_{13}H_{17}N_3O_2$
molecular weight:	247.30 Da
LC-MS analysis:	calculated: 247.13 Da; found: not determined
purity:	not determined
^{1}H NMR:	500 MHz, DMSO-d_6, δ 5.67 (s, 2H), 4.49-4.40 (m, 2H), 4.21 (q, J = 7.1 Hz, 2H), 2.77-2.73 (m, 2H), 1.76-1.70 (m, 2H), 1.60-1.54 (m, 4H), 1.25 (t, J = 7.1 Hz, 3H)
^{13}C NMR:	126 MHz, DMSO-d_6, δ 160.7, 148.6, 145.3, 115.3, 104.1, 80.7, 59.2, 46.1, 29.8, 27.5, 26.1, 25.6, 14.6

6.1.3.5.3. Synthesis of **ethyl 3-amino-4-cyano-1-methyl-1*H*-pyrrole-2-carboxylate (19)**

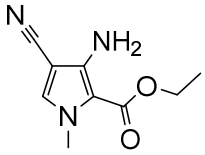

synonyms:	SMS-**A-228** compound **8a** (*J. Med. Chem.* **2016**, *59*, 3018–3033) compound **2a** (*Biochim. Biophys. Acta* **2017**, *1859*, 69–79)
educts:	2-((methylamino)methylene)malononitrile (**6**) and ethyl bromoacetate (1 eq.)
yield:	53%
visual appearance:	brown powder
chemical formula:	$C_9H_{11}N_3O_2$
molecular weight:	193.21 Da
LC-MS analysis:	calculated: 193.09 Da; found: not determined
purity:	not determined
^{1}H NMR:	500 MHz, DMSO-d_6, δ 7.50 (s, 1H), 5.71 (s, 2H), 4.21 (q, J = 7.1 Hz, 2H), 3.69 (s, 3H), 1.26 (t, J = 7.1 Hz, 3H)
^{13}C NMR:	not determined

6.1.3.5.4. Synthesis of **ethyl 3-amino-4-cyano-1-ethyl-1*H*-pyrrole-2-carboxylate (20)**

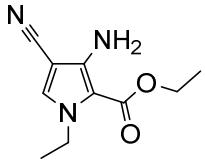

synonyms:	SMS-**A-473** compound **8b** (*J. Med. Chem.* **2016**, *59*, 3018–3033)
educts:	2-((ethylamino)methylene)malononitrile (**7**) and ethyl bromoacetate (1 eq.)
yield:	23%
visual appearance:	brown powder
chemical formula:	$C_{10}H_{13}N_3O_2$
molecular weight:	207.23 Da
LC-MS analysis:	calculated: 207.10 Da; found: not determined
purity:	not determined
^{1}H NMR:	500 MHz, DMSO-d_6, δ 7.59 (s, 1H), 5.74 (s, 2H), 4.23 (q, J = 7.1 Hz, 2H), 4.13 (q, J = 7.1 Hz, 2H), 1.27 (t, J = 7.1 Hz, 3H), 1.23 (t, J = 7.1 Hz, 3H)
^{13}C NMR:	not determined

6.1.3.5.5. Synthesis of **ethyl 3-amino-4-cyano-1-propyl-1*H*-pyrrole-2-carboxylate (21)**

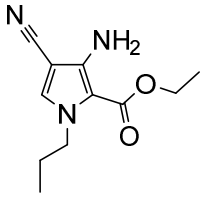

synonyms:	SMS-**A-480** compound **8c** (*J. Med. Chem.* **2016**, *59*, 3018–3033)
educts:	2-((propylamino)methylene)malononitrile (**8**) and ethyl bromoacetate (1 eq.)
yield:	66%
visual appearance:	orange powder
chemical formula:	$C_{11}H_{15}N_3O_2$
molecular weight:	221.26 Da
LC-MS analysis:	calculated: 221.12 Da; found: not determined
purity:	not determined
^{1}H NMR:	500 MHz, DMSO-d_6, δ 7.58 (s, 1H), 5.76 (s, 2H), 4.22 (q, J = 7.1 Hz, 2H), 4.06 (t, J = 7.1 Hz, 2H), 1.66-1.58 (m, 2H), 1.26 (t, J = 7.1 Hz, 3H), 0.77 (t, J = 7.4 Hz, 3H)
^{13}C NMR:	not determined

6.1.3.5.6. Synthesis of **ethyl 3-amino-4-cyano-1-isopropyl-1*H*-pyrrole-2-carboxylate (22)**

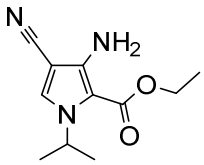

synonyms:	SMS-**A-487** compound **8d** (*J. Med. Chem.* **2016**, *59*, 3018–3033)
educts:	2-((isopropylamino)methylene)malononitrile (**9**) and ethyl bromoacetate (1 eq.)
yield:	quantitative
visual appearance:	white powder
chemical formula:	$C_{11}H_{15}N_3O_2$
molecular weight:	221.26 Da
LC-MS analysis:	calculated: 221.12 Da; found: not determined
purity:	not determined
^{1}H NMR:	500 MHz, DMSO-d_6, δ 7.73 (s, 1H), 5.73 (s, 2H), 5.09 (m, 1H), 4.23 (q, J = 7.1 Hz, 2H), 1.31 (d, J = 6.7 Hz, 6H), 1.27 (t, J = 7.1 Hz, 3H)
^{13}C NMR:	not determined

6.1.3.5.7. Synthesis of **ethyl 3-amino-4-cyano-1-cyclopropyl-1*H*-pyrrole-2-carboxylate (23)**

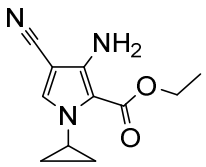

synonyms:	SMS-**A-494** compound **8e** (*J. Med. Chem.* **2016**, *59*, 3018–3033)
educts:	2-((cyclopropylamino)methylene)malononitrile (**10**) and ethyl bromoacetate (1 eq.)
yield:	85%
visual appearance:	white powder
chemical formula:	$C_{11}H_{13}N_3O_2$
molecular weight:	219.24 Da
LC-MS analysis:	calculated: 219.10 Da; found: not determined
purity:	not determined
^{1}H NMR:	500 MHz, DMSO-d_6, δ 7.55 (s, 1H), 5.77 (s, 2H), 4.23 (q, J = 7.1 Hz, 2H), 3.62-3.56 (m, 1H), 1.27 (t, J = 7.1 Hz, 3H), 0.91-0.87 (m, 4H)
^{13}C NMR:	not determined

6.1.3.5.8. Synthesis of **ethyl 3-amino-4-cyano-1-phenyl-1*H*-pyrrole-2-carboxylate (24)**

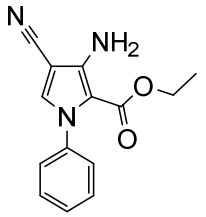

synonyms:	SMS-**A-185** compound **8f** (*J. Med. Chem.* **2016**, *59*, 3018–3033) compound **2b** (*Biochim. Biophys. Acta* **2017**, *1859*, 69–79)
educts:	2-((phenylamino)methylene)malononitrile (**11**) and ethyl bromoacetate (1 eq.)
yield:	77%
visual appearance:	brown powder
chemical formula:	$C_{14}H_{13}N_3O_2$
molecular weight:	255.28 Da
LC-MS analysis:	calculated: 255.10 Da; found: not determined
purity:	not determined
^{1}H NMR:	500 MHz, DMSO-d_6, δ 7.72 (s, 1H), 7.45-7.38 (m, 3H), 7.33-7.30 (m, 2H), 5.96 (s, 2H), 3.99 (q, J = 7.1 Hz, 2H), 0.95 (t, J = 7.1 Hz, 3H)
^{13}C NMR:	not determined

6.1.3.5.9. Synthesis of **ethyl 3-amino-4-cyano-1-(2-methoxyphenyl)-1*H*-pyrrole-2-carboxylate (25)**

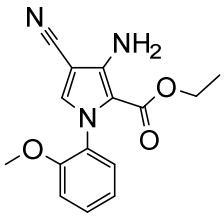

synonyms:	SMS-**A-293** compound **32a** (*J. Med. Chem.* **2017**, *accepted 10th of October, 2017*)
educts:	2-(((2-methoxyphenyl)amino)methylene)malononitrile (**12**) and (ethoxymethylene)malononitrile (1 eq.)
yield:	quantitative
visual appearance:	brown powder
chemical formula:	$C_{15}H_{15}N_3O_3$
molecular weight:	285.30 Da
LC-MS analysis:	calculated: 285.11 Da; found: not determined
purity:	not determined
^{1}H NMR:	500 MHz, DMSO-d_6, δ 7.63 (s, 1H), 7.21 (d, J = 8.9 Hz, 2H), 6.93 (d, J = 9.0, 2H), 5.90 (s, 2H), 4.05 (q, J = 7.0), 3.99 (q, J = 7.1 Hz, 2H), 1.33 (t, J = 7.0 Hz, 3H), 0.97 (t, J = 7.1 Hz, 3H)
^{13}C NMR:	not determined

6.1.3.5.10. Synthesis of **ethyl 3-amino-4-cyano-1-(4-ethoxyphenyl)-1*H*-pyrrole-2-carboxylate (26)**

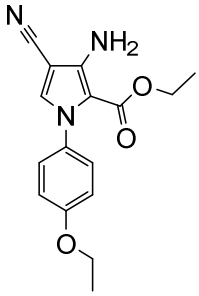

synonyms:	SMS-**A-278** compound **32b** (*J. Med. Chem.* **2017**, *accepted 10th of October, 2017*)
educts:	2-(((4-ethoxyphenyl)amino)methylene)malononitrile (**13**) and (ethoxymethylene)malononitrile (1 eq.)
yield:	92%
visual appearance:	brown powder
chemical formula:	$C_{16}H_{17}N_3O_3$
molecular weight:	299.33 Da

LC-MS analysis:	calculated: 299.13 Da; found: not determined
purity:	not determined
^{1}H NMR:	not determined
^{13}C NMR:	not determined

6.1.3.5.11. Synthesis of **ethyl 3-amino-1-benzyl-4-cyano-1*H*-pyrrole-2-carboxylate (27)**

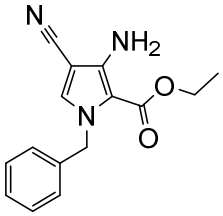

synonyms:	SMS-**A-198** compound **8g** (*J. Med. Chem.* **2016**, *59*, 3018–3033) compound **2c** (*Biochim. Biophys. Acta* **2017**, *1859*, 69–79)
educts:	2-((benzylamino)methylene)malononitrile (**14**) and ethyl bromoacetate (1 eq.)
yield:	71%
visual appearance:	brown powder
chemical formula:	$C_{15}H_{15}N_3O_2$
molecular weight:	269.30 Da
LC-MS analysis:	calculated: 269.12 Da; found: not determined
purity:	not determined
^{1}H NMR:	500 MHz, DMSO-d_6, δ 7.78 (s, 1H), 7.33-7.29 (m, 2H), 7.26-7.22 (m, 1H), 7.09-7.05 (m, 2H), 5.82 (s, 2H), 5.36 (s, 2H), 4.12 (q, J = 7.1 Hz, 2H), 1.13 (t, J = 7.1 Hz, 3H)
^{13}C NMR:	not determined

6.1.3.5.12. Synthesis of **ethyl 3-amino-4-cyano-1-phenethyl-1*H*-pyrrole-2-carboxylate (28)**

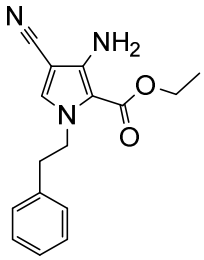

synonyms:	SMS-**A-203** compound **8h** (*J. Med. Chem.* **2016**, *59*, 3018–3033) compound **2d** (*Biochim. Biophys. Acta* **2017**, *1859*, 69–79)
educts:	2-((phenethylamino)methylene)malononitrile (**15**) and ethyl bromoacetate (1 eq.)

yield:	90%
visual appearance:	brown powder
chemical formula:	$C_{16}H_{17}N_3O_2$
molecular weight:	283.33 Da
LC-MS analysis:	calculated: 283.13 Da; found: not determined
purity:	not determined
^{1}H NMR:	500 MHz, DMSO-d_6, δ 7.39 (s, 1H), 7.30-7.26 (m, 2H), 7.23-7.18 (m, 1H), 7.15-7.12 (m, 2H), 5.78 (s, 2H), 4.33 (t, J = 7.4 Hz, 2H), 4.26 (q, J = 7.1 Hz, 2H), 2.91 (t, J = 7.2 Hz, 2H), 1.29 (t, J = 7.1 Hz, 3H)
^{13}C NMR:	not determined

6.1.3.5.13. Synthesis of **ethyl 3-amino-4-cyano-1-(3-phenylpropyl)-1*H*-pyrrole-2-carboxylate (29)**

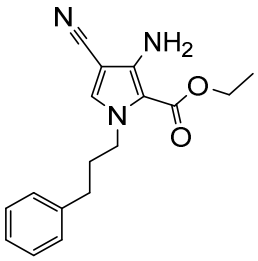

synonyms:	SMS-**A-208** compound **8i** (*J. Med. Chem.* **2016**, *59*, 3018–3033)
educts:	2-(((3-phenylpropyl)amino)methylene)malononitrile (**16**) and ethyl bromoacetate (1 eq.)
yield:	92%
visual appearance:	brown powder
chemical formula:	$C_{17}H_{19}N_3O_2$
molecular weight:	297.36 Da
LC-MS analysis:	calculated: 297.15 Da; found: not determined
purity:	not determined
^{1}H NMR:	500 MHz, DMSO-d_6, δ 7.59 (s, 1H), 7.28-7.24 (m, 2H), 7.19-7.15 (m, 3H), 5.78 (s, 2H), 4.19 (q, J = 7.1, 2H), 4.13 (t, J = 7.2 Hz, 2H), 2.52 (t, J = 7.6 Hz, 2H), 1.97-1.89 (m, 2H), 1.17 (t, J = 7.1 Hz, 3H)
^{13}C NMR:	not determined

6.1.3.5.14. Synthesis of **ethyl 3-amino-1*H*-indole-2-carboxylate (30)**

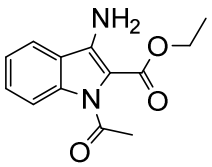

synonyms:	SMS-**A-166** compound **37** (*J. Med. Chem.* **2017**, *accepted 10th of October, 2017*)
educts:	N-(2-cyanophenyl)acetamide (**5**) and (ethoxymethylene)malononitrile (1 eq.)
yield:	62%
visual appearance:	brown powder
chemical formula:	$C_{13}H_{14}N_2O_3$
molecular weight:	246.27 Da
LC-MS analysis:	calculated: 246.10 Da; found: not determined
purity:	not determined
^{1}H NMR:	500 MHz, DMSO-d_6, δ 8.05 (dt, J = 8.4, 0.8 Hz, 1H), 7.96 (ddd, J 7.9, 1.2, 0.7 Hz, 1H), 7.48 (ddd, J = 8.5, 7.2, 1.3, 1H), 7.27 (ddd, J =8.0, 7.2, 1.0, 1H), 6.70 (s, 2H), 4.29 (q, J = 7.0 Hz, 2H), 2.37 (s, 3H), 1.30 (t, J = 7.1 Hz, 3H)
^{13}C NMR:	126 MHz, DMSO-d_6, δ 171.3, 162.1, 144.5, 138.5, 130.0, 122.0, 121.8, 121.2, 115.2, 104.3, 59.9, 26.5, 14.6

6.1.3.6. Chain Elongation to Form the Formimidamid Derivatives.

To a solution of the corresponding pyrrole derivative in *N*,*N*-dimethylformamide 3.5 to 5 equivalents of *N*,*N*-dimethylformamide dimethyl acetale were added and the mixture was heated to 100 °C. After 2 to 5 hours the solvent was evaporated and petroleum ether was added to the viscous liquid. Full crystallization was achieved after stirring for 5 to 60 minutes, yielding the title compound, which was rinsed with petroleum ether and dried. Compounds that did not crystalize were used without further purification or characterization.

6.1.3.6.1. Synthesis of **ethyl 1-cyano-2-(((dimethylamino)methylene)amino)-5,6,7,8-tetrahydroindolizine-3-carboxylate (31)**

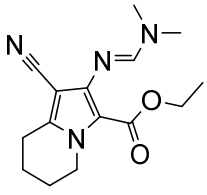

synonyms:	SMS-**A-4** compound **4a** (*J. Med. Chem.* **2016**, *59*, 3018–3033)

educts:	ethyl 2-amino-1-cyano-5,6,7,8-tetrahydroindolizine-3-carboxylate (**17**) and *N*,*N*-dimethylformamide dimethyl acetale (3-5 eq.)
yield:	75%
visual appearance:	yellow needles
chemical formula:	$C_{15}H_{20}N_4O_2$
molecular weight:	288.35 Da
LC-MS analysis:	calculated: 288.16 Da; found: not determined
purity:	not determined
^{1}H NMR:	500 MHz, DMSO-d_6, δ 7.52 (s, 1H), 4.12 (t, J = 6.1 Hz, 2H), 4.07 (q, J = 7.1 Hz, 2H), 2.97 (s, 3H), 2.91 (s, 3H), 2.75 (t, J = 6.4 Hz, 2H), 1.91-1.85 (m, 2H), 1.77-1.71 (m, 2H), 1.17 (t, J = 7.1 Hz, 3H)
^{13}C NMR:	126 MHz, DMSO-d_6, δ 160.5, 156.2 (2C), 148.7, 141.6, 115.7, 110.3, 86.5, 59.2, 46.0, 33.8, 22.5, 22.5, 18.4, 14.0

6.1.3.6.2. Synthesis of **ethyl 1-cyano-2-(((dimethylamino)methylene)amino)-6,7,8,9-tetrahydro-5*H*-pyrrolo[1,2-*a*]azepine-3-carboxylate (32)**

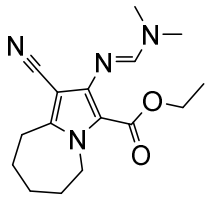

synonyms:	SMS-**A-31** compound **4b** (*J. Med. Chem.* **2016**, *59*, 3018–3033)
educts:	ethyl 2-amino-1-cyano-6,7,8,9-tetrahydro-5H-pyrrolo[1,2-a]azepine-3-carboxylate (**18**) and *N*,*N*-dimethylformamide dimethyl acetale (3-5 eq.)
yield:	40%
visual appearance:	yellow powder
chemical formula:	$C_{16}H_{22}N_4O_2$
molecular weight:	302.38 Da
LC-MS analysis:	calculated: 302.17 Da; found: not determined
purity:	not determined
^{1}H NMR:	not determined
^{13}C NMR:	not determined

6.1.3.6.3. Synthesis of **ethyl 4-cyano-3-(((dimethylamino)methylene)amino)-1-methyl-1*H*-pyrrole-2-carboxylate (33)**

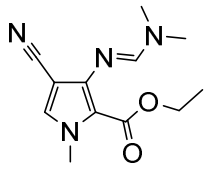

synonyms:	SMS-**A-229**
	compound **9a** (*J. Med. Chem.* **2016**, *59*, 3018–3033)
	compound **3a** (*Biochim. Biophys. Acta* **2017**, *1859*, 69–79)
educts:	ethyl 3-amino-4-cyano-1-methyl-1*H*-pyrrole-2-carboxylate (**19**) and *N*,*N*-dimethylformamide dimethyl acetale (3-5 eq.)
yield:	quantitative
visual appearance:	brown oil
chemical formula:	$C_{12}H_{16}N_4O_2$
molecular weight:	248.29 Da
LC-MS analysis:	calculated: 248.13 Da; found: not determined
purity:	not determined
^{1}H NMR:	not determined
^{13}C NMR:	not determined

6.1.3.6.4. Synthesis of **ethyl 4-cyano-3-(((dimethylamino)methylene)amino)-1-ethyl-1*H*-pyrrole-2-carboxylate (34)**

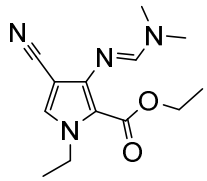

synonyms:	SMS-**A-474**
	compound **9b** (*J. Med. Chem.* **2016**, *59*, 3018–3033)
educts:	ethyl 3-amino-4-cyano-1-ethyl-1*H*-pyrrole-2-carboxylate (**20**) and *N*,*N*-dimethylformamide dimethyl acetale (3-5 eq.)
yield:	quantitative
visual appearance:	brown oil
chemical formula:	$C_{13}H_{18}N_4O_2$
molecular weight:	262.31 Da
LC-MS analysis:	calculated: 262.14 Da; found: not determined
purity:	not determined
^{1}H NMR:	not determined
^{13}C NMR:	not determined

6.1.3.6.5. Synthesis of **ethyl 4-cyano-3-(((dimethylamino)methylene)amino)-1-propyl-1*H*-pyrrole-2-carboxylate (35)**

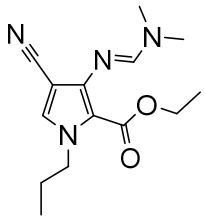

synonyms:	SMS-**A-481** compound **9c** (*J. Med. Chem.* **2016**, *59*, 3018–3033)
educts:	ethyl 3-amino-4-cyano-1-propyl-1*H*-pyrrole-2-carboxylate (**21**) and *N,N*-dimethylformamide dimethyl acetale (3-5 eq.)
yield:	quantitative
visual appearance:	orange powder
chemical formula:	$C_{14}H_{20}N_4O_2$
molecular weight:	276.34 Da
LC-MS analysis:	calculated: 276.16 Da; found: not determined
purity:	not determined
^{1}H NMR:	500 MHz, DMSO-d_6, δ 7.68 (s, 1H), 7.55 (s, 1H), 4.14 (t, J = 7.2 Hz, 2H), 4.11 (q, J = 7.1 Hz, 2H), 2.98 (s, 3H), 2.91 (s, 3H), 1.68-1.59 (m, 2H), 1.18 (t, J = 7.1 Hz, 3H), 0.78 (t, J = 7.4 Hz, 3H)
^{13}C NMR:	not determined

6.1.3.6.6. Synthesis of **ethyl 4-cyano-3-(((dimethylamino)methylene)amino)-1-isopropyl-1*H*-pyrrole-2-carboxylate (36)**

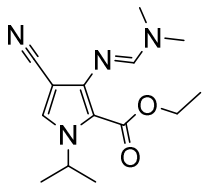

synonyms:	SMS-**A-488** compound **9d** (*J. Med. Chem.* **2016**, *59*, 3018–3033)
educts:	ethyl 3-amino-4-cyano-1-isopropyl-1*H*-pyrrole-2-carboxylate (**22**) and *N,N*-dimethylformamide dimethyl acetale (3-5 eq.)
yield:	quantitative
visual appearance:	brown oil
chemical formula:	$C_{14}H_{20}N_4O_2$
molecular weight:	276.34 Da
LC-MS analysis:	calculated: 276.16 Da; found: not determined
purity:	not determined

^{1}H NMR:	500 MHz, DMSO-d_6, δ 7.68 (s, 1H), 7.55 (s, 1H), 4.14 (t, J = 7.2 Hz, 2H), 4.11 (q, J = 7.1 Hz, 2H), 2.98 (s, 3H), 2.91 (s, 3H), 1.68-1.59 (m, 2H), 1.18 (t, J = 7.1 Hz, 3H), 0.78 (t, J = 7.4 Hz, 3H)
^{13}C NMR:	not determined

6.1.3.6.7. Synthesis of **ethyl 4-cyano-1-cyclopropyl-3-(((dimethylamino)methylene)amino)-1*H*-pyrrole-2-carboxylate (37)**

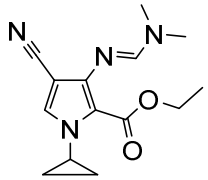

synonyms:	SMS-**A**-**495** compound **9e** (*J. Med. Chem.* **2016**, *59*, 3018–3033)
educts:	ethyl 3-amino-4-cyano-1-cyclopropyl-1*H*-pyrrole-2-carboxylate (**23**) and *N,N*-dimethylformamide dimethyl acetale (3-5 eq.)
yield:	quantitative
visual appearance:	brown oil
chemical formula:	$C_{14}H_{18}N_4O_2$
molecular weight:	274.32 Da
LC-MS analysis:	calculated: 274.14 Da; found: not determined
purity:	not determined
^{1}H NMR:	500 MHz, DMSO-d_6, δ 7.68 (s, 1H), 7.55 (s, 1H), 4.14 (t, J = 7.2 Hz, 2H), 4.11 (q, J = 7.1 Hz, 2H), 2.98 (s, 3H), 2.91 (s, 3H), 1.68-1.59 (m, 2H), 1.18 (t, J = 7.1 Hz, 3H), 0.78 (t, J = 7.4 Hz, 3H)
^{13}C NMR:	not determined

6.1.3.6.8. Synthesis of **ethyl 4-cyano-3-(((dimethylamino)methylene)amino)-1-phenyl-1*H*-pyrrole-2-carboxylate (38)**

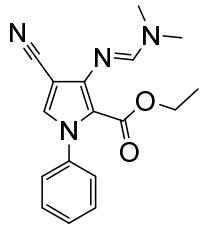

synonyms:	SMS-**A**-**186** compound **9f** (*J. Med. Chem.* **2016**, *59*, 3018–3033) compound **3b** (*Biochim. Biophys. Acta* **2017**, *1859*, 69–79)
educts:	ethyl 3-amino-4-cyano-1-phenyl-1*H*-pyrrole-2-carboxylate (**24**) and *N,N*-dimethylformamide dimethyl acetale (3-5 eq.)

yield:	quantitative
visual appearance:	yellow needles
chemical formula:	$C_{17}H_{18}N_4O_2$
molecular weight:	310.36 Da
LC-MS analysis:	calculated: 310.14 Da; found: not determined
purity:	not determined
^{1}H NMR:	500 MHz, DMSO-d_6, δ 7.82 (s, 1H), 7.74 (s, 1H), 7.47-7.38 (m, 3H), 7.32-7.28 (m, 2H), 3.92 (q, J = 7.1 Hz), 3.01 (s, 3H), 2.94 (s, 3H), 0.94 (t, J = 7.1 Hz, 3H)
^{13}C NMR:	not determined

6.1.3.6.9. Synthesis of **ethyl 4-cyano-3-(((dimethylamino)methylene)amino)-1-(2-methoxyphenyl)-1*H*-pyrrole-2-carboxylate (39)**

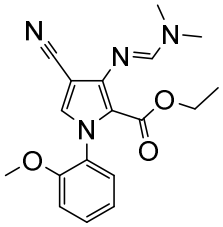

synonyms:	SMS-**A**-**294** compound **33a** (*J. Med. Chem.* **2017**, *accepted 10th of October, 2017*)
educts:	ethyl 3-amino-4-cyano-1-(2-methoxyphenyl)-1*H*-pyrrole-2-carboxylate (**25**) and (ethoxymethylene)malononitrile (1 eq.)
yield:	94%
visual appearance:	brown oil
chemical formula:	$C_{18}H_{20}N_4O_3$
molecular weight:	340.38 Da
LC-MS analysis:	calculated: 340.15 Da; found: not determined
purity:	not determined
^{1}H NMR:	not determined
^{13}C NMR:	not determined

6.1.3.6.10. Synthesis of **ethyl 4-cyano-3-(((dimethylamino)methylene)amino)-1-(4-ethoxyphenyl)-1*H*-pyrrole-2-carboxylate (40)**

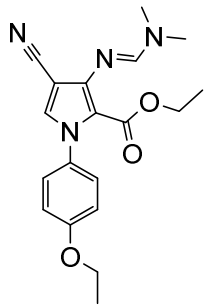

synonyms:	SMS-**A-279** compound **33b** (*J. Med. Chem.* **2017**, *accepted 10th of October, 2017*)
educts:	ethyl 3-amino-4-cyano-1-(4-ethoxyphenyl)-1*H*-pyrrole-2-carboxylate (**26**) and (ethoxymethylene)malononitrile (1 eq.)
yield:	94%
visual appearance:	brown oil
chemical formula:	$C_{19}H_{22}N_4O_3$
molecular weight:	354.41 Da
LC-MS analysis:	calculated: 354.17 Da; found: not determined
purity:	not determined
^{1}H NMR:	not determined
^{13}C NMR:	not determined

6.1.3.6.11. Synthesis of **ethyl 1-benzyl-4-cyano-3-(((dimethylamino)methylene)amino)-1*H*-pyrrole-2-carboxylate (41)**

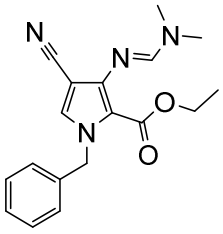

synonyms:	SMS-**A-199** compound **9g** (*J. Med. Chem.* **2016**, *59*, 3018–3033) compound **3c** (*Biochim. Biophys. Acta* **2017**, *1859*, 69–79)
educts:	ethyl 3-amino-1-benzyl-4-cyano-1*H*-pyrrole-2-carboxylate (**27**) and *N*,*N*-dimethylformamide dimethyl acetale (3-5 eq.)
yield:	quantitative
visual appearance:	brown powder
chemical formula:	$C_{18}H_{20}N_4O_2$
molecular weight:	324.38 Da

LC-MS analysis:	calculated: 324.16 Da; found: not determined
purity:	not determined
^{1}H NMR:	500 MHz, DMSO-d_6, δ 7.87 (s, 1H), 7.56 (s, 1H), 7.33-7.29 (m, 2H), 7.27-7.22 (m, 1H), 7.10-7.06 (m, 2H), 5.46 (s, 2H), 4.03 (q, J = 7.1 Hz, 2H), 2.97 (s, 3H), 2.91 (s, 3H), 1.10 (t, J = 7.1 Hz, 3H)
^{13}C NMR:	not determined

6.1.3.6.12. Synthesis of **ethyl 4-cyano-3-(((dimethylamino)methylene)amino)-1-phenethyl-1*H*-pyrrole-2-carboxylate (42)**

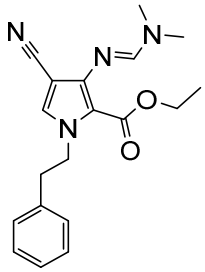

synonyms:	SMS-**A**-**204** compound **9h** (*J. Med. Chem.* **2016**, *59*, 3018–3033) compound **3d** (*Biochim. Biophys. Acta* **2017**, *1859*, 69–79)
educts:	ethyl 3-amino-4-cyano-1-phenethyl-1*H*-pyrrole-2-carboxylate (**28**) and *N*,*N*-dimethylformamide dimethyl acetale (3-5 eq.)
yield:	quantitative
visual appearance:	orange powder
chemical formula:	$C_{19}H_{22}N_4O_2$
molecular weight:	338.41 Da
LC-MS analysis:	calculated: 338.17 Da; found: not determined
purity:	not determined
^{1}H NMR:	500 MHz, DMSO-d_6, δ 7.55 (s, 1H), 7.49 (s, 1H), 7.30-7.26 (m, 2H), 7.23-7.19 (m, 1H), 7.16-7.13 (m, 2H), 4.40 (t, J = 7.5 Hz, 2H), 4.14 (q, J = 7.1 Hz), 2.99 (s, 3H), 2.94 (t, J = 7.7 Hz, 2H), 2.92 (s, 3H), 1.19 (t, J = 7.1 Hz, 3H)
^{13}C NMR:	not determined

6.1.3.6.13. Synthesis of **ethyl 4-cyano-3-(((dimethylamino)methylene)amino)-1-(3-phenylpropyl)-1*H*-pyrrole-2-carboxylate (43)**

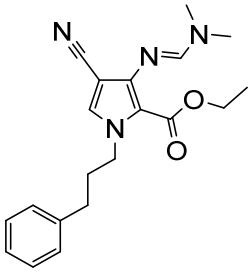

synonyms:	SMS-**A-209** compound **9i** (*J. Med. Chem.* **2016**, *59*, 3018–3033)
educts:	ethyl 3-amino-4-cyano-1-(3-phenylpropyl)-1*H*-pyrrole-2-carboxylate (**29**) and *N*,*N*-dimethylformamide dimethyl acetale (3-5 eq.)
yield:	quantitative
visual appearance:	orange powder
chemical formula:	$C_{20}H_{24}N_4O_2$
molecular weight:	352.44 Da
LC-MS analysis:	calculated: 352.19 Da; found: not determined
purity:	not determined
^{1}H NMR:	500 MHz, DMSO-d_6, δ 7.69 (s, 1H), 7.54 (s, 1H), 7.29-7.24 (m, 2H), 7.19-7.15 (m, 3H), 4.23 (t, J = 7.1 Hz, 2H), 4.10 (q, *J* = 7.1 Hz, 2H), 2.98 (s, 3H), 2.91 (s, 3H), 2.53 (t, *J* = 7.6 Hz, 2H), 1.99-1.92 (m, 2H), 1.17 (t, *J* = 7.1 Hz, 3H)
^{13}C NMR:	not determined

6.1.3.6.14. Synthesis of **ethyl 1-acetyl-3-(((dimethylamino)methylene)amino)-1*H*-indole-2-carboxylate (44)**

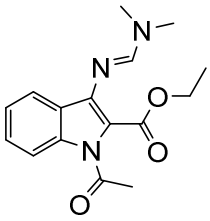

synonyms:	SMS-**A-167** compound **38** (*J. Med. Chem.* **2017**, *accepted 10th of October, 2017*)
educts:	ethyl 3-amino-1*H*-indole-2-carboxylate (**30**) and (ethoxymethylene)malononitrile (1 eq.)
yield:	29%
visual appearance:	brown oil
chemical formula:	$C_{16}H_{19}N_3O_3$
molecular weight:	301.35 Da

LC-MS analysis:	calculated: 301.14 Da; found: not determined
purity:	not determined
^{1}H NMR:	not determined
^{13}C NMR:	not determined

6.1.3.7. Cyclization to Pyrrimidinon Ring System

A saturated solution of the corresponding pyrrole derivative in ethanol was piped with gaseous ammonia for 5 hours. After solvent evaporation, 10% (m/m) sodium hydroxide solution was added while stirring. After 30 minutes, the solution was neutralized using acetic acid, precipitating the title compound, which was rinsed with fresh water and dried.

6.1.3.7.1. Synthesis of **4-oxo-3,4,6,7,8,9-hexahydropyrimido[4,5-*b*]indolizine-10-carbonitrile (45)**

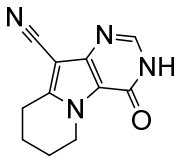

synonyms:	SMS-**A-5** compound **5a** (*J. Med. Chem.* **2016**, *59*, 3018–3033)
educts:	ethyl 1-cyano-2-(((dimethylamino)methylene)amino)-5,6,7,8-tetrahydroindolizine-3-carboxylate (**31**) and gaseous ammonia (excess)
yield:	68%
visual appearance:	white powder
chemical formula:	$C_{11}H_{10}N_4O$
molecular weight:	214.23 Da
LC-MS analysis:	calculated: 214.09 Da; found: not determined
purity:	not determined
^{1}H NMR:	500 MHz, DMSO-d_6, δ 12.21 (s, 1H), 7.90 (s, 1H), 4.35 (t, J = 6.4 Hz, 2H), 2.95 (t, J = 6.4 Hz, 2H), 1.99-1.93 (m, 2H), 1.87-1.80 (m, 2H)
^{13}C NMR:	126 MHz, DMSO-d_6, δ 153.2, 146.3, 145.5, 144.8, 116.7, 114.3, 84.0, 45.6, 22.4, 21.8, 18.3

6.1.3.7.2. Synthesis of **4-oxo-4,6,7,8,9,10-hexahydro-3*H*-pyrimido[4',5':4,5]pyrrolo[1,2-*a*]azepine-11-carbonitrile (46)**

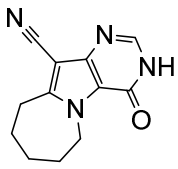

synonyms:	SMS-**A-32** compound **5b** (*J. Med. Chem.* **2016**, *59*, 3018–3033)
educts:	ethyl 1-cyano-2-(((dimethylamino)methylene)amino)-6,7,8,9-tetrahydro-5H-pyrrolo[1,2-a]azepine-3-carboxylate (**32**) and gaseous ammonia (excess)
yield:	12%
visual appearance:	white powder
chemical formula:	$C_{12}H_{12}N_4O$
molecular weight:	228.26 Da
LC-MS analysis:	calculated: 228.10 Da; found: not determined
purity:	not determined
^{1}H NMR:	500 MHz, DMSO-d_6, δ 12.30 (s, 1H), 4.82-4.69 (m, 2H), 2.01-2.95 (m, 2H), 1.85-1.79 (m, 2H), 1.72-1.63 (m, 4H)
^{13}C NMR:	126 MHz, DMSO-d_6, δ 153.5, 152.2, 144.8, 144.5, 117.0, 114.5, 85.5, 47.1, 30.0, 27.8, 26.4, 25.7

6.1.3.7.3. Synthesis of **5-methyl-4-oxo-4,5-dihydro-3*H*-pyrrolo[3,2-*d*]pyrimidine-7-carbonitrile (47)**

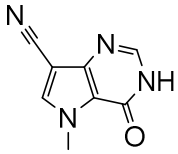

synonyms:	SMS-**A-230** compound **10a** (*J. Med. Chem.* **2016**, *59*, 3018–3033) compound **4a** (*Biochim. Biophys. Acta* **2017**, *1859*, 69–79)
educts:	ethyl 4-cyano-3-(((dimethylamino)methylene)amino)-1-methyl-1*H*-pyrrole-2-carboxylate (**33**) and gaseous ammonia (excess)
yield:	49%
visual appearance:	white powder
chemical formula:	$C_8H_6N_4O$
molecular weight:	174.16 Da
LC-MS analysis:	calculated: 174.05 Da; found: not determined
purity:	not determined

^{1}H NMR:	500 MHz, DMSO-d_6, δ 12.31 (s, 1H), 8.14 (s, 1H), 7.94 (s, 1H), 4.01 (s, 3H)
^{13}C NMR:	not determined

6.1.3.7.4. Synthesis of **5-ethyl-4-oxo-4,5-dihydro-3*H*-pyrrolo[3,2-*d*]pyrimidine-7-carbonitrile (48)**

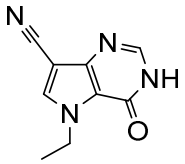

synonyms:	SMS-**A-475** compound **10b** (*J. Med. Chem.* **2016**, *59*, 3018–3033)
educts:	ethyl 4-cyano-3-(((dimethylamino)methylene)amino)-1-ethyl-1*H*-pyrrole-2-carboxylate (**34**) and gaseous ammonia (excess)
yield:	45%
visual appearance:	brown powder
chemical formula:	$C_9H_8N_4O$
molecular weight:	188.19 Da
LC-MS analysis:	calculated: 188.07 Da; found: not determined
purity:	not determined
^{1}H NMR:	500 MHz, DMSO-d_6, δ 12.34 (s, 1H), 8.25 (s, 1H), 7.95 (s, 1H), 4.40 (q, J = 7.2 Hz, 2H), 1.37 (t, J = 7.2 Hz, 3H)
^{13}C NMR:	not determined

6.1.3.7.5. Synthesis of **4-oxo-5-propyl-4,5-dihydro-3*H*-pyrrolo[3,2-*d*]pyrimidine-7-carbonitrile (49)**

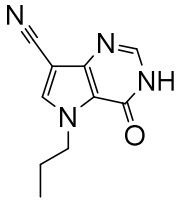

synonyms:	SMS-**A-482** compound **10c** (*J. Med. Chem.* **2016**, *59*, 3018–3033)
educts:	ethyl 4-cyano-3-(((dimethylamino)methylene)amino)-1-propyl-1*H*-pyrrole-2-carboxylate (**35**) and gaseous ammonia (excess)
yield:	24%
visual appearance:	brown powder
chemical formula:	$C_{10}H_{10}N_4O$
molecular weight:	202.22 Da
LC-MS analysis:	calculated: 202.08 Da; found: not determined
purity:	not determined

^{1}H NMR:	500 MHz, DMSO-d_6, δ 12.33 (s, 1H), 8.24 (s, 1H), 7.95 (s, 1H), 4.34 (t, J = 7.0 Hz, 2H), 1.81-1.74 (m, *2*H), 0.80 (t, J = 7.4 Hz, 3H)
^{13}C NMR:	not determined

6.1.3.7.6. Synthesis of **5-isopropyl-4-oxo-4,5-dihydro-3*H*-pyrrolo[3,2-*d*]pyrimidine-7-carbonitrile (50)**

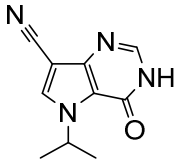

synonyms:	SMS-**A-489** compound **10d** (*J. Med. Chem.* **2016**, *59*, 3018–3033)
educts:	ethyl 4-cyano-3-(((dimethylamino)methylene)amino)-1-isopropyl-1*H*-pyrrole-2-carboxylate (**36**) and gaseous ammonia (excess)
yield:	56%
visual appearance:	brown powder
chemical formula:	$C_{10}H_{10}N_4O$
molecular weight:	202.22 Da
LC-MS analysis:	calculated: 202.08 Da; found: not determined
purity:	not determined
^{1}H NMR:	500 MHz, DMSO-d_6, δ 12.26 (s, 1H), 8.41 (s, 1H), 7.96 (s, 1H), 5.30 (m, 1H), 1.44 (d, J = 6.7 Hz, 6H)
^{13}C NMR:	not determined

6.1.3.7.7. Synthesis of **5-cyclopropyl-4-oxo-4,5-dihydro-3*H*-pyrrolo[3,2-*d*]pyrimidine-7-carbonitrile (51)**

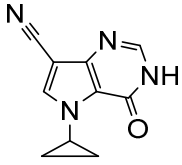

synonyms:	SMS-**A-496** compound **10e** (*J. Med. Chem.* **2016**, *59*, 3018–3033)
educts:	ethyl 4-cyano-1-cyclopropyl-3-(((dimethylamino)methylene)amino)-1*H*-pyrrole-2-carboxylate (**37**) and gaseous ammonia (excess)
yield:	6%
visual appearance:	brown powder
chemical formula:	$C_{10}H_8N_4O$
molecular weight:	200.20 Da
LC-MS analysis:	calculated: 200.07 Da; found: not determined
purity:	not determined

^{1}H NMR:	500 MHz, DMSO-d_6, δ 8.13 (s, 1H), 7.94 (s, 1H), 4.10-4.04 (m, 1H), 1.09-0.98 (m, 4H)
^{13}C NMR:	not determined

6.1.3.7.8. Synthesis of **4-oxo-5-phenyl-4,5-dihydro-3*H*-pyrrolo[3,2-*d*]pyrimidine-7-carbonitrile (52)**

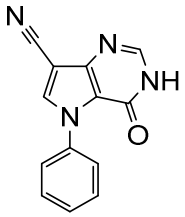

synonyms:	SMS-**A-187** compound **10f** (*J. Med. Chem.* **2016**, *59*, 3018–3033) compound **4b** (*Biochim. Biophys. Acta* **2017**, *1859*, 69–79)
educts:	ethyl 4-cyano-3-(((dimethylamino)methylene)amino)-1-phenyl-1*H*-pyrrole-2-carboxylate (**38**) and gaseous ammonia (excess)
yield:	21%
visual appearance:	white powder
chemical formula:	$C_{13}H_8N_4O$
molecular weight:	236.23 Da
LC-MS analysis:	calculated: 236.07 Da; found: not determined
purity:	not determined
^{1}H NMR:	500 MHz, DMSO-d_6, δ 12.44 (s, 1H), 8.48 (s, 1H), 8.05 (s, 1H), 7.56-7.45 (m, 5H)
^{13}C NMR:	not determined

6.1.3.7.9. Synthesis of **5-(2-methoxyphenyl)-4-oxo-4,5-dihydro-3*H*-pyrrolo[3,2-*d*]pyrimidine-7-carbonitrile (53)**

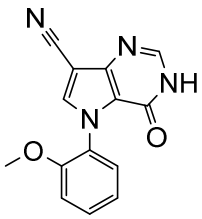

synonyms:	SMS-**A-295** compound **34a** (*J. Med. Chem.* **2017**, *accepted 10th of October, 2017*)
educts:	ethyl 4-cyano-3-(((dimethylamino)methylene)amino)-1-(2-methoxyphenyl)-1*H*-pyrrole-2-carboxylate (**39**) and gaseous ammonia (excess)
yield:	quantitative
visual appearance:	greywhite powder

chemical formula:	$C_{14}H_{10}N_4O_2$
molecular weight:	266.26 Da
LC-MS analysis:	calculated: 266.08 Da; found: not determined
purity:	not determined
^{1}H NMR:	not determined
^{13}C NMR:	not determined

6.1.3.7.10. Synthesis of **5-(4-ethoxyphenyl)-4-oxo-4,5-dihydro-3*H*-pyrrolo[3,2-*d*]pyrimidine-7-carbonitrile (54)**

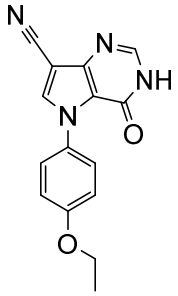

synonyms:	SMS-**A**-**280**
	compound **34b** (*J. Med. Chem.* **2017**, *accepted 10th of October, 2017*)
educts:	ethyl 4-cyano-3-(((dimethylamino)methylene)amino)-1-(4-ethoxyphenyl)-1*H*-pyrrole-2-carboxylate (**40**) and gaseous ammonia (excess)
yield:	quantitative
visual appearance:	greywhite powder
chemical formula:	$C_{15}H_{12}N_4O_2$
molecular weight:	280.10 Da
LC-MS analysis:	calculated: 280.29 Da; found: not determined
purity:	not determined
^{1}H NMR:	not determined
^{13}C NMR:	not determined

6.1.3.7.11. Synthesis of **5-benzyl-4-oxo-4,5-dihydro-3*H*-pyrrolo[3,2-*d*]pyrimidine-7-carbonitrile (55)**

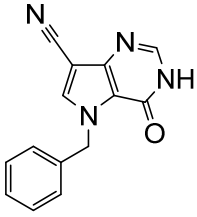

synonyms:	SMS-**A**-**200**
	compound **10g** (*J. Med. Chem.* **2016**, *59*, 3018–3033)
	compound **4c** (*Biochim. Biophys. Acta* **2017**, *1859*, 69–79)

educts:	ethyl 1-benzyl-4-cyano-3-(((dimethylamino)methylene)amino)-1*H*-pyrrole-2-carboxylate (**41**) and gaseous ammonia (excess)
yield:	47%
visual appearance:	yellow powder
chemical formula:	$C_{14}H_{10}N_4O$
molecular weight:	250.26 Da
LC-MS analysis:	calculated: 250.09 Da; found: not determined
purity:	not determined
^{1}H NMR:	500 MHz, DMSO-d_6, δ 8.31 (s, 1H), 7.97 (s, 1H), 7.35-7.24 (m, 5H), 5.63 (s, 2H)
^{13}C NMR:	not determined

6.1.3.7.12. Synthesis of **4-oxo-5-phenethyl-4,5-dihydro-3*H*-pyrrolo[3,2-*d*]pyrimidine-7-carbonitrile (56)**

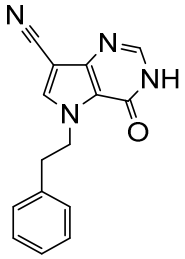

synonyms:	SMS-**A-205** compound **10h** (*J. Med. Chem.* **2016**, *59*, 3018–3033) compound **4d** (*Biochim. Biophys. Acta* **2017**, *1859*, 69–79)
educts:	ethyl 4-cyano-3-(((dimethylamino)methylene)amino)-1-phenethyl-1*H*-pyrrole-2-carboxylate (**42**) and gaseous ammonia (excess)
yield:	43%
visual appearance:	yellow powder
chemical formula:	$C_{15}H_{12}N_4O$
molecular weight:	264.29 Da
LC-MS analysis:	calculated: 264.10 Da; found: not determined
purity:	not determined
^{1}H NMR:	500 MHz, DMSO-d_6, δ 7.97 (s, 1H), 7.96 (s, 1H), 7.28-7.24 (m, 2H), 7.21-7.17 (m, 1H), 7.15-7.12 (m, 2H), 4.61 (t, J = 7.2), 3.08 (t, J = 7.3, 2H)
^{13}C NMR:	not determined

6.1.3.7.13. Synthesis of **4-oxo-5-(3-phenylpropyl)-4,5-dihydro-3*H*-pyrrolo[3,2-*d*]pyrimidine-7-carbonitrile (57)**

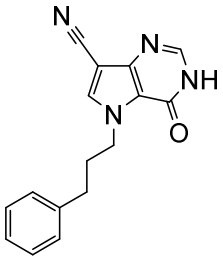

synonyms:	SMS-**A-210** compound **10i** (*J. Med. Chem.* **2016**, *59*, 3018–3033)
educts:	ethyl 4-cyano-3-(((dimethylamino)methylene)amino)-1-(3-phenylpropyl)-1*H*-pyrrole-2-carboxylate (**43**) and gaseous ammonia (excess)
yield:	21%
visual appearance:	white powder
chemical formula:	$C_{16}H_{14}N_4O$
molecular weight:	278.32 Da
LC-MS analysis:	calculated: 278.12 Da; found: not determined
purity:	not determined
^{1}H NMR:	500 MHz, DMSO-d_6, δ 8.09 (s, 1H), 7.93 (s, 1H), 7.26-7.22 (m, 2H), 7.18-7.14 (m, 3H), 4.43 (t, J = 7.0, 2H), 2.54 (t, J = 7.7, 2H), 2.13-2.05 (m, 2H)
^{13}C NMR:	not determined

6.1.3.7.14. Synthesis of **3,5-dihydro-4*H*-pyrimido[5,4-*b*]indole-4-one (58)**

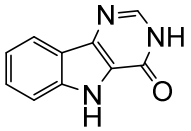

synonyms:	SMS-**A-133** compound **39** (*J. Med. Chem.* **2017**, *accepted 10th of October, 2017*)
educts:	ethyl 1-acetyl-3-(((dimethylamino)methylene)amino)-1*H*-indole-2-carboxylate (**44**) and (ethoxymethylene)malononitrile (1 eq.)
yield:	40%
visual appearance:	grey powder
chemical formula:	$C_{10}H_7N_3O$
molecular weight:	185.19 Da
LC-MS analysis:	calculated: 185.06 Da; found: not determined
purity:	not determined
^{1}H NMR:	500 MHz, DMSO-d_6, δ 12.32 (s, 1H), 12.03 (s, 1H), 7.98 (s, 1H), 7.98 (dt, J 8.0, 0.9 Hz, 1H), 7.52 (dt, J = 8.3, 0.8, 1H), 7.45 (ddd, J = 8.2, 6.9, 1.2, 2H), 7.22 (ddd, J = 7.9, 6.9, 1.0, 1H)
^{13}C NMR:	126 MHz, DMSO-d_6, δ 154.7, 141.5, 138.7, 138.3, 127.1, 122.7, 121.3, 120.4, 120.3, 112.9

6.1.3.8. Chlorination and Aromatization to Pyrimidine Ring System

The corresponding pyrimidinon derivative was dissolved in phosphoryl chloride (10 mL) and refluxed overnight. The reaction mixture was poured into ice cold water and the pyrimidine derivative was precipitated, which was filtered off, rinsed with fresh water and dried in a hot-air cabinet.

6.1.3.8.1. Synthesis of **4-chloro-6,7,8,9-tetrahydropyrimido[4,5-*b*]indolizine-10-carbonitrile (59)**

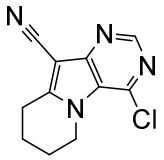

synonyms:	SMS-**A**-**6** compound **6a** (*J. Med. Chem.* **2016**, *59*, 3018–3033)
educts:	4-oxo-3,4,6,7,8,9-hexahydropyrimido[4,5-*b*]indolizine-10-carbonitrile (**45**) and phosphoryl chloride (excess)
yield:	42%
visual appearance:	white needles
chemical formula:	$C_{11}H_9ClN_4$
molecular weight:	232.67 Da
LC-MS analysis:	calculated: 232.05 Da; found: not determined
purity:	not determined
^{1}H NMR:	500 MHz, DMSO-d_6, δ 8.71 (s, 1H), 4.52 (t, J = 6.2 Hz, 2H), 3.15 (t, J = 6.4 Hz, 2H), 2.09-2.03 (m, 2H), 1.91-1.85 (m, 2H)
^{13}C NMR:	126 MHz, DMSO-d_6, δ 154.8, 151.3, 150.8, 142.1, 123.5, 113.4, 83.8, 46.0, 23.6, 21.8, 17.8

6.1.3.8.2. Synthesis of **4-chloro-7,8,9,10-tetrahydro-6*H*-pyrimido[4',5':4,5]pyrrolo[1,2-*a*]azepine-11-carbonitrile (60)**

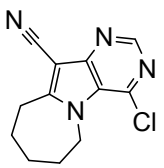

synonyms:	SMS-**A**-**33** compound **6b** (*J. Med. Chem.* **2016**, *59*, 3018–3033)
educts:	4-oxo-4,6,7,8,9,10-hexahydro-3*H*-pyrimido[4',5':4,5]pyrrolo[1,2-*a*]azepine-11-carbonitrile (**46**) and phosphoryl chloride (excess)

yield:	71%
visual appearance:	brown needles
chemical formula:	$C_{12}H_{11}ClN_4$
molecular weight:	246.70 Da
LC-MS analysis:	calculated: 246.07 Da; found: not determined
purity:	not determined
^{1}H NMR:	500 MHz, DMSO-d_6, δ 8.73 (s, 1H), 4.80-4.75 (m, 2H), 3.20-3.16 (m, 2H), 1.90-1.71 (m, 6H)
^{13}C NMR:	126 MHz, DMSO-d_6, δ 160.1, 150.8, 150.8, 141.5, 123.6, 113.6, 85.4, 47.00, 29.3, 27.1, 26.9, 25.2

6.1.3.8.3. Synthesis of **4-chloro-5-methyl-5*H*-pyrrolo[3,2-*d*]pyrimidine-7-carbonitrile (61)**

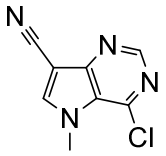

synonyms:	SMS-**A-231** compound **11a** (*J. Med. Chem.* **2016**, *59*, 3018–3033) compound **5a** (*Biochim. Biophys. Acta* **2017**, *1859*, 69–79)
educts:	5-methyl-4-oxo-4,5-dihydro-3*H*-pyrrolo[3,2-*d*]pyrimidine-7-carbonitrile (**47**) and phosphoryl chloride (excess)
yield:	66%
visual appearance:	brown powder
chemical formula:	$C_8H_5ClN_4$
molecular weight:	192.61 Da
LC-MS analysis:	calculated: 192.02 Da; found: not determined
purity:	not determined
^{1}H NMR:	500 MHz, DMSO-d_6, δ 8.79 (s, 1H), 8.76 (s, 1H), 4.14 (s, 3H)
^{13}C NMR:	not determined

6.1.3.8.4. Synthesis of **4-chloro-5-ethyl-4,5-dihydro-3*H*-pyrrolo[3,2-*d*]pyrimidine-7-carbonitrile (62)**

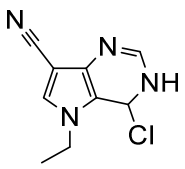

synonyms:	SMS-**A-476** compound **11b** (*J. Med. Chem.* **2016**, *59*, 3018–3033)
educts:	5-ethyl-4-oxo-4,5-dihydro-3*H*-pyrrolo[3,2-*d*]pyrimidine-7-carbonitrile (**48**) and phosphoryl chloride (excess)

yield:	79%
visual appearance:	brown powder
chemical formula:	$C_9H_9ClN_4$
molecular weight:	208.65 Da
LC-MS analysis:	calculated: 208.05 Da; found: not determined
purity:	not determined
1H NMR:	500 MHz, DMSO-*d6*, *δ* 8.86 (s, 1H), 8.80 (s, 1H), 4.56 (q, *J* = 7.2 Hz, 2H), 1.45 (t, *J* = 7.2 Hz, 3H)
13C NMR:	not determined

6.1.3.8.5. Synthesis of **4-chloro-5-propyl-5*H*-pyrrolo[3,2-*d*]pyrimidine-7-carbonitrile (63)**

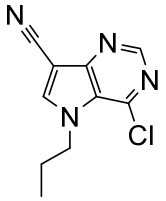

synonyms:	SMS-**A-483** compound **11c** (*J. Med. Chem.* **2016**, *59*, 3018–3033)
educts:	4-oxo-5-propyl-4,5-dihydro-3*H*-pyrrolo[3,2-*d*]pyrimidine-7-carbonitrile (**49**) and phosphoryl chloride (excess)
yield:	94%
visual appearance:	brown powder
chemical formula:	$C_{10}H_9ClN_4$
molecular weight:	220.66 Da
LC-MS analysis:	calculated: 220.05 Da; found: not determined
purity:	not determined
^{1}H NMR:	500 MHz, DMSO-d_6, *δ* 8.86 (s, 1H), 8.81 (s, 1H), 4.48 (t, *J* = 7.2 Hz, 2H), 1.88-1.81 (m, *2*H), 0.87 (t, *J* = 7.4 Hz, 3H)
^{13}C NMR:	not determined

6.1.3.8.6. Synthesis of **4-chloro-5-isopropyl-5*H*-pyrrolo[3,2-*d*]pyrimidine-7-carbonitrile (64)**

synonyms:	SMS-**A-490** compound **11d** (*J. Med. Chem.* **2016**, *59*, 3018–3033)
educts:	5-isopropyl-4-oxo-4,5-dihydro-3*H*-pyrrolo[3,2-*d*]pyrimidine-7-carbonitrile (**50**) and phosphoryl chloride (excess)

yield:	32%
visual appearance:	brown powder
chemical formula:	$C_{10}H_9ClN_4$
molecular weight:	220.66 Da
LC-MS analysis:	calculated: 220.05 Da; found: not determined
purity:	not determined
^{1}H NMR:	500 MHz, DMSO-d_6, δ 9.05 (s, 1H), 8.80 (s, 1H), 5.40 (m, 1H), 1.54 (d, J = 6.6 Hz, 6H)
^{13}C NMR:	not determined

6.1.3.8.7. Synthesis of **4-chloro-5-cyclopropyl-5*H*-pyrrolo[3,2-*d*]pyrimidine-7-carbonitrile (65)**

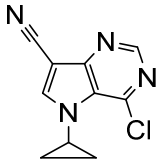

synonyms:	SMS-**A-497**
	compound **11e** (*J. Med. Chem.* **2016**, *59*, 3018–3033)
educts:	5-cyclopropyl-4-oxo-4,5-dihydro-3*H*-pyrrolo[3,2-*d*]pyrimidine-7-carbonitrile (**51**) and phosphoryl chloride (excess)
yield:	quantitative
visual appearance:	brown powder
chemical formula:	$C_{10}H_7ClN_4$
molecular weight:	218.64 Da
LC-MS analysis:	calculated: 218.04 Da; found: not determined
purity:	not determined
^{1}H NMR:	500 MHz, DMSO-d_6, δ 8.83 (s, 1H), 8.80 (s, 1H), 3.93-3.88 (m, 1H), 1.28-1.14 (m, 4H)
^{13}C NMR:	not determined

6.1.3.8.8. Synthesis of **4-chloro-5-phenyl-5*H*-pyrrolo[3,2-*d*]pyrimidine-7-carbonitrile (66)**

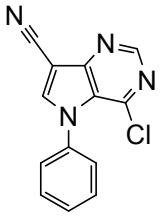

synonyms:	SMS-**A-188**
	compound **11f** (*J. Med. Chem.* **2016**, *59*, 3018–3033)
	compound **5b** (*Biochim. Biophys. Acta* **2017**, *1859*, 69–79)

educts:	4-oxo-5-phenyl-4,5-dihydro-3*H*-pyrrolo[3,2-*d*]pyrimidine-7-carbonitrile (**52**) and phosphoryl chloride (excess)
yield:	94%
visual appearance:	brown powder
chemical formula:	$C_{13}H_7ClN_4$
molecular weight:	254.68 Da
LC-MS analysis:	calculated: 254.04 Da; found: not determined
purity:	not determined
^{1}H NMR:	500 MHz, DMSO-d_6, δ 9.01 (s, 1H), 8.91 (s, 1H), 7.68-7.65 (m, 2H), 7.63-7.57 (m, 3H)
^{13}C NMR:	not determined

6.1.3.8.9. Synthesis of **4-chloro-5-(2-methoxyphenyl)-5*H*-pyrrolo[3,2-*d*]pyrimidine-7-carbonitrile (67)**

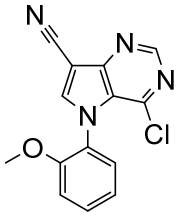

synonyms:	SMS-**A-296** compound **35a** (*J. Med. Chem.* **2017**, *accepted 10th of October, 2017*)
educts:	5-(2-methoxyphenyl)-4-oxo-4,5-dihydro-3*H*-pyrrolo[3,2-*d*]pyrimidine-7-carbonitrile (**53**) and phosphoryl chloride (excess)
yield:	quantitative
visual appearance:	greywhite powder
chemical formula:	$C_{14}H_9ClN_4O$
molecular weight:	284.70 Da
LC-MS analysis:	calculated: 284.05 Da; found: not determined
purity:	not determined
^{1}H NMR:	500 MHz, DMSO-d_6, δ 8.94 (s, 1H), 8.89 (s, 1H), 7.63-7.58 (m, 2H), 7.28 (dd, J = 8.8, 1.1 Hz, 1H), 7.15 (td, J = 7.6, 1.2 Hz, 1H), 3.74 (s, 3H)
^{13}C NMR:	not determined

6.1.3.8.10. Synthesis of **4-chloro-5-(4-ethoxyphenyl)-5*H*-pyrrolo[3,2-*d*]pyrimidine-7-carbonitrile (68)**

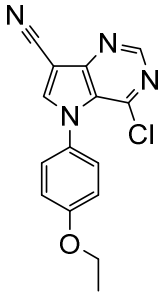

synonyms:	SMS-**A-281** compound **35b** (*J. Med. Chem.* **2017**, *accepted 10th of October, 2017*)
educts:	5-(4-ethoxyphenyl)-4-oxo-4,5-dihydro-3*H*-pyrrolo[3,2-*d*]pyrimidine-7-carbonitrile (**54**) and phosphoryl chloride (excess)
yield:	quantitative
visual appearance:	greywhite powder
chemical formula:	$C_{15}H_{11}ClN_4O$
molecular weight:	298.73 Da
LC-MS analysis:	calculated: 298.06 Da; found: not determined
purity:	not determined
^{1}H NMR:	not determined
^{13}C NMR:	not determined

6.1.3.8.11. Synthesis of **5-benzyl-4-chloro-5*H*-pyrrolo[3,2-*d*]pyrimidine-7-carbonitrile (69)**

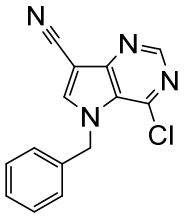

synonyms:	SMS-**A-201** compound **11g** (*J. Med. Chem.* **2016**, *59*, 3018–3033) compound **5c** (*Biochim. Biophys. Acta* **2017**, *1859*, 69–79)
educts:	5-benzyl-4-oxo-4,5-dihydro-3*H*-pyrrolo[3,2-*d*]pyrimidine-7-carbonitrile (**55**) and phosphoryl chloride (excess)
yield:	83%
visual appearance:	brown powder
chemical formula:	$C_{14}H_9ClN_4$
molecular weight:	268.70 Da
LC-MS analysis:	calculated: 268.05 Da; found: not determined
purity:	not determined

^{1}H NMR:	500 MHz, DMSO-d_6, δ 8.98 (s, 1H), 8.83 (s, 1H), 7.36-7.32 (m, 2H), 7.31-7.27 (m, 1H), 7.16- 7.12 (m, 2H), 5.81 (s, 2H)
^{13}C NMR:	not determined

6.1.3.8.12. Synthesis of **4-chloro-5-phenethyl-5*H*-pyrrolo[3,2-*d*]pyrimidine-7-carbonitrile (70)**

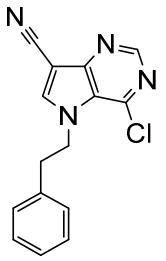

synonyms:	SMS-**A-206** compound **11h** (*J. Med. Chem.* **2016**, *59*, 3018–3033) compound **5d** (*Biochim. Biophys. Acta* **2017**, *1859*, 69–79)
educts:	4-oxo-5-phenethyl-4,5-dihydro-3*H*-pyrrolo[3,2-*d*]pyrimidine-7-carbonitrile (**56**) and phosphoryl chloride (excess)
yield:	88%
visual appearance:	brown powder
chemical formula:	$C_{15}H_{11}ClN_4$
molecular weight:	282.73 Da
LC-MS analysis:	calculated: 282.07 Da; found: not determined
purity:	not determined
^{1}H NMR:	500 MHz, DMSO-d_6, δ 8.81 (s, 1H), 8.65 (s, 1H), 7.28-7.24 (m, 2H), 7.21-7.19 (m, 1H), 7.15-7.11 (m, 2H), 4.77 (t, J = 7.4, 2H), 3.15 (t, J = 7.4, 2H)
^{13}C NMR:	not determined

6.1.3.8.13. Synthesis of **4-chloro-5-(3-phenylpropyl)-5*H*-pyrrolo[3,2-*d*]pyrimidine-7-carbonitrile (71)**

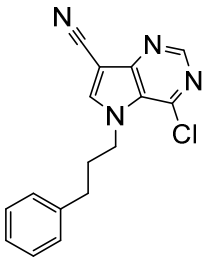

synonyms:	SMS-**A-211** compound **11i** (*J. Med. Chem.* **2016**, *59*, 3018–3033)
educts:	4-oxo-5-(3-phenylpropyl)-4,5-dihydro-3*H*-pyrrolo[3,2-*d*]pyrimidine-7-carbonitrile (**57**) and phosphoryl chloride (excess)
yield:	69%

visual appearance:	brown powder
chemical formula:	$C_{16}H_{13}ClN_4$
molecular weight:	296.76 Da
LC-MS analysis:	calculated: 296.08 Da; found: not determined
purity:	not determined
^{1}H NMR:	500 MHz, DMSO-d_6, δ 8.84 (s, 1H), 8.79 (s, 1H), 7.26-7.22 (m, 2H), 7.20-7.13 (m, 3H), 4.55 (t, J = 7.3, 2H), 2.66 (t, J = 7.5, 2H), 2.20-2.13 (m, 2H)
^{13}C NMR:	not determined

6.1.3.8.14. Synthesis of **4-chloro-5*H*-pyrimido[5,4-*b*]indole (72)**

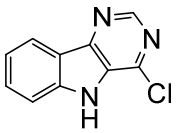

synonyms:	SMS-**A**-**134**
	compound **40** (*J. Med. Chem.* **2017**, *accepted 10th of October, 2017*)
educts:	3,5-dihydro-4*H*-pyrimido[5,4-*b*]indole-4-one (**44**) and phosphoryl chloride (excess)
yield:	52%
visual appearance:	brown powder
chemical formula:	$C_{10}H_6ClN_3$
molecular weight:	203.63 Da
LC-MS analysis:	calculated: 203.03 Da; found: not determined
purity:	not determined
^{1}H NMR:	500 MHz, DMSO-d_6, δ 12.33 (s, 1H), 8.84 (s, 1H), 8.25 (dt, J 8.0, 1.0 Hz, 1H), 7.70 (ddd, J = 7.8, 6.6, 1.0, 1H), 7.68 (dt, J = 8.3, 1.3, 2H), 7.37 (ddd, J = 8.0, 6.6, 1.4, 1H)
^{13}C NMR:	126 MHz, DMSO-d_6, δ 148.7, 147.0, 141.9, 141.4, 130.9, 128.2, 121.7, 121.2, 120.0, 113.1

6.1.3.9. Alkylation of Piperazine

To 3-(2-bromoethyl)-1*H*-indole dissolved in 50 mL acetonitrile was added to a saturated solution of piperazine (4 eq.) in the same solvent at room temperature. The reaction was started by addition of 6 eq. Hünig's base started the reaction at room temperature. After 24 hours, the Hünig's base hydrochloride was filtered off and the clear filtrate was evaporated, resulting in an orange oil containing the piperazine derivative. Column chromatography performed as stated above yielded the purified alkylated product.

6.1.3.9.1. Synthesis of **3-(2-(piperazine-1-yl)ethyl)-1*H*-indole (73)**

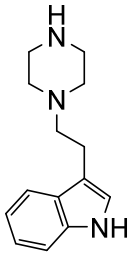

synonyms:	SMS-**A**-**8** compound **30** (*J. Med. Chem.* **2017**, *accepted 10th of October, 2017*)
educts:	3-(2-bromoethyl)-1*H*-indole, piperazine (4 eq.) and Hünig's base (6 eq.)
yield:	quantitative
visual appearance:	orange oil
chemical formula:	$C_{14}H_{19}N_3$
molecular weight:	229.33 Da
LC-MS analysis:	calculated: 229.16 Da; found: not determined
purity:	not determined
^{1}H NMR:	500 MHz, DMSO-d_6, δ 10.74 (s, 1H), 7.49 (d, J = 7.9 Hz, 1H), 7.31 (d, J = 8.1 Hz, 1H), 7.13 (d, 2.3 Hz, 1H), 7.04 (ddd, J = 8.1, 7.0, 1.1 Hz), 6.95 (ddd, J = 7.9 Hz, 7.0, 1.0 Hz), 2.85-2.81 (m, 2H), 2.81-2.76 (m, 4H), 2.59-2.53 (m, 2H), 2.48-2.40 (m, 4H), 1.87 (s, 1H)
^{13}C NMR:	126 MHz, DMSO-d_6, δ 136.3, 127.4, 122.6, 120.9, 118.4, 118.2, 112.7, 111.4, 59.5, 53.2 (2C), 45.2 (2C), 22.3

6.1.4. Synthesis and Characterization of Target Compounds via Nucleophilic Substitution at the Aromatic Ring System

The purine or 9-deazapurine intermediates **59**-**72** were dissolved in 0.5 mL *N*,*N*-dimethylformamide and added to 1.5 eq. of the corresponding primary or secondary amine in 0.5 mL of *N*,*N*-dimethylformamide. Additionally, 1.5 eq. of TEA were added. The reaction was performed using microwave-assisted synthesis at 200 W and 110 °C for 20-60 minutes. The reaction mixture was directly put onto a column and purified as stated above. The products were crystallized from a mixture of ethanol and petroleum ether (1:1).

6.1.4.1. Synthesis of **4-(4-phenethylpiperazine-1-yl)-6,7,8,9-tetrahydropyrimido[4,5-*b*]indolizine-10-carbonitrile (74)**

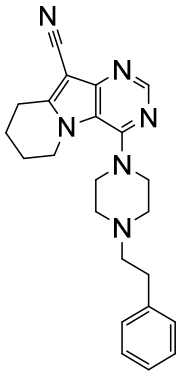

synonyms:	SMS-**A**-**50** compound **12** (*J. Med. Chem.* **2016**, *59*, 3018–3033) compound **SC12** (*Biochim. Biophys. Acta* **2017**, *1859*, 69–79) compound **75** (*J. Med. Chem.* **2017**, *accepted 10th of October, 2017*)
educts:	4-chloro-6,7,8,9-tetrahydropyrimido[4,5-*b*]indolizine-10-carbonitrile (**59**), 1-(2-phenethyl)piperazine (1.5 eq.) and TEA (1.5 eq.)
yield:	66%
visual appearance:	yellow needles
chemical formula:	$C_{23}H_{26}N_6$
molecular weight:	386.50 Da
LC-MS analysis:	calculated: 386.22 Da; found: 387.4 Da $[M+H]^+$
purity:	95%
^{1}H NMR:	500 MHz, DMSO-d_6, δ 8.46 (s, 1H), 7.29-7.22 (m, 4H), 7.19-7.15 (m, J = 7.1, 1.6 Hz, 1H), 3.34-3.29 (m, 4H), 4.35 (t, J = 5.6 Hz, 2H), 3.11 (t, J = 6.5 Hz, 2H), 2.78 (t, J = 7.2 Hz, 2H), 2.61-2.68 (m, 4H), 2.58 (t, J = 7.4 Hz, 2H), 1.98-1.87 (m, 4H)
^{13}C NMR:	126 MHz, DMSO-d_6, δ 154.4, 151.2, 151.0, 150.2, 140.5, 128.8 (2C), 128.4 (2C), 126.0, 118.2, 114.4, 83.6, 59.8, 52.2 (2C), 50.4 (2C), 46.1, 32.84, 22.9, 22.6, 18.4

6.1.4.2. Synthesis of **4-(4-benzylpiperazine-1-yl)-6,7,8,9-tetrahydropyrimido[4,5-*b*]indolizine-10-carbonitrile (75)**

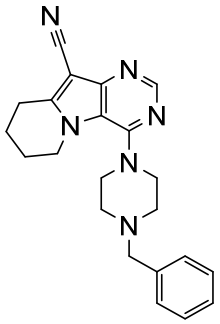

synonyms:	SMS-**A**-**53** compound **13** (*J. Med. Chem.* **2016**, *59*, 3018–3033)
educts:	4-chloro-6,7,8,9-tetrahydropyrimido[4,5-*b*]indolizine-10-carbonitrile (**59**), 1-benzylpiperazine (1.5 eq.) and TEA (1.5 eq.)
yield:	48%
visual appearance:	yellow needles
chemical formula:	$C_{22}H_{24}N_6$
molecular weight:	372.48 Da
LC-MS analysis:	calculated: 372.21 Da; found: 372.5 Da $[M+H]^+$
purity:	94%
^{1}H NMR:	500 MHz, DMSO-d_6, δ 8.45 (s, 1H), 7.34-7.31 (m, 4H), 7.28-7.23 (m, 1H), 4.33 (t, J = 5.6 Hz, 2H), 3.36-3.30 (m, 4H), 3.54 (s, 2H), 3.10 (t, J = 6.5 Hz, 2H), 2.66-2.51 (m, 4H), 2.03-1.81 (m, 4H)
^{13}C NMR:	126 MHz, DMSO-d_6, δ 154.3, 151.2, 150.9, 150.2, 138.1, 129.1 (2C), 128.3 (2C), 127.1, 118.2, 114.4, 83.6, 62.2, 52.3 (2C), 50.3 (2C), 46.1, 22.9, 22.6, 18.4

6.1.4.3. Synthesis of **4-(4-benzhydrylpiperazine-1-yl)-6,7,8,9-tetrahydropyrimido[4,5-*b*]indolizine-10-carbonitrile (76)**

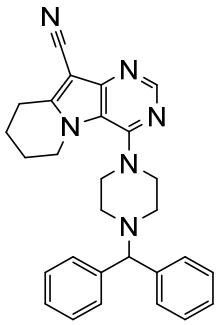

synonyms:	SMS-**A**-**51** compound **14** (*J. Med. Chem.* **2016**, *59*, 3018–3033)
educts:	4-chloro-6,7,8,9-tetrahydropyrimido[4,5-*b*]indolizine-10-carbonitrile (**59**), 1-benzhydrylpiperazine (1.5 eq.) and TEA (1.5 eq.)

yield:	70%
visual appearance:	white needles
chemical formula:	$C_{28}H_{28}N_6$
molecular weight:	448.57 Da
LC-MS analysis:	calculated: 448.24 Da; found: 449.4 Da $[M+H]^+$
purity:	92%
^{1}H NMR:	500 MHz, DMSO-d_6, δ 8.45 (s, 1H), 7.49-7.47 (m, 4H), 7.33-7.27 (m, 4H), 7.21-7.16 (m, 2H), 4.37 (s, 1H, CH), 4.31 (t, 5.5 Hz, 2H), 3.30-3.40 (m, 4H), 3.09 (t, J = 6.5 Hz, 2H), 2.49-2.60 (m, 4H), 1.82-1.95 (m, 4H)
^{13}C NMR:	126 MHz, DMSO-d_6, δ 154.2, 151.3, 150.9, 150.13, 142.9 (2C), 128.7 (4C), 127.7 (4C), 127.1 (2C), 118.2, 114.4, 83.6, 75.4, 51.3 (2C), 50.4 (2C), 46,0, 22.9, 22.6, 18.4

6.1.4.4. Synthesis of **4-(4-phenylpiperazine-1-yl)-6,7,8,9-tetrahydropyrimido[4,5-*b*]indolizine-10-carbonitrile (77)**

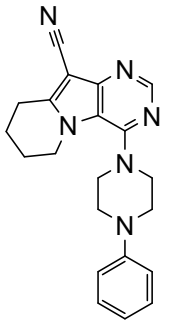

synonyms:	SMS-**A-52** compound **15** (*J. Med. Chem.* **2016**, *59*, 3018–3033)
educts:	4-chloro-6,7,8,9-tetrahydropyrimido[4,5-*b*]indolizine-10-carbonitrile (**59**), 1-phenylpiperazine (1.5 eq.) and TEA (1.5 eq.)
yield:	13%
visual appearance:	white needles
chemical formula:	$C_{21}H_{22}N_6$
molecular weight:	358.45 Da
LC-MS analysis:	calculated: 358.19 Da; found: 359.4 Da $[M+H]^+$
purity:	92%
^{1}H NMR:	500 MHz, DMSO-d_6, δ 8.50 (s, 1H), 7.24 (dd, J = 8.7, 7.3 Hz, 2H), 7.00 (d, J = 8.6 Hz, 2H), 6.81 (t, J = 7.3 Hz 1H), 4.40 (t, J = 5.6 Hz, 2H), 3.50-3.43 (m, 4H), 3.36-3.31 (m, 4H), 3.13 (t, J = 6.4 Hz, 2H), 2.00-1.88 (m, 4H)
^{13}C NMR:	126 MHz DMSO-d_6) δ 154.3, 151.3, 150.1, 150.1, 150.3, 129.1 (2C), 119.4, 118.4, 115.8 (2C), 114.4, 83.6, 50.3 (2C), 48.1 (2C), 46.1, 23.0, 22.6, 18.4

6.1.4.5. Synthesis of **4-(4-methylpiperazine-1-yl)-6,7,8,9-tetrahydropyrimido[4,5-b]indolizine-10-carbonitrile (78)**

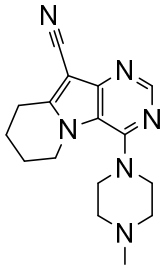

synonyms:	SMS-**A-123** compound **16** (*J. Med. Chem.* **2016**, *59*, 3018−3033)
educts:	4-chloro-6,7,8,9-tetrahydropyrimido[4,5-*b*]indolizine-10-carbonitrile (**59**), 1-methylpiperazine (1.5 eq.) and TEA (1.5 eq.)
yield:	45%
visual appearance:	white powder
chemical formula:	$C_{21}H_{22}N_6$
molecular weight:	296.38 Da
LC-MS analysis:	calculated: 296.17 Da; found: 297.2 Da $[M+H]^+$
purity:	100%
^{1}H NMR:	500 MHz, DMSO-d_6, δ 8.45 (s, 1H), 4.34 (t, J = 5.6 Hz, 2H), 3.31-3.25 (m, 4H), 3.10 (t, J = 6.5 Hz, 2H), 2.56-2.51 (m, 4H), 2.23 (s, 3H), 1.99-1.88 (m, 4H)
^{13}C NMR:	126 MHz DMSO-d_6, δ 154.4, 151.2, 151.0, 150.2, 118.2, 114.5, 83.6, 54.2 (2C), 50.2 (2C), 46.1, 45.8, 22.9, 22.6, 18.4

6.1.4.6. Synthesis of **4-(piperazine-1-yl)-6,7,8,9-tetrahydropyrimido[4,5-*b*]indolizine-10-carbonitrile (79)**

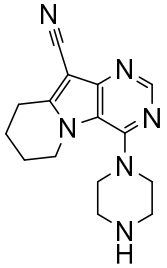

synonyms:	SMS-**A-7** compound **17** (*J. Med. Chem.* **2016**, *59*, 3018−3033)
educts:	4-chloro-6,7,8,9-tetrahydropyrimido[4,5-*b*]indolizine-10-carbonitrile (**59**), 1-piperazine (4 eq.) and TEA (1.5 eq.)
yield:	59%
visual appearance:	white powder
chemical formula:	$C_{15}H_{18}N_6$
molecular weight:	282.35 Da

LC-MS analysis:	calculated: 282.16 Da; found: 283.2 Da $[M+H]^+$
purity:	100%
^{1}H NMR:	500 MHz, DMSO-d_6, δ 8.45 (s, 1H), 4.34 (t, J = 5.6 Hz, 2H), 3.23 (t, J = 4.6 Hz, 4H), 3.10 (t, J 6.5 Hz, 2H), 2.86 (J = 4.8 Hz, 4H), 1.98-1.86 (m, 4H)
^{13}C NMR:	126 MHz DMSO-d_6, δ 154.7, 151.3, 150.8, 150.2, 118.2, 114.5, 83.6, 51.6 (2C), 46.1, 45.2 (2C), 22.9, 22.6, 18.4

6.1.4.7. Synthesis of **4-((3-phenylpropyl)amino)-6,7,8,9-tetrahydropyrimido[4,5-*b*]indolizine-10-carbonitrile (80)**

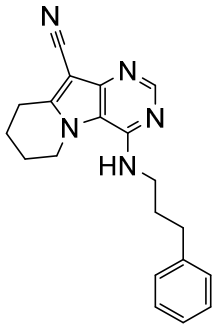

synonyms:	SMS-**A-694** compound **18** (*J. Med. Chem.* **2016**, *59*, 3018–3033)
educts:	4-chloro-6,7,8,9-tetrahydropyrimido[4,5-*b*]indolizine-10-carbonitrile (**59**), phenylpropylamine (1.5 eq.) and TEA (1.5 eq.)
yield:	40%
visual appearance:	yellow needles
chemical formula:	$C_{20}H_{21}N_5$
molecular weight:	331.42 Da
LC-MS analysis:	calculated: 331.18 Da; found: 332.1 Da $[M+H]^+$
purity:	99%
^{1}H NMR:	500 MHz, DMSO-d_6, δ 8.20 (s, 1H), 7.25 (t, J = 7.5 Hz, 2H), 7.20 (d, J = 7.2 Hz, 2H), 7.15 (t, J = 7.2 Hz, 1H), 6.80 (t, J 5.4 Hz, 1H), 4.37 (t, J = 6.1 Hz, 2H), 3.52-3.47 (m, 2H), 2.99 (t, J = 6.3 Hz, 2H), 2.65 (t, J = 7.6 Hz, 2H), 2.03-1.98 (m, 2H), 1.95-1.89 (m, 2H), 1.86-1.80 (m, 2H)
^{13}C NMR:	126 MHz DMSO-d_6, δ 152.2, 150.0, 147.7, 147.7, 142.1, 128.5 (2C), 128.5 (2C), 125.9, 115.1, 114.0, 82.8, 45.7, 33.0, 30.7, 23.1, 22.1, 18.2

6.1.4.8. Synthesis of **4-(phenethylamino)-6,7,8,9-tetrahydropyrimido[4,5-*b*]indolizine-10-carbonitrile (81)**

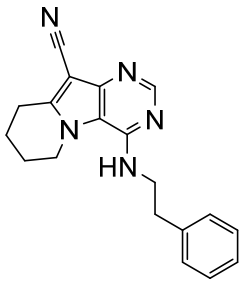

synonyms:	SMS-**A-652** compound **19** (*J. Med. Chem.* **2016**, *59*, 3018–3033)
educts:	4-chloro-6,7,8,9-tetrahydropyrimido[4,5-*b*]indolizine-10-carbonitrile (**59**), phenethylamine (1.5 eq.) and TEA (1.5 eq.)
yield:	18%
visual appearance:	yellow needles
chemical formula:	$C_{19}H_{19}N_5$
molecular weight:	317.40 Da
LC-MS analysis:	calculated: 317.16 Da; found: 318.1 Da $[M+H]^+$
purity:	100%
^{1}H NMR:	500 MHz, DMSO-d_6, δ 8.24 (s, 1H), 7.29 (t, J = 7.4 Hz, 2H), 7.25 (d, J = 6.9 Hz, 2H), 7.20 (t, J = 7.3 Hz, 1H), 6.92 (t, J = 5.5 Hz, 1H), 4.34 (t, J = 6.1 Hz, 2H), 3.73-3.63 (m, 2H), 3.00 (t, J = 6.3 Hz, 2H), 2.90 (t, J = 7.4, 2H), 2.04-1.97 (m, 2H), 1.97-1.80 (m, 2H)
^{13}C NMR:	126 MHz DMSO-d_6, δ 152.2, 149.7, 147.7, 147.6, 139.8, 128.8 (2C), 128.5 (2C), 126.2, 114.9, 114.0, 82.9, 45.6, 42.1, 35.1, 23.0, 22.0, 18.1

6.1.4.9. Synthesis of **4-(benzylamino)-6,7,8,9-tetrahydropyrimido[4,5-*b*]indolizine-10-carbonitrile (82)**

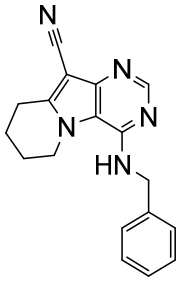

synonyms:	SMS-**A-604** compound **20** (*J. Med. Chem.* **2016**, *59*, 3018–3033)
educts:	4-chloro-6,7,8,9-tetrahydropyrimido[4,5-*b*]indolizine-10-carbonitrile (**59**), benzylamine (1.5 eq.) and TEA (1.5 eq.)
yield:	26%
visual appearance:	yellow needles

chemical formula:	$C_{18}H_{17}N_5$
molecular weight:	303.37 Da
LC-MS analysis:	calculated: 303.15 Da; found: 304.1 Da $[M+H]^+$
purity:	100%
^{1}H NMR:	500 MHz, DMSO-d_6, δ 8.17 (s, 1H), 7.46 (d, J = 6.4 Hz, 1H), 7.36 (d, J = 7.3 Hz, 2H), 7.28 (t, J = 7.6 Hz, 2H), 7.20 (t, J = 7.3 Hz, 1H), 4.71 (d, J = 5.8 Hz, 2H), 4.47 (t, J = 6.1 Hz, 2H), 3.01 (t, J = 6.3 Hz, 2H), 2.06-2.00 (m, 2H), 1.88-1.82 (m, 2H)
^{13}C NMR:	126 MHz DMSO-d_6, δ 152.1, 149.6, 148.8, 147.8, 140.1, 128.3 (2C), 127.3 (2C), 126.7, 114.9, 113.9, 82.9, 45.8, 43.5, 23.1, 22.1, 18.2

6.1.4.10. Synthesis of **4-(phenylamino)-6,7,8,9-tetrahydropyrimido[4,5-*b*]indolizine-10-carbonitrile (83)**

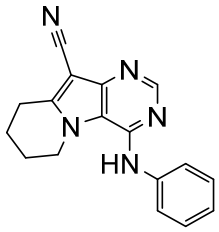

synonyms:	SMS-**A-556** compound **21** (*J. Med. Chem.* **2016**, *59*, 3018−3033)
educts:	4-chloro-6,7,8,9-tetrahydropyrimido[4,5-*b*]indolizine-10-carbonitrile (**59**), aniline (1.5 eq.) and TEA (1.5 eq.)
yield:	19%
visual appearance:	yellow needles
chemical formula:	$C_{17}H_{15}N_5$
molecular weight:	289.34 Da
LC-MS analysis:	calculated: 289.13 Da; found: 290.1 Da $[M+H]^+$
purity:	98%
^{1}H NMR:	500 MHz, DMSO-d_6, δ 8.49 (s, 1H), 8.31 (s, 1H), 7.55 (d, J = 7.7 Hz, 2H), 7.33 (t, J = 7.9 Hz, 2H), 7.07 (t, J = 7.4 Hz, 1H), 4.57 (t, J = 6.1 Hz, 2H), 3.08 (t, J = 6.4 Hz, 2H), 2.07-2.02 (m, 2H), 1.90-1.85 (m, 2H)
^{13}C NMR:	126 MHz DMSO-d_6, δ 151.5, 149.6, 149.2, 147.8, 139.6, 128.6 (2C), 123.4, 122.4 (2C), 114.9, 114.7, 83.22, 45.7, 23.2, 22.1, 18.3

6.1.4.11. Synthesis of **4-(4-phenethylpiperazine-1-yl)-7,8,9,10-tetrahydro-6*H*-pyrimido[4',5':4,5]pyrrolo[1,2-*a*]azepine-11-carbonitrile (84)**

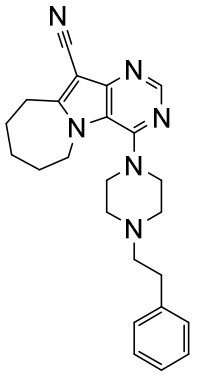

synonyms:	SMS-**A**-**64** compound **22** (*J. Med. Chem.* **2016**, *59*, 3018–3033)
educts:	4-chloro-7,8,9,10-tetrahydro-6*H*-pyrimido[4',5':4,5]pyrrolo[1,2-*a*]azepine-11-carbonitrile (**60**), 1-(2-phenethyl)piperazine (1.5 eq.) and TEA (1.5 eq.)
yield:	16%
visual appearance:	yellow needles
chemical formula:	$C_{24}H_{28}N_6$
molecular weight:	400.53 Da
LC-MS analysis:	calculated: 400.24 Da; found: 401.3 Da $[M+H]^+$
purity:	96%
^{1}H NMR:	500 MHz, DMSO-d_6, δ 8.47 (s, 1H), 7.29-7.22 (m, 4H), 7.19-7.15 (m, 1H), 4.59-4.39 (m, 2H), 3.40-3.28 (m, 4H), 3.14-3.03 (m, 2H), 2.77 (t, J = 7.2 Hz, 2H), 2.69-2.62 (m, 4H), 2.59 (t, J = 7.2 Hz, 2H), 1.90-1.81 (m, 2H), 1.81-1.70 (m, 4H)
^{13}C NMR:	126 MHz, DMSO-d_6, δ 156.6, 153.7, 151.0, 149.6, 140.5, 128.8 (2C), 128.3 (2C), 126.0, 117.9, 114.6, 85.4, 59.7, 52.1 (2C), 49.8 (2C), 47.4, 32.8, 29.9, 27.9, 27.1, 25.6

6.1.4.12. Synthesis of **4-(4-phenethylpiperazine-1-yl)-7,8,9,10-tetrahydro-6*H*-pyrimido[4',5':4,5]pyrrolo[1,2-*a*]azepine-11-carbonitrile (85)**

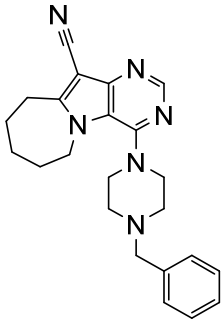

synonyms:	SMS-**A**-**67** compound **23** (*J. Med. Chem.* **2016**, *59*, 3018–3033)
educts:	4-chloro-7,8,9,10-tetrahydro-6*H*-pyrimido[4',5':4,5]pyrrolo[1,2-*a*]azepine-11-carbonitrile (**60**), 1-benzylpiperazine (1.5 eq.) and TEA (1.5 eq.)

yield:	36%
visual appearance:	white needles
chemical formula:	$C_{23}H_{26}N_6$
molecular weight:	386.50 Da
LC-MS analysis:	calculated: 386.22 Da; found: 387.4 Da $[M+H]^+$
purity:	99%
^{1}H NMR:	500 MHz, DMSO-d_6, δ 8.46, (s, 1H), 7.35-7.31 (m, 4H), 7.28-7.22 (m, 1H), 4.52-4.40 (m, 2H), 3.36-3.28 (m, 4H), 3.54 (s, 2H), 3.12-3.04 (m, 2H), 2.69-2.51 (m, 4H), 1.87-1.79 (m, 2H), 1.80-1.67 (m, 4H)
^{13}C NMR:	126 MHz, DMSO-d_6, δ 156.6, 153.7, 151.1, 149.6, 138.1, 129.0 (2C), 128.4 (2C), 127.2, 117.9, 114.6, 85.3, 62.1, 52.1 (2C), 49.7 (2C), 47.4, 27.9, 27.9, 27.1, 25.6

6.1.4.13. Synthesis of 4-(4-benzhydrylpiperazine-1-yl)-7,8,9,10-tetrahydro-6*H*-pyrimido[4',5':4,5]pyrrolo[1,2-*a*]azepine-11-carbonitrile (86)

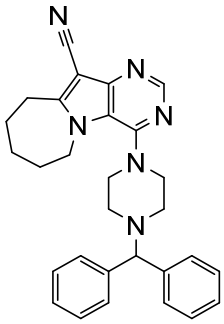

synonyms:	SMS-**A**-**65** compound **24** (*J. Med. Chem.* **2016**, *59*, 3018–3033)
educts:	4-chloro-7,8,9,10-tetrahydro-6*H*-pyrimido[4',5':4,5]pyrrolo[1,2-*a*]azepine-11-carbonitrile (**60**), 1-benzhydrylpiperazine (1.5 eq.) and TEA (1.5 eq.)
yield:	51%
visual appearance:	white needles
chemical formula:	$C_{29}H_{30}N_6$
molecular weight:	462.60 Da
LC-MS analysis:	calculated: 462.25 Da; found: 463.3 Da $[M+H]^+$
purity:	98%
^{1}H NMR:	500 MHz, DMSO-d_6, δ 8.46 (s, 1H), 7.48-7.43 (m, 4H), 7.32-7.27 (m, 4H), 7.21-7.16 (m, 2H), 4.49-4.39 (m, 2H), 4.38 (s, 1H), 3.40-3.29 (m, 4H), 3.11-2.99 (m, 2H), 2.56-2.50 (m, 4H), 1.84-1.76 (m, 2H), 1.76-1.63 (m, 4H)
^{13}C NMR:	126 MHz, DMSO-d_6, δ 156.5, 153.6, 151.1, 149.8, 142.8 (2C), 128.7 (4C), 127.7 (4C), 127.1 (2C), 114.6, 117.9, 85.2, 75.2, 51.1 (2C), 49.8 (2C), 47.4, 29.9, 27.8, 27.1, 25.6

6.1.4.14. Synthesis of 4-(4-phenylpiperazine-1-yl)-7,8,9,10-tetrahydro-6*H*-pyrimido[4',5':4,5]pyrrolo[1,2-*a*]azepine-11-carbonitrile (87)

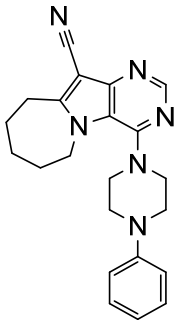

synonyms:	SMS-**A-66** compound **25** (*J. Med. Chem.* **2016**, *59*, 3018–3033)
educts:	4-chloro-7,8,9,10-tetrahydro-6*H*-pyrimido[4',5':4,5]pyrrolo[1,2-*a*]azepine-11-carbonitrile (**60**), 1-phenylpiperazine (1.5 eq.) and TEA (1.5 eq.)
yield:	52%
visual appearance:	yellow needles
chemical formula:	$C_{22}H_{24}N_6$
molecular weight:	372.48 Da
LC-MS analysis:	calculated: 372.21 Da; found: 373.4 Da $[M+H]^+$
purity:	99%
^{1}H NMR:	500 MHz, DMSO-d_6, δ 8.51 (s, 1H), 7.27-7.20 (m, 2H), 7.03-6.98 (m, 2H), 6.84-6.78 (m, 1H), 4.56-4.49 (m, 2H), 3.47-3.41 (m, 4H), 3.38-3.31 (m, 4H), 3.14-3.09 (m, 2H), 1.90 - 1.72 (m, 6H)
^{13}C NMR:	126 MHz, DMSO-d_6, δ 156.8, 153.7, 151.1, 151.0, 149.7, 129.1 (2C), 119.4, 118.0, 115.9 (2C), 114.6, 85.3, 49.7 (2C), 47.9 (2C), 47.5, 29,9, 27.8, 27.1, 25.6

6.1.4.15. Synthesis of 5-methyl-4-(4-phenethylpiperazine-1-yl)-5*H*-pyrrolo[3,2-*d*]pyrimidine-7-carbonitrile (88)

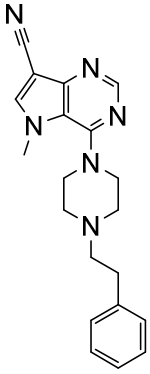

synonyms:	SMS-**A-340** compound **26** (*J. Med. Chem.* **2016**, *59*, 3018–3033)
educts:	4-chloro-5-methyl-5*H*-pyrrolo[3,2-*d*]pyrimidine-7-carbonitrile (**61**), 1-(2-phenethyl)piperazine (1.5 eq.) and TEA (1.5 eq.)

yield:	72%
visual appearance:	yellow needles
chemical formula:	$C_{20}H_{22}N_6$
molecular weight:	346.44 Da
LC-MS analysis:	calculated: 346.19 Da; found: 347.2 Da $[M+H]^+$
purity:	100%
^{1}H NMR:	500 MHz, DMSO-d_6, δ 8.50 (s, 1H), 8.44 (s, 1H), 7.29-7.25 (m, 2H), 7.25-7.22 (m, 2H), 7.19-7.15 (m, 1H), 4.01 (s, 3H), 3.41-3.34 (m, 4H), 2.77 (t, J = 7.3 Hz, 2H), 2.68-2.61 (m, 4H), 2.58 (t, J = 7.4 Hz, 2H)
^{13}C NMR:	126 MHz, DMSO-d_6, δ 154.9, 151.3, 150.1, 141.5, 140.5, 128.8 (2C), 128.4 (2C), 126.0, 118.6, 114.4, 85.4, 59.8, 52.2 (2C), 50.1 (2C), 36.8, 32.8

6.1.4.16. Synthesis of **5-ethyl-4-(4-phenethylpiperazine-1-yl)-5*H*-pyrrolo[3,2-*d*]pyrimidine-7-carbonitrile (89)**

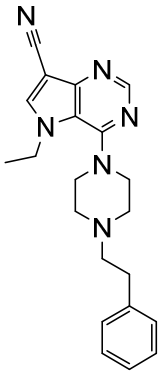

synonyms:	SMS-**A-478** compound **27** (*J. Med. Chem.* **2016**, *59*, 3018–3033)
educts:	4-chloro-5-ethyl-5*H*-pyrrolo[3,2-*d*]pyrimidine-7-carbonitrile (**62**), 1-(2-phenethyl)piperazine (1.5 eq.) and TEA (1.5 eq.)
yield:	64%
visual appearance:	white needles
chemical formula:	$C_{21}H_{24}N_6$
molecular weight:	360.47 Da
LC-MS analysis:	calculated: 360.21 Da; found: 361.2 Da $[M+H]^+$
purity:	100%
^{1}H NMR:	500 MHz, DMSO-d_6, δ 8.61 (s, 1H), 8.54 (s, 1H), 7.29-7.22 (m, 4H), 7.19-7.15 (m, 1H), 4.34 (q, J = 7.2 Hz, 2H), 3.36-3.30 (m, 4H), 2.78 (t, J = 7.2 Hz, 2H), 2.70-2.62 (m, 4H), 2.59 (t, J = 7.3 Hz, 2H), 1.37 (t, J = 7.2 Hz, 3H)
^{13}C NMR:	126 MHz, DMSO-d_6, δ 154.9, 151.4, 150.6, 140.6, 140.5, 128.8 (2C), 128.4 (2C), 126.0, 117.8, 114.3, 86.1, 59.7, 52.2 (2C), 50.1 (2C), 44.1, 32.8, 16.1

6.1.4.17. Synthesis of **4-(4-phenethylpiperazine-1-yl)-5-propyl-5*H*-pyrrolo[3,2-*d*]pyrimidine-7-carbonitrile (90)**

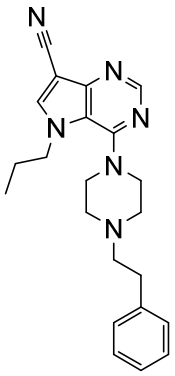

synonyms:	SMS-**A-485** compound **28** (*J. Med. Chem.* **2016**, *59*, 3018–3033)
educts:	4-chloro-5-propyl-5*H*-pyrrolo[3,2-*d*]pyrimidine-7-carbonitrile (**63**), 1-(2-phenethyl)piperazine (1.5 eq.) and TEA (1.5 eq.)
yield:	72%
visual appearance:	white needles
chemical formula:	$C_{22}H_{26}N_6$
molecular weight:	374.49 Da
LC-MS analysis:	calculated: 374.22 Da; found: 375.2 Da $[M+H]^+$
purity:	100%
^{1}H NMR:	500 MHz, DMSO-d_6, δ 8.61 (s, 1H), 8.54 (s, 1H), 7.29-7.22 (m, 4H), 7.19-7.15 (m, 1H), 4.34 (q, J = 7.2 Hz, 2H), 3.36-3.30 (m, 4H), 2.78 (t, J = 7.2 Hz, 2H), 2.70-2.62 (m, 4H), 2.59 (t, J = 7.3 Hz, 2H), 1.37 (t, J = 7.2 Hz, 3H)
^{13}C NMR:	126 MHz, DMSO-d_6, δ 154.9, 151.4, 150.6, 140.6, 140.5, 128.8 (2C), 128.4 (2C), 126.0, 117.8, 114.3, 86.1, 59.7, 52.2 (2C), 50.1 (2C), 44.1, 32.8, 16.1

6.1.4.18. Synthesis of **5-isopropyl-4-(4-phenethylpiperazine-1-yl)-5*H*-pyrrolo[3,2-*d*]pyrimidine-7-carbonitrile (91)**

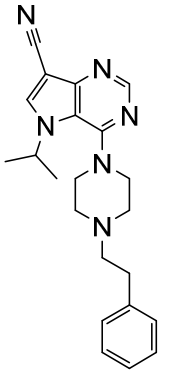

synonyms:	SMS-**A-492** compound **29** (*J. Med. Chem.* **2016**, *59*, 3018–3033)

educts:	4-chloro-5-isopropyl-5*H*-pyrrolo[3,2-*d*]pyrimidine-7-carbonitrile (**64**), 1-(2-phenethyl)piperazine (1.5 eq.) and TEA (1.5 eq.)
yield:	18%
visual appearance:	pale yellow needles
chemical formula:	$C_{22}H_{26}N_6$
molecular weight:	374.49 Da
LC-MS analysis:	calculated: 374.22 Da; found: 373.3 Da $[M+H]^+$
purity:	100%
^{1}H NMR:	500 MHz, DMSO-d_6, δ 8.81 (s, 1H), 8.55 (s, 1H), 7.29-7.22 (m, 4H), 7.19-7.15 (m, 1H), 4.99 (hept, J = 6.7 Hz, 1H), 3.32-3.30 (m, 4H), 2.78 (t, J = 7.2 Hz, 2H), 2.70-2.61 (m, 4H), 2.59 (t, J = 7.2 Hz, 2H), 1.44 (d, J = 6.6 Hz, 6H)
^{13}C NMR:	126 MHz, DMSO-d_6, δ 154.9, 151.3, 150.3, 140.5, 138.3, 128.8 (2C), 128.4 (2C), 126.0, 117.3, 114.4, 87.0, 59.7, 52.1 (2C), 50.0, 49.9 (2C), 32.8, 23.1 (2C)

6.1.4.19. Synthesis of 5-cyclopropyl-4-(4-phenethylpiperazine-1-yl)-5*H*-pyrrolo[3,2-*d*]pyrimidine-7-carbonitrile (92)

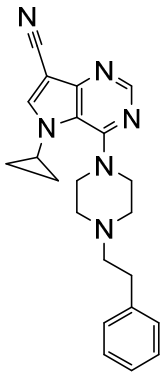

synonyms:	SMS-**A-499** compound **30** (*J. Med. Chem.* **2016**, *59*, 3018–3033)
educts:	4-chloro-5-cyclopropyl-5*H*-pyrrolo[3,2-*d*]pyrimidine-7-carbonitrile (**65**), 1-(2-phenethyl)piperazine (1.5 eq.) and TEA (1.5 eq.)
yield:	47%
visual appearance:	yellow needles
chemical formula:	$C_{22}H_{24}N_6$
molecular weight:	372.48 Da
LC-MS analysis:	calculated: 372.21 Da; found: 373.3 Da $[M+H]^+$
purity:	100%
^{1}H NMR:	500 MHz, DMSO-d_6, δ 8.46 (s, 1H), 8.45 (s, 1H), 7.29-7.21 (m, 4H), 7.19-7.15 (m,1H), 3.97 (quint, J = 3.8 Hz, 1H), 3.56-3.48 (m, 4H), 2.77 (t, J = 7.2 Hz, 2H), 2.64-2.60 (m, 4H), 2.57 (t, J = 7.4 Hz, 2H), 1.14-1.03 (m, 4H)
^{13}C NMR:	126 MHz, DMSO-d_6, δ 154.4, 151.3, 150.3, 140.5, 140.2, 128.8 (2C), 128.4 (2C), 126.0, 118.6, 114.4, 85.7, 59.8, 52.4 (2C), 49.7 (2C), 32.8, 32.2, 8.5 (2C)

6.1.4.20. Synthesis of **4-(4-phenethylpiperazine-1-yl)-5-phenyl-5*H*-pyrrolo[3,2-*d*]pyrimidine-7-carbonitrile (93)**

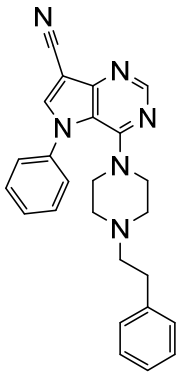

synonyms:	SMS-**A-308** compound **31** (*J. Med. Chem.* **2016**, *59*, 3018–3033)
educts:	4-chloro-5-phenyl-5*H*-pyrrolo[3,2-*d*]pyrimidine-7-carbonitrile (**66**), 1-(2-phenethyl)piperazine (1.5 eq.) and TEA (1.5 eq.)
yield:	50%
visual appearance:	yellow needles
chemical formula:	$C_{25}H_{24}N_6$
molecular weight:	408.51 Da
LC-MS analysis:	calculated: 408.21 Da; found: 409.4 Da $[M+H]^+$
purity:	100%
^{1}H NMR:	500 MHz, DMSO-d_6, δ 8.74 (s, 1H), 8.58 (s, 1H), 7.61-7.57 (m, 2H), 7.54-7.48 (m, 3H), 7.25-7.21 (m, 2H), 7.17-7.12 (m, 3H), 3.12-3.00 (m, 4H), 2.61 (t, J = 7.4 Hz, 2H) 2.34 (t, J = 7.5 Hz, 2H), 2.12-2.02 (m, 4H)
^{13}C NMR:	126 MHz, DMSO-d_6, δ 153.2, 151.8, 151.2, 141.4, 140.4, 137.9, 129.6 (2C), 128.7 (2C), 128.5, 128.3 (2C), 125.9, 125.3 (2C), 115.3, 114.1, 88.2, 59.6, 51.4 (2C), 48.7 (2C), 32.5

6.1.4.21. Synthesis of **4-(4-benzylpiperazine-1-yl)-5-phenyl-5*H*-pyrrolo[3,2-*d*]pyrimidine-7-carbonitrile (94)**

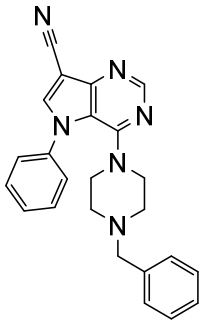

synonyms:	SMS-**A-311** compound **32** (*J. Med. Chem.* **2016**, *59*, 3018–3033)

educts:	4-chloro-5-phenyl-5*H*-pyrrolo[3,2-*d*]pyrimidine-7-carbonitrile (**66**), 1-benzylpiperazine (1.5 eq.) and TEA (1.5 eq.)
yield:	15%
visual appearance:	yellow needles
chemical formula:	$C_{24}H_{22}N_6$
molecular weight:	394.48 Da
LC-MS analysis:	calculated: 394.19 Da; found: 395.3 Da $[M+H]^+$
purity:	100%
^{1}H NMR:	500 MHz, DMSO-d_6, δ 8.73 (s, 1H), 8.57 (s, 1H), 7.58-7.49 (m, 3H), 7.49-7.45 (m, 2H), 7.30-7.25 (m, 2H), 7.25-7.21 (m, 1H), 719-7.16 (m, 2H), 3.31 (s, 2H), 312-3.00 (m, 4H), 2.04-1.91 (m, 4H)
^{13}C NMR:	126 MHz, DMSO-d_6, δ 153.1, 151.8, 151.2, 141.4, 137.9, 137.7, 129.6 (2C), 128.9 (2C), 128.5, 128.3 (2C), 127.1, 125.3 (2C), 115.3, 114.1, 88.1, 61.9, 51.3 (2C), 48.7 (2C)

6.1.4.22. Synthesis of **4-(4-benzylpiperazine-1-yl)-5-phenyl-5*H*-pyrrolo[3,2-*d*]pyrimidine-7-carbonitrile (95)**

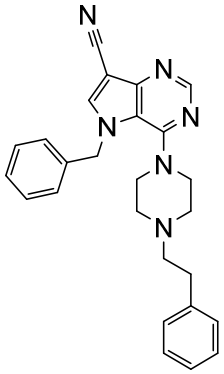

synonyms:	SMS-**A-316** compound **33** (*J. Med. Chem.* **2016**, *59*, 3018–3033)
educts:	5-benzyl-4-chloro-5*H*-pyrrolo[3,2-*d*]pyrimidine-7-carbonitrile (**69**), 1-(2-phenethyl)piperazine (1.5 eq.) and TEA (1.5 eq.)
yield:	41%
visual appearance:	yellow needles
chemical formula:	$C_{26}H_{26}N_6$
molecular weight:	422.54 Da
LC-MS analysis:	calculated: 422.22 Da; found: 423.3 Da $[M+H]^+$
purity:	100%
^{1}H NMR:	500 MHz, DMSO-d_6, δ 8.65 (s, 1H), 8.56 (1H), 7.33-7.11 (m, 10H), 5.52 (s, 2H), 3.39-3.30 (m, 4H), 2.76 (t, J = 7.2 Hz, 2H), 2.68-2.60 (m, 4H), 2.58 (t, J = 7.2 Hz, 2H)
^{13}C NMR:	126 MHz, DMSO-d_6, δ 155.2, 151.7, 151.0, 141.7, 140.5, 137.0, 128.9 (2C), 128.8 (2C), 128.4 (2C), 128.1, 127.1 (2C), 126.0, 117.9, 114.1, 87.0, 59.7, 52.2 (2C), 52.1, 50.0 (2C), 32.8

6.1.4.23. Synthesis of **5-benzyl-4-(4-benzylpiperazine-1-yl)-5*H*-pyrrolo[3,2-*d*]pyrimidine-7-carbonitrile (96)**

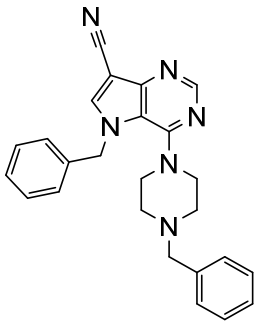

synonyms:	SMS-**A-319** compound **34** (*J. Med. Chem.* **2016**, *59*, 3018–3033)
educts:	5-benzyl-4-chloro-5*H*-pyrrolo[3,2-*d*]pyrimidine-7-carbonitrile (**69**), 1-benzylpiperazine (1.5 eq.) and TEA (1.5 eq.)
yield:	13%
visual appearance:	yellow solid
chemical formula:	$C_{25}H_{24}N_6$
molecular weight:	408.51 Da
LC-MS analysis:	calculated: 408.21 Da; found: 409.4 Da $[M+H]^+$
purity:	98%
^{1}H NMR:	500 MHz, DMSO-d_6, δ 8.64 (s, 1H), 8.55 (s, 1H), 7.35-7.22 (m, 8H), 7.13-7.09 (m, 2H), 5.51 (s, 2H), 3.54 (m, 2H), 3.36-3.30 (m, 4H), 2.57-2.52 (m, 4H)
^{13}C NMR:	126 MHz, DMSO-d_6, δ 155.1, 151.7, 151.0, 141.7, 138.0, 136.9, 129.1 (2C), 128.9 (2C), 128.3 (2C), 128.1, 127.2, 127.1 (2C), 117.9, 114.0, 86.9, 62.1, 52.1 (2C), 52.1, 49.9

6.1.4.24. Synthesis of **5-phenethyl-4-(4-phenethylpiperazine-1-yl)-5*H*-pyrrolo[3,2-*d*]pyrimidine-7-carbonitrile (97)**

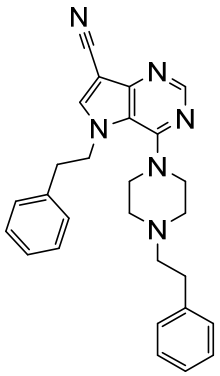

synonyms:	SMS-**A-324** compound **35** (*J. Med. Chem.* **2016**, *59*, 3018–3033)
educts:	4-chloro-5-phenethyl-5*H*-pyrrolo[3,2-*d*]pyrimidine-7-carbonitrile (**70**), 1-(2-phenethyl)piperazine (1.5 eq.) and TEA (1.5 eq.)

yield:	60%
visual appearance:	yellow needles
chemical formula:	$C_{27}H_{28}N_6$
molecular weight:	436.56 Da
LC-MS analysis:	calculated: 436.24 Da; found: 437.5 Da $[M+H]^+$
purity:	100%
^{1}H NMR:	500 MHz, DMSO-d_6, δ 8.55 (s, 1H), 8.49 (s, 1H), 730-7.21 (m, 4H), 7.20-7.09 (m, 4H), 7.00-6.96 (m, 2H), 4.55 (t, J = 7.1 Hz, 2H), 3.27-3.18 (m, 4H), 3.00 (t, J = 7.1 Hz, 2H), 2.77 (t, J = 7.2 Hz, 2H), 2.69-2.60 (m, 4H), 2.58 (t, J = 7.3 Hz, 2H)
^{13}C NMR:	126 MHz, DMSO-d_6, δ 154.9, 151.3, 150.4, 141.1, 140.5, 137.3, 128.8 (2C), 128.7 (2C), 128.4 (2C), 128.2 (2C), 126.7, 126.0, 118.1, 114.3, 86.2, 59.8, 52.2 (2C), 50.3, 50.0 (2C), 37.2, 32.7

6.1.4.25. Synthesis of 4-(4-benzylpiperazine-1-yl)-5-phenethyl-5*H*-pyrrolo[3,2-*d*]pyrimidine-7-carbonitrile (98)

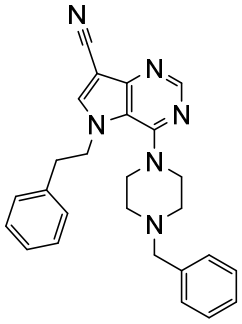

synonyms:	SMS-**A-327** compound **36** (*J. Med. Chem.* **2016**, *59*, 3018–3033)
educts:	4-chloro-5-phenethyl-5*H*-pyrrolo[3,2-*d*]pyrimidine-7-carbonitrile (**70**), 1-benzylpiperazine (1.5 eq.) and TEA (1.5 eq.)
yield:	25%
visual appearance:	white needles
chemical formula:	$C_{26}H_{26}N_6$
molecular weight:	422.54 Da
LC-MS analysis:	calculated: 422.22 Da; found: 423.3 Da $[M+H]^+$
purity:	100%
^{1}H NMR:	500 MHz, DMSO-d_6, δ 8.54 (s, 1H), 8.48 (s, 1H), 7.36-7.30 (m, 4H), 7.29-7.24 (m, 1H), 7.18-7.10 (m, 3H), 6.99-6.95 (m, 2H), 4.52 (t, J = 7.2 Hz, 2H), 3.54 (s, 2H), 3.27-3.20 (m, 4H), 3.00 (t, J = 7.1 Hz, 2H), 2.61-2.52 (m, 4H)
^{13}C NMR:	126 MHz, DMSO-d_6, δ = 154.8, 151.3, 150.4, 141.0, 137.9, 137.2, 129.0 (2C), 128.7 (2C), 128.3 (2C). 128,2 (2C), 127.1, 126.7, 118.0, 117.2, 86.1, 62.2, 52.1 (2C), 50.2, 49.9 (2C), 37.1

6.1.4.26. Synthesis of **4-(4-phenethylpiperazine-1-yl)-5-(3-phenylpropyl)-5*H*-pyrrolo[3,2-*d*]pyrimidine-7-carbonitrile (99)**

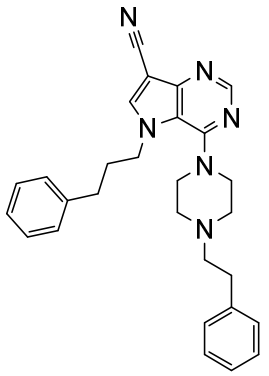

synonyms:	SMS-**A**-**332** compound **37** (*J. Med. Chem.* **2016**, *59*, 3018–3033)
educts:	4-chloro-5-(3-phenylpropyl)-5*H*-pyrrolo[3,2-*d*]pyrimidine-7-carbonitrile (**71**), 1-(2-phenethyl)piperazine (1.5 eq.) and TEA (1.5 eq.)
yield:	37%
visual appearance:	yellow needles
chemical formula:	$C_{28}H_{30}N_6$
molecular weight:	450.59 Da
LC-MS analysis:	calculated: 450.25 Da; found: 451.5 Da $[M+H]^+$
purity:	99%
^{1}H NMR:	500 MHz, DMSO-d_6, δ 8.62 (s, 1H), 8.53 (s, 1H), 7.30-7.25 (m, 2H), 7.25-7.21 (m, 4H), 7.20-7.16 (m, 1H), 7.16-7.12 (m, 1H), 7.10-7.07 (m, 2H), 4.31 (t, J = 7.5 Hz, 2H), 3.25-3.15 (m, 4H), 2.75 (t, J = 7.2 Hz, 2H), 2.54 (t, J = 7.4 Hz, 2H), 2.53-2.50 (m, 4H), 2.48-2.45 (m, 2H), 2.13-2.05 (m, 2H)
^{13}C NMR:	126 MHz, DMSO-d_6, δ 155.0, 151.4, 150.4, 140.9, 140.5, 128.8 (2C), 128.5 (2C), 128.4 (2C), 128.3 (2C), 126.2, 126.0, 118.0, 114.3, 86.2, 59.6, 52.1 (2C), 50.0 (2C), 48.6, 32.8, 32.0, 32.0

6.1.4.27. Synthesis of **4-(4-benzylpiperazine-1-yl)-5-(3-phenylpropyl)-5*H*-pyrrolo[3,2-*d*]pyrimidine-7-carbonitrile (100)**

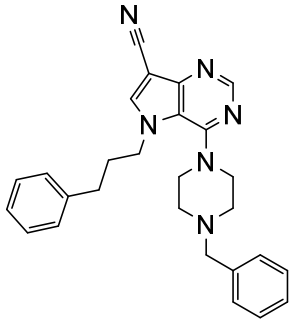

synonyms:	SMS-**A**-**335** compound **38** (*J. Med. Chem.* **2016**, *59*, 3018–3033)

educts:	4-chloro-5-(3-phenylpropyl)-5*H*-pyrrolo[3,2-*d*]pyrimidine-7-carbonitrile (**71**), 1benzylpiperazine (1.5 eq.) and TEA (1.5 eq.)
yield:	29%
visual appearance:	yellow needles
chemical formula:	$C_{27}H_{28}N_6$
molecular weight:	436.56 Da
LC-MS analysis:	calculated: 436.24 Da; found: 437.5 Da $[M+H]^+$
purity:	100%
^{1}H NMR:	500 MHz, DMSO-d_6, δ 8.61 (s, 1H), 8.52 (s, 1H), 7.35-7.30 (m, 4H), 7.27-7.22 (m, 3H), 7.20-7.16 (m, 1H), 7.10-7.06 (m, 2H), 4.30 (t, J = 7.4 Hz, 2H), 3.50 (s, 2H), 3.25-3.14 (m, 4H), 2.46 (t, J = 7.3 Hz, 2H), 2.45-2.37 (m, 4H), 2.11-2.04 (m, 2H)
^{13}C NMR:	126 MHz, DMSO-d_6, δ 154.9, 151.4, 150.4, 140.9, 140.5, 138.0, 129.0 (2C), 128.5 (2C), 128.3 (4C), 127.2, 126.2, 118.0, 114.3, 86.2, 62.0, 52.0 (2C), 50.0 (2C), 48.6, 32.0, 32.0

6.1.4.28. Synthesis of **4-(benzylamino)-5-methyl-5*H*-pyrrolo[3,2-*d*]pyrimidine-7-carbonitrile (101)**

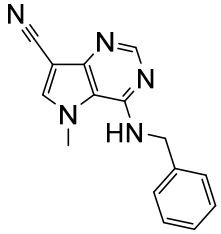

synonyms:	SMS-**A-715** compound **6** (*Biochim. Biophys. Acta* **2017**, *1859*, 69–79)
educts:	4-chloro-5-methyl-5*H*-pyrrolo[3,2-*d*]pyrimidine-7-carbonitrile (**61**), benzylamine (1.5 eq.) and TEA (1.5 eq.)
yield:	33%
visual appearance:	pale yellow crystals
chemical formula:	$C_{15}H_{13}N_5$
molecular weight:	263.30 Da
LC-MS analysis:	calculated: 263.12 Da; found: 264.0 Da $[M+H]^+$
purity:	95%
^{1}H NMR:	500 MHz, DMSO-d_6, δ 8.21 (s, 2H), 7.59 (t, J = 5.8 Hz, 1H), 7.37 (d, J = 7.3 Hz, 2H), 7.29 (t, J = 7.6 Hz, 2H), 7.20 (t, J = 7.3 Hz, 2H) 4.74 (d, J = 5.9 Hz, 2H), 4.12 (s, 3H)
^{13}C NMR:	126 MHz, DMSO-d_6, δ 152.3, 150.4, 148.3, 139.9, 128.3 (2C), 127.2 (2C), 126.7, 114.9, 114.8, 84.2, 43.5, 37.7

6.1.4.29. Synthesis of **4-(benzylamino)-5-phenyl-5*H*-pyrrolo[3,2-*d*]pyrimidine-7-carbonitrile (102)**

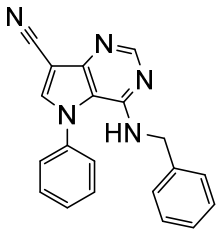

synonyms:	SMS-**A-700** compound **7** (*Biochim. Biophys. Acta* **2017**, *1859*, 69–79)
educts:	4-chloro-5-phenyl-5*H*-pyrrolo[3,2-*d*]pyrimidine-7-carbonitrile (**66**), benzylamine (1.5 eq.) and TEA (1.5 eq.)
yield:	42%
visual appearance:	pale yellow crystals
chemical formula:	$C_{20}H_{15}N_5$
molecular weight:	325.38 Da
LC-MS analysis:	calculated: 325.13 Da; found: 326.1 Da $[M+H]^+$
purity:	98%
^{1}H NMR:	500 MHz, DMSO-d_6, δ 8.54 (s, 1H), 8.39 (s, 1H), 7.64-7.54 (m, 5H), 7.28 (t, J = 7.6 Hz, 2H), 7.20 (t, J = 7.3 Hz, 3H), 5.59 (t, J = 5.6 Hz, 1H), 4.60 (d, J = 5.6 Hz, 2H)
^{13}C NMR:	126 MHz, DMSO-d_6, δ 152.7, 149.8, 148.4, 139.6, 139.0, 137.4, 130.1 (2C), 129.7, 128.5 (2C), 127.1 (2C), 127.0, 126.4 (2C), 114.4, 113.7, 87.4, 43.9

6.1.4.30. Synthesis of **5-benzyl-4-(benzylamino)-5*H*-pyrrolo[3,2-*d*]pyrimidine-7-carbonitrile (103)**

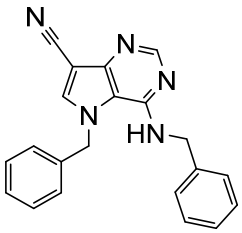

synonyms:	SMS-**A-705** compound **8** (*Biochim. Biophys. Acta* **2017**, *1859*, 69–79)
educts:	5-benzyl-4-chloro-5*H*-pyrrolo[3,2-*d*]pyrimidine-7-carbonitrile (**69**), benzylamine (1.5 eq.) and TEA (1.5 eq.)
yield:	54%
visual appearance:	brown crystals
chemical formula:	$C_{21}H_{17}N_5$
molecular weight:	339.40 Da
LC-MS analysis:	calculated: 339.15 Da; found: 340.4 Da $[M+H]^+$
purity:	98%

^{1}H NMR:	500 MHz, DMSO-d_6, δ 8.46 (s, 1H), 8.23 (s, 1H), 7.35-7.26 (m, 4H), 7.20-7.13 (m, 3H), 7.02 (dd, J = 6.5, 3.0 Hz, 2H), 6.96 (t, J = 7.3, 2.1 Hz, 2H), 5.78 (s, 2H), 4.65 (d, J = 5.8 Hz, 2H)
^{13}C NMR:	126 MHz, DMSO-d_6, δ 152.4, 149.9, 149.0, 139.7, 139.4, 137.1, 129.1 (2C), 128.3 (2C), 128.1, 126.9 (2C), 126.7, 126.4 (2C), 114.6, 114.2, 85.6, 52.6, 43.3

6.1.4.31. Synthesis of **5-benzyl-4-((3-phenylpropyl)amino)-5*H*-pyrrolo[3,2-*d*]pyrimidine-7-carbonitrile (104)**

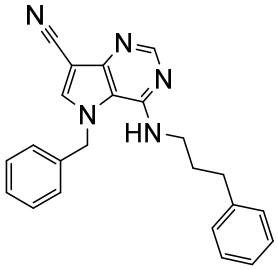

synonyms:	SMS-**A**-**707** compound **9** (*Biochim. Biophys. Acta* **2017**, *1859*, 69–79)
educts:	5-benzyl-4-chloro-5*H*-pyrrolo[3,2-*d*]pyrimidine-7-carbonitrile (**69**), phenylpropylamine (1.5 eq.) and TEA (1.5 eq.)
yield:	22%
visual appearance:	pale yellow crystals
chemical formula:	$C_{23}H_{21}N_5$
molecular weight:	367.46 Da
LC-MS analysis:	calculated: 367.18 Da; found: 368.1 Da $[M+H]^+$
purity:	97%
^{1}H NMR:	500 MHz, DMSO-d_6, δ 8.41 (s, 1H), 8.26 (s, 1H), 7.34-7.29 (m, 2H), 7.27-7.22 (m, 3H), 7.16-7.12 (m, 1H), 7.08-7.03 (m, 4H), 6.65 (t, J = 5.5, 1H), 5.74 (s, 2H), 3.41 (dd, J = 12.5, 6.9 Hz, 2H), 2.40-2.35 (m, 2H), 1.72 (dt, J = 14.6, 7.3 Hz, 2H)
^{13}C NMR:	126 MHz, DMSO-d_6, δ 152.6, 150.2, 148.8, 141.9, 139.5, 137.2, 129.2 (2C), 128.5 (4C), 128.2, 126.4 (2C), 125.9, 114.7, 114.3, 85.5, 52.6, 32.5, 30.4

6.1.4.32. Synthesis of **5-phenethyl-4-(phenethylamino)-5*H*-pyrrolo[3,2-*d*]pyrimidine-7-carbonitrile (105)**

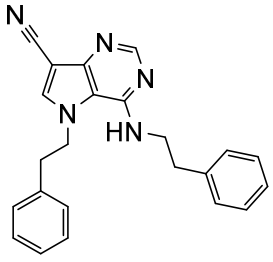

synonyms:	SMS-**A**-**711** compound **10** (*Biochim. Biophys. Acta* **2017**, *1859*, 69–79)

educts:	4-chloro-5-phenethyl-5*H*-pyrrolo[3,2-*d*]pyrimidine-7-carbonitrile (**70**), phenethylamine (1.5 eq.) and TEA (1.5 eq.)
yield:	16%
visual appearance:	white crystals
chemical formula:	$C_{23}H_{21}N_5$
molecular weight:	367.46 Da
LC-MS analysis:	calculated: 367.18 Da; found: 368.1 Da $[M+H]^+$
purity:	97%
^{1}H NMR:	500 MHz, DMSO-d_6, δ 8.33 (s, 1H), 7.95 (s, 1H), 7.30-7.13 (m, 8H), 7.00 (t, J = 5.3 Hz, 1H), 6.93-6.90 (m, 2H), 4.62 (t, J = 7.1 Hz, 2H), 3.80-3.74 (m, 2H), 2.97 (t, J = 7.2 Hz, 2H), 2.83 (t, J = 7.1 Hz, 2H)
^{13}C NMR:	126 MHz, DMSO-d_6, δ 152.3, 150.1, 148.6, 139.7, 138.8, 137.2, 128.9 (2C), 128.9 (2C), 128.5 (2C), 128.4 (2C), 126.8, 126.3, 114.7, 114.0, 84.5, 50.8, 42.0, 37.2. 34.8

6.1.4.33. Synthesis of 5-phenethyl-4-((3-phenylpropyl)amino)-5*H*-pyrrolo[3,2-*d*]pyrimidine-7-carbonitrile (106)

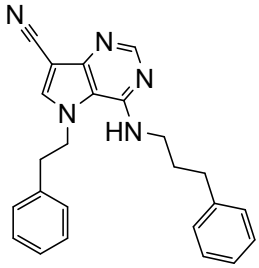

synonyms:	SMS-**A-712** compound **11** (*Biochim. Biophys. Acta* **2017**, *1859*, 69–79)
educts:	4-chloro-5-phenethyl-5*H*-pyrrolo[3,2-*d*]pyrimidine-7-carbonitrile (**70**), phenylpropylamine (1.5 eq.) and TEA (1.5 eq.)
yield:	29%
visual appearance:	white crystals
chemical formula:	$C_{24}H_{23}N_5$
molecular weight:	381.48 Da
LC-MS analysis:	calculated: 381.20 Da; found: 382.1 Da $[M+H]^+$
purity:	97%
^{1}H NMR:	500 MHz, DMSO-d_6, δ 8.28 (s, 1H), 8.00 (s, 1H), 7.27 (t, J = 7.5 Hz, 2H), 7.23-7.20 (m, 4H), 7.20-7.14 (m, 2H) 7.02 (d, J = 6.8 Hz, 2H), 6.94 (t, J = 5.4 Hz, 1H), 4.69 (t, J = 7.2 Hz, 2H), 3.54 (dd, J = 13.0, 6.9 Hz, 2H), 2.99 (t, J = 7.1 Hz, 2H), 2.69 (t, J = 7.6 Hz, 2H), 1.99-1.92 (m, 2H)
^{13}C NMR:	126 MHz, DMSO-d_6, δ 152.2, 150.3, 148.6, 141.9, 138.7, 137.2, 128.9 (2C), 128.5 (2C), 128.4 (2C), 128.4 (2C), 126.8, 125.9, 114.7, 114.0, 84.5, 50.8, 42.0, 37.4. 32.9, 30.7

6.1.4.34. Synthesis of **6-(4-phenethylpiperazine-1-yl)-7*H*-purine (107)**

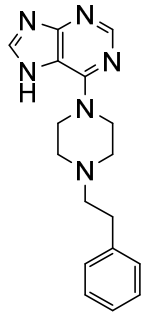

synonyms:	SMS-**H-3**
	compound **12** (*Biochim. Biophys. Acta* **2017**, *1859*, 69–79)
educts:	6-chloropurine, 1-(2-phenethyl)piperazine (1.5 eq.) and TEA (1.5 eq.)
yield:	52%
visual appearance:	white crystals
chemical formula:	$C_{17}H_{20}N_6$
molecular weight:	308.39 Da
LC-MS analysis:	calculated: 308.17 Da; found: 309.1 Da $[M+H]^+$
purity:	98%
^{1}H NMR:	500 MHz, DMSO-d_6, δ 13.00 (s, 1H), 8.19 (s, 1H), 8.09 (s, 1H), 7.29-7.21 (m, 4H), 7.19-7.15 (m, 1H), 4.32-4.08 (m, 4H), 2.78 (t, J = 7.3 Hz, 2H), 2.64-2.51 (m, 6H)
^{13}C NMR:	126 MHz, DMSO-d_6, δ 153.3, 151.9, 151.5, 140.5, 138.2, 128.8, 128.4, 126.0, 118.9, 59.8, 52.8 (2C), 45.8 (2C), 32.7

6.1.4.35. Synthesis of **6-(4-benzylpiperazine-1-yl)-7*H*-purine (108)**

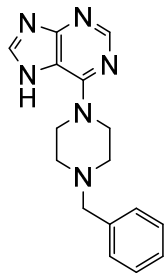

synonyms:	SMS-**H-6**
	compound **13** (*Biochim. Biophys. Acta* **2017**, *1859*, 69–79)
educts:	6-chloropurine, 1-benzylpiperazine (1.5 eq.) and TEA (1.5 eq.)
yield:	41%
visual appearance:	white crystals
chemical formula:	$C_{16}H_{18}N_6$
molecular weight:	294.36 Da
LC-MS analysis:	calculated: 294.16 Da; found: 294.2 Da $[M+H]^+$
purity:	99%
^{1}H NMR:	500 MHz, DMSO-d_6, δ 12.98 (s, 1H), 8.18 (s, 1H), 8.09 (s, 1H), 7.32 (d, J = 4.5 Hz, 4H), 7.27-7.23 (m, 1H), 4.32-4.15 (m, 4H), 3.29 (s, 2H), 2.48-2.45 (m, 4H)

^{13}C NMR:	126 MHz, DMSO-d_6, δ 153.3, 151.9, 151.6, 138.3, 138.0, 129.1 (2C), 128.3 (2C), 127.1, 118.9, 62.2, 52.8 (2C), 44.6 (2C)

6.1.4.36. Synthesis of **6-(4-benzhydrylpiperazine-1-yl)-7*H*-purine (109)**

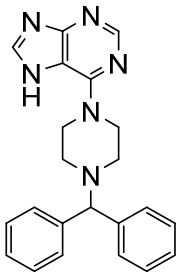

synonyms:	SMS-**H-4** compound **14** (*Biochim. Biophys. Acta* **2017**, *1859*, 69–79)
educts:	6-chloropurine, 1-benzhydrylpiperazine (1.5 eq.) and TEA (1.5 eq.)
yield:	48%
visual appearance:	white crystals
chemical formula:	$C_{22}H_{22}N_6$
molecular weight:	370.46 Da
LC-MS analysis:	calculated: 370.19 Da; found: 294.2 Da $[M+H]^+$
purity:	97%
^{1}H NMR:	500 MHz, DMSO-d_6, δ 12.97 (s, 1H), 8.17 (s, 1H), 8.07 (s, 1H), 7.14 (dd, J = 8.2, 1.1 Hz, 4H), 7.32-7.28 (m, 4H), 7.21-7.17 (m, 2H), 4.35 (s, 1H), 4.31-4.11 (m, 4H), 2.44-2.40 (m, 4H)
^{13}C NMR:	126 MHz, DMSO-d_6, δ 153.2, 151.9, 151.5, 142.6 (2C), 138.2, 128.7 (4C), 127.8 (4C), 127.1 (2C), 118.9, 75.0, 51.6 (2C), 44.8 (2C)

6.1.4.37. Synthesis of **6-(4-phenylpiperazine-1-yl)-7*H*-purine (110)**

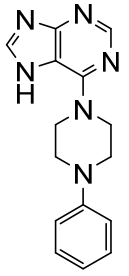

synonyms:	SMS-**H-5** compound **15** (*Biochim. Biophys. Acta* **2017**, *1859*, 69–79)
educts:	6-chloropurine, 1-phenylpiperazine (1.5 eq.) and TEA (1.5 eq.)
yield:	50%
visual appearance:	white crystals
chemical formula:	$C_{15}H_{16}N_6$
molecular weight:	280.34 Da

LC-MS analysis:	calculated: 280.14 Da; found: 281.1 Da $[M+H]^+$
purity:	99%
^{1}H NMR:	500 MHz, DMSO-d_6, δ 13.03 (s, 1H), 8.23 (s, 1H), 8.13 (s, 1H), 7.26-7.20 (m, 2H), 6.99 (dt, J = 9.2, 1.7 Hz, 2H), 6.80 (tt, J 7.4, 1.0 Hz, 1H), 4.48-4.22 (m, 4H), 2.27-2.24 (m, 4H)
^{13}C NMR:	126 MHz, DMSO-d_6, δ 153.3, 152.0, 151.6, 151.1, 138.4, 129.1 (2C), 119.4, 119.0, 116.0 (2C), 48.6 (2C), 44.6 (2C)

6.1.4.38. Synthesis of 4-(4-(2-(1*H*-indole-3-yl)ethyl)piperazine-1-yl)-6,7,8,9-tetrahydropyrimido[4,5-*b*]indolizine-10-carbonitrile (111)

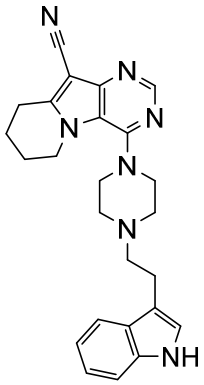

synonyms:	SMS-**A**-**9** compound **41** (*J. Med. Chem.* **2017**, *accepted 10th of October, 2017*)
educts:	4-chloro-6,7,8,9-tetrahydropyrimido[4,5-*b*]indolizine-10-carbonitrile (**59**), 3-(2-(piperazine-1-yl)ethyl)-1*H*-indole (**73**) and (1.5 eq.) and TEA (1.5 eq.)
yield:	58%
visual appearance:	yellow powder
chemical formula:	$C_{25}H_{27}N_7$
molecular weight:	425.54 Da
LC-MS analysis:	calculated: 425.23 Da; found: 426.4 Da $[M+H]^+$
purity:	91%
^{1}H NMR:	500 MHz, DMSO-d_6, δ 10.76 (s, 1H), 8.47 (s, 1H), 7.52 (d, J = 7.9 Hz, 1H), 7.32 (dt, J = 8.2, 0.8 Hz, 1H), 7.15 (d, J = 2.3 Hz, 1H), 7.05 (ddd, J = 8.1, 7.1, 1.1 Hz, 1H), 6.96 (ddd, J = 7.9, 7.0; 1.0 Hz, 1H), 4.36 (t, J = 5.6 Hz, 2H), 3.37-3.32 (m, 4H), 3.11 (t, J = 6.5 Hz, 2H), 2.89 (t, J = 7.3 Hz, 2H), 2.71-2.65 (m, 6H), 1.98-1.88 (m, 4H)
^{13}C NMR:	126 MHz, DMSO-d_6, δ 154.4, 151.3, 151.0, 150.2, 136.3, 127.4, 123.6, 120.9 (2C), 118.4, 118.3, 114.5, 112.7, 111.5, 83.6, 58.9, 52.4 (2C), 50.4 (2C), 46.1, 22.9, 22.6, 22.6, 18.4

6.1.4.39. Synthesis of 4-(4-(2-(1*H*-indole-3-yl)ethyl)piperazine-1-yl)-7,8,9,10-tetrahydro-6*H*-pyrimido[4',5':4,5]pyrrolo[1,2-*a*]azepine-11-carbonitrile (112)

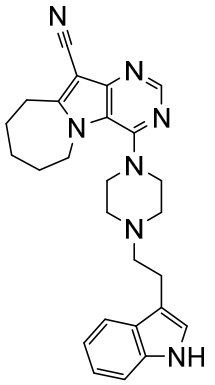

synonyms:	SMS-**A-35** compound **42** (*J. Med. Chem.* **2017**, *accepted 10th of October, 2017*)
educts:	4-chloro-7,8,9,10-tetrahydro-6*H*-pyrimido[4',5':4,5]pyrrolo[1,2-*a*]azepine-11-carbonitrile (**60**), 3-(2-(piperazine-1-yl)ethyl)-1*H*-indole (**73**) and (1.5 eq.) and TEA (1.5 eq.)
yield:	58%
visual appearance:	pale yellow crystals
chemical formula:	$C_{26}H_{29}N_7$
molecular weight:	439.57 Da
LC-MS analysis:	calculated: 439.25 Da; found: 440.3 Da $[M+H]^+$
purity:	99%
^{1}H NMR:	500 MHz, DMSO-d_6, δ 10.74 (s, 1H), 8.48 (s, 1H), 7.52 (d, J = 7.9 Hz, 1H), 7.32 (d, J = 8.1, 1H), 7.16 (d, J = 2.2 Hz, 1H), 7.05 (ddd, J = 8.0, 7.0, 1.0 Hz, 1H), 6.96 (ddd, J = 7.9, 7.1; 0.8 Hz, 1H), 4.55-4.42 m, 2H), 3.41-3.30 (m, 4H), 3.09 (t, J = 5.5 Hz, 2H), 2.89 (t, J = 7.3 Hz, 2H), 2.75-2.62(m, 6H), 1.91-1.82 (m, 2H), 1.80-1.71 (m, 4H)
^{13}C NMR:	126 MHz, DMSO-d_6, δ 156.6, 153.7, 151.1, 149.6, 136.2, 127.4, 122.6, 120.9, 118.4, 118.3, 117.9, 114.6, 112.6, 111.4, 85.3, 58.9, 52.2 (2C), 49.8 (2C), 47.4, 29.9, 27.9, 27.1, 25.6, 22.5

6.1.4.40. Synthesis of 4-((2-(1*H*-indole-3-yl)ethyl)amino)-6,7,8,9-tetrahydropyrimido[4,5-*b*]indolizine-10-carbonitrile (113)

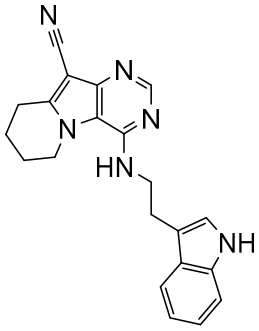

synonyms:	SMS-**A-695** compound **43** (*J. Med. Chem.* **2017**, *accepted 10th of October, 2017*)

educts:	4-chloro-6,7,8,9-tetrahydropyrimido[4,5-*b*]indolizine-10-carbonitrile (**59**), tryptamine (1.5 eq.) and TEA (1.5 eq.)
yield:	13%
visual appearance:	pale yellow crystals
chemical formula:	$C_{21}H_{20}N_6$
molecular weight:	356.43 Da
LC-MS analysis:	calculated: 356.17 Da; found: 357.2 Da $[M+H]^+$
purity:	96%
^{1}H NMR:	500 MHz, DMSO-d_6, δ 10.80 (s, 1H), 8.27 (s, 1H), 7.60 (d, J = 7.8 Hz, 1H), 7.33 (d, J = 8.1 Hz, 1H), 7.20 (d, J = 2.1 Hz, 1H), 7.06 (t, J = 7.5 Hz, 1H), 6.97 (t, J = 7.4 Hz, 1H), 6.92 (t, J = 5.6 Hz, 1H), 4.32 (t, J = 6.2 Hz, 2H), 3.75 (dd, J = 14.0, 6.0 Hz, 2H), 3.04-2.98 (m, 4H), 2.03-1.95 (m, 2H), 1.86-1.79 (m, 2H)
^{13}C NMR:	126 MHz, DMSO-d_6, δ 152.2, 149.8, 147.6, 147.5, 136.4, 127.6, 122.8, 121.1, 118.5, 118.3, 115.0, 113.9, 112.1, 111.5, 82.1, 45.6, 41.4, 25.0, 23.0, 22.1, 18.1

6.1.4.41. Synthesis of 4-(4-(2-(pyridin-4-yl)ethyl)piperazine-1-yl)-6,7,8,9-tetrahydropyrimido[4,5-*b*]indolizine-10-carbonitrile (114)

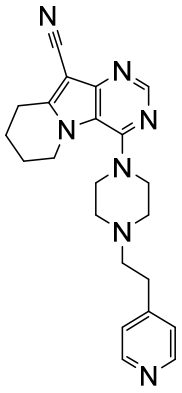

synonyms:	SMS-**A-129** compound **44** (*J. Med. Chem.* **2017**, *accepted 10th of October, 2017*)
educts:	4-chloro-6,7,8,9-tetrahydropyrimido[4,5-*b*]indolizine-10-carbonitrile (**59**), 1-(2-(pyridin-4-yl)ethyl)piperazine (1.5 eq.) and TEA (1.5 eq.)
yield:	42%
visual appearance:	yellow powder
chemical formula:	$C_{22}H_{25}N_7$
molecular weight:	387.49 Da
LC-MS analysis:	calculated: 387.22 Da; found: 388.3 Da $[M+H]^+$
purity:	96%
^{1}H NMR:	500 MHz, DMSO-d_6, δ 8.46 (s, 1H), 8.44 (dd, J = 4.4, 1.6. Hz, 2H), 7.28 (dd, J = 4.4, 1.6 Hz, 2H), 4.34 (t, J = 5.6 Hz, 2H), 3.38-3.31 (m, 4H), 3.11 (t, J = 6.5 Hz, 2H), 2.80 (t, J = 7.3 Hz, 2H), 2.71-2.60 (m, 6H), 1.98-1.87 (m, 4H)
^{13}C NMR:	126 MHz, DMSO-d_6, δ 154.3, 151.2, 151.0, 150.2, 149.5 (2C), 136.3, 124.4 (3C), 118.2, 114.4, 83.6, 58.1, 52.6 (2C), 50.2, 46.0 (2C), 31.8, 22.9, 22.6, 18.4

6.1.4.42. Synthesis of 4-(4-(2-(pyridin-4-yl)ethyl)piperazine-1-yl)-7,8,9,10-tetrahydro-6*H*-pyrimido[4',5':4,5]pyrrolo[1,2-*a*]azepine-11-carbonitrile (115)

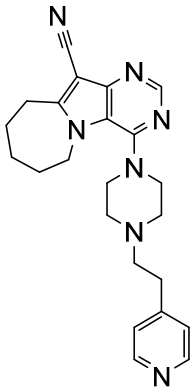

synonyms:	SMS-**A-130** compound **45** (*J. Med. Chem.* **2017**, *accepted 10th of October, 2017*)
educts:	4-chloro-7,8,9,10-tetrahydro-6*H*-pyrimido[4',5':4,5]pyrrolo[1,2-*a*]azepine-11-carbonitrile (**60**), 1-(2-(pyridin-4-yl)ethyl)piperazine and (1.5 eq.) and TEA (1.5 eq.)
yield:	42%
visual appearance:	pale yellow crystals
chemical formula:	$C_{23}H_{27}N_7$
molecular weight:	401.52 Da
LC-MS analysis:	calculated: 401.23 Da; found: 402.2 Da $[M+H]^+$
purity:	100%
^{1}H NMR:	500 MHz, DMSO-d_6, δ 8.49 (s, 1H), 8.46 (d, J = 4.6 Hz, 2H), 7.29 (d, J = 4.7 Hz, 2H), 4.52-4.45 (m, 2H), 3.20-3.17 (m, 4H), 3.12 (t, J = 6.4 Hz, 2H), 2.82 (t, J = 7.3 Hz, 2H), 2.70-2.59 (m, 6H), 1.91-1.83 (m, 2H), 1.83-1.71 (m, 4H)
^{13}C NMR:	126 MHz, DMSO-d_6, δ 156.6, 153.7, 151.1, 149.6, 149.5, 149.5 (2C), 124.4 (3C), 117.9, 114.6, 85.3, 58.2, 52.0 (2C), 49.7 (2C), 47.4, 31.8, 29.9, 27.9, 27.1, 25.6

6.1.4.43. Synthesis of 4-(4-(pyridin-2-yl)piperazine-1-yl)-6,7,8,9-tetrahydropyrimido[4,5-*b*]indolizine-10-carbonitrile (116)

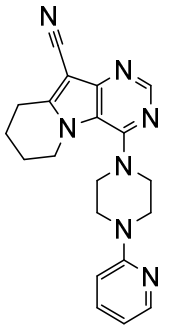

synonyms:	SMS-**A-158** compound **46** (*J. Med. Chem.* **2017**, *accepted 10th of October, 2017*)
educts:	4-chloro-6,7,8,9-tetrahydropyrimido[4,5-*b*]indolizine-10-carbonitrile (**59**), 1-(pyridin-2-yl)piperazine (1.5 eq.) and TEA (1.5 eq.)

yield:	55%
visual appearance:	pale yellow crystals
chemical formula:	$C_{20}H_{21}N_7$
molecular weight:	359.44 Da
LC-MS analysis:	calculated: 359.19 Da; found: 360.1 Da $[M+H]^+$
purity:	93%
^{1}H NMR:	500 MHz, DMSO-d_6, δ 8.49 (s, 1H), 8.15-8.12 (m, 1H), 7.56 (ddd, J = 8.9, 6.9, 2.0 Hz 1H), 6.88 (d, J = 8.6 Hz), 6.68 (dd, J = 7.1, 4.9 Hz, 1H), 4.42 (t, J = 5.5 Hz, 2H), 3.67 (t, J = 5.3 Hz, 4H), 3.42 (t, J = 5.2 Hz, 4H), 3.13 (t, J = 6.4 Hz, 2H), 1.99-1.88 (m, 4H)
^{13}C NMR:	126 MHz, DMSO-d_6, δ 159.2, 154.4, 151.3, 151.1, 150.3, 147.7, 137.8, 118.4, 114.4, 113.6, 107.5, 83.6, 50.1 (2C), 46.1, 44.5 (2C), 23.0, 22.6, 18.4

6.1.4.44. Synthesis of 4-(4-(pyridin-2-yl)piperazine-1-yl)-7,8,9,10-tetrahydro-6*H*-pyrimido[4',5':4,5]pyrrolo[1,2-*a*]azepine-11-carbonitrile (117)

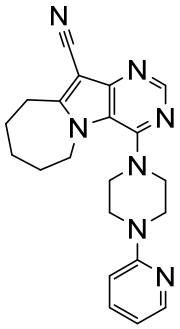

synonyms:	SMS-**A-160** compound **47** (*J. Med. Chem.* **2017**, *accepted 10th of October, 2017*)
educts:	4-chloro-7,8,9,10-tetrahydro-6*H*-pyrimido[4',5':4,5]pyrrolo[1,2-*a*]azepine-11-carbonitrile (**60**), 1-(pyridin-2-yl)piperazine and (1.5 eq.) and TEA (1.5 eq.)
yield:	58%
visual appearance:	yellow crystals
chemical formula:	$C_{21}H_{23}N_7$
molecular weight:	373.46 Da
LC-MS analysis:	calculated: 373.20 Da; found: 374.2Da $[M+H]^+$
purity:	100%
^{1}H NMR:	500 MHz, DMSO-d_6, δ 8.51 (s, 1H), 8.14 (ddd, J = 4.8, 1.9, 0.7 Hz, 1H), 7.57 (ddd, J = 8.8, 6.8, 2.0 Hz, 1H), 6.90 (d, J = 8.6 Hz), 6.68 (ddd, J = 7.1, 4.9, 0.6 Hz, 1H), 4.57-4.50 (m, 2H), 3.76-3.63 (m, 4H), 3.44-3.35 (m, 4H), 3.11 (t, J = 5.0 Hz, 2H), 1.89-1.73 (m, 6H)
^{13}C NMR:	126 MHz, DMSO-d_6, δ 159.1, 156.8, 155.6, 154.3, 149.7, 141.1, 137.8, 118.3, 114.6, 113.6, 107.5, 79.6, 49.5 (2C), 47.5, 44.3 (2C), 30.3, 30.0, 27.8, 25.6

6.1.4.45. Synthesis of 4-(4-(2-(1*H*-indole-3-yl)ethyl)piperazine-1-yl)-5-methyl-5*H*-pyrrolo[3,2-*d*]pyrimidine-7-carbonitrile (118)

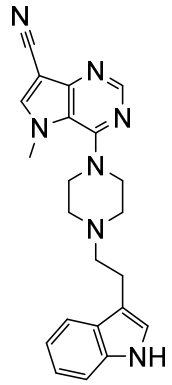

synonyms:	SMS-**A-339** compound **48** (*J. Med. Chem.* **2017**, *accepted 10th of October, 2017*)
educts:	4-chloro-5-methyl-5*H*-pyrrolo[3,2-*d*]pyrimidine-7-carbonitrile (**61**), 3-(2-(piperazine-1-yl)ethyl)-1*H*-indole (**73**) and (1.5 eq.) and TEA (1.5 eq.)
yield:	29%
visual appearance:	yellow crystals
chemical formula:	$C_{22}H_{23}N_7$
molecular weight:	385.47 Da
LC-MS analysis:	calculated: 385.20 Da; found: 386.3 Da $[M+H]^+$
purity:	100%
^{1}H NMR:	500 MHz, DMSO-d_6, δ 10.74 (s, 1H), 8.51 (s, 1H), 8.44 (s, 1H), 7.52 (d, J = 7.9 Hz, 1H), 7.32 (dt, J = 8.1, 0.9 Hz, 1H), 7.16 (d, J = 2.3 Hz, 1H), 7.05 (ddd, J = 8.1, 7.0, 1.1 Hz, 1H), 6.96 (ddd, J = 7.9, 7.0; 1.0 Hz, 1H), 4.01 (s, 3H), 3.42-3.37 (m, 4H), 2.89 (t, J = 7.3 Hz, 2H), 2.73-2.65 (m, 6H)
^{13}C NMR:	126 MHz, DMSO-d_6, δ 154.9, 151.4, 150.1, 141.5, 136.3, 127.4, 122.6, 121.0, 118.6, 118.4, 118.3, 114.4, 112.6, 111.5, 85.4, 58.9, 52.3 (2C), 50.2 (2C), 36.8, 22.5

6.1.4.46. Synthesis of 4-(4-(2-(1*H*-indole-3-yl)ethyl)piperazine-1-yl)-5-ethyl-5*H*-pyrrolo[3,2-*d*]pyrimidine-7-carbonitrile (119)

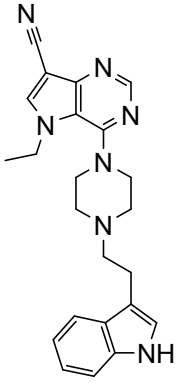

synonyms:	SMS-**A-477** compound **49** (*J. Med. Chem.* **2017**, *accepted 10th of October, 2017*)

educts:	4-chloro-5-ethyl-5*H*-pyrrolo[3,2-*d*]pyrimidine-7-carbonitrile (**62**), 3-(2-(piperazine-1-yl)ethyl)-1*H*-indole (**73**) and (1.5 eq.) and TEA (1.5 eq.)
yield:	25%
visual appearance:	yellow crystals
chemical formula:	$C_{23}H_{25}N_7$
molecular weight:	399.50 Da
LC-MS analysis:	calculated: 399.22 Da; found: 400.2 Da $[M+H]^+$
purity:	97%
^{1}H NMR:	500 MHz, DMSO-d_6, δ 10.76 (s, 1H), 8.61 (s, 1H), 8.55 (s, 1H), 7.52 (d, J = 7.9 Hz, 1H), 7.32 (d, J = 8.1 Hz, 1H), 7.16 (d, J = 2.2 Hz, 1H), 7.06 (ddd, J = 8.0, 7.0, 1.1 Hz, 1H), 6.96 (ddd, J = 7.9, 7.0; 1.0 Hz, 1H), 4.35 (q, J = 7.2 Hz, 2H) 3.38-3.33 (m, 4H), 2.90 (t, J = 7.4 Hz, 2H), 2.76-2.66 (m, 6H), 1.38 (t, J = 7.2 Hz, 3H)
^{13}C NMR:	126 MHz, DMSO-d_6, δ 155.0, 151.4, 150.6, 140.6, 136.3, 127.4, 122.7, 121.0, 118.4, 118.3, 117.9, 114.4, 112.6, 111.5, 86.2, 58.9, 52.4 (2C), 50.2 (2C), 44.1, 22.6, 16.1

6.1.4.47. Synthesis of 4-(4-(2-(1*H*-indole-3-yl)ethyl)piperazine-1-yl)-5-propyl-5*H*-pyrrolo[3,2-*d*]pyrimidine-7-carbonitrile (120)

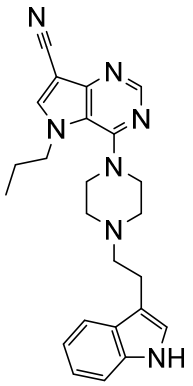

synonyms:	SMS-**A-484** compound **50** (*J. Med. Chem.* **2017**, *accepted 10th of October, 2017*)
educts:	4-chloro-5-propyl-5*H*-pyrrolo[3,2-*d*]pyrimidine-7-carbonitrile (**63**), 3-(2-(piperazine-1-yl)ethyl)-1*H*-indole (**73**) and (1.5 eq.) and TEA (1.5 eq.)
yield:	21%
visual appearance:	white crystals
chemical formula:	$C_{24}H_{27}N_7$
molecular weight:	413.53 Da
LC-MS analysis:	calculated: 413.23 Da; found: 414.3 Da $[M+H]^+$
purity:	91%
^{1}H NMR:	500 MHz, DMSO-d_6, δ 10.74 (s, 1H), 8.60 (s, 1H), 8.56 (s, 1H), 7.52 (d, J = 7.9 Hz, 1H), 7.32 (dt, J = 8.1, 0.8 Hz, 1H), 7.16 (d, J = 2.3 Hz, 1H), 7.05 (ddd, J = 8.1, 7.0, 1.1 Hz, 1H), 6.96 (ddd, J = 7.9, 7.0; 1.0 Hz, 1H), 4.27 (t, J = 7.4 Hz, 2H) 3.38-3.32 (m, 4H), 2.90 (t, J = 7.3 Hz, 2H), 2.72-2.64 (m, 6H), 1.76 (p, J = 7.3 Hz, 2H), 0.72 (t, J = 7.4 Hz, 3H)
^{13}C NMR:	126 MHz, DMSO-d_6, δ 155.1, 151.4, 150.6, 141.2, 136.3, 127.4, 122.6, 120.9, 118.4, 118.3, 118.0, 114.3, 112.6, 111.5, 85.9, 58.9, 52.5 (2C), 50.8, 50.2 (2C), 24.2, 22.5, 10.7

6.1.4.48. Synthesis of 4-(4-(2-(1*H*-indole-3-yl)ethyl)piperazine-1-yl)-5-cyclopropyl-5*H*-pyrrolo[3,2-*d*]pyrimidine-7-carbonitrile (121)

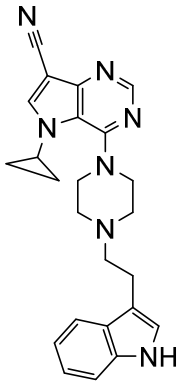

synonyms:	SMS-**A-498** compound **51** (*J. Med. Chem.* **2017**, *accepted 10th of October, 2017*)
educts:	4-chloro-5-cyclopropyl-5*H*-pyrrolo[3,2-*d*]pyrimidine-7-carbonitrile (**65**), 3-(2-(piperazine-1-yl)ethyl)-1*H*-indole (**73**) and (1.5 eq.) and TEA (1.5 eq.)
yield:	39%
visual appearance:	white crystals
chemical formula:	$C_{24}H_{25}N_7$
molecular weight:	411.51 Da
LC-MS analysis:	calculated: 411.22 Da; found: 412.2 Da $[M+H]^+$
purity:	96%
^{1}H NMR:	500 MHz, DMSO-d_6, δ 10.74 (s, 1H), 8.47 (s, 1H), 8.46 (s, 1H), 7.51 (d, J = 7.9 Hz, 1H), 7.32 (d, J = 8.1, 1H), 7.15 (d, J = 2.3 Hz, 1H), 7.04 (ddd, J = 8.1, 7.1, 1.1 Hz, 1H), 6.96 (ddd, J = 7.9, 7.1; 1.0 Hz, 1H), 3.97 (p, J = 3.6 Hz, 1H) 3.60-3.50 (m, 4H), 2.88 (t, J = 7.8 Hz, 2H), 2.70-2.62 (m, 6H), 1.15-1.02 (m, 4H)
^{13}C NMR:	126 MHz, DMSO-d_6, δ 154.4, 151.3, 150.1, 140.2, 136.3, 127.4, 122.6, 120.9, 118.5, 118.4, 118.2, 114.4, 112.6, 111.4, 85.6, 58.9, 52.5 (2C), 49.8 (2C), 32.1, 22.5, 8.5 (2C)

6.1.4.49. Synthesis of 4-(4-(2-(1*H*-indole-3-yl)ethyl)piperazine-1-yl)-5-phenyl-5*H*-pyrrolo[3,2-*d*]pyrimidine-7-carbonitrile (122)

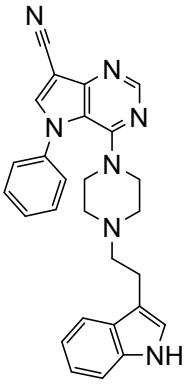

synonyms:	SMS-**A-307** compound **52** (*J. Med. Chem.* **2017**, *accepted 10th of October, 2017*)

educts:	4-chloro-5-phenyl-5*H*-pyrrolo[3,2-*d*]pyrimidine-7-carbonitrile (**66**), 3-(2-(piperazine-1-yl)ethyl)-1*H*-indole (**73**) and (1.5 eq.) and TEA (1.5 eq.)
yield:	11%
visual appearance:	yellow crystals
chemical formula:	$C_{27}H_{25}N_7$
molecular weight:	447.55 Da
LC-MS analysis:	calculated: 447.22 Da; found: 448.1 Da $[M+H]^+$
purity:	93%
^{1}H NMR:	500 MHz, DMSO-d_6, δ 10.70 (s, 1H), 8.74 (s, 1H), 8.58 (s, 1H), 7.62-7.58 (m, 2H), 7.54-7.50 (m, 3H), 7.43 (d, J = 7.8 Hz, 1H), 7.30 (dt, J = 8.1, 0.8 Hz, 1H), 7.07 (d, J = 2.3 Hz, 1H), 7.03 (ddd, J = 8.1, 7.1, 1.1 Hz, 1H), 6.94 (ddd, J = 7.9, 7.0; 1.0 Hz, 1H), 3.12-3.06 (m, 4H) 2.71 (t, J = 8.3 Hz, 2H), 2.44 (t, J = 8.2 Hz, 2H), 2.16-2.08 (m, 4H)
^{13}C NMR:	126 MHz, DMSO-d_6, δ 153.2, 151.9, 150.2, 141.4, 137.9, 136.3, 129.6 (2C), 128.5, 127.3, 125.3 (2C), 122.5, 120.9, 118.3, 118.2, 115.3, 114.1, 112.5, 111.4, 88.1, 58.7, 51.5 (2C), 48.8 (2C), 22.2

6.1.4.50. Synthesis of 4-(4-(2-(1*H*-indole-3-yl)ethyl)piperazine-1-yl)-5-benzyl-5*H*-pyrrolo[3,2-*d*]pyrimidine-7-carbonitrile (123)

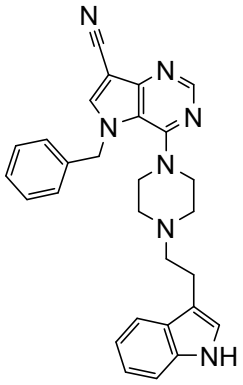

synonyms:	SMS-**A-315** compound **53** (*J. Med. Chem.* **2017**, *accepted 10th of October, 2017*)
educts:	4-chloro-5-benzyl-5*H*-pyrrolo[3,2-*d*]pyrimidine-7-carbonitrile (**69**), 3-(2-(piperazine-1-yl)ethyl)-1*H*-indole (**73**) and (1.5 eq.) and TEA (1.5 eq.)
yield:	18%
visual appearance:	white crystals
chemical formula:	$C_{28}H_{27}N_7$
molecular weight:	461.57 Da
LC-MS analysis:	calculated: 461.23 Da; found: 462.0 Da $[M+H]^+$
purity:	97%
^{1}H NMR:	500 MHz, DMSO-d_6, δ 10.74 (s, 1H), 8.65 (s, 1H), 8.56 (s, 1H), 7.51 (d, J = 7.9 Hz, 1H), 7.33-7.28 (m, 3H), 7.27-7.23 (m, 1H), 7.16-7.14 (m, 1H), 7.14-7.13 (m, 1H), 7.43 (d, J = 7.8 Hz, 1H), 7.04 (ddd, J = 8.1, 7.0, 1.2 Hz, 1H), 6.96 (ddd, J = 7.9, 7.0; 1.0 Hz, 1H), 5.54 (s, 2H), 3.39-3.33 (m, 4H) 2.90-2.85 (m, 2H), 2.71-2.61 (m, 6H)
^{13}C NMR:	126 MHz, DMSO-d_6, δ 155.2, 151.7, 150.9, 141.7, 137.0, 136.3, 128.8 (2C), 128.1, 127.4, 127.1 (2C), 122.6, 120.9, 118.4, 118.3, 117.9, 114.00, 112.6, 111.4, 87.0, 58.3, 52.3 (2C), 52.1, 50.0 (2C), 22.5

6.1.4.51. Synthesis of 4-(4-(2-(1H-indole-3-yl)ethyl)piperazine-1-yl)-5-phenethyl-5H-pyrrolo[3,2-d]pyrimidine-7-carbonitrile (124)

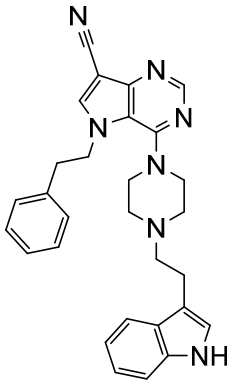

synonyms:	SMS-**A-323** compound **54** (*J. Med. Chem.* **2017**, *accepted 10th of October, 2017*)
educts:	4-chloro-5-phenethyl-5*H*-pyrrolo[3,2-*d*]pyrimidine-7-carbonitrile (**70**), 3-(2-(piperazine-1-yl)ethyl)-1*H*-indole (**73**) and (1.5 eq.) and TEA (1.5 eq.)
yield:	9%
visual appearance:	white crystals
chemical formula:	$C_{29}H_{29}N_7$
molecular weight:	475.60 Da
LC-MS analysis:	calculated: 475.25 Da; found: 476.2 Da $[M+H]^+$
purity:	97%
^{1}H NMR:	500 MHz, DMSO-d_6, δ 10.73 (s, 1H), 8.55 (s, 1H), 8.50 (s, 1H), 7.51 (d, J = 7.9 Hz, 1H), 7.33 (dt, J = 8.1, 0.8 Hz, 1H), 7.18-7.09 (m, 4H), 7.05 (ddd, J = 8.2, 7.0, 1.1 Hz, 1H), 7.01-6.95 (m, 3H), 4.56 (t, J = 7.2 Hz, 2H), 3.29-3.26 (m, 4H) 3.01 (t, J = 7.1 Hz, 2H), 2.88 (t, J = 7.2 Hz, 2H), 2.71-2.61 (m, 6H)
^{13}C NMR:	126 MHz, DMSO-d_6, δ 155.0, 151.4, 150.4, 141.1, 137.3, 136.3, 128.7 (2C), 128.2 (2C), 127.4, 126.7, 122.6, 121.0, 118.4, 118.3, 118.1, 114.3, 112.6, 111.5, 86.2, 59.0, 52.3 (2C), 50.3, 50.0 (2C), 37.2, 22.4

6.1.4.52. Synthesis of 4-(4-(2-(1*H*-indole-3-yl)ethyl)piperazine-1-yl)-5-(3-phenylpropyl)-5*H*-pyrrolo[3,2-*d*]pyrimidine-7-carbonitrile (125)

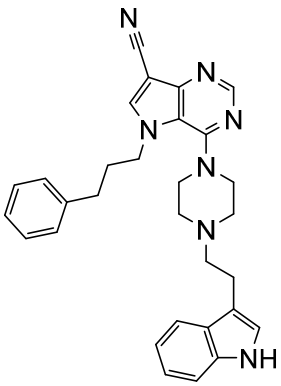

synonyms:	SMS-**A-331** compound **55** (*J. Med. Chem.* **2017**, *accepted 10th of October, 2017*)

educts:	4-chloro-5-phenylpropyl-5*H*-pyrrolo[3,2-*d*]pyrimidine-7-carbonitrile (**71**), 3-(2-(piperazine-1-yl)ethyl)-1*H*-indole (**73**) and (1.5 eq.) and TEA (1.5 eq.)
yield:	16%
visual appearance:	pale yellow crystals
chemical formula:	$C_{30}H_{31}N_7$
molecular weight:	489.63Da
LC-MS analysis:	calculated: 489.26 Da; found: 490.3 Da $[M+H]^+$
purity:	95%
^{1}H NMR:	500 MHz, DMSO-d_6, δ 10.75 (s, 1H), 8.62 (s, 1H), 8.54 (s, 1H), 7.52 (d, J = 7.9 Hz, 1H), 7.33 (d, J = 8.1 Hz, 1H), 7.23 (t, J = 7.5 Hz, 2H), 7.16 (d, J = 2.1 Hz, 1H), 7.14 (t, J = 7.4 Hz, 1H), 7.09 (d, J = 7.0 Hz, 2H), 7.05 (m, 1H), 6.97 (m, 1H), 4.33 (t, J = 7.3 Hz, 2H) 3.27-3.23 (m, 6H), 2.87 (t, J = 7.2 Hz, 2H), 2.62 (t, J = 7.2 Hz, 2H), 2.59-2.51 (m, 4H), 2.09 (p, J = 7.5 Hz, 2H)
^{13}C NMR:	126 MHz, DMSO-d_6, δ 155.0, 151.4, 150.4, 140.9, 140.5, 136.3, 128.5 (2C), 128.3 (2C), 127.3, 126.2, 122.6, 120.9, 118.4, 118.3, 118.0, 114.3, 112.6, 111.5, 86.2, 58.8, 52.2 (2C), 50.1 (2C), 48.6, 32.0, 32.0, 22.5

6.1.4.53. Synthesis of **4-(4-(benzo[*d*][1,3]dioxol-5-ylmethyl)piperazine-1-yl)-6,7,8,9-tetrahydropyrimido[4,5-*b*]indolizine-10-carbonitrile (126)**

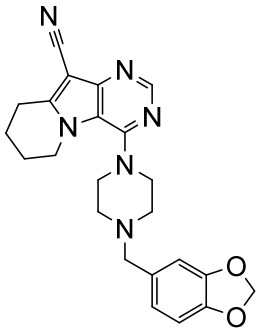

synonyms:	SMS-**A**-**54** compound **56** (*J. Med. Chem.* **2017**, *accepted 10th of October, 2017*)
educts:	4-chloro-6,7,8,9-tetrahydropyrimido[4,5-*b*]indolizine-10-carbonitrile (**59**), 1-piperonylpiperazine (1.5 eq.) and TEA (1.5 eq.)
yield:	46%
visual appearance:	white crystals
chemical formula:	$C_{23}H_{24}N_6O_2$
molecular weight:	416.48 Da
LC-MS analysis:	calculated: 416.20 Da; found: 417.1 Da $[M+H]^+$
purity:	98%
^{1}H NMR:	500 MHz, DMSO-d_6, δ 8.45 (s, 1H), 6.88 (d, J = 1.5 Hz, 1H), 6.84 (d, J = 7.9 Hz, 1H), 6.77 (dd, J = 7.9, 1.5 Hz, 1H), 5.98 (s, 2H), 4.33 (t, J = 5.6 Hz, 2H), 3.45 (s, 2H), 3.36-3.29 (m, 4H), 3.10 (t, J = 6.4 Hz, 2H), 2.61-2.50 (m, 4H), 1.98-1.84 (m, 4H)
^{13}C NMR:	126 MHz, DMSO-d_6, δ 154.3, 151.2, 150.9, 150.2, 147.4, 146.4, 131.9, 122.2, 118.2, 114.4, 109.3, 108.0, 100.9, 83.6, 61.9, 52.1 (2C), 50.4 (2C), 46.1, 22.9, 22.6, 18.4

6.1.4.54. Synthesis of 4-(4-(benzo[*d*][1,3]dioxol-5-ylmethyl)piperazine-1-yl)-7,8,9,10-tetrahydro-6*H*-pyrimido[4',5':4,5]pyrrolo[1,2-*a*]azepine-11-carbonitrile (127)

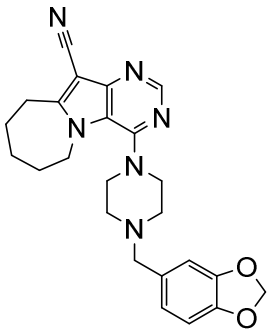

synonyms:	SMS-**A**-**68** compound **57** (*J. Med. Chem.* **2017**, *accepted 10th of October, 2017*)
educts:	4-chloro-7,8,9,10-tetrahydro-6*H*-pyrimido[4',5':4,5]pyrrolo[1,2-*a*]azepine-11-carbonitrile (**60**), 1-piperonylpiperazine (1.5 eq.) and TEA (1.5 eq.)
yield:	35%
visual appearance:	pale yellow crystals
chemical formula:	$C_{24}H_{26}N_6O_2$
molecular weight:	430.51 Da
LC-MS analysis:	calculated: 430.21 Da; found: 431.2 Da $[M+H]^+$
purity:	100%
^{1}H NMR:	500 MHz, DMSO-d_6, δ 8.46 (s, 1H), 6.88 (d, J = 1.5 Hz, 1H), 6.84 (d, J = 7.8 Hz, 1H), 6.77 (dd, J = 7.9, 1.6 Hz, 1H), 5.98 (s, 2H), 4.54-4.40 (m, 2H), 3.45 (s, 2H), 3.35-3.29 (m, 4H), 3.12-3.04 (m, 2H), 2.61-2.49 (m, 4H), 1.89-1.80 (m, 2H), 180-168 m, 2H)
^{13}C NMR:	126 MHz, DMSO-d_6, δ 156.6, 153.7, 151.1, 149.6, 147.4, 146.3, 131.9, 122.2, 117.9, 114.6, 109.3, 108.0, 100.9, 85.3, 61.8, 51.9 (2C), 49.8 (2C), 47.4, 29.9, 27.9, 27.2, 25.6

6.1.4.55. Synthesis of 4-(4-(benzo[*d*][1,3]dioxol-5-ylmethyl)piperazine-1-yl)-5-phenyl-5*H*-pyrrolo[3,2-*d*]pyrimidine-7-carbonitrile (128)

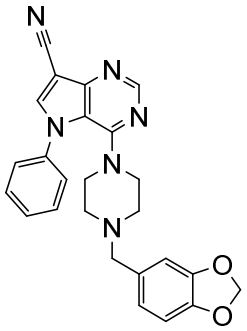

synonyms:	SMS-**A**-**703** compound **58** (*J. Med. Chem.* **2017**, *accepted 10th of October, 2017*)
educts:	4-chloro-5-phenyl-5*H*-pyrrolo[3,2-*d*]pyrimidine-7-carbonitrile (**66**), 1-piperonylpiperazine (1.5 eq.) and TEA (1.5 eq.)

yield:	37%
visual appearance:	yellow crystals
chemical formula:	$C_{25}H_{22}N_6O_2$
molecular weight:	438.49 Da
LC-MS analysis:	calculated: 438.18 Da; found: 439.1 Da $[M+H]^+$
purity:	98%
^{1}H NMR:	500 MHz, DMSO-d_6, δ 8.80 (s, 1H), 8.64 (s, 1H), 7.58-7.46 (m, 5H), 707 (s, 1H), 6.97 (s, 1H), 6.90 (s, 1H), 6.06 (s, 1H), 4.17-3.97 (m, 2H), 3.73-3.40 (m, 4H), 315-2.96 (m, 4H)
^{13}C NMR:	126 MHz, DMSO-d_6, δ 151.7, 151.4, 147.5, 141.7, 137.5, 129.5 (3C), 128.6, 125.4 (3C), 115.5, 113.9, 101.6, 88.2, 49.1 (2C), 45.2 (2C)

6.1.4.56. Synthesis of **4-(4-(benzo[*d*][1,3]dioxol-5-ylmethyl)piperazine-1-yl)-5-phenethyl-5*H*-pyrrolo[3,2-*d*]pyrimidine-7-carbonitrile (129)**

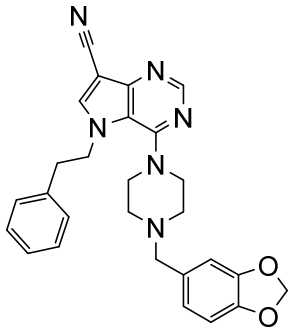

synonyms:	SMS-**A-713** compound **59** (*J. Med. Chem.* **2017**, *accepted 10th of October, 2017*)
educts:	4-chloro-5-phenethyl-5*H*-pyrrolo[3,2-*d*]pyrimidine-7-carbonitrile (**70**), 1-piperonylpiperazine (1.5 eq.) and TEA (1.5 eq.)
yield:	20%
visual appearance:	white crystals
chemical formula:	$C_{27}H_{26}N_6O_2$
molecular weight:	466.55 Da
LC-MS analysis:	calculated: 466.21 Da; found: 467.3 Da $[M+H]^+$
purity:	99%
^{1}H NMR:	500 MHz, DMSO-d_6, δ 8.55 (s, 1H), 8.48 (s, 1H), 7.17-7.11 (m, 3H), 6.98-6.95 (m, 2H), 6.87 (d, J = 1.4 Hz, 1H), 6.85 (d, J = 7.9 Hz, 1H), 6.76 (dd, J = 7.9, 1.5 Hz, 1H), 5.98 (s, 2H) ,4.52 (t, J = 7.2 Hz, 2H), 3.44 (s, 2H), 3.26-3.20 (m, 4H), 3.00 (t, J = 7.1 Hz, 2H), 2.57-2.51 (m, 4H)
^{13}C NMR:	126 MHz, DMSO-d_6, δ 154.9, 151.4, 150.5, 147.4, 146.4, 141.1, 137.3, 131.8, 128.7 (2C), 128.3 (2C), 126.8, 122.3, 118.1, 114.3, 109.3, 108.3, 101.0, 86.2, 61.8, 52.0 (2C), 50.3, 50.0 (2C), 37.2

6.1.4.57. Synthesis of 4-(4-(furan-2-carbonyl)piperazine-1-yl)-6,7,8,9-tetrahydropyrimido[4,5-*b*]indolizine-10-carbonitrile (130)

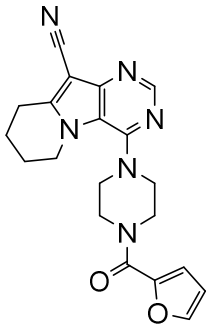

synonyms:	SMS-**A-127** compound **60** (*J. Med. Chem.* **2017**, *accepted 10th of October, 2017)*
educts:	4-chloro-6,7,8,9-tetrahydropyrimido[4,5-*b*]indolizine-10-carbonitrile (**59**), 1-(2-furoyl)piperazine (1.5 eq.) and TEA (1.5 eq.)
yield:	37%
visual appearance:	yellow crystals
chemical formula:	$C_{20}H_{20}N_6O_2$
molecular weight:	376.42 Da
LC-MS analysis:	calculated: 376.16 Da; found: 377.2 Da $[M+H]^+$
purity:	99%
^{1}H NMR:	500 MHz, DMSO-d_6, δ 8.49 (s, 1H), 7.85 (dd, J = 1.7, 0.7 Hz, 1H), 7.03 (dd, J = 3.5, 0.7 Hz, 1H), 6.64 (dd, J = 3.4, 1.8 Hz, 1H), 4.40 (t, J = 5.6 Hz, 2H), 3.94-3.82 (m, 4H), 3.39 (t, J = 5.0 Hz, 4H), 3.13 (t, J = 6.4 Hz, 2H), 2.02-1.86 (m, 4H)
^{13}C NMR:	126 MHz, DMSO-d_6, δ 158.7, 153.9, 151.2, 151.1, 150.3, 147.0, 144.9, 118.2, 115.9, 114.4, 111.5, 83.6, 60.4, 46.0 (2C), 40.4 (2C), 23.0, 22.6, 18.3

6.1.4.58. Synthesis of 4-(4-(furan-2-carbonyl)piperazine-1-yl)-7,8,9,10-tetrahydro-6*H*-pyrimido[4',5':4,5]pyrrolo[1,2-*a*]azepine-11-carbonitrile (131)

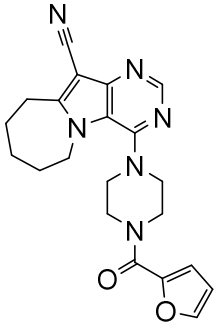

synonyms:	SMS-**A-128** compound **61** (*J. Med. Chem.* **2017**, *accepted 10th of October, 2017*)
educts:	4-chloro-7,8,9,10-tetrahydro-6*H*-pyrimido[4',5':4,5]pyrrolo[1,2-*a*]azepine-11-carbonitrile (**60**), 1-(2-furoyl)piperazine (1.5 eq.) and TEA (1.5 eq.)

yield:	37%
visual appearance:	white crystals
chemical formula:	$C_{21}H_{22}N_6O_2$
molecular weight:	390.45 Da
LC-MS analysis:	calculated: 390.18 Da; found: 391.2 Da $[M+H]^+$
purity:	96%
^{1}H NMR:	500 MHz, DMSO-d_6, δ 8.50 (s, 1H), 7.85 (dd, J = 1.8, 0.8 Hz, 1H), 7.04 (dd, J = 3.5, 0.8 Hz, 1H), 6.64 (dd, J = 3.5, 1.8 Hz, 1H), 4.54-4.46 (m, 2H), 3.95-3.81 (m, 4H), 3.40-3.35 (m, 4H), 3.11 (t, J = 5.4 Hz, 2H), 1.89-1.72 (m, 6H)
^{13}C NMR:	126 MHz, DMSO-d_6, δ 158.7, 156.9, 153.4, 151.0, 149.8, 147.0, 145.0, 117.9, 116.0, 114.5, 111.5, 85.3, 56.1 (2C), 49.8, 47.5 (2C), 29.9, 27.8, 27.2, 25.6

6.1.4.59. Synthesis of 5-(2-methoxyphenyl)-4-(4-phenethylpiperazine-1-yl)-5*H*-pyrrolo[3,2-*d*]pyrimidine-7-carbonitrile (132)

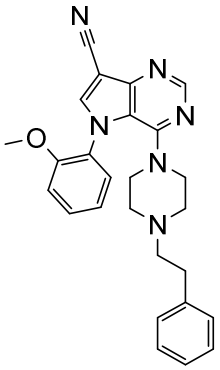

synonyms:	SMS-**A**-**436** compound **62** (*J. Med. Chem.* **2017**, *accepted 10th of October, 2017*)
educts:	4-chloro-5-(2-methoxyphenyl)-5*H*-pyrrolo[3,2-*d*]pyrimidine-7-carbonitrile (**67**), 1-(2-phenethyl)piperazine (1.5 eq.) and TEA (1.5 eq.)
yield:	22%
visual appearance:	pale yellow crystals
chemical formula:	$C_{26}H_{26}N_6O$
molecular weight:	438.54 Da
LC-MS analysis:	calculated: 438.22 Da; found: 439.3 Da $[M+H]^+$
purity:	100%
^{1}H NMR:	500 MHz, DMSO-d_6, δ 8.57 (s, 1H), 8.56 (s, 1H), 7.54 (ddd, J = 8.4, 7.5, 1.7 Hz, 1H), 7.42 (dd, J = 7.8, 1.6 Hz, 1H), 7.30 (dd, J = 8.4, 1.1 Hz, 1H), 7.26-7.20 (m, 2H), 7.19-7.08 (m, 4H), 3.74 (s, 3H), 3.10-2.59 (m, 4H), 2.63-2.57 (m, 2H), 2.38-2.31 (m, 2H), 2.05-1.93 (m, 4H)
^{13}C NMR:	126 MHz, DMSO-d_6, δ 158.5, 153.1, 151.7, 150.9, 141.4, 137.8, 130.9, 128.9 (2C), 128.3 (2C), 127.1, 126.7 (2C), 115.6, 115.2 (2C), 114.2, 87.6, 63.8, 62.1, 51.5 (2C), 48.8 (2C), 14.7

6.1.4.60. Synthesis of **4-(4-benzylpiperazine-1-yl)-5-(2-methoxyphenyl)-5*H*-pyrrolo[3,2-*d*]pyrimidine-7-carbonitrile (133)**

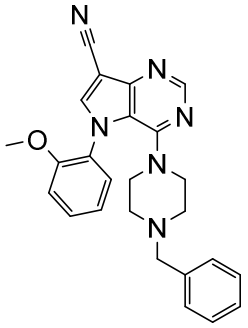

synonyms:	SMS-**A-439** compound **63** (*J. Med. Chem.* **2017**, *accepted 10th of October, 2017*)
educts:	4-chloro-5-(2-methoxyphenyl)-5*H*-pyrrolo[3,2-*d*]pyrimidine-7-carbonitrile (**67**), 1-benzylpiperazine (1.5 eq.) and TEA (1.5 eq.)
yield:	20%
visual appearance:	yellow crystals
chemical formula:	$C_{25}H_{24}N_6O$
molecular weight:	424.51 Da
LC-MS analysis:	calculated: 424.20 Da; found: 425.2 Da $[M+H]^+$
purity:	100%
^{1}H NMR:	500 MHz, DMSO-d_6, δ 8.56 (s, 1H), 8.55 (s, 1H), 7.53 (ddd, J = 8.4, 7.5, 1.7 Hz, 1H), 7.41 (dd, J = 7.8, 1.6 Hz, 1H), 7.32-7.21 (m, 4H), 7.20-7.16 (m, 2H), 7.10 (td, J 7.6, 1.2 Hz, 1H), 3.71 (s, 3H), 3.31 (s, 2H), 3.09-2.96 (m, 4H), 1.97-1.87 (m, 4H)
^{13}C NMR:	126 MHz, DMSO-d_6, δ 153.9, 153.8, 151.7, 150.2, 141.5, 137.7, 130.7, 128.9 (2C), 128.3 (2C), 128.0, 127.1, 126.6, 120.8, 117.0, 114.0, 112.9, 87.7, 61.9, 56.0, 51.4 (2C), 49.1 (2C)

6.1.4.61. Synthesis of **5-(4-ethoxyphenyl)-4-(4-phenethylpiperazine-1-yl)-5*H*-pyrrolo[3,2-*d*]pyrimidine-7-carbonitrile (134)**

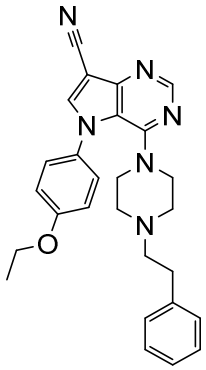

synonyms:	SMS-**A-412** compound **64** (*J. Med. Chem.* **2017**, *accepted 10th of October, 2017*)

educts:	4-chloro-5-(4-ethoxyphenyl)-5*H*-pyrrolo[3,2-*d*]pyrimidine-7-carbonitrile (**68**), 1-(2-phenethyl)piperazine (1.5 eq.) and TEA (1.5 eq.)
yield:	22%
visual appearance:	pale yellow crystals
chemical formula:	$C_{27}H_{28}N_6O$
molecular weight:	452.56 Da
LC-MS analysis:	calculated: 452.23 Da; found: 453.2 Da $[M+H]^+$
purity:	99%
^{1}H NMR:	500 MHz, DMSO-d_6, δ 8.66 (s, 1H), 8.55 (s, 1H), 7.41 (d, J = 8.8 Hz, 2H), 7.42 (t, J = 7.5 Hz, 2H), 7.15 (t, J = 7.9 Hz, 3H), 7.11 (d, J = 8.8 Hz, 2H), 4.11 (q, J = 6.9 Hz, 2H), 3.11-3.04 (m, 4H), 2.60 (t, J = 8.3 Hz, 2H), 2.38 (t, J = 8.4 Hz, 2H), 2.13-2.07 (m, 4H), 1.33 (t, J = 6.9 Hz, 3H)
^{13}C NMR:	126 MHz, DMSO-d_6, δ 158.5, 153.2, 151.7, 150.9, 141.4, 140.4, 130.9, 128.7 (2C), 128.4 (2C), 126.8 (2C), 126.0, 115.7, 115.2 (2C), 114.2, 87.6, 63.8, 59.7, 51.4 (2C), 48.9 (2C), 32.4, 14.7

6.1.4.62. Synthesis of **4-(4-benzylpiperazine-1-yl)-5-(4-ethoxyphenyl)-5*H*-pyrrolo[3,2-*d*]pyrimidine-7-carbonitrile (135)**

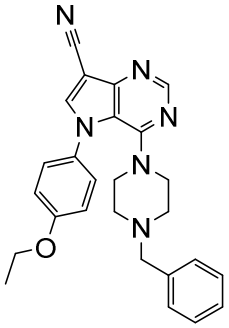

synonyms:	SMS-**A-415** compound **65** (*J. Med. Chem.* **2017**, *accepted 10th of October, 2017*)
educts:	4-chloro-5-(4-ethoxyphenyl)-5*H*-pyrrolo[3,2-*d*]pyrimidine-7-carbonitrile (**68**), 1-benzylpiperazine (1.5 eq.) and TEA (1.5 eq.)
yield:	20%
visual appearance:	pale yellow crystals
chemical formula:	$C_{26}H_{26}N_6O$
molecular weight:	438.54 Da
LC-MS analysis:	calculated: 438.22 Da; found: 439.1 Da $[M+H]^+$
purity:	97%
^{1}H NMR:	500 MHz, DMSO-d_6, δ 8.64 (s, 1H), 8.54 (s, 1H), 7.40-7.36 (m, 2H), 7.31-7.26 (m, 2H), 7.24-7.20 (m, 1H), 7.20-7.17 (m, 2H), 7.11-7.07 (m, 2H), 4.14 (q, J = 7.0 Hz, 2H), 3.31 (s, 2H), 3.14-3.02 (m, 4H), 2.08-1.96 (m, 4H), 1.39 (t, J = 7.0 Hz, 3H)
^{13}C NMR:	126 MHz, DMSO-d_6, δ 158.5, 153.1, 151.7, 150.9, 141.4, 137.8, 130.9, 128.9 (2C), 128.3 (2C), 127.1, 126.7 (2C), 115.6, 115.2 (2C), 114.2, 87.6, 63.8, 62.1, 51.5 (2C), 48.8 (2C), 14.7

6.1.4.63. Synthesis of **4-(4-phenethylpiperazine-1-yl)-5*H*-pyrimido[5,4-*b*]indole (136)**

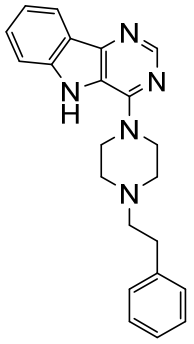

synonyms:	SMS-**A-137** compound **69** (*J. Med. Chem.* **2017**, *accepted 10th of October, 2017*)
educts:	4-chloro-5*H*-pyrimido[5,4-*b*]indole (**72**), 1-(2-phenethyl)piperazine (1.5 eq.) and TEA (1.5 eq.)
yield:	18%
visual appearance:	pale yellow crystals
chemical formula:	$C_{22}H_{23}N_5$
molecular weight:	357.46 Da
LC-MS analysis:	calculated: 357.20 Da; found: 358.1 Da $[M+H]^+$
purity:	94%
^{1}H NMR:	500 MHz, DMSO-d_6, δ 11.27 (s, 1H), 8.46 (s, 1H), 8.09 (d, J = 7.8 Hz, 1H), 7.61 (dt, J = 8.3, 0.9 Hz, 1H), 7.53 (ddd, J = 8.2, 7.0, 1.2 Hz, 1H), 7.30-7.21 (m, 5H), 7.20-7.16 (m, 1H), 3.80 (t, J = 4.9 Hz, 4H), 2.80 (dd, J = 9.1, 6.6 Hz, 2H), 2.65 (t, J = 5.0 Hz, 4H), 2.61 (dd, J = 9.0, 6.7 Hz, 2H)
^{13}C NMR:	126 MHz, DMSO-d_6, δ 151.1, 149.1, 144.8, 140.5, 140.0, 128.8 (2C), 128.4 (3C), 126.0, 120.7, 120.5, 119.9, 118.5, 112.7, 59.8, 52.8 (2C), 46.1 (2C), 32.8

6.1.4.64. Synthesis of **4-(4-benzylpiperazine-1-yl)-5*H*-pyrimido[5,4-*b*]indole (137)**

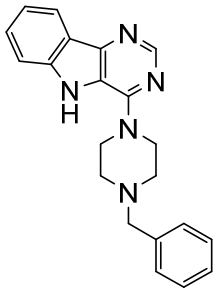

synonyms:	SMS-**A-140** compound **70** (*J. Med. Chem.* **2017**, *accepted 10th of October, 2017*)
educts:	4-chloro-5*H*-pyrimido[5,4-*b*]indole (**72**), 1-benzylpiperazine (1.5 eq.) and TEA (1.5 eq.)
yield:	36%
visual appearance:	yellow crystals
chemical formula:	$C_{21}H_{21}N_5$
molecular weight:	343.43 Da

LC-MS analysis:	calculated: 343.18 Da; found: 344.1 Da $[M+H]^+$
purity:	97%
^{1}H NMR:	500 MHz, $CDCL_3$, δ 9.09 (s, 1H), 8.61 (s, 1H), 8.20 (d, J = 7.9 Hz, 1H), 7.50-7.42 (m, 2H), 7.33-7.30 (m, 4H), 7.27-7.25 (m, 1H), 7.24-7.20 (m, 1H), 3.90 (t, J = 4.9 Hz, 4H), 3.55 (s, 2H), 2.61 (t, J = 4.9 Hz, 4H)
^{13}C NMR:	126 MHz, $CDCl_3$, δ 151.3, 149.6, 145.1, 139.9, 137.1, 129.3 (2C), 128.9, 128.4 (2C), 127.4, 121.2, 121.2, 120.8, 118.9, 112.1, 62.9, 52.8 (2C), 46.3 (2C)

6.1.4.65. Synthesis of **4-(4-benzhydrylpiperazine-1-yl)-5*H*-pyrimido[5,4-*b*]indole (138)**

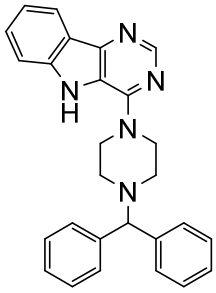

synonyms:	SMS-**A**-**138** compound **71** (*J. Med. Chem.* **2017**, *accepted 10th of October, 2017*)
educts:	4-chloro-5*H*-pyrimido[5,4-*b*]indole (**72**), 1-benzhydrylpiperazine (1.5 eq.) and TEA (1.5 eq.)
yield:	54%
visual appearance:	pale yellow crystals
chemical formula:	$C_{27}H_{25}N_5$
molecular weight:	419.53 Da
LC-MS analysis:	calculated: 419.21 Da; found: 420.4 Da $[M+H]^+$
purity:	97%
^{1}H NMR:	500 MHz, $CDCL_3$, δ 9.02 (s, 1H), 8.47 (s, 1H), 8.18 (d, J = 7.9 Hz, 1H), 7.49-7.37 (m, 6H), 7.30-7.25 (m, 4H), 7.21-7.17 (m, 3H), 4.28 (s, 1H), 3.95-3.89 (m, 4H), 2.61-2.54 (m, 4H)
^{13}C NMR:	126 MHz, $CDCL_3$, δ 151.2, 142.0, 139.8 (2C), 129.1, 128.7 (4C), 128.7 (4C), 127.2 (3C), 121.3, 121.0, 118.3, 112.2, 76.0, 51.8, 52.8 (2C), 46.7 (2C)

3.1.4.66. Synthesis of **(4-phenylpiperazine-1-yl)-5*H*-pyrimido[5,4-*b*]indole (139)**

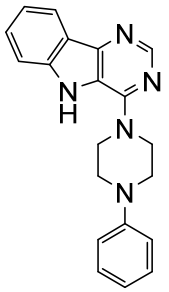

synonyms:	SMS-**A**-**139** compound **72** (*J. Med. Chem.* **2017**, *accepted 10th of October, 2017*)

educts:	4-chloro-5*H*-pyrimido[5,4-*b*]indole (**72**), 1-phenylpiperazine (1.5 eq.) and TEA (1.5 eq.)
yield:	41%
visual appearance:	pale yellow crystals
chemical formula:	$C_{20}H_{19}N_5$
molecular weight:	329.41 Da
LC-MS analysis:	calculated: 329.16 Da; found: 330.1 Da $[M+H]^+$
purity:	96%
^{1}H NMR:	500 MHz, $CDCL_3$, δ 8.70 (s, 1H), 8.39 (s, 1H), 8.27 (d, J = 7.9 Hz, 1H), 7.56-7.48 (m, 2H), 7.32-7.26 (m, 3H), 6.97-6.93 (m, 2H), 6.90 (t, J = 7.3 Hz, 1H), 4.01 (t, J = 5.2 Hz, 4H), 3.37 (t, J = 5.1 Hz, 4H)
^{13}C NMR:	126 MHz, $CDCL_3$, δ 151.4, 151.0, 150.4, 146.4, 139.9, 129.3 (2C), 129.0, 121.8, 121.4, 121.0, 120.4, 119.3, 116.4 (2C), 111.9, 49.3 (2C), 46.5 (2C)

6.1.4.67. Synthesis of 4-(4-(2-(1*H*-indole-3-yl)ethyl)piperazine-1-yl)-5*H*-pyrimido[5,4-*b*]indole (140)

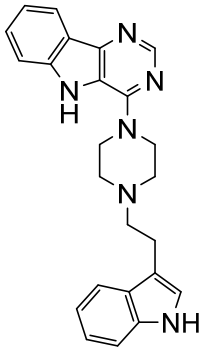

synonyms:	SMS-**A**-**136** compound **66** (*J. Med. Chem.* **2017**, *accepted 10th of October, 2017*)
educts:	4-chloro-5*H*-pyrimido[5,4-*b*]indole (**72**), 3-(2-(piperazine-1-yl)ethyl)-1*H*-indole (**73**, 1.5 eq.) and TEA (1.5 eq.)
yield:	28%
visual appearance:	white crystals
chemical formula:	$C_{24}H_{24}N_6$
molecular weight:	396.50 Da
LC-MS analysis:	calculated: 396.21 Da; found: 397.2 Da $[M+H]^+$
purity:	99%
^{1}H NMR:	500 MHz, DMSO-d_6, δ 11.70 (s, 1H), 11.34 (s, 1H), 10.97 (s, 1H), 8.57 (s, sH), 8.33 (d, J = 7.9 Hz, 1H), 7.65 (t, J = 7.8 Hz, 1H), 7.57 (ddd, J = 8.2, 7.0, 1.2 Hz, 1H), 7.37 (d, J = 8.1 Hz, 1H) ,7.29-7.24 (m, 2H), 7.11-7.07 (m, 1H), 7.03-6.98 (m, 1H), 4.70-4.48 (m, 2H), 3.85-3.60 (m, 4H), 3.49-3.38 (m, 2H), 3.27-3.03 (m, 4H)
^{13}C NMR:	126 MHz, DMSO-d_6, δ 150.4, 148.8, 145.1, 140.4, 136.4, 128.8, 126.9, 123.3, 121.4, 120.7, 120.5, 120.2, 118.8, 118.6, 118.5, 112.8, 111.7, 119.4, 55.9, 50.8 (2C), 43.4 (2C), 19.8

6.1.4.68. Synthesis of 4-(4-(2-(pyridin-2-yl)ethyl)piperazine-1-yl)-5*H*-pyrimido[5,4-*b*]indole (141)

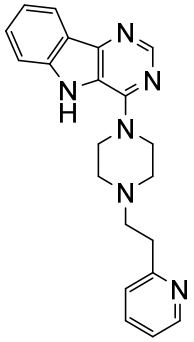

synonyms:	SMS-**A-143** compound **67** (*J. Med. Chem.* **2017**, *accepted 10th of October, 2017*)
educts:	4-chloro-5*H*-pyrimido[5,4-*b*]indole (**72**), 4-(2-(pyridin-2-yl)ethyl)piperazine (1.5 eq.) and TEA (1.5 eq.)
yield:	33%
visual appearance:	pale yellow crystals
chemical formula:	$C_{21}H_{22}N_6$
molecular weight:	358.45 Da
LC-MS analysis:	calculated: 358.19 Da; found: 359.0 Da $[M+H]^+$
purity:	89%
^{1}H NMR:	500 MHz, $CDCL_3$, δ 9.15 (s, 1H), 8.65 (s, 1H), 8.51 (d, J = 4.5 Hz, 1H), 8.23 (d, J = 7.9 Hz, 1H), 7.60 (td, J = 7.7, 1.6 Hz, 1H), 7.53-7.47 (m, 2H), 7.27-7.24 (m, 1H), 7.18 (d, J = 7.8 Hz, 1H), 7.13 (dd, J = 7.1, 5.2 Hz, 1H), 3.87 (t, J = 4.5 Hz, 4H), 3.02-2.97 (m, 2H), 2.84-2.80 (m, 2H), 2.64 (t, J = 4.6 Hz, 4H)
^{13}C NMR:	126 MHz, $CDCL_3$, δ 159.7, 151.3, 150.0, 149.2, 146.0, 140.1, 136.6, 128.9, 123.3, 121.6, 121.5, 121.3, 120.8, 119.2, 112.1, 58.1, 52.7 (2C), 46.2 (2C), 35.3

6.1.4.69. Synthesis of 4-(4-(pyridin-2-yl)piperazine-1-yl)-5*H*-pyrimido[5,4-*b*]indole (142)

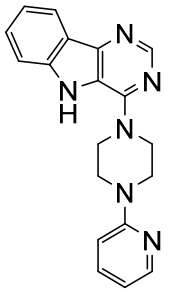

synonyms:	SMS-**A-177** compound **68** (*J. Med. Chem.* **2017**, *accepted 10th of October, 2017*)
educts:	4-chloro-5*H*-pyrimido[5,4-*b*]indole (**72**), 1-(pyridin-2-yl)piperazine (1.5 eq.) and TEA (1.5 eq.)

yield:	46%
visual appearance:	pale yellow crystals
chemical formula:	$C_{19}H_{18}N_6$
molecular weight:	330.39 Da
LC-MS analysis:	calculated: 330.16 Da; found: 331.1 Da $[M+H]^+$
purity:	96%
^{1}H NMR:	500 MHz, $CDCL_3$, δ 8.92 (s, 1H), 8.69 (s, 1H), 8.24 (d, J = 7.9 Hz, 1H), 8.19 (dd, J = 5.3, 1.6 Hz, 1H), 7.53-7.45 (m, 3H), 7.30-7.25 (m, 1H), 6.66 (t, J = 3.4 Hz, 1H), 6.64 (s, 1H), 4.00 (t, J = 5.2 Hz, 4H), 3.73 (t, J = 5.2 Hz, 4H)
^{13}C NMR:	126 MHz, $CDCL_3$, δ 159.1, 151.5, 150.1, 148.0, 146.1, 140.0, 137.7, 129.0, 121.6, 121.3, 120.9, 119.3, 113.8, 112.0, 107.1, 46.1 (2C), 44.9 (2C)

6.1.4.70. Synthesis of 4-(4-(benzo[*d*][1,3]dioxol-5-ylmethyl)piperazine-1-yl)-5*H*-pyrimido[5,4-*b*]indole (143)

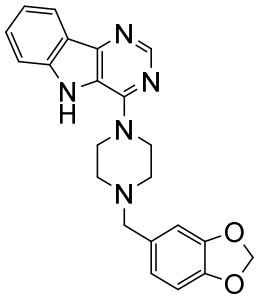

synonyms:	SMS-**A**-**141** compound **73** (*J. Med. Chem.* **2017**, *accepted 10th of October, 2017*)
educts:	4-chloro-5*H*-pyrimido[5,4-*b*]indole (**72**), 1-piperonylpiperazine (1.5 eq.) and TEA (1.5 eq.)
yield:	43%
visual appearance:	pale yellow crystals
chemical formula:	$C_{22}H_{21}N_5O_2$
molecular weight:	387.44 Da
LC-MS analysis:	calculated: 387.17 Da; found: 388.2 Da $[M+H]^+$
purity:	98%
^{1}H NMR:	500 MHz, DMSO-d_6, δ 11.26 (s, 1H), 8.45 (s, 1H), 8.08 (d, J = 7.9 Hz, 1H), 7.60 (d, J = 8.2 Hz, 1H), 7.55-7.49 (m, 1H), 7.25-7.20 (m, 1H), 6.93-6.89 (m, 1H), 6.86 (d, J = 7.8 Hz, 1H), 6.80 (d, J = 7.9 Hz, 1H), 5.99 (s, 2H), 3.84-3.71 (m, 4H), 3.54-3.43 (m, 2H), 2.64-2.51 (m, 4H)
^{13}C NMR:	126 MHz, DMSO-d_6, δ 151.1, 149.1, 147.4, 146.4, 144.8, 140.0, 131.8, 128.4, 122.3, 120.7, 120.5, 119.9, 118.5, 112.7, 109.4, 198.0, 100.9, 61.8, 52.5 (2C), 46.1 (2C)

6.1.4.71. Synthesis of **(4-(5*H*-pyrimido[5,4-*b*]indole-4-yl)piperazine-1-yl)(furan-2-yl)methanone (144)**

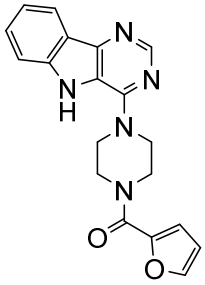

synonyms:	SMS-**A**-**142** compound **74** (*J. Med. Chem.* **2017**, *accepted 10th of October, 2017*)
educts:	4-chloro-5*H*-pyrimido[5,4-*b*]indole (**72**), 1-(2-furoyl)piperazine (1.5 eq.) and TEA (1.5 eq.)
yield:	75%
visual appearance:	pale yellow crystals
chemical formula:	$C_{19}H_{17}N_5O_2$
molecular weight:	347.38 Da
LC-MS analysis:	calculated: 347.14 Da; found: 348.0 Da $[M+H]^+$
purity:	98%
^{1}H NMR:	500 MHz, DMSO-d_6, δ 11.39 (s, 1H), 8.50 (s, 1H), 8.11 (d, J = 7.9 Hz, 1H), 7.87 (dd, J = 1.7, 0.7 Hz, 1H), 7.63 (d, J = 8.2 Hz, 1H), 7.55 (ddd, J = 8.2, 7.1, 1.1 Hz, 1H), 7.25 (ddd, J = 7.8, 7.0, 0.8 Hz, 1H), 7.06 (dd, J = 3.4, 0.7 Hz, 1H), 6.65 (dd, J = 3.4, 1.8 Hz, 1H), 3.95-3.90 (m, 4H), 3.90-3.84 (m, 4H)
^{13}C NMR:	126 MHz, DMSO-d_6, δ 158.6, 150.9, 149.1, 147.1, 145.0, 144.9, 140.1, 128.5, 120.7, 120.6, 120.0, 118.6, 115.9, 112.7, 111.5, 55.7 (2C), 46.0 (2C)

6.2. Materials and Methods for Biological Investigation

6.2.1. Materials

6.2.1.1. Chemicals for Biological Testing

Table 6.10 summarizes reference compounds, fluorescence dyes, chemicals and solvents used in the cell laboratory.

Table 6.10. Summary of used reference compounds, fluorescence dyes, chemicals and solvents.

chemical	provider
calcein AM	Calbiochem (EMD Chemicals (San Diego, CA, USA), supplied by Merck KGaA (Damstadt, Germany)
calcium chloride dihydrate	Merck KGaA (Darmstadt, Germany)
cyclosporine A	Tocris Bioscience (Bristol, IO, USA)
daunorubicin	Sigma (Oakville, ON, Canada)
$_{D}$-glucose monohydrate	Merck KGaA (Darmstadt, Germany)
DMSO	Sigma-Aldrich Chemie GmbH (Steinheim, Germany)
HEPES	Carl Roth GmbH & Co KG (Karlsruhe, Germany)
indomethacin	Sigma-Aldrich (St. Louis, MO, USA)
Ko143	Tocris Bioscience (Bristol, IO, USA)
magnesium sulfate heptahydrate	Merck KGaA (Darmstadt, Germany)
methanol	Sigma-Aldrich Chemie GmbH (Steinheim, Germany)
MK571 sodium salt hydrate	Sigma-Aldrich Chemie GmbH (Steinheim, Germany)
MTT	Carl Roth GmbH & Co KG (Karlsruhe, Germany)
pheophorbide A	Frontier Scientific Inc. (Logan, UT, USA)
potassium chloride	Merck KGaA (Darmstadt, Germany)
potassium dihydrogen phosphate	Merck KGaA (Darmstadt, Germany)
pranlukast hemihydrate	Sigma-Aldrich Chemie GmbH (Steinheim, Germany)
sodium chloride	Th.Greyer GmbH & Co KG (Renningen, Germany)
sodium hydrogen carbonate	Merck KGaA (Darmstadt, Germany)
sodium hydroxide	VWR Chemicals (Darmstadt, Germany)
Water, ultrapure (Elix Millipore)	Merck KGaA (Darmstadt, Germany)

6.2.1.2. Buffers for Biological Testing

Since cell culture media and their ingredients (see section 6.2.1.3) contain enzymes, proteins or other macromolecules that might interfere with fluorescence measurement, the Krebs-HEPES-buffer (KHB) was used for measurement with the microplate reader (see section 6.2.1.5). The buffer ensured survival of cells over the assay time. Since the KHB was used extensively for serial dilution, fluorescence dye dilutions, or cell-based fluorescence assays in general, the stock solution of KHB was prepared fivefold concentrated. Table 6.11 gives the ingredients. The weighed salts were dissolved in 500 mL of ultra pure water, aliquoted into 50 mL falcons and stored at -20 °C.

Table 6.11. Ingredients and necessary weighed portion for 500 mL of a fivefold concentrated Krebs-HEPES-buffer solution.

ingredient	molecular weight [Da]	weighed portion [g]
$_D$-glucose monohydrate	198.17	5.796
HEPES	238.31	5.958
potassium chloride	74.54	0.876
potassium dihydrogen phosphate	136.09	0.408
sodium chloride	58.44	17.330
sodium hydrogen carbonate	84.01	0.882

The onefold KHB solution was prepared as follows: eight 50 mL aliquots of the fivefold concentrated, frozen KHB solution were defrosted. The resultant 400 mL of fivefold concentrated KHB was diluted to 1.8 L with ultrapure water followed by addition of 2.6 mL and 2.4 mL of a calcium chloride and magnesium sulfate solution, respectively (both 1 mol · L^{-1}). The solution was adjusted to pH = 7.4 with sodium hydroxide (10 mol · L^{-1}). The buffer was filled up to 2.0 L with ultrapure water and aliquoted into 50 mL tubes. Table 6.12 gives the prevailing concentration of every ingredient in the onefold concentrated KHB solution.

Table 6.12. Calculated concentrations of the incredients in the onefold Krebs-HEPES-buffer as used in the assays.

ingredient	concentration [mmol · L^{-1}]
calcium chloride dihydrate	1.3
$_D$-glucose	11.7
HEPES	10.0
potassium chloride	4.7
potassium dihydrogen phosphate	1.2
magnesium sulfate	1.2
sodium chloride	118.6
sodium hydrogen carbonate	4.2

6.2.1.3. Solutions for Cell Culture

Different solutions were used for cell maintenance, rinsing, counting or subculturing (see section 6.2.3). Table 6.13 gives the used cell culture media and with cell culture associated solutions.

Tabl. 6.13. Cell culture media and necessary ingredients for cell culture used in the cell laboratory and assays.

equipment	provider
CASY ton solution	OMNI Life Science GmbH + Co. KG (Bremen, Germany)
Dulbecco's modified Eagle's medium ("DMEM")	Sigma Life Science (Steinheim, Germany)
Fetal Bovine Serum (FBS)	Sigma Life Science (Steinheim, Germany)
L-glutamine ("L-Glu")	PAN Biotech GmbH (Aidenbach, Germany)
Penicillin G / 50 Streptomycin ("PenStrep")	PAN Biotech GmbH (Aidenbach, Germany)
phosphate-buffered saline (PBS)	PAN Biotech GmbH (Aidenbach, Germany)
RPMI-1640 cell culture medium	PAN Biotech GmbH (Aidenbach, Germany)
Trypsin-EDTA solution 0.05%/0.02%	PAN Biotech GmbH (Aidenbach, Germany)

6.2.1.4. Materials for Biological Testing

Several appliances were used for different operations in the cell laboratory, e.g. cryopreservation (6.2.3.1.2), subculturing (see section 6.2.3.3), or preparation of serial dilution (6.2.4.1). Table 6.14 gives an overview of all used appliances.

Table 6.14. Summary of used materials for cell culture, assay preparation and execution.

equipment	provider
accu-jet pro	Brand GmbH + Co. KG (Wertheim, Germany)
96-well microplate, F-bottom, clear	Greiner bio one (Frickenhausen, Germany)
96-well microplate, U-shaped, clear	Greiner bio one (Frickenhausen, Germany)
96-well tissue-culture treated plates	Starlab GmbH (Hamburg, Germany)
cryopreservation tank MVE cryosystem 4000	cryo solutions (GmbH Rheinberg, Germany)
falcon tube 15 mL	Greiner bio one (Frickenhausen, Germany)
falcon tube 50 mL	Greiner bio one (Frickenhausen, Germany)
Finnpipette 0.5-10 μL	Thermo Fisher Scientific (Waltham, MA, USA)
Finnpipette 2-20 μL	Thermo Fisher Scientific (Waltham, MA, USA)
Finnpipette 5-50 μL	Thermo Fisher Scientific (Waltham, MA, USA)
Finnpipette 10-100 μL	Thermo Fisher Scientific (Waltham, MA, USA)
Finnpipette 20-200 μL	Thermo Fisher Scientific (Waltham, MA, USA)
Finnpipette 200-1000 μL	Thermo Fisher Scientific (Waltham, MA, USA)
Finnpipette 1000-5000 μL	Thermo Fisher Scientific (Waltham, MA, USA)
glass Pasteur pipettes (230 mm)	Brand GmbH + Co. KG (Wertheim, Germany)
Microflex xceed powder-free nitrile examination gloves (M)	Microflex (Reno, NV, USA)
microtubes 1.5 mL	Sarstedt, AG & Co. (Nürnbrecht, Germany)
microtubes 2.0 mL MCT-200-C	Axygen scientific (Union City, CA, USA)
Nalgene System 100 cryogenic tubes	Thermo Fisher Scientific (Waltham, MA, USA)
pipette 0.5-10 μL	Eppendorf (Hamburg, Germany)

equipment	provider
pipette 10-100 µL	Eppendorf (Hamburg, Germany)
pipette 20-200 µL	Eppendorf (Hamburg, Germany)
pipette 100-1000 µL	Eppendorf (Hamburg, Germany)
reagent reservoirs, sterile	VWR International GmbH (Darmstadt, Germany)
serological pipette 10 mL	Sarstedt, AG & Co. (Nürnbrecht, Germany)
serological pipette 25 mL	Sarstedt, AG & Co. (Nürnbrecht, Germany)
syringe Braun Injekt 20 mL	ALMO-Erzeugnisse, Erwin Busch GmbH (Bad Arolsen, Germany)
T25 cell culture flasks	Greiner bio one (Frickenhausen, Germany)
T75 cell culture flasks	Greiner bio one (Frickenhausen, Germany)
T175 cell culture flasks	Greiner bio one (Frickenhausen, Germany)
tip, 5 mL	Brand GmbH + Co. KG (Wertheim, Germany)
TipOne 10 µL graduated tips	Starlab GmbH (Hamburg, Germany)
TipOne 200 µL yellow, bevelled tips	Starlab GmbH (Hamburg, Germany)
TipOne 1000 µL blue, graduated tips	Starlab GmbH (Hamburg, Germany)
Transferpipette S 1000 µL	Brand GmbH + Co. KG (Wertheim, Germany)
Transferpipette S 5000 µL	Brand GmbH + Co. KG (Wertheim, Germany)
Whatman FP 30/0.2 µM CA-S filter units	GE Healthcare UK limited (Buckinghamshire, UK)

6.2.1.5. Instruments for Basic Operations

Many instruments were used in the cell laboratory for preparation or postprocessing of assays, aseptic operations or proper storage of cells or stock solutions. Table 6.15 shows all used instruments except for analytical instruments (see section 6.2.1.6).

Table 6.15. List of used instruments for basic operations in the cell laboratory.

equipment	provider
autoclave VX-95	Systec GmbH (Wettenberg, Germany)
Avanti J-25 centrifuge	Beckmann Coulter (Krefeld, Germany)
coulter counter CASY1 model TT with Epson LQ-400 printer	Schärfe System GmbH (Reutlingen, Germany)
cell culture incubator	Münchener Medizin Mechanik GmbH (Planegg, Germany)
Herafreezer -80 °C	Heraeus Holding GmbH (Hanau, Germany)
laminar air flow	Bio-Flow Technik GmbH (Meckenheim, Germany)
microscope Axiovert 25	Carl Zeiss AG (Feldbach, Swizzerland)
refrigerator	Bosch (Stuttgart, Germany)
refrigerator Premium NoFrost -20 °C	Liebherr-International Deutschland GmbH (Biberach an der Riß, Germany)
multi channel pipette Transferpette©-8 electronic 10-200 µL	Brand GmbH + Co. KG (Wertheim, Germany)

equipment	provider
multi channel pipette Xplorer plus	Eppendorf (Hamburg, Germany)
ThermoStat plus	Eppendorf (Hamburg, Germany)
scale KERN 430-33	Kern &Sohn GmbH (Balingen-Frommern, Germany)
vortexer vortex-genie 2	Scientific Industries (Bohemia, NY, USA)
waterbath Julabo TW 12	Julabo GmbH (Seelbach, Germany)
vacuum pump unit BVC 21	Vacuubrand GmbH + Co. KG (Wertheim, Germany)

6.2.1.6. Instruments for Biological Investigations

Table 6.16 gives an overview of the used analytical instruments for cell-based fluorescence assays, MTT-viability or MDR reversal-efficacy assays.

Table 6.16. Listing of analytical instruments used in this thesis.

equipment	provider
Ex Multiscan microplate photometer	Thermo Fisher Scientific (Waltham, MA, USA)
FACSCalibur© flow cytometer	Becton Dickinson Biosciences (Heidelberg, Germany)
Fluostar Optima microplate reader	BMG-Labtech (Ortenberg, Germany; software version 2.00R2 and 2.20)
Fluostar Polarstar microplate reader	BMG-Labtech (Ortenberg, Germany; software version 4.11-0)
LS 55 Luminescence Spectrometer	Perkin Elmer (Waltham, MA, USA)

6.2.2. Cell lines

6.2.2.1. H69AR and H69

The adherent growing doxorubicin-selected small cell lung cancer cell line H69AR overexpressing MRP1 and its sensitive counterpart H69 (syn. NCL-H69) growing as suspension were provided by American Type Culture Collection (ATCC CRL-11351 and ATCC HTB-119, respectively). The cells were cultivated using RPMI-1640 cell culture medium supplemented with 20% (V/V) FBS, 2 mmol · L^{-1} L-glutamine, 50 U/mL penicillin G and 50 μg/mL streptomycin.

6.2.2.2. MDCK II MRP1 and MDCK II

The Madin-Darby Canine Kidney (MDCK) cell line transfected with the cDNA of human MRP1 (MDCK II MRP1) and their sensitive counterpart MDCK II were a generous gift of Prof. Dr. P. Borst and Dr. A. Schinkel from The Netherlands Cancer Institute (Amsterdam, The

Netherlands). Cultivation was performed using Dulbecco's modified Eagle's medium complemented with 10% (V/V) FBS, 2 mmol · L^{-1} L-glutamine, 50 U/mL penicillin G and 50 μg/mL streptomycin.

6.2.2.3. 2008/MRP1 and 2008

The human ovarian carcinoma cell line 2008/MRP1 stably transfected with human MRP1 cDNA and their sensitive counterpart 2008 were a generous gift of Prof. Dr. P. Borst and Dr. A. Schinkel from The Netherlands Cancer Institute (Amsterdam, The Netherlands). The cells were cultivated using RPMI-1640 cell culture medium supplemented with 10% (V/V) FBS, 2 mmol · L^{-1} L-glutamine, 50 U/mL penicillin G and 50 μg/mL streptomycin.

6.2.2.4. A2780/ADR and A2780

The doxorubicin-selected human ovarian carcinoma cell line A2780/ADR (ECACC no. 931123120) overexpressing P-gp as well as its sensitive counterpart A2780 (ECACC no. 93112519) were provided by European Collection of Animal Cell Culture (ECACC). Cultivation was performed in RPMI-1640 medium complemented with 10% FBS, 2 mmol · L^{-1} L-glutamine, 50 U/mL penicillin G and 50 μg/mL streptomycin.

6.2.2.5. MDCK II BCRP

The MDCK II BCRP cell line is stably transfected with human wildtype cDNA of BCRP and additionally *C*-terminally linked to green fluorescent protein (GFP), which allowed the observation of the expression level of BCRP. The cells were also a generous gift by Prof. Dr. P. Borst and Dr. A. Schinkel (The Netherlands Cancer Institute, Amsterdam, The Netherlands). Cultivation was performed as stated for the MDCK II MRP1 and MDCK II cell lines.

6.2.3. Cell Culture

6.2.3.1. Cell Line Back-Ups

6.2.3.1.1. Defrosting

The cryopreservation vials were taken out of the cryopreservation tank and handwarmed. The content was transferred into a 15 mL conic tube and 5 mL of warmed (37 °C) cell culture medium was added. The cell suspension was centrifuged at 266 x *g* and 4 °C for 4 minutes. The supernatant was sucked off with a vacuum pump. After resuspension in fresh, warmed

cell culture medium, the pellet was transferred into a T25, T75 or T175 cell culture flask followed by storage at 37 °C and under 5% CO_2-humidified atmosphere. The cells were subcultured as stated below (see section 6.2.3.3) before using in biological experiments.

6.2.3.1.2. Cryopreservation

Cryopreservation was performed under liquid nitrogen (Air Liquide, Düsseldorf, Germany) in a cryoconservation tank at approximately -196 °C. At a confluence of 90-100%, the cells were trypsinated as stated below (6.2.3.2). The obtained cell pellet from six T175 cell culture flasks was suspended in 20 mL cell culture medium. 900 μL cell suspension was pipetted into 1 mL cryopreservation vials followed by addition of 100 μL of DMSO to prevent cell damage by freezing. The vials were transferred quickly into a -80 °C refrigerator and kept for 30 minutes with frequent shaking every 10 minutes to maintain homogenous conditions within the vials. After one day, the vials were transferred into the liquid nitrogen tank.

6.2.3.2. Trypsination

The necessary cell culture medium, the trypsin-EDTA solution or any other needed buffer (KHB, PBS) was taken out of the storage refrigerator and transferred into a warmed 37 °C water bath. All work with living cells used for defrosting, subculturing, biological testing or cryopreservation was performed in the laminar air flow cabinet to maintain aseptic conditions. The cell culture flasks containing the adherent growing cells at a confluence between 90-100% were taken out of the incubator. The cell layer was rinsed three times with PBS, and the supernatant containing cell debris was sucked off. The necessary amount of warmed trypsin-EDTA solution (0.05%/0.02%) was transferred into the cell culture flasks (T25 cell culture flask: 1 mL; T75 cell culture flask: 3-5 mL; T175 cell culture flask: 5-10 mL; dependent on the cell confluence). Incubation time depended on confluence and cell type (H69AR; A2780/ADR, A2780, 2008/MRP1 and 2008: ≤ 5 min; transfected and parental MDCK II cell lines: 15-30 min). Afterwards, the trypsin was deactivated by pouring fresh and warmed culture medium into the flasks. The bottom was rinsed at least three times to remove still adherent cells using an electronic pipette and a 10 mL serological pipette. The whole volume was transferred into a 15 mL or 50 mL tube, dependent on the volume, and centrifuged at 266 x *g* and 4 °C for 4 minutes. The supernatant was sucked off by a pump using 3 mL Pasteur pipettes and the resultant pellet was suspended in fresh warmed cell culture medium. The resultant suspension was prepared for cell counting or subculturing.

For the suspension cells H69 no trypsination was necessary, since the cell culture medium can easily be put into the 50 mL tubes and centrifuged at 266 x *g* and 4 °C for 4 minutes. The resultant pellet was treated as stated above.

6.2.3.3. Subculturing

The necessary amount of cells was taken either after cell counting as stated below (6.2.3.4) or as partial volume (percentage) and transferred into an already with warmed cell culture medium filled cell culture flask. For T25 flasks, 10 mL of medium was sufficient for each cell line. For the T75 flasks, 18-20 mL of cell culture medium was taken in case of 2008/MRP1, 2008, A2780 adr, A2780 and all MDCK II cells (transfected or parental). H69AR cells grow slowly while consuming cell culture medium in high magnitude. Hence, a higher volume of cell culture medium was needed (at least 30 mL). T175 flasks were used to generate cell line back-ups. Here, between 50 and 100 mL cell culture medium was used, dependent on the state of growing.
While for all other cell lines a population of 3-4 million cells is sufficient to start reproductive cell growth and reach a confluence of up to 100% after 3-5 days, H69AR cells must be transferred at least with approximately 30% of the total volume or 8-10 million cells, to guarantee a homogenous and constant cell growth. The same policy accounts for the parental cell line H69.

6.2.3.4. Cell Counting

20 µL of the freshly prepared cell suspension (see section 6.2.3.2) was transferred into 10 mL of CASY® solution, which was sterilized by filtration with membrane filters (0.2 µm pore diameter) using a 20 mL syringe. The solution was shaked carefully at least 10 times. The created suspension was counted employing a coulter counter CASY1 model TT using a 150 µm capillary. Measuring the electric resistance dependent on the cell diameter, the necessary amount of cells was taken to conduct the procedures stated below. The cell diameter was individually limited dependent on the cell lines. Table 6.17 summarizes used cell lines, their usage in fluorescence-based assays, needed amount of cells and the measured cell diameter.

Table 6.17. Summary of used cell lines in different cell-based fluorescence assays and needed cell amount as well as the determined cell diameters.

cell line	assay (section)	cell amount	cell diameter [μm]
H69AR (MRP1)	calcein AM assay (6.2.4.2)	60,000	7.5-30
	daunorubicin assay (6.2.4.3)	60,000	
H69	daunorubicin assay (6.2.4.3)	60,000	3-30
MDCK II MRP1	calcein AM assay (6.2.4.2)	60,000	8-30
	daunorubicin assay (6.2.4.3)	60,000	
MDCK II	calcein AM assay (6.2.4.2)	60,000	8-30
	daunorubicin assay (6.2.4.3)	60,000	
	pheophorbide A assay (6.2.4.4)	45,000	
2008/MRP1	calcein AM assay (6.2.4.2)	30,000	8-30
A2780/ADR (P-gp)	calcein AM assay (6.2.4.2)	30,000	8-30
A2780	calcein AM assay (6.2.4.2)	30,000	8-30
MDCK II BCRP	pheophorbide A assay (6.2.4.4)	45,000	8-30

6.2.4. Cell-based Fluorescence Assays

6.2.4.1. Preparation of Serial Dilution and 96 Well Plate

The serial dilution for biological evaluation was prepared in KHB. The 10 mmol · L^{-1} compound stock solution in DMSO was used as starting concentration. The solubility of compounds depended on temperature and solvent content. The 1 mmol · L^{-1} concentration was prepared by dilution of 100 μL stock solution and adjusted to 1000 μL with either methanol or a mixture of methanol and KHB, in case the solubility of the compound allowed this procedure. Further dilutions were created using mixtures of KHB and methanol to the 100 μmol · L^{-1} concentration, continued by usage of KHB only. 20 μL of every compound dilution was pipetted to each well of a 96-well microplate with duplicate determination. The compounds were usually evaluated in a concentration range from 10 nM to 10 μM. In case of transport activators, lower concentrations were applied. Compounds with low inhibitory potential were sometimes also evaluated up to 100 μM, as far as solubility, intrinsic toxicity, and solvent content allowed a reproducible determination.

6.2.4.2. Calcein AM Assay

6.2.4.2.1. General Information

Calcein AM is a substrate of MRP1 and P-gp.[357,358] While this hydrophobic molecule diffuses easily through cell membranes, it becomes effluxed out of cells mediated by these two transport proteins. In case of efflux inhibition the intracellular calcein AM gets hydrolyzed by intracellular unspecific esterases to the fluorescence dye calcein. This molecule is due to its five carboxy groups highly hydrophilic and not able to leave cells through passive diffusion. In P-gp overexpressing cells, the amount of built calcein is completely trapped intracellularly. In case of MRP1 overexpressing cells, the produced calcein is still a substrate of MRP1, which is generally known to transport organic anions. But the affinity toward calcein is by a factor of 5000 lower than to the acetoxymethyl ester calcein AM,[357] and the effluxed calcein is still measured in a microplate reader as it registers all fluorescence inside a well.

The amount of intracellularly persisting calcein AM is dependent on the pump rate of the transport protein. If the transport protein is inhibited, the amount of calcein AM increases, which automatically leads to an increased cleavage of the ester to the fluorescent product calcein. Vice versa, transport activation leads to a decreased presence of calcein AM and therefore to a decreased fluorescence. In the beginning of an experiment, the extracellular concentration of calcein AM is almost constant due to the large excess in the extracellular space and the intracellular concentration equals zero. Due to active export and hydrolysis sink conditions exist, that lead to a constant passive diffusion into the cell in spite of reduction of total amount of calcein AM. Though, the instantaneous fluorescence increase is linear, and the slope can be calculated using a specific time interval, which was checked per assay individually. In general, the slope was evaluated between minutes 5 and 20 to 35. Figure 6.1 gives a simplified overview of the prevailing processes.

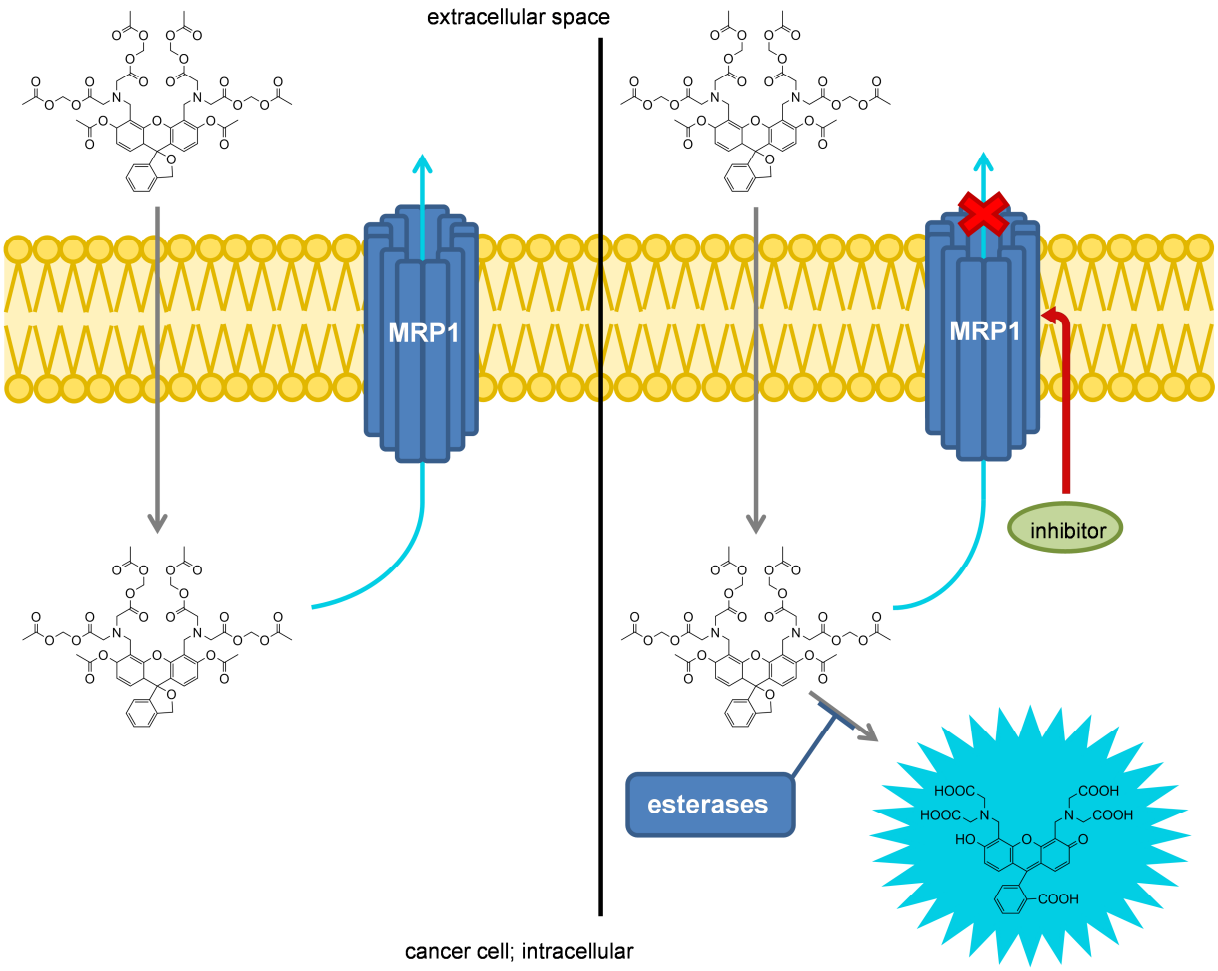

Figure 6.1. Simplified depiction of processes involved in the calcein AM assay. Calcein AM diffuses through biomembranes into e.g. MRP1 overexpressing cells and gets pumped out by this transporter. In case of inhibition, the persistence of calcein AM leads to increased cleavage to the fluorescence dye calcein mediated by unspecific intracellular esterases. The same mechanism applies for P-gp overexpressing cells.

6.2.4.2.2 General Procedure

The calcein AM assay for MRP1[258,260,293,359] and P-gp[359,360,361,362] was performed as already described before with small adaptions. The biological data presented in subchapter 4.3 was determined by Katja Stefan. The cell suspension was prepared as described above (see section 6.2.3.2) and the necessary amount of cells was calculated (see section 6.2.3.4). Table 6.18 gives used parameters of the assays.

In short, a 96 well plate was pipetted with 20 μL of the compounds at different concentrations between 100 nM and 100 μM. The plate was incubated for 30 minutes at 37 °C and CO_2-humidified atmosphere after addition of 160 μL of a cell suspension containing the necessary amount of cells per well. A 3.125 μmol · L^{-1} solution of calcein AM was added (20 μL) before measuring the fluorescence increase as a function of time in a microplate reader.

Table 6.18. Summary of important parameters for the calcein AM assay for MRP1 and P-gp.

calcein AM assay	parameter
cell lines and cells per well (transporter)	H69AR, 60,000 (MRP1) MDCKII MRP1, 60,000 (MRP1) MDCK II, 60,000 2008/MRP1, 30,000 (MRP1) 2008, 30,000 A2780/ADR, 30,000 (P-gp)
compound dilution	20 μL
cell suspension volume per well	160 μL
incubation time and conditions	30 min, 37 °C, CO_2-humidified atmosphere
calcein AM and final concentration	20 μL of 3.125 μmol · L^{-1} stock final: 0.3125 μmol · L^{-1}
analytical instrument and instrument parameters	microplate reader plate scan mode horizontal measurement 485 nm excitation wavelength 520 nm emission wavelength 60 cycles à 10 stimuli · s^{-1} 20% required value

The fluorescence increase over time is a function of the degree of inhibition of the corresponding transport protein. Plotting of the slope of the linear fluorescence increase (between minutes 5 and 20 to 35) and the logarithmic compound concentration gave sigmoidal concentration-effect curves, that were evaluated with respect to their IC_{50} and I_{max} value by nonlinear regression analysis using GraphPad Prism (four-parameter logistic equation with either variable Hill slope (4 parameter model) or Hill slope = 1 (three parameter model); see section 6.3.2.2).

6.2.4.2.3 Characterization of H69AR Cells via Calcein AM Assay

The MDCK II MRP1 as well as the 2008/MRP1 cell lines were already characterized with respect to calcein AM and calcein accumulation by Stefan Leyers before.[293] The linear correlation between calcein accumulation in uninhibited H69AR cells dependent on the used calcein AM concentration can be seen in Figure 6.2 A. The fluorescence increase over time

is linear between 0.1 and 0.7 μmol · L^{-1}. The already established concentration[293,363] of 0.3125 μmol · L^{-1} was also used for the calcein AM assay and H69AR cells. Figure 6.2 B shows the linear correlation between used calcein AM concentration and the slope of the fluorescence increase over time.

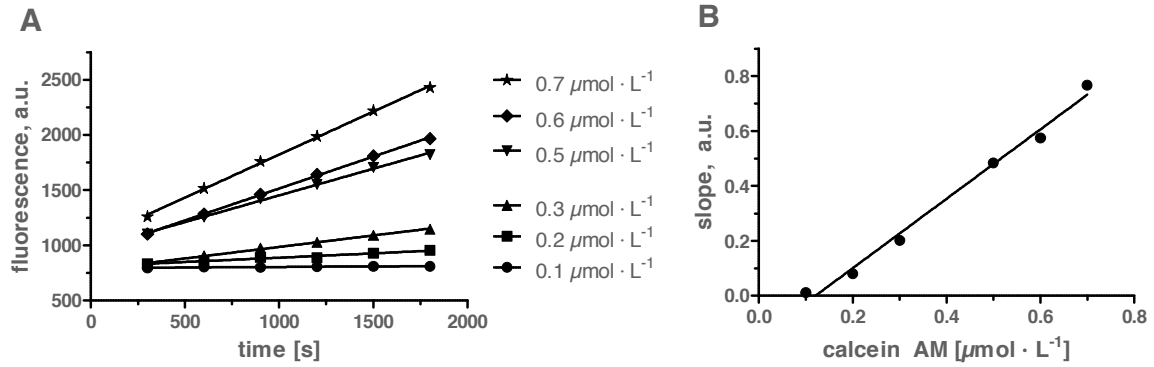

Figure 6.2. (A): Fluorescence increase over time dependent on the used calcein AM concentration. (B): Linear correlation between used calcein AM concentration and slope of fluorescence increase calculated from lines of graphic (A) determined between minutes 5 and 35. Depicted is a representative experiment out of at least three independent experiments; a.u. = arbitrary units.

The fact that the second line does not cross the origin might be caused by unspecific secondary effects, e.g. protein binding. But the linear relationship makes the assay applicable for compound evaluation. The next step was to see whether inhibition of MRP1 leads to a saturable increase of fluorescence. Figures 6.3 A-B show corresponding graphics for indomethacin.

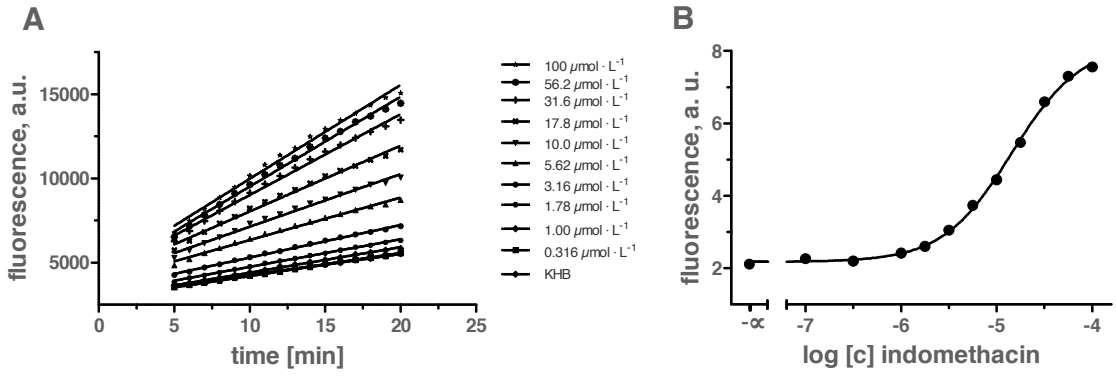

Figure 6.3. (A): Indomethacin as a representative of a known inhibitor of MRP1-mediated transport of calcein AM. Increase of the indomethacin concentration enhances intracellular calcein accumulation and fluorescence. The calculated slopes plotted against the logarithmic indomethacin concentrations give a sigmoidal concentration-effect curve as seen in graphic (B). Shown is a representative experiment out of at least three independent experiments; a.u. = arbitrary units.

The effect of indomethacin as a representative of a specific MRP1 inhibitor and cyclosporine A as representative of an unspecific MRP1 inhibitor was determined in three MRP1 overexpressing cell lines, H69AR, MDCK II MRP1 and 2008/MRP1. Tables 6.19 A-B summarize the obtained biological data.

Table 6.19 A. Summary of IC_{50} values obtained using H69AR, MDCK II MRP1 and 2008/MRP1 cells with respect to the MRP1 standard inhibitors indomethacin (specific) and cyclosporine A (unspecific).

standard inhibitor	H69AR IC_{50} ± SEM [μmol · L^{-1}]	MDCK II MRP1 IC_{50} ± SEM [μmol · L^{-1}]	2008/MRP1 IC_{50} ± SEM [μmol · L^{-1}]
indomethacin	8.69 ± 0.722	10.8 ± 0.725	8.34 ± 0.400
cyclosporine A	3.55 ± 0.225	3.37 ± 0.483	3.30 ± 0.237

Table 6.19 B. Summary of pIC_{50} values and Hill slopes deduced from concentration-effect curves obtained using H69AR, MDCK II MRP1 and 2008/MRP1 cells with respect to the MRP1 standard inhibitors indomethacin (specific) and cyclosporine A (unspecific); n_H = Hill slope.

standard inhibitor	H69AR pIC_{50} ± SEM	n_H ± SEM	MDCK II MRP1 pIC_{50} ± SEM	n_H ± SEM	2008/MRP1 pIC_{50} ± SEM	n_H ± SEM
indomethacin	5.062 ± 0.055	= 1	4.966 ± 0.044	= 1	5.030 ± 0.028	= 1
cyclosporine A	5.450 ± 0.041	2.56 ± 0.18	5.477 ± 0.094	1.90 ± 0.48	5.483 ± 0.047	2.25 ± 0.32

Cyclosporine A is a rare example of a compound in this thesis with a Hill coefficient significantly different from one, so that the three parameter model of the logistic equation was inappropriate (see section 6.3.2.2). Most compounds including indomethacin had a slope of one, which is an indicator of the molecularity of the reaction.[364] Furthermore, several known MRP1 inhibitors were compared to IC_{50} and pIC_{50} values determined by Stefan Leyers in the calcein AM assay using 2008/MRP1 cells as can be seen in Table 6.20.

Table 6.20. Inhibition data using H69AR cells of the leukotriene receptor antagonists MK571 (verlukast) and ONO-1078 (pranlukast) as well as indomethacin and cyclosporine A compared to the data determined by Stefan Leyers with 2008/MRP1 cells;[293] n_H = Hill slope.

standard inhibitor	H69 AR IC_{50} ± SEM [μmol · L^{-1}]	H69 AR pIC_{50} ± SEM	n_H ± SEM	2008/MRP1[293] IC_{50} ± SEM [μmol · L^{-1}]	2008/MRP1[293] pIC_{50} ± SEM
MK571	7.73 ± 0.178	5.112 ± 0.015	3.97 ± 0.29	6.51 ± 0.72	5.189 ± 0.073
ONO-1078	6.94 ± 0.224	5.159 ± 0.021	3.91 ± 0.18	n.t.	n.t.
indomethacin	8.69 ± 0.722	5.062 ± 0.055	= 1	11.4 ± 0.779	4.945 ± 0.045
cyclosporine A	3.55 ± 0.225	5.450 ± 0.041	2.56 ± 0.18	4.83 ± 0.293	5.317 ± 0.040

6.2.4.2.3. Anomalies of the Calcein AM Assay

Figure 6.4 shows found concentration-effect curves of the standard inhibitors cyclosporine A and indomethacin as well as compounds **74**, **119** and **126**. These differ with respect to the maximum inhibition level (I_{max}). This effect occurs not only in H69AR cells, but also in MDCK II MRP1 and 2008/MRP1 cells (see Figures 6.5 A-B), and was already found in P-gp overexpressing cells, too.[281]

As already shown before by Leyers et al.,[293] the MDCK II MRP1 as well as 2008/MRP1 cells express a natively occurring P-gp. This applies also to the parental cell lines. Figure 6.5 C shows a representative experiment of compound **74** using MDCK II MRP1 and wild type cells. The sensitive cell line gives also a sigmoidal concentration effect curve. This effect was obtained for most herein presented compounds. Though, this effect disguises the real value of full inhibition. Hence, the alleged top value indicated by the sensitive cell lines cannot be used.

Although the sensitive H69 cells have not been reported to express other transport proteins, their use in microplate reader-based assays was not applicable due to several reasons: (i) these suspension cells are morphologically different compared to their selected counterparts, as they are smaller and grow as agglomerates. This affects partitioning of test compounds and fluorescence dyes; (ii) the cell counting is difficult, since the cells are partially smaller than the measurement window of the coulter-counting system, which makes the calculation of the correct amount of cells difficult; (iii) as the cells are not attached on the cell culture flask bottom, dead cells or other cell debris cannot be separated, which makes the measurement in the microplate reader problematic.

Otherwise, the evaluation of the compounds using the sensitive H69 cells was possible in the daunorubicin assay (see section 6.2.4.3) since this assay is based on the measurement of intracellular fluorescence of single cells. Furthermore, this effect of partial inhibition could not be observed in the daunorubicin assay (Figure 6.5 D) despite of rare exceptions (compounds **136**-**144**).

Different I_{max} values could be explained by disturbance of the membrane integrity, which would lead to different passive diffusion velocities of the fluorescence probes. But flow cytometry data excluded this possibility since no effect could be seen in sensitive cell lines (see Figure 4.19). Furthermore, MTT-viability assays showed that the evaluated compounds did not have a negative influence on cell growth in a long-term period (see sections 4.1.5, 4.2.5 and 4.3.6).

Taken together, this makes a substrate specific effect and even partial inhibition of MRP1-mediated calcein AM transport more likely. This assumption is supported by experiments showing the compounds to be noncompetitive inhibitors of MRP1-mediated transport of

calcein AM as well as daunorubicin (see sections 4.1.2 and 4.3.5), except for the activation part (see section 4.2.7).

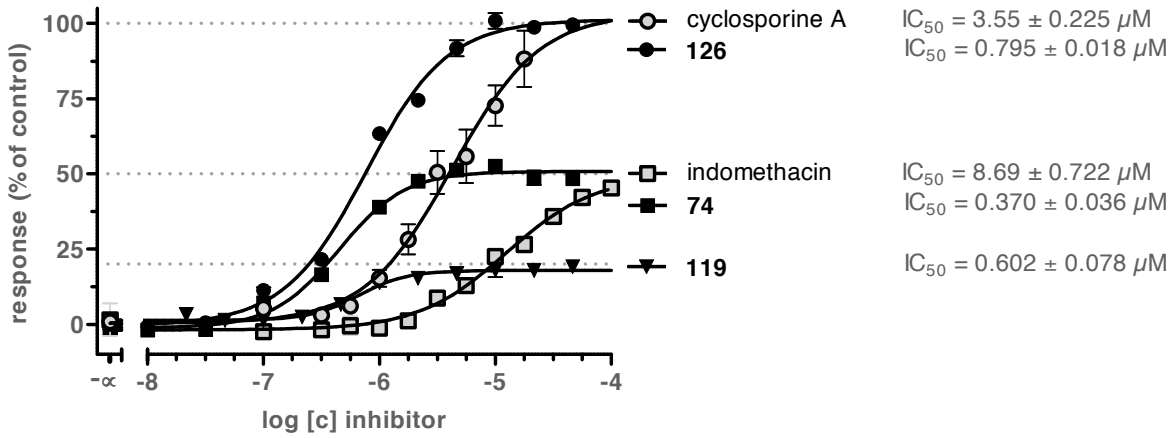

Figure 6.4. Concentration-effect curves of the known MRP1 standard inhibitors cyclosporine A (open circles) and indomethacin (open squares) in comparison to compounds of this thesis giving different I_{max} values (**74**, black closed squares; **119**, black closed downward triangles; **126**, black closed circles) determined in the calcein AM assay. Shown are at least three independent experiments.

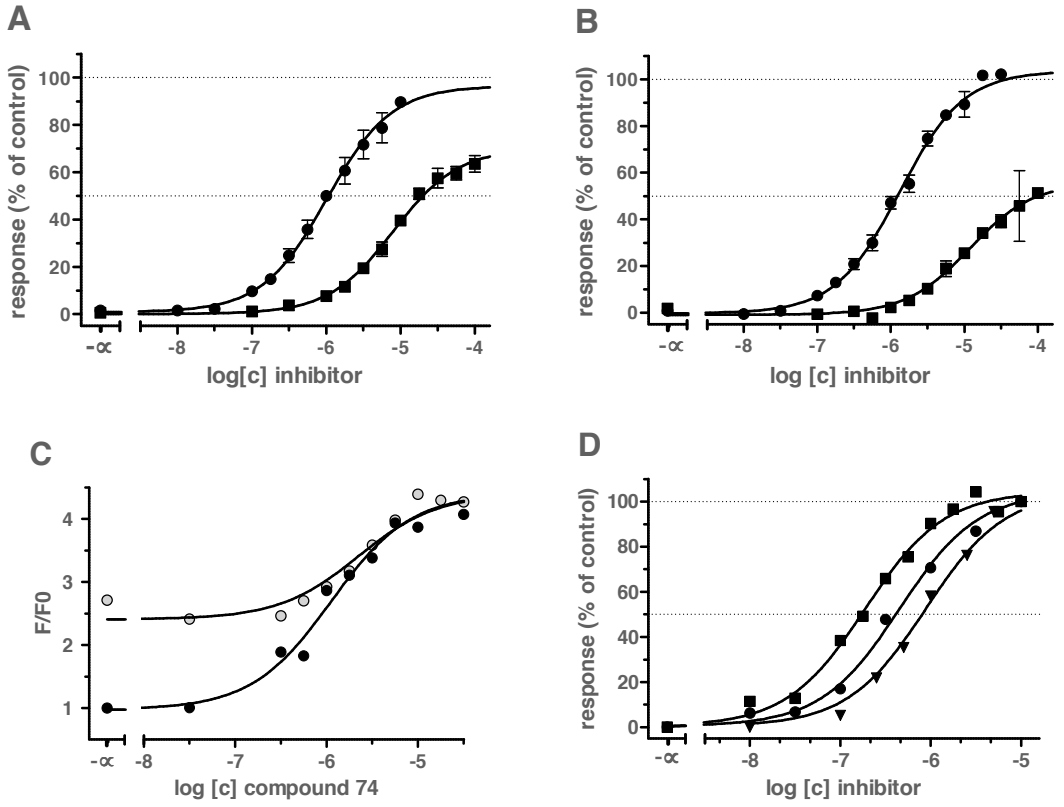

Figure 6.5. (A): Concentration-effect curves of cyclosporine A (closed circles) and indomethacin (closed squares) using MDCK II MRP1 cells (calcein AM). (B): Concentration-effect curves of cyclosporine A (closed circles) and indomethacin (closed squares) using 2008/MRP1 cells (calcein AM). (C): Representative experiment of compound **74** using MDCK II MRP1 (closed circles) and MDCK II (open circles) determined in the calcein AM assay. (D): Representative concentration-effect curves of compound **74** (closed squares), **119** (closed downward triangles) and **126** (closed circles) in the daunorubicin assay.

Since most compounds resulted in the same top value in the daunorubicin assay but nearly none did so in the calcein AM assay, the question arose whether the IC_{50} value calculated constraining to the I_{max} indicated by a standard inhibitor is a proper measure for compound evaluation. This specific IC_{50} value will be termed absolute IC_{50} in the following. Figure 6.6 gives the concentration-effect curves of compounds **74**, **119** and **126**. The latter represented 100% transport inhibition since it gave similar I_{max} values like cyclosporine A, MK571 or ONO-1078 but with much better inhibitory activity. As one can see, the absolute IC_{50} changed dependent on the I_{max} of the unconstrained concentration-effect curve as seen in Figure 6.4. The lower the I_{max} value of a concentration-effect curve, the higher the absolute IC_{50} value.

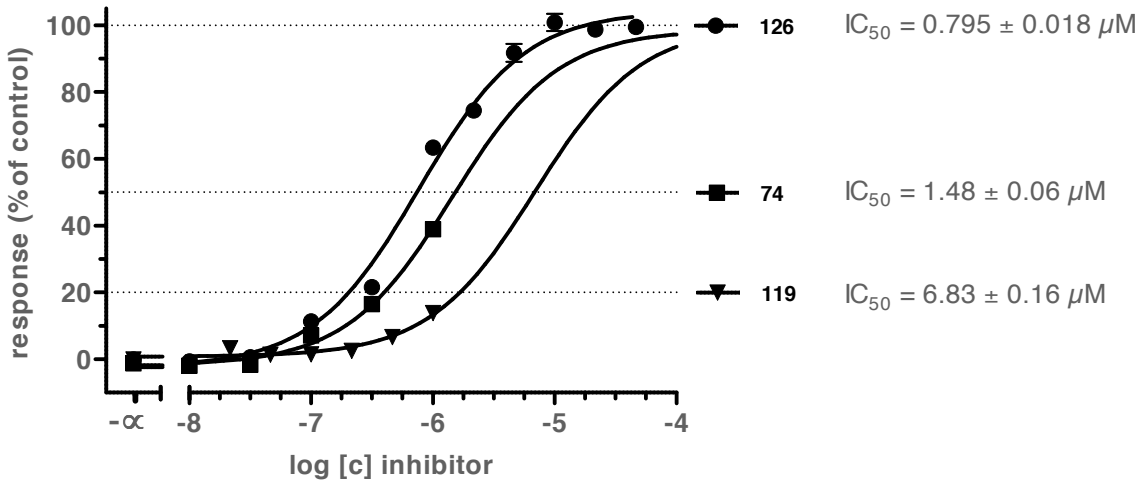

Figure 6.6. Concentration-effect curves of compounds **74** (closed squares), **119** (closed downward triangles) and **126** (closed circles) with I_{max} values constrained to compound **126** (calcein AM assay). Shown are at least three independent experiments with duplicate measurements.

The absolute pIC_{50} values were experimentally determined using compound **126** as 100% control and plotted against the absolute pIC_{50} obtained in the daunorubicin assay (Figure 6.7 A). This data did not correlate well, as the slope of 0.69 ± 0.08 and the R^2 value of 0.75 indicate. In other words, the daunorubicin assay gives inhibitory activity data indicating a higher potency of the compounds than the data obtained in the calcein AM assay. For example, pIC_{50} values in the daunorubicin assay of 5.5, 6.0 or 6.5 give absolute pIC_{50} values in the calcein AM assay of approximately 4.0, 4.75 and 5.5, respectively.

On the other hand, the relative pIC_{50} values of the calcein AM assay correlated much better with the data of the daunorubicin assay (Figure 6.7 B), as can be seen from the slope of 0.93 ± 0.07 and a R^2 value of 0.88. This led to the conclusion that the calcein AM assay is a proper measure and reflects the inhibitory power of the compounds in the right manner. This

was also shown in Figures 4.1 A and 4.13 A. The latter gave the evidence that the relative pIC_{50} value of the calcein AM assay correlated directly with the MDR reversal potency of the compound. Table 6.21 gives the determined relative and absolute IC_{50} values, pIC_{50} values, and I_{max} values obtained in the calcein AM assay for compounds **74**-**100** in comparison to the determined daunorubicin assay data as already shown in Tables 4.1-3.

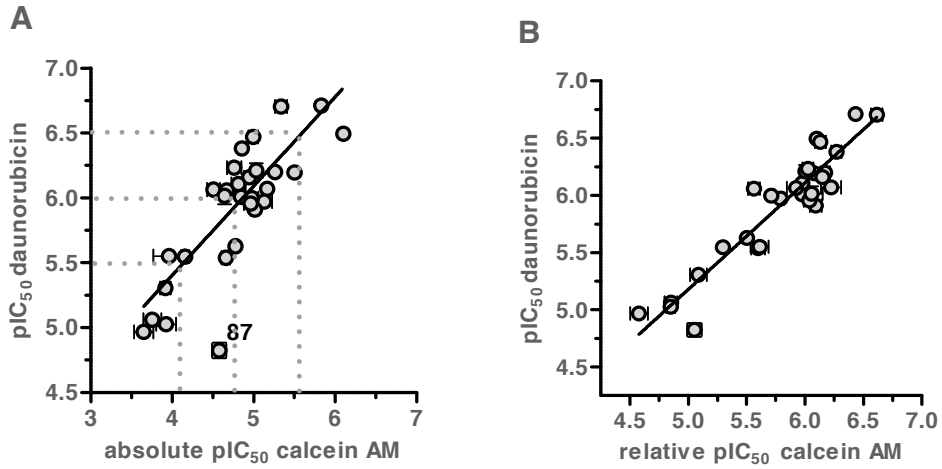

Figure 6.7. (A): Correlation between absolute pIC_{50} values determined in the calcein AM and daunorubicin assays of compounds **74**-**100**. The slope of the linear regression line is 0.69 ± 0.08, the R^2 = 0.75. (B): Correlation of relative pIC_{50} values obtained in the calcein AM assay and the absolute pIC_{50} value determined in the daunorubicin assay; the slope of the linear regression line is 0.93 ± 0.07, the R^2 = 0.88.

Table 6.21. List of relative IC_{50} values, pIC_{50} values, and corresponding I_{max} values obtained in the calcein AM assay as already presented in Tables 4.1-3 in comparison to the absolute IC_{50} values of the calcein AM (I_{max} constrained to compound **126**) and daunorubicin (see Tables 4.1-3) assays of compounds **74**-**100**.

no.	calcein AM relative IC_{50} ± SEM [μmol · L^{-1}]	calcein AM relative pIC_{50} ± SEM	calcein AM I_{max} [%] ± SEM	calcein AM absolute IC_{50} ± SEM [μmol · L^{-1}]	calcein AM absolute pIC_{50} ± SEM	daunorubicin IC_{50} ± SEM [μmol · L^{-1}]	daunorubicin pIC_{50} ± SEM
74	0.369 ± 0.007	6.433 ± 0.012	51.1 ± 1.7	1.48 ± 0.06	5.829 ± 0.024	0.195 ± 0.012	6.710 ± 0.041
75	0.672 ± 0.041	6.173 ± 0.040	26.6 ± 2.3	5.47 ± 0.24	5.262 ± 0.029	0.634 ± 0.028	6.198 ± 0.029
76	1.62 ± 0.07	5.791 ± 0.027	37.1 ± 4.2	10.2 ± 1.5	5.128 ± 0.098	1.07 ± 0.03	5.971 ± 0.020
77	2.54 ± 0.23	5.598 ± 0.059	27.7 ± 2.5	20.1 ± 1.7	4.658 ± 0.054	2.90 ± 0.07	5.538 ± 0.015
78	5.06 ± 0.15	5.296 ± 0.020	17.7 ± 0.8	69.7 ± 5.3	4.157 ± 0.050	2.85 ± 0.19	5.546 ± 0.043
79	26.6 ± 3.0	4.578 ± 0.075	25.7 ± 2.2	228 ± 41	3.649 ± 0.117	10.8 ± 0.2	4.966 ± 0.015
80	2.46 ± 0.28	5.611 ± 0.076	19.3 ± 4.5	114 ± 34	3.959 ± 0.192	2.82 ± 0.18	5.550 ± 0.042
81	8.22 ± 0.90	5.088 ± 0.072	23.5 ± 2.2	118 ± 11	3.915 ± 0.064	4.97 ± 0.27	5.305 ± 0.036
82	14.2 ± 1.2	4.851 ± 0.054	29.0 ± 6.0	179 ± 30	3.754 ± 0.110	8.72 ± 0.66	5.061 ± 0.050
83	14.1 ± 0.8	4.850 ± 0.037	36.9 ± 7.2	121 ± 22	3.924 ± 0.120	9.40 ± 0.30	5.027 ± 0.021

no.	calcein AM relative IC_{50} ± SEM [$\mu mol \cdot L^{-1}$]	calcein AM relative pIC_{50} ± SEM	calcein AM I_{max} [%] ± SEM	calcein AM absolute IC_{50} ± SEM [$\mu mol \cdot L^{-1}$]	calcein AM absolute pIC_{50} ± SEM	daunorubicin IC_{50} ± SEM [$\mu mol \cdot L^{-1}$]	daunorubicin pIC_{50} ± SEM
84	0.833 ± 0.022	6.080 ± 0.022	42.7 ± 0.5	3.15 ± 0.16	5.502 ± 0.033	0.641 ± 0.037	6.194 ± 0.038
85	1.06 ± 0.02	5.976 ± 0.013	18.7 ± 2.8	14.3 ± 1.1	4.845 ± 0.051	0.980 ± 0.041	6.009 ± 0.028
86	1.94 ± 0.08	5.712 ± 0.026	34.1 ± 3.7	10.6 ± 1.3	4.976 ± 0.081	1.01 ± 0.02	5.998 ± 0.016
87	8.90 ± 0.84	5.053 ± 0.062	13.4 ± 0.8	73.5 ± 9.8	4.578 ± 0.088	15.1 ± 1.4	4.824 ± 0.060
88	0.712 ± 0.032	6.148 ± 0.029	12.3 ± 0.6	11.4 ± 1.1	4.945 ± 0.062	0.695 ± 0.049	6.159 ± 0.046
89	1.05 ± 0.05	5.977 ± 0.031	13.9 ± 1.5	15.6 ± 2.1	4.812 ± 0.087	0.785 ± 0.053	6.106 ± 0.045
90	0.540 ± 0.035	6.269 ± 0.043	11.8 ± 0.7	14.0 ± 0.8	4.855 ± 0.038	0.417 ± 0.016	6.380 ± 0.025
91	0.813 ± 0.064	6.091 ± 0.052	12.2 ± 1.3	9.72 ± 0.64	5.013 ± 0.043	1.23 ± 0.07	5.909 ± 0.036
92	0.243 ± 0.018	6.615 ± 0.049	12.1 ± 0.8	4.65 ± 0.53	5.335 ± 0.075	0.199 ± 0.014	6.703 ± 0.047
93	0.752 ± 0.052	6.130 ± 0.046	18.8 ± 4.2	10.2 ± 0.9	4.992 ± 0.058	0.340 ± 0.004	6.469 ± 0.008
94	1.20 ± 0.14	5.923 ± 0.079	10.2 ± 2.2	31.4 ± 3.7	4.506 ± 0.077	0.863 ± 0.042	6.064 ± 0.032
95	1.00 ± 0.05	6.002 ± 0.031	18.2 ± 3.0	9.30 ± 0.32	5.032 ± 0.023	0.619 ± 0.052	6.210 ± 0.055
96	2.74 ± 0.21	5.563 ± 0.051	33.9 ± 4.8	21.7 ± 3.0	4.668 ± 0.091	0.876 ± 0.019	6.058 ± 0.015
97	0.920 ± 0.067	6.037 ± 0.048	22.6 ± 7.3	11.0 ± 1.4	4.962 ± 0.082	1.11 ± 0.08	5.955 ± 0.046
98	0.891 ± 0.131	6.055 ± 0.096	26.5 ± 4.4	22.9 ± 0.4	4.640 ± 0.011	0.973 ± 0.097	6.014 ± 0.066
99	0.947 ±	6.025 ± 0.046	13.8 ± 1.8	17.5 ± 2.3	4.761 ± 0.088	0.585 ± 0.015	6.233 ± 0.017
100	3.15 ± 0.11	5.502 ± 0.024	31.4 ± 2.3	16.8 ± 0.7	4.775 ± 0.027	2.36 ± 0.07	5.628 ± 0.020

6.2.4.2.3. Establishing of Compounds **74** and **126** as Standard Inhibitors

The previous section showed that known inhibitors of MRP1 gave different I_{max} values in the calcein AM assay. Additionally, most standard compounds of MRP1 are not reliable and give severely varying concentration-effect curves. Cyclosporine A for example, a compound widely used as standard MRP1 inhibitor, differs in its solubility, dependent on the batch. This results mostly in concentration-effect curve with reduced response, as depicted in Figure 6.8 A. Here, two different experiments are shown. The upper curve shows the concentration-effect curve of cyclosporine A resulting in a measured plateau, and indicated the maximum inhibition of this test system. Otherwise, the lower curve shows cyclosporine A with solubility issues. The values between 10 and 56 $\mu mol \cdot L^{-1}$ are too low, resulting in fluorescence values different from the absolute maximum as indicated by the upper curve (~ 18 $\mu mol \cdot L^{-1}$). This raises also the question whether the upper curve is a real plateau or is likewise caused by solubility problems.

The solution could be using cyclosporine A only up to a concentration of 10 $\mu mol \cdot L^{-1}$, as this is common for screening evaluations. But this reveals another problem: As one can see in Figure 6.8 B, the resulting concentration-effect curve with a final used concentration of 10 $\mu mol \cdot L^{-1}$ depends on the effect value (fluorescence measure) of exactly this concentration. It is a critical concentration range (dashed grey circle), in which small changes

in the measured fluorescence can result in severe changes of the extrapolated concentration-effect curves (dark and light grey curves).

Though, relative IC_{50} values are measurable, but cyclosporine A is not a proper standard compound when it comes to determe the maximum inhibition level or as fix point for multiple data sets. Furthermore, the inhibitory activity of cyclosporine A is rather poor, which also disqualifies it as a proper standard inhibitor.

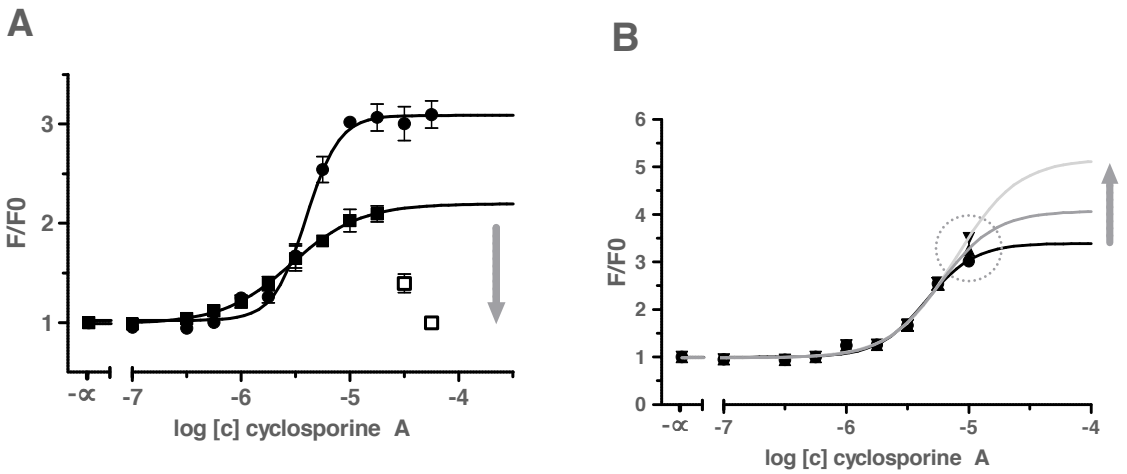

Figure 6.8 Concentration-effect curves of cyclosporine A in the calcein AM assay using H69AR cells. (A): different experiments of cyclosporine A that resulted in a measured plateau (closed circles) or curves with reduced response (closed squares) due to solubility issues. Data points not used are marked as open squares. The tendency of the measured effect with decreased solubility is marked as grey arrow. Shown are at least three independent experiments with duplicate measurements. (B): The concentration-effect curve of graphic (A) marked as black curve (closed circles) in comparison to simulated concentration-effect curves (dark and light grey curves) with slightly varying effect-value of the last concentration (10 μmol · L^{-1}). The grey arrow indicates the tendency of resultant top values.

The leukotriene receptor antagonist MK571 (verlukast), the most used standard inhibitor of MRP1 in the literature, gives the same problems as already stated for cyclosporine A (Figure 6.9 A). But contrary to the latter, solubility issues have never been observed. As it contains a carboxylic acid function, it is a rather water- and buffer-soluble molecule. Though, the reason for the observed effect must be a different one, e.g. influence on intracellular pH or cell toxicity. Although an IC_{50} can be determined by not considering the highest concentrations, this method increases the uncertainty, since it is not clear which concentrations should be left out. Here applies the same argumentation as for cyclosporine A: the mere existence of a measured plateau does not automatically mean that this represents the maximal possible inhibition of the MRP1-mediated transport.

Figure 6.9 B shows the concentration-effect curve of another leukotriene receptor antagonist, ONO-1078. Here, an opposite effect is observed compared to MK571. Effect values observed at concentrations above 10 μmol · L^{-1} contain a huge error. There is up to now no

explanation for this effect. Fluorescence measurements at these concentrations showed this compound not having any auto-fluorescence. Neither was this observed for other herein evaluated compounds. Again, reasonable concentration-effect curves can be obtained by omitting the questionable concentrations, but this leaves the question which concentration should be considered and which should not and disqualifies this compound as standard inhibitor for MRP1 in the calcein AM assay.

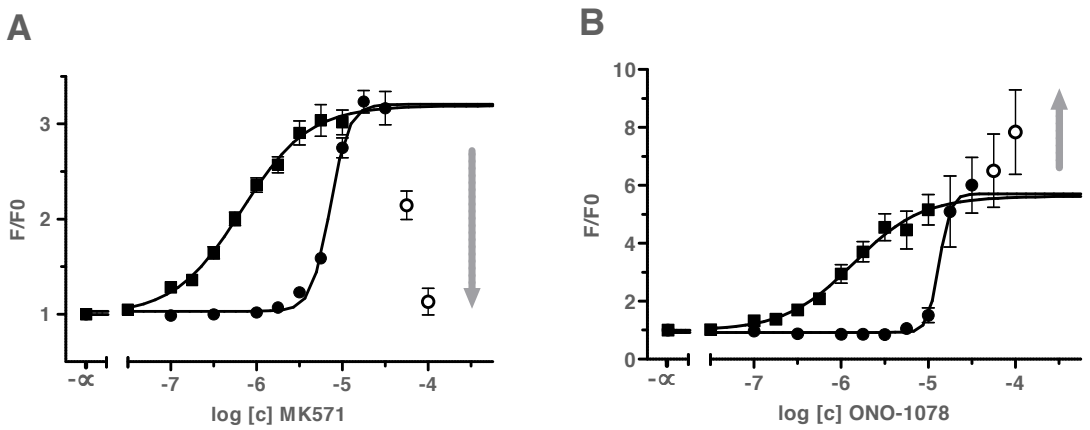

Figure 6.9. Concentration-effect curves of MK571 (verlukast; A; closed circles) and ONO-1078 (pranlukast; B; closed circles) in the calcein AM assay using H69AR cells in comparison to compound **126** (closed squares). The questionable concentrations of the standard MRP1 inhibitors are shown as open circles, and the tendency of the observed effect is depicted as grey arrow. Shown are at least three independent experiments with duplicate measurements.

Taken together, the commonly used standard inhibitors of MRP1, cyclosporine A, indomethacin, MK571 or ONO-1078, cannot be used in the calcein AM assay as these compounds give no reliable data. Although relative IC_{50} values can be determined, and these calculated values have been shown to correlate with literature data, the maximum inhibition level varies significantly. The sensitive cell line H69 cannot be used as a reference since these cells are morphologically different to their selected counterpart. Though, another solution must be found to define the boundaries of the microplate reader-based calcein AM assay to determine the quality and quantity of MRP1 inhibition.

Hence, compound **74** as an already known, very effective MRP1 inhibitor[271] as well as compound **126** were established as standard inhibitors of MRP1 in the calcein as well as daunorubicin assay. Figures 6.10 A-B show the fluorescence increase of totally inhibited H69AR cells mediated by the stated compounds. These graphics are in analogy to Figure 6.2 B and prove that the measured fluorescence is linear within the used concentration range. This makes the cell number of 60,000 cells per well as well as the used calcein AM

concentration applicable for the assay. Furthermore, these compounds are more reliable, because the inhibitory activity is in nanomolar range.

Finally, since compound **74** was shown to be a noncompetitive inhibitor of calcein AM transport mediated by MRP1 (see section 4.1.2), Figure 6.11 shows the evaluation of compound **126** with respect to this manner. As one can see, compound **126** is also a noncompetitive inhibitor of calcein AM transport.

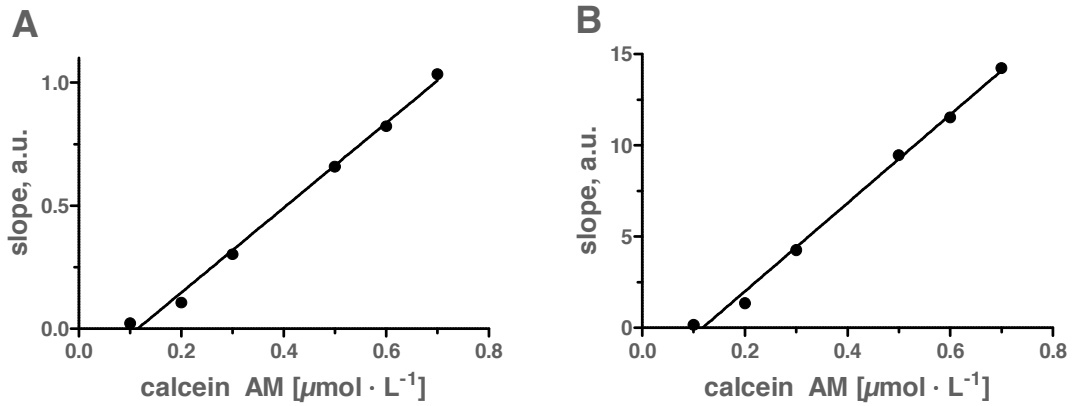

Figure 6.10. Fluorescence increase dependent on the used calcein AM concentration in fully inhibited H69AR cells caused by compounds **74** (A) and **126** (B). These are two representative experiments out of at least three independent experiments; a.u. = arbitrary units.

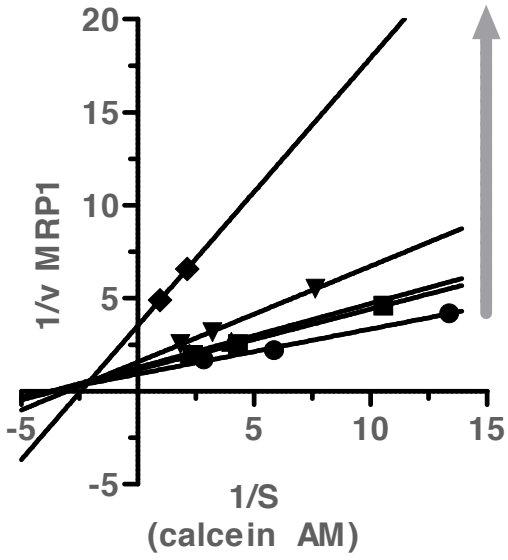

Figure 6.11. Lineweaver-Burk plot of the standard inhibitor **126** with respect to MRP1-mediated transport of calcein AM. Calcein AM was used at concentrations of 0.2, 0.3, 0.5, 0.6 and 0.7 μmol · L^{-1}; compound **126** was used at concentrations of 0.10 (closed squares), 0.21 (closed upward triangles), 0.47 (closed downward triangles) 1.00 (closed rhombs) μmol · L^{-1}. The control is depicted as closed circles. The grey upward oriented arrow indicates the inhibitory manner.

6.2.4.3. Daunorubicin Assay

6.2.4.3.1. General Information

The daunorubicin assay was performed as stated before.[281,282,284,365,366] It was adapted and established for MRP1 overexpressing cells by Katja Stefan. In short, daunorubicin diffuses through the cell membrane and becomes effluxed by MRP1 since it is a good MRP1 substrate. Inhibition of MRP1 enhances the presence of daunorubicin inside the cell and therefore increases the measured fluorescence. Figure 6.12 summarizes the prevailing processes.

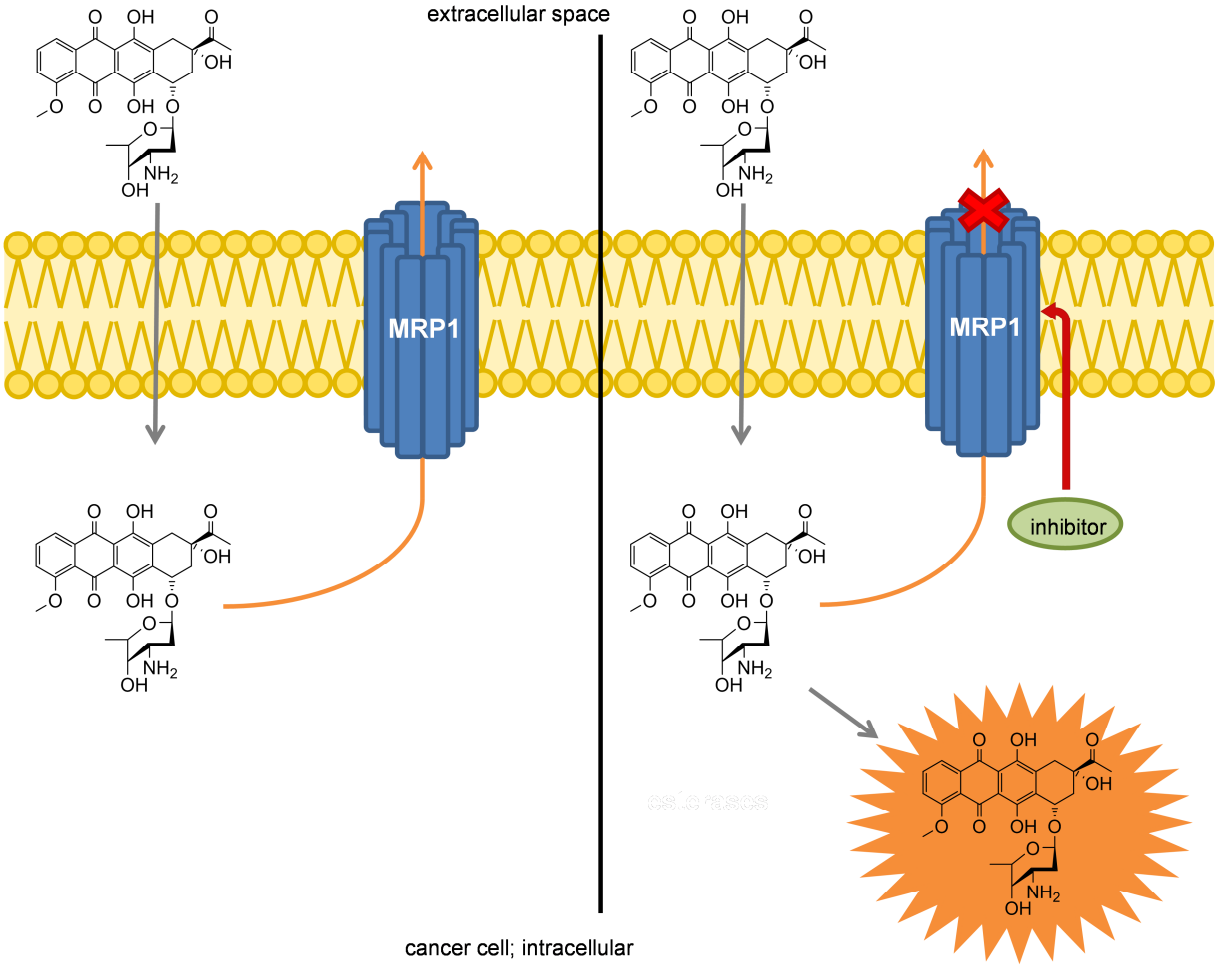

Figure 6.12. Schematic presentation of the daunorubicin assay. Daunorubicin accumulates inside the cell through passive diffusion. Since it is a good MRP1 subtrate, it gets effluxed out of the cell (left). In case of inhibition (right), the increased intracellular concentration of daunorubicin can be detected by fluorescence measurement and is linear to the degree of inhibition.

6.2.4.3.2. General Procedure

The cell suspension was prepared as stated above (see section 6.2.3.2) and the necessary amount of cells was calculated (see section 6.2.3.4). Table 6.22 gives the parameters of this assay.

In short, a 96 well plate was pipetted with 20 μL of the compounds at different concentrations between 100 nmol · L^{-1} and 100 μmol · L^{-1}. After addition of 160 μL of a cell suspension containing the necessary amount of cells per well, the plate was pre-incubated for 15 minutes at 37 °C and CO_2-humidified. Afterwards, 20 μL of a 30 μmol · L^{-1} solution of daunorubicin was added followed by a second incubation period. The plate was evaluated in a flow-cytometer.

Table 6.22. Summary of important parameters for the daunorubicin assay for MRP1.

daunorubicin assay	**parameter**
cell lines and cells per well (transporter)	H69AR, 60,000 (MRP1) H69, 60,000 MDCKII MRP1, 60,000 (MRP1) MDCK II, 60,000
compound dilution	20 μL
cell suspension volume per well	160 μL
pre-incubation and conditions	15 min, 37 °C, CO_2-humidified atmosphere
daunorubicin and final concentration	20 μL of 30 μmol · L^{-1} stock final: 3 μmol · L^{-1}
incubation time	180 min, 37 °C, CO_2-humidified atmosphere
analytical instrument and instrument parameter	fluorescence-activated cell sorting resuspension of cells before measurement 488 nm excitation wavelength ≥ 670 nm emission wavelength (FL3 channel)

The amount of fluorescence is a function of the degree of inhibition of MRP1. The linearity with respect to used daunorubicin concentrations can be seen in Figure 6.13. Plotting of the measured fluorescence values and the logarithmic corresponding compound concentration gave sigmoidal concentration-effect curves, which were analyzed by nonlinear regression,

using GraphPad Prism (four-parameter logistic equation with either variable Hill slope (4 parameter model) or Hill slope = 1 (three parameter model); see section 6.3.2.2). In case of transport activation, the intracellular fluorescence was decreased in comparison to the basal value (no compound supplementation). In this case the sigmoidal curve was evaluated with respect to the AC_{50} value and A_{max} value (as shown in Table 4.13 B).

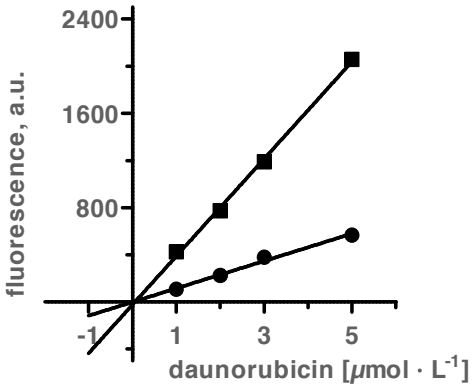

Figure 6.13. Linearity between effect value (measured fluorescence) and used daunorubicin concentration in fully activated state (by compound **101** at 10 nmol · L^{-1}; closed circles) and fully inhibited state (by compound **74** at 10 μmol · L^{-1}; closed squares). Shown is a representative experiment out of at least three independent experiments.

6.2.4.4. Pheophorbide A Assay

6.2.4.4.1. General Information

The pheophorbide A assay was performed as already stated in the literature[317,337,367,368] by Katja Stefan via flow cytometry. In short, the chlorophyll breakdown product pheophorbide A is a substrate of BCRP, which diffuses passively through the membrane and becomes effluxed by BCRP. Inhibition of BCRP increases the presence of pheophorbide A inside the cell and therefore increases the measured fluorescence. Figure 6.14 gives a simplified overview.

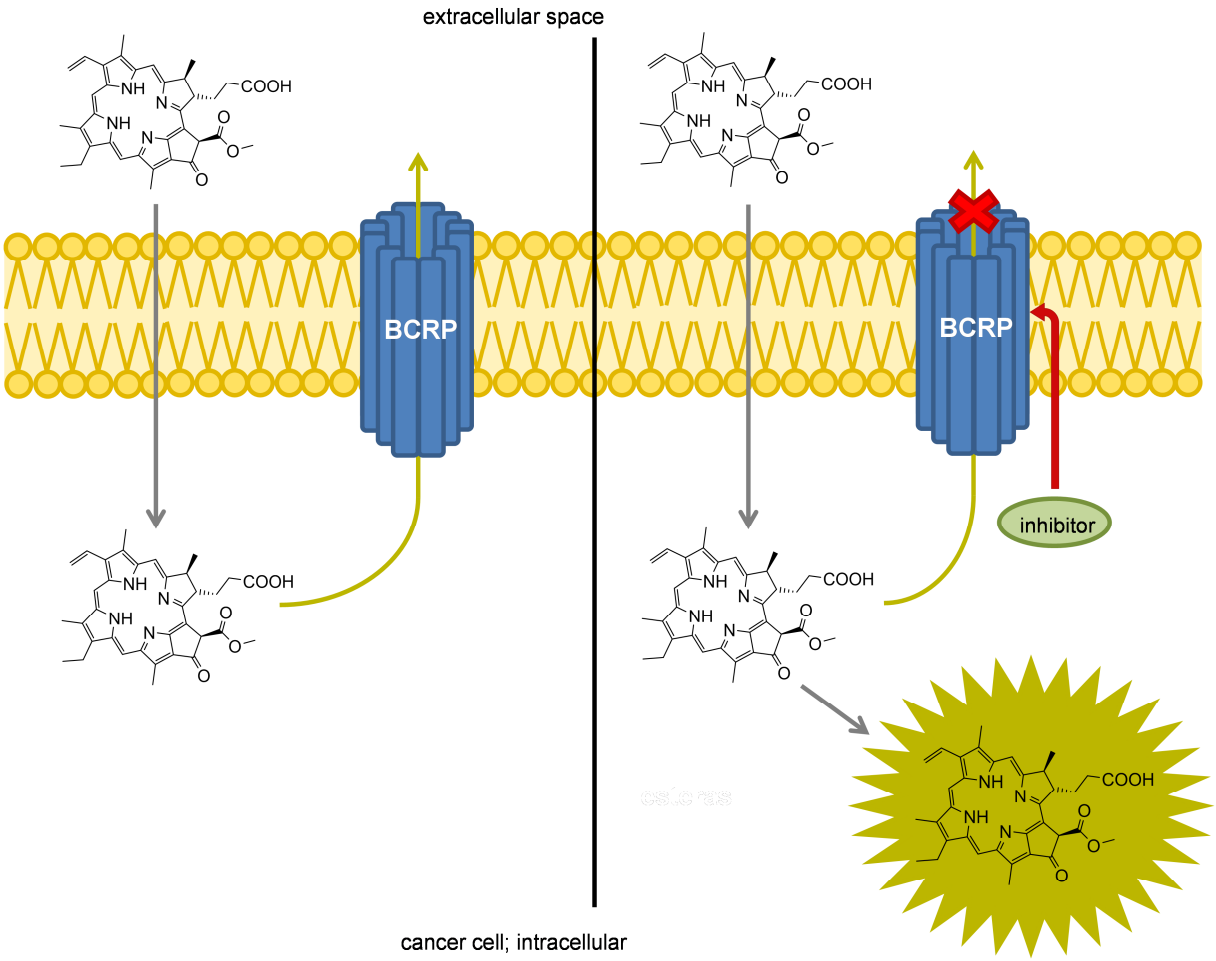

Figure 6.14. Summary of the pheophorbide A assay. While this fluorescence dye can easily diffuse passively through the cell membrane, pheophorbide A gets effluxed by BCRP (left). In analogy to the daunorubicin assay, BCRP inhibition leads to increased intracellular fluorescence (right).

6.2.4.4.2. General Procedure

In short, the cell suspension was prepared as described above (see section 6.2.3.2) and the necessary cell amount determined (see section 6.2.3.4). Table 6.23 shows the most important parameters of this assay.

In short, a 96 well plate was pipetted with 20 μL of compound at different concentrations between 100 nmol · L^{-1} and 100 μmol · L^{-1}. After addition of 160 μL of a cell suspension containing the necessary amount of cells per well, the plate was pre-incubated for 20 minutes at 37 °C and CO_2-humidified atmosphere. Afterwards, 20 μL of a 5 μmol · L^{-1} solution of pheophorbide A was added followed by a second incubation period. The plate was evaluated in a flow-cytometer.

Table 6.23. Summary of important parameters for the pheophorbide A assay for BCRP.

pheophorbide A assay	parameter
cell lines and cells per well (transporter)	MDCK II BCRP, 45,000 (BCRP) MDCK II, 45,000
compound dilution	20 μL
cell suspension volume per well	160 μL
pre-incubation and conditions	20 min, 37 °C, CO_2-humidified atmosphere
pheophorbide A and final concentration	20 μL of 5 μmol · L^{-1} stock final: 0.5 μmol · L^{-1}
incubation time	120 min, 37 °C, CO_2-humidified atmosphere
analytical instrument and instrument parameter	fluorescence-activated cell sorting resuspension of cells before measurement 488 nm excitation wavelength ≥ 670 nm emission wavelength (FL3 channel)

The amount of fluorescence reflects the degree of BCRP inhibition. The measured intracellular fluorescence and the logarithmic corresponding compound concentration can be plotted against each other, resulting in sigmoidal concentration-effect curves that were analyzed by nonlinear regression using GraphPad Prism. The four-parameter logistic equation with either variable hill slope (4 parameter model) or Hill slope = 1 (three parameter model; see section 6.3.2.2), were used whichever was statistically preferred. Transport activation would lead to decreased intracellular fluorescence in comparison to basal transport velocity (no compound supplementation).

6.2.4.5. MTT-viability Assay

6.2.5.5.1. General Information

Intrinsic toxicity is an important value for the evaluation of a compound, e.g. for clinical purpose or calculation of the therapeutic ratio. Due to several reasons xenobiotics can lead to reduced cell growth and enhanced cell death. Dead cells contain no functional mitochondria. Reductase enzymes located in mitochondria can reduce the tetrazole ring system of MTT to the blue colored formazan. From the magnitude of formazan production

the cell viability and half-maximal growth inhibition value (GI_{50}) can be deduced.[369] Figure 6.15 shows a simplified view of the reaction.

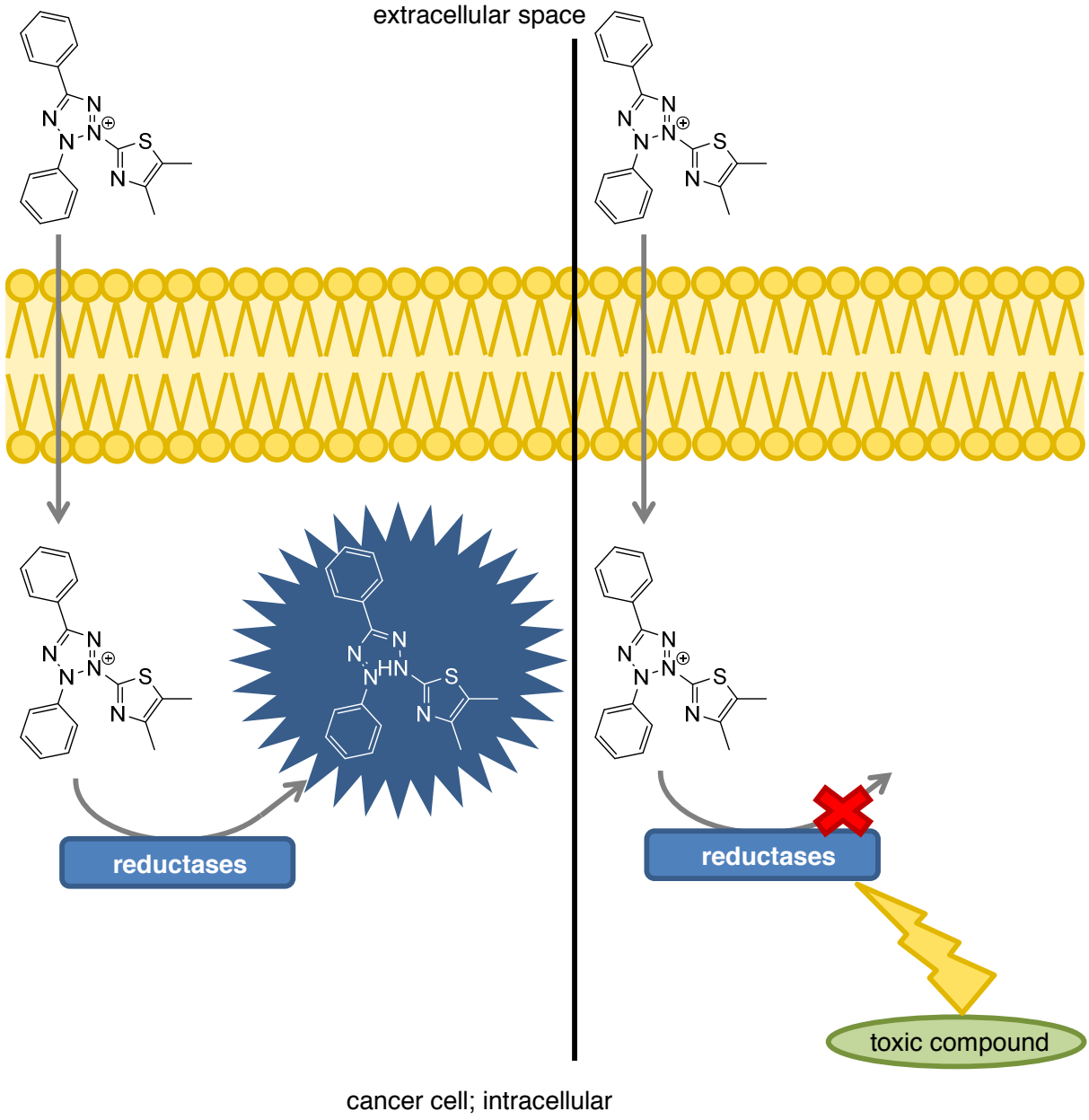

Figure 6.15. Principle of the MTT-viability assay. MTT diffuses passively through the membrane and becomes reduced by intra-mitochondrial reductases to the blue coloured formazane. Dead cells are not able to do so, which allows an evaluation of the influence of compounds on the cell viability.

6.2.5.5.2. General Procedure

The assay was performed as already reported in the literature[359,369,370] by Katja Stefan. The serial dilution of the compounds was performed with cell culture medium. Table 6.24 summarizes the main parameter of this assay.

In short, a 96 well plate was pipetted with 20 μL of compound at different concentrations between 100 nM and 100 μM. 180 μL of a cell suspension containing the necessary amount of cells per well was added followed by an incubation period of 72 hours at 37 °C and CO_2-humidified atmosphere. After that, 40 μL of a 0.015 μmol · L^{-1} solution of MTT was added per well. The plate was incubated a second time for 60 minutes at 37 °C and CO_2-humidified atmosphere. The supernatant was removed and 100 μL of DMSO was added. Colorimetric measurement of the absorbance of the built formazan followed.

Table 6.24. Summary of important parameters for the MTT-viability assay.

MTT-viability assay	**parameter**
cell lines and cells per well (transporter)	H69AR, 20,000 (MRP1) H69, 20,000 MDCKII MRP1, 3,000 (MRP1) MDCK II, 3,000 2008/MRP1, 8,000 (MRP1) 2008, 8,000 A2780/ADR, 8,000 (P-gp) A2780, 8,000 MDCK II BCRP, 3,000 (BCRP)
compound dilution	20 μL
cell suspension volume per well	180 μL
first incubation and conditions	72 h, 37 °C, CO_2-humidified atmosphere
MTT	40 μL of 0.015 μmol · L^{-1} stock final: 0.003 μmol · L^{-1}
incubation time and further process	60 min, 37 °C, CO_2-humidified atmosphere followed by supernatant removal and addition of 100 μL DMSO
analytical instrument and instrument parameter	microplate photometer 570 nm absorbance wavelength 690 nm background correction

6.2.4.6. MDR reversal-efficacy Assay

6.2.5.5.1. General Information

One major measure of compound evaluation is the possibility of the compounds to sensitize MDR cells. In principle, the assay equals the MTT-viability assay. But additionally, an anticancer agent is present. If a compound is a good inhibitor of the corresponding transport protein, the intracellular concentration of the antineoplastic drug is increased, resulting in enhanced cell death. As already stated in the MTT-viability assay, cell death can be deduced from the lack of formazan production by the cells. Figure 6.16 gives a simplified picture of the principle reactions.

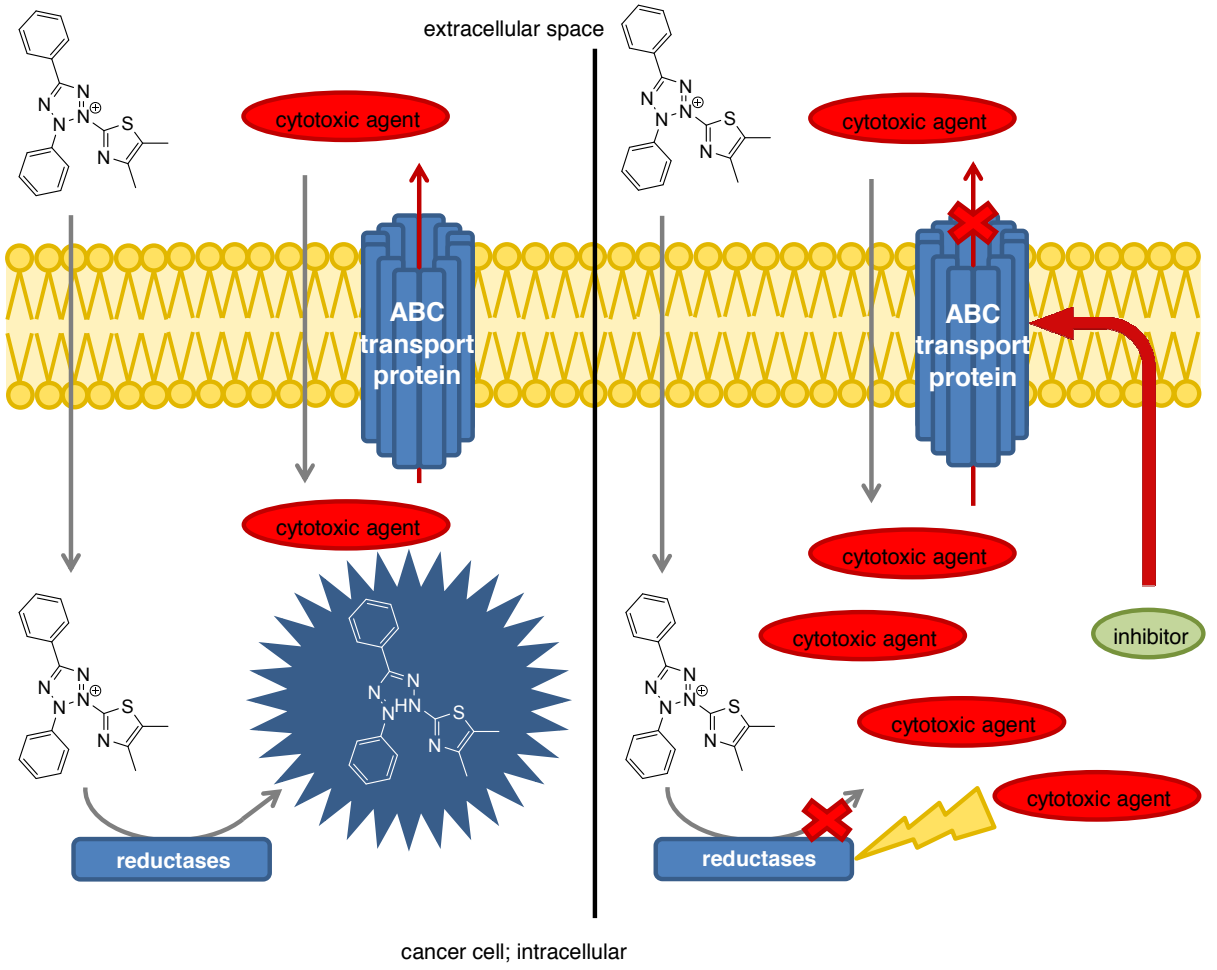

Figure 6.16. Summary of the prevailing processes of the MDR reversal-efficacy assay. The antineoplastic drug (red) diffuses passively through the membrane and gets effluxed by a transport protein. In case of inhibition of the transporter, the cytotoxic agent accumulates intracellularly (right). The degree of cell death is reflected in the amount of built formazan mediated by intra-mitochondrial reductases as already stated in 6.2.4.5.

6.2.5.5.2. General Procedure

Table 6.25 summarizes the parameters used in the MDR reversal-efficacy assay, which was performed by Katja Stefan. The main difference to the MTT-viability assay is the presence of an antineoplastic compound.

In short, a 96 well plate was pipetted with 20 μL of compound at specific concentrations, mostly 0.1, 1, 5 and 10 μmol · L^{-1}. 160 μL of a cell suspension containing the necessary amount of cells was added. Additionally, 20 μL of a dilution series of the corresponding cytotoxic agent was added to the wells. An incubation period of 72 hours at 37 °C and CO_2-humidified atmosphere followed. After that, 40 μL of a 0.015 μmol · L^{-1} solution of MTT was added per well. The plate was incubated a second time for 60 minutes at 37 °C and CO_2-humidified atmosphere. The supernatant was removed and 100 μL of DMSO was added to each well. Colorimetric measurement of the absorbance of the formed formazan followed.

Table 6.25. Summary of important parameters for the MDR reversal-efficacy assay

MDR reversal-efficacy assay	parameter
cell lines and cells per well (transporter)	H69AR, 20,000 (MRP1) H69, 20,000 MDCK II MRP1, 3,000 (MRP1) A2780/ADR, 8,000 (P-gp) A2780, 8,000 MDCK II BCRP, 3,000 (BCRP) MDCK II, 3,000
compound (1,10,50 and 100 μmol · L^{-1})	20 μL
cell suspension volume per well	160 μL
dilution of antineoplastic drug	20 μL of daunorubicin (MRP1 and P-gp) 20 μL of SN-38 (BCRP)
first incubation and conditions	72 h, 37 °C, CO_2-humidified atmosphere
MTT	40 μL of 0.015 μmol · L^{-1} stock final: 0.003 μmol · L^{-1}
incubation time and further process	60 min, 37 °C, CO_2-humidified atmosphere followed by supernatant removal and addition of 100 μL DMSO
analytical instrument and instrument parameter	microplate photometer 570 nm absorbance wavelength 690 nm background correction

6.3. Mathematical Operations

6.3.1. Statistical Values

6.3.1.1. Average ($\bar{x}$)

$$\bar{x} = \frac{\sum_{i=1}^{n} x_i}{n}$$

Equation 6.1. Basic mathematical equation for determination of the arithmetic mean; x_i = measured value; n = sample size.

6.3.1.2. Standard Error of the Mean (SEM)

$$SEM = \frac{\sqrt{\sum_{i=1}^{n}(x_i - \bar{x})^2}}{n}$$

Equation 6.2. Basic mathematical equation for determination of the standard error of the mean. $\bar{x}$ = arithmetic mean (see 6.3.1.1 and Equation 6.1); x_i = measured value; n = sample size.

6.3.1.3. One-sample *t*-Test

The one-sample *t*-test compares the mean of a measurement with a hypothetical value. In this thesis, this hypothetical value was defined as basal transport velocity in presence of DMSO (see Figures 4.17 and 4.18 A-B). From the formula below, GraphPad Prism calculated a P value dependent on the degree of freedom, which is defined as sample size minus one. The resultant significance is given as *: P ≤ 0.05, **: P ≤ 0.01, ***: P ≤ 0.001, ****: P ≤ 0.0001.

$$t = \frac{\bar{x}_{sample} - \bar{x}_{hypothetical}}{SEM}$$

Equation 6.3. Basic mathematical equation to perform the one-sample *t*-test; $\bar{x}_{\text{sample}}$ = arithmetic mean of the sample; $\bar{x}_{\text{hypothetical}}$ = arithmetic mean of the reference; SEM = standard error of the mean.

6.3.2. Regression

6.3.2.1. Linear Regression

The basic function of linear regression is as follows:

$$y = a \cdot x + b$$

Equation 6.4. Mathematical basis behind linear regression; a = slope; b = Y-intercept.

6.3.2.2. Nonlinear Regression of Concentration-Effect curves

For compound evaluation the logistic equation was used, either with variable slope or with standard slope (Hill slope = 1). The equation can be seen below (Eq. 6.5).

$$y = \text{bottom} + \frac{(top - bottom)}{1 + 10^{(\log(EC_{50}) - \log[c]) \cdot n_H)}}$$

Equation 6.5. Four-parameter logistic equation. y represents the measured fluorescence value in arbitrary units. The bottom and top value is defined as the intra- and extrapolation of the calculated sigmoidal concentration-effect curve. The EC_{50} value represents the inflection of the sigmoidal concentration-effect curve and is the half-maximal effect between bottom and top. In case of inhibition, it is called half-maximum inhibition concentration (IC_{50}); in case of activation, it is called half-maximal activation concentration (AC_{50}); in case of growth inhibition (MTT-viability or MDR reversal-efficacy assays) it is called half-maximal growth inhibition concentration (GI_{50}). n_H represents the Hill slope. Four-parameter model: n_H variable; three-parameter model: $n_H = 1$.

All standard inhibitors and synthesized target compounds were evaluated with respect to their Hill slope. Statistical analysis showed that most yielded concentration-effect curves with slopes not significantly different from one, which indicates a 1:1 reaction between transport protein and inhibitor. The only exceptions were cyclosporine A, MK571 and ONO-1078.

6.3.2.3. Logit Transformation

Inhibitory activity was always correlated to the logit of the I_{max} value of the screening results of the corresponding compound. The logit function can be expressed as inversed concentration-effect curves according to the logistic equation as was stated above (see section 6.3.2.2).

$$\text{logit} = \log\left(\frac{effect\ value\ [\%]}{100 - effect\ value\ [\%]}\right)$$

Equation 6.6. Mathematical basis behind the logit transformation. The effect value was taken as expressed percentage from screening experiments referred to a standard compound at a specific concentration.

6.3.3. Calculation of the Maximal Inhibition Level (I_{max})

The I_{max} value represents the maximal inhibition of a calculated concentration-effect curve in comparison to a standard compound. In this thesis, compound **126** was used in the calcein AM assay to define 100% inhibition. 0% inhibition is defined by the point without compound supplementation (basal transport velocity). The used equation to determine the I_{max} value is given below.

$$I_{max} = \frac{(top_{compound} - bottom_{compound})}{(top_{standard\ inhibitor} - bottom_{standard\ inhibitor})} \cdot 100$$

Equation 6.7. Calculation of the maximal inhibition level in the calcein AM assay. Numerator: response of the evaluated compound. Denominator: response of the standard inhibitor. In case of the calcein AM assay, compound **126** was used as 100% control, while compound **74** was the 50% control.

6.3.4. Calculation of Transport Velocity-related Values

6.3.4.1. Calculation of the Flux Ratio (Pump Rate)

Assuming first order kinetics, the influx or efflux velocity of a substrate (in this thesis a cytotoxic agent or fluorescence dye) can be expressed as the product of substrate concentration and velocity constant (Eq. 6.8 A).

$$v = k \cdot c$$

Equation 6.8 A. Influx or efflux velocity (v) of a substrate described as the product of the velocity constant (k) and the used concentration of the substrate (c).

Considering both, passive and active transport, under steady state conditions the simultaneous process of influx and efflux can be expressed as shown in equation 6.8 B.

$$v_{p,out} = v_{p,in} + v_{a,in}$$

Equation 6.8 B. Under steady state conditions the passive influx velocity ($v_{p,out}$) equals the sum of passive ($v_{p,in}$) and active ($v_{a,in}$) efflux; out = from outside to inside the cell; in = from inside to outside the cell.

Combining Equations 6.8 A and B yields Equation 6.8 C.

$$k_p \cdot c_{out} = (k_p + k_a) \cdot c_{in}$$

Equation 6.8 C. Under steady state conditions the passive influx expressed as product of the velocity constant of passive diffusion through the cell membrane (k_p) and the extracellular concentration (c_{out}) equals the sum of passive (k_p) and active (k_a) efflux velocity constants multiplied with the intracellular concentration (c_{in}).

Equation 6.8 C can be rearranged giving the flux ratio, also called pump rate. This value represents the ratio of active efflux to passive diffusion. It can also be expressed as the ratio between intra- and extracellular concentration. Equation 6.8 D gives the derivation of the relationship.

$$\frac{(k_a + k_p)}{k_p} = \frac{c_{out}}{c_{in}} \quad \rightarrow \quad \frac{k_a}{k_p} = \frac{c_{out}}{c_{in}} - 1 \quad or \quad \frac{c_{in}}{c_{out}} = \frac{k_p}{(k_a + k_p)} \quad \rightarrow \quad \frac{c_{in}}{c_{out}} = \frac{k_{in}}{k_{out}}$$

Equation 6.8 D. Calculation of the flux ratio (pump rate) as the division of extra- and intracellular concentration of the used substrate minus one; $k_{out} = k_a + k_p$.

This mathematical relationship between active efflux and passive diffusion can also be graphically presented as a hyperbolic relationship (Figure 6.17). It is in agreement with findings with respect to specific anthracyclines, where cancer cells were less resistant to more lipophilic compounds with higher diffusion velocity.[371] Since the intracellular calcein and daunorubicin concentration correlated with the measured fluorescence over a wide concentration range as shown in Figures 6.10 A-B and 6.13, the calculated bottom and top value of a sigmoidal concentration-effect curve can be taken as surrogates for c_{in} and c_{out}. At low k_{out}, small changes in the pump velocity lead to significant reduction of intracellular concentrationon of the substrate or fluorescence dye. In resistant cells (e.g. H69AR), a high active efflux (k_a) is already present, which makes a strong increase in the pump velocity necessary for a noticeable further decrease of the intracellular concentration of the substrate or fluorescence dye.

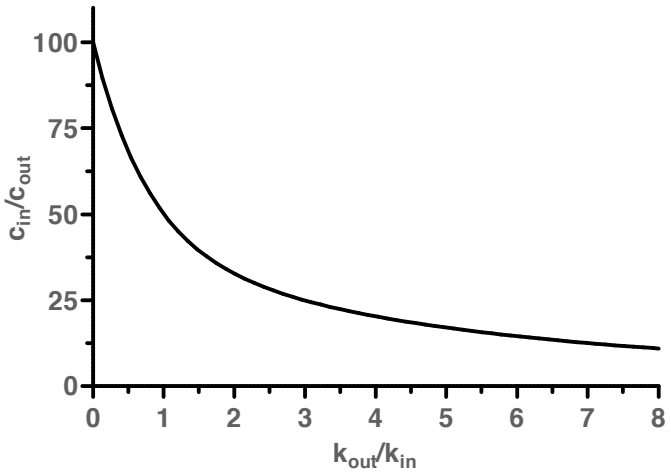

Figure. 6.17. Hyperbolic relationship between active and passive transport (k_{out}/k_{in}) and ratio of intra- (c_{in}) and extracellular (c_{out}) substrate concentration.

6.3.4.2. Calculation of the Activation Ratio (A_r)

The activation ratio is the ratio between the flux ratio of a compound and the standard inhibitor **126** (or 2 times the flux ratio of compound **74**) in the calcein AM assay or both compounds with equal magnitude in the daunorubicin assay and is calculated according to Equation 6.9.

$$activation\ ratio = \frac{flux\ ratio_{compound}}{flux\ ratio_{standard\ inhibitor}} = \frac{(\frac{top_{standard\ inhibitor}}{bottom_{compound}} - 1)}{(\frac{top_{standard\ inhibitor}}{bottom_{standard\ inhibitor}} - 1)}$$

Equation 6.9. Calculation of the activation ratio of a compound in comparison to standard inhibitors **74** or **126**.

6.3.5. Calculation of the Selectivity Ratio (sr)

The selectivity ratio gives the factor by which an inhibitor is more potent toward one target. It is calculated by division of the IC_{50} value of both targets.

$$\mathrm{sr} = \frac{IC_{50\ (target\ A)}}{IC_{50\ (target\ B)}}$$

Equation 6.10. Calculation of the selectivity ratio (sr).

6.3.6. Calculation of the Therapeutic Ratio (tr)

The therapeutic ratio gives the factor by which the tested compound is more potent toward a target than toxic toward the cells. It can easily be calculated by division of the corresponding half-maximal growth inhibition value (GI_{50}) and the determined half-maximal inhibitory concentration (IC_{50}).

$$\mathrm{tr} = \frac{GI_{50\ (compound)}}{IC_{50\ (compound)}}$$

Equation 6.11. Calculation of the therapeutic ratio (tr).

6.3.7. Calculation of the Resistance Factor (rf)

The resistance factor gives the ratio between the GI_{50} value of a compound toward the sensitive and resistant cell line. It is determined by division of the GI_{50} of the corresponding antineoplastic agents in the resistant cell line and the GI_{50} of the sensitive cell line.

$$\mathrm{rf} = \frac{GI_{50\ (resistant\ cell\ line)}}{GI_{50\ (sensitive\ cell\ line)}}$$

Equation 6.12. Calculation of the resistance factor (rf).

6.3.8. Calculation of the Potentiation Factor (pf)

The potentiation factor gives the factor by which a compound (e.g. inhibitor of a transporter) enhances sensitivity toward an antineoplastic drug. It is defined as the division of the GI_{50} of the cytotoxic agent in the resistant cell line and the GI_{50} of the same cytotoxic agent in combination with an inhibitor.

$$\mathrm{pf} = \frac{GI_{50\ (resistant\ cell\ line)}}{GI_{50\ (resistant\ cell\ line\ in\ combination\ with\ compound)}}$$

Equation 6.13. Potentiation factor (pf) as calculated using a resistant cell line.

6.3.9. Calculation of the Degree of Sensitization (°s)

The degree of sensitization (°s) is the ratio between potentiation factor of the compound at a specific concentration and the resistance factor of the resistant cell line. It gives the percentage of how much the cells have been sensitized compared to the maximal resistance.

$$°s = \frac{pf_{(resistant\ cell\ line\ with\ compound)}}{rf_{(resistant\ cell\ line\ without\ compound)}}$$

Equation 6.13. Potentiation factor (pf) as calculated using a resistant cell line.

6.3.10. Kinetic Evaluations

6.3.10.1. Lineweaver-Burk

The double-reciprocal plot of Lineweaver-Burk is based on the Michaelis-Menten kinetic as depicted below:

$$v = \frac{V_{max} \cdot [S]}{K_m + [S]}$$

Equation 6.14. Michaelis-Menten equation.

Inverting of equation 6.14. gives the Lineweaver-Burk equation.

$$\frac{1}{v} = \frac{K_m}{V_{max}} \cdot \frac{1}{[S]} + \frac{1}{V_{max}}$$

Equation 6.15. Double-reciprocal Lineweaver-Burk equation.

Four basic types of inhibition are present: competitive, noncompetitive, mixed-type or uncompetitive inhibition. In case of the first, the intersection of lines is on the ordinate. This means that V_{max} remains constant while K_m increases, which equals a lowered affinity of the substrate toward the target protein caused by competition with the inhibitor. In case of noncompetitive inhibition, the V_{max} value decreases while the substrate affinity (K_m) remains

constant. This can be seen by an intersection on the negative abscissa. A mixed-type inhibitor gives a mixture of both and can be explained by a compound that interacts with two binding sites, where one is the same as for the substrate. The intersection in this case is in the upper left quadrant of the coordinate system. A rare case is uncompetitive inhibition, which is indicated by parallel lines. This occurs rarely and was not observed in this thesis. Additionally, nonessential activation can occur, which can be seen as noncompetitive or mixed-type activation of the enzyme. The latter case occurs with activators that also have an inhibitory property. One must be aware that these kinetical equations are limited to enzymatic systems, and transporters are different from those proteins.

6.3.10.2. Hanes-Woolf

Rearrangement and inversion of the Michaelis-Menten equation (6.14) results in the Hanes-Woolf equation.

$$\frac{[S]}{v} = \frac{[S]}{V_{max}} + \frac{K_m}{V_{max}}$$

Equation 6.16. Hanes-Woolf equation.

A competitive inhibition type can be recognized by parallel lines. A noncompetitive inhibition is indicated by an intersection of the lines at the negative abscissa.

6.3.10.3. Cornish-Bowden

Rearrangement and inversion of the Michaelis-Menten equation (6.14) results in the basic mathematical coherence of Cornish-Bowden.

$$\frac{1}{V_{max}} = \frac{1}{v} - \frac{K_m}{V_{max} \cdot [S]}$$

Equation 6.17. Cornish-Bowden equation.

7. References

[1] Mutschler, E.; Geisslinger, G.; Kroemer, H. K.; Ruth, P.; Schäfer-Korting, M. Mutschler Arzneimittelwirkungen. Lehrbuch der Pharmakologie und Toxikologie. *WVG Suttgard mbH* **2008**, *9th edition*, 907-950.

[2] Lüllmann, H.; Mohr, K.; Hein, L. Pharmakologie und Toxikologie. Arzneimittelwirkungen verstehen – Medikamente gezielt einsetzen. *Theime Verlag* **2006**, *16th edition*, 418-432.

[3] Steinhilber, D.; Schubert-Zsilavecz, M.; Roth, H. J. Medizinische Chemie. Targets. Arzneistoffe. Chemische Biologie. *DAV* **2010**, *2nd edition*, 461-517.

[4] Bellamy, W. T.; Dalton, W. S.; Dorr, R. T. The Clinical Relevance of Multidrug Resistance. *Cancer Invest.* **1990**, *8*, 5, 547-562.

[5] Szakacs, G.; Paterson, J. K.; Ludwig, J. A.; Booth-Genthe, C.; Gottesman, M. M. Targeting Multidrug Resistance in Cancer. *Nat. Rev. Drug. Discov.* **2006**, *5*, 219-234.

[6] Gottesman, M. M.; Fojo, T.; Bates, S. E. Multidrug Resistance in Cancer: Role of ATP-Dependent Transporters. *Nat. Rev. Cancer* **2002**, *2*, 48-58.

[7] Dean, M.; Rzhetsky, A.; Allikmets, R. The Human ATP-Binding Cassette (ABC) Transporter Superfamily. *Genome Res.* **2001**, *11*, 7, 1156-1166.

[8] George, A. M. ABC Transporters – 40 Years on. *Springer* **2016**.

[9] Westlake, C. J.; Cole, S. P. C.; Deeley, R. G. Role of the NH2-terminal Membrane Spanning Domain of Multidrug Resistance Protein 1/ABCC1 in Protein Processing and Trafficking. *Mol. Biol. Cell* **2005**, *16*, 2483-2492.

[10] Gao, M.; Yamazaki, M.; Loe, D. W.; Westlake, C. J.; Grant, C. E. G.; Cole, S. P. C.; Deeley, R. G. Multidrug Resistance Protein. Identification of Regions Required for Active Transport of Leukotriene C4. *J. Biol. Chem.* **1998**, *17*, 10733-10740.

[11] Conseil, G.; Deeley, R. G.; Cole, S. P. C. Role of Two Adjacent Cytoplasmic Tyrosine Residues in MRP1 (ABCC1) Transport Activity and Sensitivity to Sulfonylureas. *Biochem. Pharmacol.* **2005**, *69*, 451-461.

[12] Ito, K.-I.; Olsen, S. L.; Qiu, W.; Deeley, R. G.; Cole, S. P. C. Mutation of a Single Conserved Tryptophan in Multidrug Resistance Protein 1 (MRP1/ABCC1) Results in Loss of Drug Resistance and Selective Loss of Organic Anion Transport. *J. Biol. Chem.* **2001**, *19*, 15616-15624.

[13] Koike, K.; Oleschuk, C. J.; Haimeur, A.; Olsen, S. L.; Deeley, R. G.; Cole, S. P. C. Multiple Membrane-associated Tryptophan Residues Contribute to the Transport Activity and Substrate Specifity of the Human Multidrug Resistance Protein, MRP1. *J. Biol. Chem.* **2002**, *51*, 49495-49503.

[14] Leslie, E. M.; Létourneau, I. J.; Deeley, R. G.; Cole, S. P. C. Functional and Structural Consequences of Cysteine Substitutions in the NH2 Proximal Region of the Human Multidrug Resistance Protein 1 (MRP1/ABCC1). *Biochem. J.* **2003**, *42*, 5214-5224.

[15] Qin, L.; Tam, S.-P.; Deeley, R. G. Effect of Multiple Cysteine Substitutions on the Functionality of Human Multidrug Resistance Protein 1 Expressed in Human Embryonic Kidney 293 cells: Identification of Residues Essential for Function. *Drug Metab. Dispos.* **2012**, *40*, 1403-1413.

[16] Zhang, D.-W.; Gu, H.-M.; Situ, D.; Haimeur, A.; Cole, S. P. C. Deeley, R. G.; Functional Importance of Polar and Charged Amino Acid Residues in Transmembrane Helix 14 of Multidrug Resistance Protein (MRP1/ABCC1). *J. Biol. Chem.* **2003**, *46*,46052-46063.

[17] Haimeur, A.; Conseil, G.; Deeley, R. G.; Cole, S. P. C. Mutations of Charged Amino Acids in or Near the Transmembrane Helices of the Second Membrane Spanning Domain Differentially Affect the Substrate Specificity and Transport Activity of the Multidrug Resistance Protein MRP1 (ABCC1). *Mol. Pharmacol.* **2004**, *65,* 1375-1385.

[18] Flens, M. J.; Zaman, G. J. R.; van der Valk, Paul, Izquierdo, M. A.; Schroeijers, A. B.; Scheffer, G. L.; van der Groep, P.; de Haas, M.; Meijer, C. J. L. M.; Scheper, R. J. Tissue Distribution of the Multidrug Resistance Protein. *Am. J. Pathol.* **1996**, *148*, 1237-1247.

[19] Kunicka, T.; Soucek, P. Importance of ABCC1 for Cancer Therapy and Prognosis. *Drug. Metab. Rev.* **2014**, *46*, 325-342.

[20] Young, L. C.; Campling, B. G.; Voskoglou-Nomikos, T.; Cole, S. P. C.; Deeley, R. G.; Gerlach, J. H. Expression of Multidrug Resistance Protein-related Genes in Lung Cancer: Correlation with Drug Response. *Clin. Cancer Res.* **1999**, *5*, 673-680.

[21] Young, L. C.; Campling, B. G.; Cole, S. P. C.; Deeley, R. G.; Gerlach, J. H. Multidrug Resistance Proteins MRP3, MRP1, and MRP2 in Lung Cancer: Correlation of Protein Levels with Drug Response and Messenger RNA Levels. *Clin. Cancer Res.* **2001**, *7*, 1798-1804.

[22] Cole, S. P. C. Targeting Multidrug Resistance Protein 1 (MRP1, ABCC1): Past, Present, and Future. *Annu. Rev. Pharmacol. Toxicol.* **2014**, *54*, 95-117.

[23] Nooter, K.; Westerman, A. M.; Flens, M. J.; Zaman, G. J. R.; Scheper, R. J.; van Wingerden, K. E.; Burger, H.; Oostrum, R.; Boersma, T.; Sonnenveld, P.; Gratama, J. W.; Kok, T.; Eggermont, A. M. M.; Bosman, F. T.; Stoter, G. Expression of the Multurdrug Resistance-associated Protein (*MRP*) Gene in Human Cancers. *Clin. Cancer Res.* **1995**, *1*, 1301-1310.

[24] Kruh, G. D.; Gaughan, K. T.; Godwin, A.; Chan, A. Expression Pattern of MRP in Human Tissues and Adult Solid Tumor Cell Lines. *J. Natl. Cancer Inst.* **1995**, *87*, 1256-1260.

[25] Lu, J. F.; Pokharel, D.; Bebawy, M. MRP1 and Its Role in Anticancer Drug Resistance. *Drug Metab. Rev.* **2015**, *47*, 4, 406-419.

[26] Zaman, G. J. R.; Flens, M. J.; van Leusden, M. R.; de Haas, M.; Muelder, H. S.; Lankelma, J.; Pinedo, H. M.; Scheper, R. J.; Baas, F.; Broxterman, H. J.; Borst, P. The Human Multidrug Resistance-associated Protein MRP Is a Plasma Membrane Drug-efflux Pump. *Proc. Natl. Acad. Sci. U.S.A.* **1994**, *91*, 8822-8826.

[27] Leier, I.; Jedlitschky, G.; Buchholz, U.; Cole, S. P. C.; Deeley, R. G.; Keppler, D. The *MRP* Gene Encodes an ATP-dependent Export Pump for Leukotriene C_4 and Structurally Related Conjungates. *J. Biol. Chem.* **1994**, *45*, 27807-27810.

[28] Jedlitschky, G.; Leier, I.; Buchholz, U.; Barnouin, K.; Kurz, G.; Keppler, D. Transport of Glutathione, Glucuronate, and Sulfate Conjungates by the *MRP* Gene-encoded conjungate Export Pump. *Cancer Res.* **1996**, *56*, 988-994.

[29] Jedlitschky, G.; Leier, I.; Buchholz, U.; Center, M.; Keppler, D. ATP-dependent Transport of Glutathione S-conjungates by the Multidrug Resistance-associated Protein. *Cancer Res.* **1994**, *54*, 4833-4836.

[30] Priebe, W.; Krawczyk, M.; Kuo, M. T.; Yamane, Y.; Savaraj, N.; Ishikawa, T. Doxorubicin- and Daunorubicin-Glutathione Conjungates, but Not Unconjungated Drugs, Competitively Inhibit Leukotriene C_4 Transport Mediated by *MRP*/*GS-X* Pump. *Biochem. Biophys. Res. Comm.* **1998**, *247*, 859-863.

[31] Leier, I.; Jedlitschky, G.; Buchholz, U.; Center, M.; Cole, S. P. C.; Deeley, R. G.; Keppler, D. ATP-dependent Glutathione Disulphide Transport Mediated by the *MRP* Gene-encoded Conjungate Export Pump. *Biochem. J.* **1996**, *314*, 433-437.

[32] Hipfner, D. R.; Deeley, R. G.; Cole, S. P. C. Structural, Mechanistic and Clinical Aspects of MRP1. *Biochim. Biophys. Acta* **1999**, *1461*, 359-376.

[33] Cole, S. P. C. Multidrug resistance protein 1 (MRP1, ABCC1), a "Multitasking" ATP-binding Cassette (ABC) Transporter. *J. Biol. Chem.* **2014**, *289*, 30880-30888.

[34] Mirski, S. E. L.; Gerlach, J. H.; Cole, S. P. C. Multidrug Resistance in a Human Small Cell Lung Cancer Cell Line Selected with Adriamycin. *Cancer Res.* **1987**, *47*, 2594-2598.

[35] Grant, C. E.; Valdimarsson, G.; Hipfner, D. R.; Almquist, K. C.; Cole, S. P. C.; Deeley, R. G. Overexpression of Multidrug Resistance-associated Protein (MRP) Increases Resistance to Natural Product Drugs. *Cancer Res.* **1994**, *54*, 357-361.

[36] Cole, S. P. C.; Sparks, K. E.; Fraser, K.; Loe, D. W.; Grant, C. E.; Wilson, G. M.; Deeley, R. G. Pharmacological Characterization of Multidrug Resistant MRP-transfected Human Tumor Cells. *Cancer Res.* **1994**, *54*, 5902-5910.

[37] Grzywacz, M. J.; Yang, J.-M.; Hait, W. N. Effect of the Multidrug Resistance Protein on the Transport of the Antiandrogene Flutamide. *Cancer Res.* **2003**, *63*, 2492-2498.

[38] Hooijberg, J. H.; Broxterman, H. J.; Kool, M.; Assaraf, Y. G.; Peters, G. J.; Noordhuis, P.; Scheper, R. J.; Borst, P.; Pinedo, H. M.; Jansen, G. Antifolate Resistance Mediated by the Multidrug Resistance Proteins MRP1 and MRP2. *Cancer Res.* **1999**, *59*, 2532-2535.

[39] Pham, A.-N.; Wang, J.; Fang, J.; Gao, X.; Zhang, Y.; Blower, P. E.; Sadee, W.; Huang, Y. Pharmacogenomics Approach Reveals MRP1 (ABCC1)-mediated Resistance to Geldanamycins. *Pharm. Res.* **2009**, *26*, 4, 936-945.

[40] Zaman, G. J. R.; Lankelma, J.; Van Tellingen, O.; Beijnen, J.; Dekker, H.; Paulusma, C.; Oude Elferink, R. P. J.; Baas, F.; Borst, P. Role of Glutathione in the Export of Compounds from Cells by the Multidrug-resistance-associated Protein. *Proc. Natl. Acad. Sci. U. S. A.* **1995**, *92*, 7690-7694.

[41] Loe, D. W.; Almquist, K. C.; Delley. R. G.; Cole. S. P. C. Multidrug Resistance Protein (MRP)-mediated Transport of Leukotriene C4 and Chemotherapeutic Agents in Membrane Vesicles. *J. Biol. Chem.* **1996**, *271*, 16, 9675-9682.

[42] Rappa, G.; Lorico, A.; Flavell, R. A.; Sartorelli, A. C. Evidence That the Multidrug Resistance Protein (MRP) Functions as a Co-Transporter of Glutathione and Natural Product Toxins. *Cancer Res.* **1997**, *57*, 5232-5237.

[43] Loe, D. W.; Deeley, R. G.; Cole, S. P. C. Characterization of Vincristine Transport by the Mr190,000 Multidrug Resistance Protein (MRP): Evidence for Cotransport with Reduced Glutathione. *Cancer Res.* **1998**, *58*, 5130-5136.

[44] Renes, J.; De Vries, E. G. E. ; Nienhuis, E. F. ; Jansen, P. L. M. ; Müller, M. ATP- and Glutathione-dependent Transport of Chemotherapeutic Drugs by the Multidrug Resistance Protein MRP1. *Br. J. Pharmacol.* **1999**, *126*, 681-688.

[45] Morrow, C. S.; Peklak-Scot, C.; Bishwokarma, B.; Kute, T. E.; Smitherman, P. K.; Townsend, A. J. Multidrug Resistance Protein 1 (MRP1, ABCC1) Mediates Resistance to Mitoxantrone via Glutathione-dependent Drug Efflux. *Mol. Pharmacol.* **2006**, *69*, 1499-1505.

[46] Rothnie, A.; Conseil, G.; Lau, Y. T. ; Deeley, R. G. ; Cole, S. P. C. Mechanistic Differences between GSH Transport by Multidrug Resistance Protein 1 (MRP1/ABCC1) and GSH Modulation of MRP1-Mediated Transport. *Mol. Pharmacol.* **2008**, *74*, 1630-1640.

[47] Arrik, B. A.; Nathan, C. F. Glutathione Metabolism as a Determinant of Therapeutic Efficacy: A Review. *Cancer Res.* **1984**, *44*, 4224-4232.

[48] Lewis, A. D.; Hickson, I. D.; Robson, C. N.; Harris, A. L.; Hayes, J. D.; Griffiths, S. A.; Manson, M. M.; Hall, A. E.; Moss, J. E.; Wolf, C. R. Amplification of increased expression of alpha class glutathione *S*-transferase-encoding genes associated with resistance to nitrogen mustards. *Proc. Natl. Acad. Sci. U. S. A.* **1988**, *85*, 8511-8515.

[49] Barnouin, K.; Leier, I.; Jedlitschky, G.; Pourtier-Manzanedo, A.; König, J.; Lehmann, W.-D.; Keppler, D. Multidrug Resistance Protein-mediated Transport of Chlorambucil and Melphalan Conjungated to Glutathione. *Br. J. Cancer* **1998**, *77*, 2, 201-209.

[50] Dulik, D. M.; Frenselau, C.; Hilton, J. Characterization of Melphalan-glutathione Adducts whose Formation Is Catalyzed by Glutathione Transferases. *Biochem. Pharmacol.* **1986**, *35*, 19, 3409-3412.

[51] Ciaccio, P. J.; Tew, K. D.; LaCreta, F. P. The Spontaneous and Glutathione *S*-transferase-mediated Reaction of Chlorambucil with Glutathione. *Cancer commun.* **1990**, *2*, 8, 279-285.

[52] Meister, A. Glutathione Metabolism and Its Selective Modification. *J. Biol. Chem.* **1988**, *263*, 33,17205-17208.

[53] Meister, A. Selective Modification of Glutathione Metabolism. *Science* **1983,** *220*, 472-477.

[54] O'Brien, M.; Kruh, G. D.; Tew, K. D. The Influence of Coordinate Overexpression of Glutathione Phase II Detoxification Gene Products on Drug Resistance. *J. Pharmacol. Exp. Ther.* **2000**, *294*, 480-487.

[55] Juliano, R. L.; Ling, V. A Surface Glycoprotein Modulating Drug Permeability in Chinese Hamster Ovary Cell Mutants. *Biochim. Biophys. Acta*, **1976**, *455*, 152-162.

[56] Leonard, G. D.; Fojo, T.; Bates, S. E. The Role of ABC Transporters in Clinical Practise. *The Oncologist*, **2003**, *8*, 411-424.

[57] Eckford, P. D. W.; Sharom, F. J. ABC Efflux Pump-Based Resistance to Chemotherapy Drugs. *Chem. Rev.* **2009**, *109*, 2989-3011.

[58] Sharom, F. J. The P-glycoprotein Multidrug Transporter. *Essays Biochem.* **2011**, *50*, 161-178.

[59] Doyle, L. A.; Yang, W. Y.; Abruzzo, L. V.; Krogmann, T.; Gao, Y.; Rishi, A. K.; Ross, D. D. A Multidrug Resistance Transporter from Human MCF-7 Breast Cancer Cells. *Proc. Natl. Acad. Sci. USA*, **1998**, *95*, 15665-15670.

[60] Xu, J.; Liu, Y.; Yang, Y.; Bates, S.; Zhang, J.-T. Characterization of Oligomeric Human Half-ABC Transporter ATP-binding Cassette G2. *J. Biol. Chem.* **2004**, *279*, 19781-19789.

[61] McDevitt, C. A.; Collins, R. F.; Conway, M.; Modok, Szabolocs; Storm, J.; Kerr, I. D.; Fort, R. C.; Callaghan, R. Purification and 3D Structural Analysis of Oligomeric Human Multidrug Transporter ABCG2. *Structure* **2006**, *14*, 11, 1623-1632.

[62] Dezi, M.; Fribourgh, P.-F.; Di Cicco, A.; Arnaud, O. ; Marco, S.; Falso, P.; Di Pietro, A.; Levy, D. The Multidrug Resistance Half-transporter ABCG2 Is Purified as a Tetramer upon Selective Extraction from Membrane. *Biochim. Biophys. Acta* **2010**, *1798*, 2094-2101.

[63] Xu, J.; Peng, H.; Chen, Q.; Liu, Y.; Dong, Z.; Zhang, J.-T. Oligomerization Domain of the Multidrug Resistance-Associated Transporter ABCG2 and Its Dominant Inhibitory Activity. *Cancer Res.* **2007**, *67*, 9, 4373-4381.

[64] Soszynski, M.; Kaluzna, A.; Rychlik, B.; Sokal, A.; Bartosz, G. Radiation Interaction Suggests that Human Multidrug Resistance-Associated Protein 1 Occurs as a Dimer in the Human Erythrocyte Membrane. *Arch. Biochem. Biophys.* **1998**, *354*, 2, 311-316.

[65] Rosenberg, M. R.; Mao, Q.; Holzenburg, A.; Ford, R. C.; Deeley, R. G.; Cole, S. P. C. The Structure of the Multidrug Resistance Protein 1 (MRP1/ABCC1). Crystallization and Single-Particle Analysis. *J. Biol. Chem.* **2001**, *276*, 19, 16076-16082.

[66] Boscoboinik, D.; Debanne, M. T.; Stafford, A. R.; Jung, C. Y.; Gupta, R. S.; Epand, R. M. Dimerization of the P-glycoprotein in Membranes. *Biochim. Biophys. Acta* **1990**, *1027*, 225-228.

[67] Poruchynsky, M. S.; Ling, V. Detection of Oligomeric and Monomeric Forms of P-glycoprotein in Multidrug Resistant Cells. *Biochemistry* **1994**, *33*, 4163-4174.

[68] Jette, L.; Potier, M.; Beliveau, R. P-glycoprotein Is a Dimer in the Kidney and Brain Capillary Membranes: Effect of Cyclosporin A and SDZ-PSC 833. *Biochemistry* **1997**, *36*, 13929-13937.

[69] Diestra, J. E.; Scheffer, G. L.; Catala, I.; Maliepaard, M.; Schellens, J. H. M.; Scheper, R. J.; Germa-Lluch, J. R.; Izquirdo, M. A. Frequent expression of the Multi-drug Resistance-associated Protein BCRP/MXR/ABCP/ABCG2 in Human Tumours Detected by the BXP-21 Monoclonal Antibody in Paraffin-embedded Material. *J. Pathol.* **2002**, *198,* 213-219.

[70] Miwa, M.; Tsukahara, S.; Ishikawa, E.; Asada, S.; Imai, Y.; Sugimoto, Y. Single Amino Acid Substitutions in the Transmembrane Domains of Breast Cancer Resistance Protein (BCRP) Alter Cross Resistance Patterns in Transfectants. *Int. J. Cancer*, **2003**, *107*, 757-763.

[71] Norman, B. H. Inhibitors of MRP1-mediated Multidrug Resistance. *Drugs Fut.* **1998**, *23*, 1001-1013.

[72] Boumendjel, A.; Baubichon-Cortay, H.; Trompier, D.; Perrotton, T.; di Pietro, A. Anticancer Multidrug Resistance Mediated by MRP1: Recent Advances in the Discovery of Reversal Agents. *Med. Res. Rev.* **2005**, *25*, 453-472.

[73] Rogan, A. M.; Hamilton, T. C.; Young, R. C.; Klecker Jr., R. W.; Ozols, R. F. Reversal of Adriamycin Resistance by Verapamil in Human Ovarian Cancer. *Science* **1984**, *224*, 994-996.

[74] Dalton, W. S.; Grogan, T. M.; Meltzer, P. S.; Scheper, R. J.; Durie, B. G. M.; Taylor, C. W.; Miller, T. P.; Salmon, S. E. Drug-Resistance in Multiple Myeloma and Non-Hodgkin's Lymphoma: Detection of P-Glycoprotein and Potential Circumvention by Addition of Verapamil to Chemotherapy. *J. Clin. Oncol.* **1989**, *7*, 4, 415-424.

[75] Perrotton, T.; Trompier, D.; Chang, X.-B.; Di Pietro, A.; Baubichon-Cortay, H. (R)- and (*S*)-Verapamil Differentially Modulate the Multidrug-resistant Protein MRP1. *J. Biol. Chem.* **2007**, *282*, 43, 31542-31548.

[76] Cole, S. P. C.; Downes, H. F.; Slovak, M. L. Effect of Calcium Antagonists on the Chemosensitivity of Two Multidrug-resistant Human Tumor Cell Lines which Do Not Overexpress P-glycoprotein. *Br. J. Cancer* **1989**, *59*, 42-46.

[77] Loe, D. W.; Oleschuk, C- J.; Deeley, R. G.; Cole, S. P. C. Structure-Activity Studies of Verapamil Analogs That Modulate Transport of Leukotriene C_4 and Reduced Glutathione by Multidrug Resistance Protein MRP1. *Biochem. Biophys. Res. Com.* **2000**, *275*, 795-803.

[78] Nogae, I.; Kohno, K.; Kikuchi, J.; Kuwano, M.; Akiyama, S.-I.; Kiue, A.; Suzuki, K.-I.; Yoshida, Y.; Cornwell, M. M.; Pastan, I.; Gottesman, M. M. Analysis of Structureal Features of Dihydropyridine Analogs Needed to Reverse Multidrug Resistance and to Inhibit Photoaffinity Labeling of P-Glycoprotein. *Biochem. Pharmacol.* **1989**, *38*, 3, 519-527.

[79] Kamiwatari, M.; Nagata, Y.; Kukuchi, H.; Yoshimura, A.; Sumizawa, T.; Shudo, N.; Sakoda, R.; Seto, K.; Akiyama, S.-I. Correlation between Reversing of Multidrug Resistance and Inhibiting of [3H]Azidopine Photolabeling of P-Glycoprotein by Newly Synthesized Dihydropyridine Analogues in a Human Cell Line. *Cancer Res.* **1989**, *49*, 3190-3195.

[80] Tasaka, S.; Ohmori, H.; Gomi, N.; Iino, M.; Machida, T.; Kiue, A.; Naito, S.; Kuwano, M. Synthesis and Structure-Activity Analysis of Novel Dihydropyridine Derivatives to Overcome Multidrug Resistance. *Bioorg. Med. Chem. Lett.* **2001**, *11*, 275-277.

[81] Shudo, N.; Mizoguchi, T.; Kiyosue, T.; Arita, M.; Yoshimura, A.; Seto, K.; Sakoda, R.; Akiyama, S.-I. Two Pyridine Analogues with More Effective Ability to Reverse Multidrug Resistance and with Lower Calcium Channel Blocking Activity Than Their Dihydropyridine Counterparts. *Cancer Res.* **1990**, *50*, 3055-3061.

[82] Abe, T.; Koike, K.; Ohga, T.; Kubo, T.; Wada, M.; Kohno, K.; Hidaka, K.; Kuwano, M. Chemosensitisation of Spontaneous Multidrug Resistance by a 1,4-dihydropyridine Analog and Verapamil in Human Glioma Cell Lines Overexpressing *MRP1* or *MDR1*. *Br. J. Cancer* **1995**, *72*, 418-423.

[83] Vanhoefer, U.; Cao, S.; Minderman, H.; Toth, K.; Scheper, R. J.; Slovak, M. L.; Rustum, Y. M. PAK-104P, a Pyridine Analogue, Reverses Paclitaxel and Doxorubicin Resistance in Cell Lines and Nude Mice Bearing Xenografts That Overexpress the Multidrug Resistance Protein. *Clin. Cancer Res.* **1996**, *2*, 369-377.

[84] Marbeuf-Gueye, C.; Salerno, M.; Quidu, P.; Garnier-Suillerot, A. Inhibition of the P-glycoprotein- and Multidrug Resistance Protein-mediated Efflux of Anthracyclines and Calceinacetoxymethyl Ester by PAK-104P. *Eur. J. Pharmacol.* **2000**, *391*, 207-216.

[85] Twentyman, P. R.; Fox, N. E.; White, D. J. G. Cyclosporin A and Its Analogues as Modifiers of Adriamycin and Vincristine Resistance in a Multidrug-resistant Human Lung Cancer Cell Line. *Br. J. Cancer* **1987**, *56*, 55-57.

[86] Twentyman, P. R. Cyclosporins as Drug Resistance Modifiers. *Biochem. Pharmacol.* **1992**, *43*, 1, 109-117.

[87] Slater, L. M.; Sweet, P.; Stupecky, M.; Gupta, S. Cyclosporin A Reverses Vincristine and Daunorubicin Resistance in Acute Lymphatic Leukemia *In Vitro*. *J. Clin. Invest.* **1986**, *77*, 1405-1408.

[88] Barrand, M. A.; Rhodes, T.; Center, M. S.; Twentyman, P. R. Chemosensitisation and Drug Accumulation Effects of Cyclosporin A, PSC-833 and Verapamil in Human MDR Large Cell Lung Cancer Cells Expressing a 190k Membrane Protein Distinct from P-glycoprotein. *Eur. J. Cancer*, **1993**, *29A*, 3, 408-415.

[89] Rowinski, E. K.; Smith, L.; Wang, Y.-M.; Chaturvedi, P.; Villalona, M.; Campbell, E.; Aylesworth, C.; Echardt, S. G.; Hammond, L.; Kraynak, M.; Drengler, R.; Stephenson, J.; Harding Jr.; M. W.; Von Hoff, D. D. Phase I and Pharmacokinetic Study of Paclitaxel in Combination With Biricodar, a Novel Agent That Reverses Multidrug Resistance Conferred by Overexpression of Both, MDR1 and MRP1. *J. Clin. Oncol.* **1998**, *16*, 9, 2964-2976.

[90] Peck, R. A.; Hewett, J.; Harding, M. W.; Wang, Y.-M.; Chaturvedi, P. R.; Bhatnagar, A.; Ziessman, H.; Atkins, F.; Hawkins, M. J. Phase I and Pharmacokinetic Study of the Novel MDR1 and MRP1 Inhibitor Biricodar Administered Alone and in Combination With Doxirubicin. *J. Clin. Oncol.* **2001**, *19*, 12, 3130-3141.

[91] Germann, U. A.; Shlyakhter D.; Mason, V. S.; Zelle, R. E.; Duffy, J. P.; Galullo, V.; Armisteaad, D. M.; Saunders, J. O.; Boger, J.; Harding M. W. Cellular and Biochemical Characterization of VX-710 as a Chemosensitizer: Reversal of P-glycoprotein-mediated Multidrug Resistance *In Vitro*. *Anticancer Drugs* **1997**, *8*, 2, 125-140.

[92] Germann, U. A; Ford, P. J.; Shylakhter, D.; Mason, V. S.; Harding, M. W. Chemosensitization and drug accumulation effects of VX-710, Verapamil, Cyclosporine A, MS-209 and GS120918 in Multidrug Resistant HL60/ADR Cells Expressing the Multidrug Resistance-associated Protein MRP1. *Anticancer Drugs* **1997**, *8*, 2, 141-155.

[93] Evers, R.; Kool, M.; Smith, A. J.; van Deemter, L.; de Haas, M.; Borst, P. Inhibitory Effect of the Reversal Agents V-104, GF120918 and Pluronic L61 on MDR1 P-gp-, MRP1- and MRP2-mediated Transport. *Br. J. Cancer* **2000**, *83*, 3, 366-374.

[94] Sato, W.; Fukuzawa, N.;Nakanashi, O.; Baba, Makoto, Suzuki, T.; Yano, O.; Naito, M.; Tsuruo, T. Reversal of Multidrug Resistance by a Novel Quinoline Derivative, MS-209. *Cancer Chemother. Pharmacol.* **1995**, *35*, 271-277.

[95] Baba, M.; Nakanashi, O.; Sato, W.; Saito, A.; Miyama, Y.; Yano, O.; Shimada, A.; Fukazawa, N.; Naito, M.; Tsuruo, T. Relationship between Multidrug Resistant Gene Expression and Multidrug Resistant-reversing Effect of MS-209 in Various Tumor Cells. *Cancer Chemother. Pharmacol.* **1995**, *36*, 361-367.

[96] Nakanishi, O.; Baba, M.; Saito, A.; Yamashita, T.; Sato, W.; Abe, H.; Fukazawa, N.; Suzuki, T.; Sato, S.; Naito, M.; Tsuruo, T. Potentiation of the Antitumor Activity by a Novel Quinolone Compound, MS-209, in Multidrug-resistant Solid Tumor Cell Lines. *Oncol. Res.* **1997**, *9*, 2, 61-69.

[97] Narasaki, F.; Oka, M.; Fukuda, M.; Nakano, R.; Ikeda, K.; Takatani, H.; Terashi, K.;Soda, H.; Yano, O.; Nakamura, T.; Doyle, L. A.; Tsuruo, T.; Kohno, S. A Novel Quinolone Derivative, MS-209, Overcomes Drug Resistance of Human Lung Cancer Cells Expressing the Multidrug Resistance-associated Protein (MRP) Gene. *Cancer Chemother. Pharmacol.* **1997**, *40*, 425-432.

[98] Doyle, L. A.; Ross, D. D.; Ordnonez, J. V.; Yang, W.; Gao, Y.; Tong, Y.; Belani, C. P.; Gutheil, J. C. An Etoposide-resistant Lung Cancer Subline Overexpresses the Multidrug Resistance-associated Protein. *Br. J. Cancer*, **1995**, *72*, 535-532.

[99] Gekeler, V.; Boer, R.; Ise, W.; Sanders, K. H.; Schächtele, C.; Beck, J. The Specific Bisindoylmaleimide PAK-Inhibitor GF 10923X Efficiently Modulates MRP-Associated Multiple Drug Resistance. *Biochem. Biophys. Res. Comm.* **1995**, *296*, 1, 119-126.

[100] Gollapudi, S.; Kim, C. H.; Tran, B.-N.; Sangha, S.; Gupta, S. Probenecid Reverses Multidrug Resistance in Multidrug Resistance-associated Protein-overexpressing HL60/ADR and H69/AR Cells but Not in P-glycoprotein-overexpressing HL60/Tax and P388/ADR Cells. *Cancer Chemother. Pharmacol*. **1997**, *40*, 150–158.

[101] Bobrowska-Hägerstrand, M.; Wrobel, A.; Mrowczynska, L.; Söderström, T.; Shirataki, Y.; Motohashi, N.; Molnar, J.; Michalak, K.; Hägerstrand, H. Flavonoids as Inhibitors of MRP1-like Efflux Activity in Human Erythrocytes. A Structure-activity Relationship Study. *Oncol. Res.* **2003**, *13*, 11, 463-469.

[102] Levy, G. N. Prostaglandin H Synthases, Nonsteroidal Anti-inflammatory Drugs, and Colon Cancer. *FASEB J.* **1997**, *11*, 234-247.

[103] Duffy, C. P.; Elliott, C. J.; O'Connor, R. R.; Heenan, M. M.; Coyle, S.; Cleary, I. M.; Kavanagh, K.; Verhaegen, S.; O'Loughlin, C. M.; NicAmhlaoibh, R.; Clynes, M. Enhancement of Chemotherapeutic Drug Toxicity to Human Tumor Cells *In Vitro* by a Subset of Non-steroidal Anti-inflammatory Drugs (NSAIDs). *Eur. J. Cancer* **1998**, *34*, 8, 1250-1259.

[104] Roller, A.; Bähr, O.; Streffer, J.; Winter, S.; Heneka, M.; Deininger, M.; Meyermann, R.; Naumann, U.; Gulbins, E.; Weller, M. Selective Potentiation of Drug Cytotoxicity by NSAID in Human Glioma Cells: The Role of Cox-1 and MRP1. *Biochem. Biophys. Res. Com.* **1999**, *259*, 600-605.

[105] Draper, M. P.; Martell, R. L.: Levy, S. B. Active Efflux of the Free Acid Form of the Fluorescent Dye 2',7'-bis(2-carboxylethyl)-5(6)-carboxyfluorescein in Multidrug-resistance-protein-overexpressing Murine and Human Leukemia Cells. *Eur. J. Biochem.* **1997**, *243*, 1-2, 219-224.

[106] Benyahia, B.; Huguet, S.; Declèves, X.; Mokhtari, K.; Crinière, E.; Bernaudin, J. F.; Scherrmann, J. M.; Delattre, J. Y. Multidrug Resistance-associated Protein MRP1 Expression in Human Gliomas: Chemosensitization to Vincristine and Etoposide by Indomethacin in Human Glioma Cell Lines Overexpressing MRP1. *J. Neurooncol.* **2004**, *66*, 65-70.

[107] Piazza, G. A.; Rahm, A. L. K.; Krutsch, M.; Sperl, G.; Paranka, N. S.; Gross, P. H.; Brendel, K.; Burt, R. W.; Alberts, D. S.; Pamukcu, R.; Ahnen, D. J. Antineoplastic Drugs, Sulindac Sulfide and Sulfone Inhibit Cell Growth by Inducing Apoptosis. *Cancer Res.* **1995**, *55*, 3110-3116.

[108] Piazza, G. A.; Rahm, A. K.; Finn, T. S.; Fryer, B. H.; Li, H.; Stoumen, A. L.; Pamukcu, R.; Ahnen, D. J. Apoptosis Primarily Accounts for the Growth-inhibitory Properties of Sulindac Metabolites and Involves a Mechanism That Is Independent of Cyclooxygenase Inhibition, Cell Cycle Arrest, and p53 Induction. *Cancer Res.* **2007**, *57*, 2452-2459.

[109] Han, E. K.; Aber, N.; Yamamoto, H.; Lim, J. T.; Dolohery, T.; Pamukcu, R.; Piazza, G. A.; Xing, W. Q.; Weinstein, I. B. Effects of Sulindac and Its Metabolites on Growth and Apoptosis in Human Mammary Epithelial and Breast Carcinoma Cell Lines. *Brest Cancer Res. Treat.* **1998**, *48*, 3, 195-203.

[110] Lim, J. T. E.; Piazza, G. A.; Han, E. K.-H.; Delohery, T. M.; Li, H.; Finn, T. S.; Buttyan, R.; Yamamoto, H.; Sperl, G. J.; Brendel, K.; Gross, P. H.; Pamukcu, R.; Weinstein, I. B. Sulindac Derivatives Inhibit Growth and Induce Apoptosis in Human Prostate Cancer Cell Lines. *Biochem. Pharmacol.* **1999**, *58*, 1097-1107.

[111] Maguire, A. R.; Plunkett, S. J. ; Papot, S. ; Clynes, M. ; O'Connor, R. ; Touhey, S. Synthesis of Indomethacin Analogues for Evaluation as Modulators of MRP1 activity. *Bioorg. Med. Chem.* **2001**, *9*, 745-762.

[112] Touhey, S.; O'Connor, R.; Plunkett, S.; Maguire, A.; Clynes, M. Structure-activity Relationship of Indomethacin Analogues for MRP-1, COX-1 and COX-2 Inhibitor: Identification of Novel Chemotherapeutic Drug Resistance Modulators. *Eur. J. Cancer* **2002**, *38*, 1661-1670.

[113] Rosenbaum, C.; Röhrs, S.; Müller, O.; Waldmann, H. Modulation of MRP-1-mediated Multidrug Resistance by Indomethacin Analogues. *J. Med. Chem.* **2005**, *48*, 1179-1187.

[114] Dai, C.-L.; Tiwari, A. K. ; Wu, C.-P.; Su, X.-D. ; Wang, S.-R. ; Liu, D.-G. ; Ashby Jr., C. R.; Huang, Y.; Robey, R. W.; Liang, Y.-J.; Chen, L.-M.; Shi, C.-J.; Ambudkar, S. V.; Chen, Z.-S.; Fu, L.-F. Lapatinib (Tykerb, GW572016) Reverses Multidrug Resistance in Cancer Cells by Inhibiting the Activity of ATP-Binding Cassette Subfamily B Member 1 and G Member 2. *Cancer Res.* **2008**, *68*, 19, 7905-7914.

[115] Kodaira, H.; Kusuhara, H.; Ushiki, J.; Fuse, E.; Sugiyama, Y. Kinetic Analysis of the Cooperation of P-glycoprotein (P-gp/*Abcb1*) and Breast Cancer Resistance Protein (Bcrp/*Abcg2*) in Limiting the Brain and Testis Penetration of Erlotinib, Flavopiridol, and Mitoxantrone. *J. Pharmacol. Exp. Ther.* **2010**, *333*, 788-796.

[116] Mi, Y.-J.; Liang, Y.-J.; Huang, H.-B.; Zhao, H.-Y.; Wu, C.-P.; Wang, F.; Tao, L.-Y.; Zhang, C.-Z.; Dai, C.-L.; Tiwari, A.-K.; Ma, X.-X.; Kin Wah To, K.; Ambudkar, S: V.; Chen, Z.; S.; Fu, L.-W. Apatinib (YN968D1) Reversis Multidrug Resistance by Inhibiting the Efflux Function of Multiple ATP-Bindung Cassette Transporters. *Cancer Res.* **2010**, *70*, 20, 7981-7991.

[117] Nakamura, Y.; Oka, M.; Soda, H.; Shiozawa, K.; Yoshikawa, M.; Itoh, A.; Ikegami, Y.; Tsurutani, J.; Nakatomi, K.;Kitazaki, T.; Doi, S.; Yoshida, H.; Kohno, S. Gefitinib ("Iressa", ZD1839), an Epidermal Growth Factor Receptor Tyrosine Kinase Inhibitor, Reverses Breast Cancer Resistance Protein/ABCG2-Mediated Drug Resistance. *Cancer Res.* **2005**, *65*, 4, 1541-1546.

[118] Yanase, K.; Tsukahara, S.; Asada, S.; Ishikawa, E.; Imai, Y.; Sugimoto, Y. Gefitinib Reverses Breast Cancer Resistance Protein-mediated Drug Resistance. *Mol. Cancer Ther.* **2004**, *3*, 9, 1119-1125.

[119] Hegedus, T.; Orfi, L.; Seprodi, A.; Varadi, A. ; Sarkadi, B. ; Keri, G. Interaction of Tyrosine Kinase Inhibitors with the Human Multidrug Transporter Proteins, MDR1 and MRP1. *Biochim. Biochys. Acta* **2002**, *1587*, 318-325.

[120] Jagiello-Gruszfeld, A.; Tjulandin, S.; Dobrovolskaya, N.; Manikhas, A.; Pienkowski, T.; DeSilvio, M.; Ridderheim, M.; Abbey, R. A Single-Arm Phase II Trial of First-Line Paclitaxel in Combination with Lapatinib in HER2-Overexpressing Metastatic Breast Cancer. *Oncology* **2010**, *79*, 129-135.

[121] Cameron, D.; Casey, M.; Press, M.; Lindquist, D.; Pienkowski, T.; Romieu, C. G.; Chan, S.; Jagiello-Gruszfeld, A.;Kaufman, B.; Crown, J.; Chan, A.; Campone, M.; Viens, P.; Davidson, N.; Gorbounova, V.; Raats, J. I.; Skarlos, D.; Newstat, B.;Roychowdhury, D.; Paoletti, P.; Olivia, C.; Rubin, S.; Stein, S.; Geyer, C. E. A phase III Randomized Comparison of Lapatinib Plus Capecitabine Versus Capecitabine Alone in Women with Advanced Breast Cancer that Has Progressed on Trastuzumab: Updated Efficacy and Biomarker Analyses. *Breast Cancer Res. Treat.* **2008**, *112*, 533-543.

[122] Geyer, C. E.; Foster, J.; Lindquist, D.; Chan, S.; Romieu, C. G. ; Pienkowski, T. ; Jagiello-Gruszfeld, A. ; Crown, J. ; Chan, A. ;Kaufman, B.; Skarlos, D.; Campone, M.; Davidson, N.; Berger, M.; Olivia, C.; Rubin, S. D.; Stein, S.; Cameron, D. Lapatinib Plus Capecitabine for HER2-Positive Advanced Breast Cancer. *N. Engl. J. Med.* **2006**, *355*, 26, 2733-2743.

[123] Ma, S.-L.; Hu, Y.-P-: Wang, F; Huang, Z.-C.; Chen, Y.-F.; Wang, X.-K.; Fu, L.-W. Lapatanib Antagonizes Multidrug Resistance-Associated Protein 1-Mediated Multidrug Resistance by Inhibiting Its Transport Function. *Mol. Med.* **2014**, *20*, 390-399.

[124] Zhang, H.; Patel, A.; Ma, S.-L.; Li, X. J.; Zhang, Y.-K.; Yang, P.-Q.; Kathawala, R. J.; Wang, Y.-J.; Anreddy, N.; Fu, L.-W.; Chen, Z.-S. *In Vitro*, *In Vivo* and *Ex Vivo* Characterization of Ibrutinib: a Potent Inhibitor of the Function of the Transporter MRP1. *Br. J. Pharmacol.* **2014**, *171*, 5845-5857.

[125] Bousquet, L.; Pruvost, A.; Didier, N.; Farinotti, R. ; Mabondzo, A. Emtricitabine : Inhibitor and Substrate of Multidrug Resistance Associated Protein. *Eur. J. Pharm. Sci.* **2008**, *35*, 247-256.

[126] Weiss, J.; Theile, D.; Ketabi-Kiyanvash, N.; Lindenmaier, H.; Haefeli, W. E. Inhibition of MRP1/ABCC1, MRP2/ABCC2, and MRP3, ABCC3 by Nucleoside, Nucleotide, and Non-nucleoside Reverse Transcriptase Inhibitors. *Drug Metab. Dispos.* **2007**, *35*, 340-344.

[127] Michot, J.-M.; Van Bambeke, F.; Mingeot-Leclercq, M.-P.; Tulkens, P. M. Active Efflux of Ciprofloxacin from J774 Macrophages through an MRP-Like Transporter. *Antimicrob. Agents Chemother.* **2004**, *48*, 7, 2673-2682.

[128] Rudin, D. E.; Gao, P. X.; Cao, C. X.; Neu, H. C.; Silverstein, S. C. Gemfibrozil Enhances the Listeriacidal Effects of Fluorquinolone Antibiotics in J744 Macrophages. *J. Exp. Med.* **1992**, *176*, 1439-1447.

[129] Cao, C. X.; Silverstein, S. C.; Neu, H. C.; Steinberg, T. H. J744 Macrophages Secrete Antibiotics via Organic Anion Transporters. *J. Infect. Dis.* **1992**, *165*, 322-328.

[130] Sasabe, H.; Kato, Y.; Suzuki, T.; Itose, M.; Miyamoto, G.; Sugiyama, Y. Differential Involvement of Multidrug Resistance-Associated Protein 1 and P-Glycoprotein in Tussue Distribution and Excretion of Grepafloxacin in Mice. *J. Pharmacol. Exp. Ther.* **2004**, *310*, 648-655.

[131] Courtois, A.; Payen, L.; Vernhet, L.; De Vries, E. G. E. ; Guillouzo, A. ; Fardel, O. Inhibition of Multidrug Resistance-associated Protein (MRP) Activity by Rifampicin in Human Multidrug-resistant Lung Tumor Cells. *Cancer Lett.* **1999**, *139*, 97-104.

[132] Payen, L.; Delugin, L.; Courtois, A.; Trinquart, Y. ; Guillouzo, A. ; Fardel, F. The Sulfonylurea Glibenclamide Inhibits Multudrg Resistance Protein (MRP1) Activity in Human Lung Cancer Cells. *Br. J. Pharmacol.* **2001**, *132*, 3, 778-784.

[133] Sauna, Z. E.; Peng, X.-H. ; Nandigama, K. ; Tekle, S. ; Ambudkar, S. V. The Molecular Basis of the Action of Disulfiram as a Modulator of the Multidrug Resistance-Linked ATP Binding Cassette Transporters MDR1 (ABCB1) and MRP1 (ABCC1). *Mol. Pharmacol.* **2004**, *65*, 675-684.

[134] Payen, L.; Delugin, L.; Courtois, A.; Trinquart, Y. ; Guillouzo, A. ; Fardel, O. Reversal of MRP-mediated Multidrug Resistance in Human Lung Cancer Cells by the Antiprogestatin Drug RU486. *Biochem. Biophys. Res. Comm.* **1999**, *258*, 513-518.

[135] Lecureur, V.; Fardel, O.; Guillouzo, A. The Antiprogestatin Drug RU 486 Potentiates Doxorubicin Cytotoxicity in Multidrug Resistant Cells through Inhibition of P-glycoprotein Function. *FEBS lett.* **1994**, *355*, 187-191.

[136] Fardel, O.; Courtois, A.; Drenou, D.; Lamy, T.; Lecureur, V.; Le Prisé, P. Y. ; Fauchet, R. Inhibition of P-glycoprotein Activity in Human Leukemic Cells by Mifepristone. *Anticancer Drugs* **1996**, *7*, 6, 671-677.

[137] Wang, E.-J.; Johnson, W. W. The Farnesyl Protein Transferase Inhibitor Lonafarnib (SCH66336) Is an Inhibitor of Multidrug Resistance Proteins 1 and 2. *Chemotherapy* **2003**, *49*, 303-308.

[138] Michaelis, M.; Rothweiler, F.;Klassert, D.; von Deimling, A.; Weber, K.; Fehse, B.; Kammerer, B.; Doerr, H. W.; Cinatl Jr., J. Reversal of P-glycoprotein-Mediated Multidrug Resistance by the Murine Double Minute 2 Antagonist Nutilin-3. *Cancer Res.* **2009**, *69*, 2, 416-421.

[139] Burkhart, C. A.; Watt, F.; Murray, J.; Pajic, M.; Prokvolit, A.; Xue, C.; Flemming, C.; Smith, J.; Purmal, A.; Isachenko, N.; Komarov, P. G.; Gurova, K. V.; Sartorelli, A. C.; Marshall, G. M.; Norris, M. D.; Gudkov, A. V.; Haber, M. Small Molecule MRP1 Inhibitor Reversan Increases the Therapeutic Index of Chemotherapy in Mouse Model of Neuroblastoma. *Cancer Res.* **2009**, *69*, 16, 6573-6580.

[140] Robey, R. W.; Shukla, S.; Finley, E. M.; Oldham, R. K.; Barnett, D.; Ambudkar, S. V.; Fojo, T.; Bates, S. E. Inhibition of P-glycoprotein (ABCB1)- and Multidrug Resistance-associated Protein 1 (ABCC1)-Mediated Transport by the Orally Administered Inhibitor, CBT-1. *Biochem. Pharmacol.* **2008**, *75*, 6, 1302-1312.

[141] Fotsis, T.; Pepper, M.; Adlercreutz, H.; Fleischmann, G.; Hase, T.; Montesano, R.; Schweigerer, L. Genistein, a Dietary-derived Inhibitor of *In Vitro* Angiogenesis. *Proc. Natl. Acad. Sci. U. S. A.* **1993**, *90*, 2690-2694.

[142] Fotsis, T.; Pepper, M.; Adlercreutz, H.; Hase, T.; Montesano, R.; Schweigerer, L. Genistein, a Dietary ingested Isoflavonoid, Inhibits Cell Proliferation and *In Vitro* Angiogenesis. *J. Nutr.* **1995**, *125*, 790-797.

[143] Fotsis, T.; Pepper, M. S.; Aktas, E.; Breit, S.; Rasku, S.; Adlercreutz, H.; Wähälä, K.; Montesano, R.; Schweigerer, L. Flavonoids, Dietary-derived Inhibitors of Cell Proliferation and *In Vitro* Angiogenesis. *Cancer Res.* **1997**, *57*, 2916-2921.

[144] Neuhouser, M. L. Dietary Flavonoids and Cancer Risk: Evidence from Human Population Studies. *Nutr. Cancer* **2004**, *50*, 1, 1-7.

[145] Castro, Ariel F.; Altenberg, G. A. Inhibition of Drug Transport by Genistein in Multidrug Resistant Cells Expressing P-Glycoprotein. *Biochem. Pharmacol.* **1996**, *53*, 89-93.

[146] Zhang, S.; Morris, M. E. Effects of the Flavonoids Biochanin A, Morin, Phloretin, and Silymarin on P-Glycoprotein-Mediated Transport. *J. Pharmacol. Exp. Ther.* **2003**, *304*, 1258-1267.

[147] Zhang, S.; Yang, X.; Morris, M. E. Flavonoids Are Inhibitors of Breast Cancer resistance Protein (ABCG2)-Mediated Transport. *Mol. Pharmacol.* **2004**, *65*, 1208-1216.

[148] Cooray, H. C.; Janvilisry, T.; Van Veen, H. W.; Hladky, S. B.; Barrand, M. A. Interaction of the Breast Cancer Resistance Protein with Plant Polyphenols. *Biochem. Biochys. Res. Comm.* **2004**, *317*, 269-275.

[149] Wesolowska, O. Interaction of Phenothiazines, Stilbenes and Flavonoids with Multidrug Resistance-associated Transporters, P-glycoprotein and MRP1. *Acta Biochim. Polon.* **2011**, *58*, 433-448.

[150] Versantvoort, C. H. M.; Schnuurhuis, G. J.; Pinedo, H. M.; Eekman, C. A.; Kuiper, C. M.; Lankelma, J.; Broxterman, H. J. Genistein Modulates the Decreased Drug Accumulation in Non-P-glycoprotein Mediated Multidrug Resistant Tumor Cells. *Br. J. Cancer* **1993**, *68*, 939-946.

[151] Nguyen, H.; Zhang, S.; Morris, M. E. Effect of Flavonoids on MRP1-Mediated Transport in Panc-1 Cells. *J. Pharm. Sci.* **2003**, *92*, 250-257.

[152] Versantvoort, C. H. M.; Rhodes, T.; Twentyman, P. R. Acceleration of MRP-associated Efflux of Rhodamine 123 by Genistein and Related Compounds. *Br. J. Cancer* **1996**, *74*. 1949-1954.

[153] Wu, C.-P.; Calcagno, A. M.; Hladky, S. B.; Ambudkar, S. V.; Barrand, M. A. Modulatory Effects of Plant Polyphenols on Human Multidrug Resistance Proteins 1, 4 and 5 (ABCC1, 4 and 5). *FEBS J.* **2005**, *272*, 18, 4725-4740.

[154] Hooijberg, J. H.; Broxterman, H. J.; Scheffer, G. L.; Vrasdonk, C.; Heijn, M.; De Jong, M. C.; Scheper, R. J.; Lankelma, J.; Pinedo, H. M. Potent Interaction of Flavopiridol with MRP1. *Br. J. Cancer*b **1999**, *81*, 2, 269-276.

[155] Leslie, E. M.; Mao, Q.; Oleschuk, C. J.; Deeley, R. G.; Cole, S. P. C. Modulation of Multidrug Resistance Protein 1 (MRP1/ABCC1) Transport and ATPase Activities by Interaction with Dietary Flavonoids. *Mol. Pharmacol.* **2001**, *59*, 1171-1180.

[156] Van Zanden, J. J.; Wortelboer, H. M.; Bijsma, S.; Punt, A.; Usta, M.; Bladeren, P. J.; Rietjens, I. M.; Cnubben, N. H. Quantitative Structure Activity Relationship Studies on the Flavonoid Mediated Inhibition of Multidrug Resistance Protein 1 and 2. *Biochem. Pharmacol.* **2005**, *69*, 4, 699-708.

[157] Wesolowska, O.; Wisniewski, J.; Sroda, K.; Krawczenko, A.; Bielawska-Pohl, A.; Papocka, M.; Dus, D.; Michalak, K. 8-Prenylnaringenin is an Inhibitor of Multidrug Resistance-associated Transporters, P-glycoprotein and MRP1. *Eur. J. Pharmacol.* **2010**, *644*, 32-40.

[158] Trompier, D.; Baubichon-Cortay, H.; Chang, X.-B.; Maitrejean, M.; Barron, D. ; Riordan, J. R. ; Di Pietro, A. Multiple Flavonoid-binding Sites within Multidrug Resistance Protein MRP1. *Cell Mol. Life Sci* **2003**, *60*, 10, 2164-2177.

[159] Wesolowska, O.; Wisniewski, J. Duarte, N.; Ferreira, M.-J. U.; Michalak, K. Inhibition of MRP1 Transport Activity by Phenolic and Terpenic Compounds Isolated from *Euphorbia* species. *Anticancer Res.* **2007***, 27*, 4127-4134.

[160] Kweon, S. H.; Song, J. H.; Kim, T. S. Resveratrol-mediated Reversal of Doxorubicin Resistance in Acute Myeloid Leukemia Cells Via Downregulation of MRP1 Expression. *Biochem. Biophys. Res. Comm.* **2010**, *395*, 104-110

[161] Bobrowska-Hägerstrand, M.; Lillas, M.; Mrowczynska, L.; Wrobel, A.; Shirataki, Y.; Motohashi, N.; Hägerstrand, H. Resveratrol Oligomers are Potent MRP1 Transport Inhibitors. *Anticancer Res.* **2006**, *26*, 2018-2084.

[162] Bible, K. C.; Kaufmann, S. H. Cytotoxic Synergy between Flavopiridol (NSC 649890, L86-8275) and Various Antineoplastic Agents: The Importance of Sequence of Administration. *Cancer Res.* **1997**, *57*, 3375-3380.

[163] Mavel, S.; Dikic, B.; Palakas, S.; Emond, P.; Greguric, I.; Gomez De Gracia, A.; Mattner, F.; Garrigos, M.; Guilloteau, D.; Katsifis, A. Synthesis and Biological Evalulation of a Series of Flavone Derivatives as Potential Radioligands for Imaging the Multidrug Resistance-associated Protein 1 (ABCC1/MRP1). *Bioorg. Med. Chem.* **2006**, *14*, 1599-1607.

[164] Wong, I. L. K.; Chan, K.-F.; Tsang, K. H.; Lam, C. Y.; Zhao, Y.; Chan, T. H.; Chow, L. M. C. Modulation of Multidrug Resistance Protein 1 (MRP1/ABCC1))-mediated Multidrug Resistance by Bivalent Apigenin Homodimers and Their Derivatives. *J. Med. Chem.* **2009**, *52*, 5311-5322.

[165] Sedlacek, H.; Czech, J.; Naik, R.; Kaur, G.; Worland, P.; Losiewicz, M.; Parker, B.; Carlson, B.; Smith, A.; Senderowicz, A.; Sausville, E. Flavopiridol (L86 8275; NSC 649890), a New Kinase Inhibitor for Tumor Therapy. *Int. J. Oncol.* **1996**, *9*, 6, 1143-1168.

[166] Senderowicz, A. M.; Flavopiridol: the First Cyclin-dependent Kinase Inhibitor in Human Clinical Trials. *Invest. New Drugs* **1999**, *17*, 3, 313-320.

[167] Kelland, K. R. Flavopiridol, the First Cyclin-dependent Inhibitor to Enter the Clinic: Current Status. *Exp. Opin. Invest. Drugs* **2000**, *9*, 12, 2903-2911.

[168] Wang, L. M.; Ren, D. M. Flavopiridol, the First Cyclin-dependent Kinase Inhibitor: Revent Advances in Combination Chemotherapy. *Mini Rev. Med. Chem.* **2010**, *10*, 11, 1058-1070.

[169] Pepper, M. S.; Hazel, S. J.; Hümpel, M.; Schleuning, W.-D. 8-Prenylnaringenin, a Novel Phytoestrogen, Inhibits Angiogenesis *In Vitro* and *In Vivo*. *J. Cell Physio.* **2004**, *199*, 98-107.

[170] Delmulle, L.; Bellahcene, A.; Dhooge, W.; Comhaire, F.; Roelens, F. ; Huvaere, K. ; Heyerick, A.; Castronovo, D.; De Keukeleire, D. Anti-proliferative Properties of Prenylated Flavonoids from Hops (*Humulus lupulus* L.) in Human Prostate Cancer Cell Lines. *Phytomedicine* **2006**, *13*, 732-734.

[171] Lee, S. H.; Kim, J. S.; Lee, J. S.; Lee, I. S.; Kang, B. Y. Inhibition of Topoisomerase I Activity and Efflux Drug Transporters' Expression by Xanthohumol from Hops. *Arch. Pharm. Res.* **2007**, *30*, 11, 1435-1439.

[172] Nabekura, T.; Yamaki, T.; Ueno, K.; Kitagawa, S. Effects of Plant Sterols on Human Multidrug Transporters ABCB1 and ABCC1. *Biochem. Biophys. Res. Comm.* **2008**, *369*, 363-368.

[173] Li, L.; Pan, Q.; Sun, M.; Lu, Q.; Hu, X. Dibenzocyclooctadiene Lignans – A class of Novel Inhibitors of Multidrug Resistance-associated Protein 1. *Life Sci.* **2007**, *80*, 741-748.

[174] Slaninova, I.; Brezinova, L.; Koubikova, L.; Slanina, J. Dibenzocyclooctadiene Lignans Overcome Drug Resistance in Lung Cancer Cells – Study of Structure-activity Relationship. *Toxicol. In Vitro* **2009**, *23*, 6, 1047-1054.

[175] Wrobel, A.; Eklund, P.; Bobrowska-Hägerstrand, M.; Hägerstrand, H. Lignans and Norlignans Inhibit Multidrug Resistance Protein 1 (MRP1/ABCC1)-mediated Transport. *Anticancer Res.* **2010**, *30*, 4423-4428.

[176] Cheng, A. L.; Hsu, C. H.; Lin, J. K.; Hsu, M. M.; Ho, Y. F.; Shen,, T. S.; Ko, J. Y:; Lin, B. R.; Mind-Shiang, W.; Yu, H. S.; Jee, S. H.; Chen, G. S.; Chen, T. M.; Chen, C. A.; Lai, M. K.; Pu, Y. S.; Pan, M. H.; Wang, Y. J.; Tsai, C. C.; Hsieh, C. Y. Phase I Clinical Trial of Curcumin, a Chemopreventive Agent, in Patients with High-risk or Pre-malignant Lesions. *Anticancer Res.* **2001**, *21*, 4B, 2895-2900.

[177] Hsu, C. H.; Cheng, A. L. Clinical Studies with Curcumin. *Adv. Exp. Med. Biol.*, **2007**, *595*, 471-480.

[178] Limtrakul, P.; Anuchapreeda, S.; Buddhasukh, D. Modulation of Human Multidrug-resistance MDR-I Gene by Natural Curcumoids. *BMC Cancer* **2004**, *4*, 13, 1-6.

[179] Wortelboer, H. M.; Usta, M.; van der Velde, A. E.; Boersma, M. G.; Spenkelink, B.; van Zanden, J. J.; Rietjens, I. M.; van Bladeren, P. J.; Cnubben, N. H. Interplay between MRP Inhibition and Metabolism of MRP Inhibitors: the Case of Curcumin. *Chem. Res. Toxicol.* **2003**, *16*, 12, 1642-1651.

[180] Wortelboer, H. M.; Usta, M.; Van Zanden, J. J.; Van Bladeren, P. J.; Rietjes, I. M. C. M.; Cnubben, N. H. P. Inhibition of Multidrug Resistance Proteins MRP1 and MRP2 by a Series of α,β-unsaturated Carbonyl Compounds. *Biochem. Pharmacol.* **2005**, *69*, 1879-1890.

[181] Rhodes, T.; Barrand, M. A.; Twentyman, P. R. Modification by Brefeldin A, Bafilomycin A1 and 7-chloro-4-nitrobenz-2-oxa-1,3-diazole (NBD) of Cellular Accumulation and Intracellular Distribution of Anthracyclines in the non-P-glycoprotein-mediated Multidrug Resistant Cell Line COR-L23/R. *Br. J. Cancer* **1994**, *70*, 60-66.

[182] Ogino, J.; Moore, R. E.; Patterson, G. M. L.;; Smith, C. D. Dendroamides, New Cyclic Hexapeptides from a Blue-Green Alga. Multidrug-Resistance Reversing Activity of Dendroamide A. *J. Nat. Prod.* **1996**, *59*, 581-586.

[183] Xia, Z.; Smith, C. D. Total Synthesis of Dendroamide A, a Novel Cyclis Peptide That Reverses Multiple Drug Resistance. *J. Org. Chem.* **2001**, *66*, 3459-3466.

[184] Aoki, S.; Yoshioka, Y.; Miyamoto, Y.; Higuchi, K.; Setiawan, A.; Murakami, N.; Chen, Z.-S.; Sumizawa, T.; Akiyama, S.-I.; Kobayashi, M. Agosterol A, a Novel Polyhydroxylated Sterol Acetate Reversing Multidrug Resistance from a Marine Sponce of *Spongia* sp. *Tetrahedron Lett.* **1998**, *39*, 6303-6306.

[185] Aoki, S.; Setiawan, A.; Yoshioka, Y.; Higuchi, K.; Fudetani, R.; Chen, Z.-S.; Sumizawa, T.; Akiyama, S.-I.; Kobayashi, M. T. Reversal of Multidrug Resistance in Human Carcinoma Cell Line by Agosterols, Marine Spongean Sterols. *Tetrahedron* **1999**, *55*, 13965-13972.

[186] Murakami, N.; Sugimoto, M.; Morita, M.; Kobayashi, M. Total Synthesis of Agosterol A: an MDR-Modulator from the Marine Sponge. *Chemistry* **2001**, *7*, 12, 2663-2670.

[187] Chen, S.-S.; Aoki, S.; Komatsu, M.; Ueda, K.; Sumizawa, T.; Furukawa, T.; Okumura, H.; Ren, X.-Q.; Belinsky, M. G.; Lee, K.; Kruh, G. D.; Kobayashi, M.; Akiyama, S.-I. Reversal of Drug Resistance Mediated by Multidrug Resistance Protein (MRP) 1 by Dual Effects of Agosterol A on MRP1 function. *Int. J. Cancer* **2001**, *93*, 107-113.

[188] Murakami, N.; Sugimoto, M.; Morita, M.; Akiyama, S.-I.; Kobayashi, M. Synthesis and Evaluation of 4-Deacetoxyagosterol A as an MDR-Modulator. *Bioorg. Med. Chem. Lett.* **2000**, *10*, 2521-2524.

[189] Cullen, K. V.; Davey, R. A.; Davey, M. W. Verapamil-stimulated Glutathione Transport by the Multidrug Resistance-associated Protein (MRP1) in Leukemia Cells. *Biochem. Pharmacol.* **2001**, *62*, 417-424.

[190] Trompier, D.; Chang, X.-B.; Barattin, R. ; Du Moulinet d'Hardemare, A. ; Di Pietro, A. ; Baubichon-Cortay, H. Verapamil and Its Derivative Trigger Apoptosis through Glutathione Extrusion by Multidrug Resistance Protein MRP1. *Cancer Res.* **2004**, *64*, 4950-4956.

[191] Barattin, R.; Perrotton, T.; Trompier, D.; Lorendeau, D.; Di Pietro, A.; Du Moulinet d'Hardemare, A.; Baubichon-Cortay, H. Iodination of Verapamil for a Stronger Induction of Death, through GSH Efflux, of Cancer Cells Overexpressing MRP1. *Bioorg. Med. Chem.* **2010**, *18*, 6265-6274.

[192] Brandmann, M.; Tulpule, K.; Schmidt, M. M. Dringen, R. The Antiretroviral Protease Inhibitors Indinavir and Nelfinavir Stimulate MRP1-mediated GSH Export from Cultured Brain Astrocytes. *J. Neurochem.* **2012**, *120*, 78-92.

[193] Zhang, K.; Wong, P. Glutathione Conjungation of Chlorambucil: Measurement and Modulation by Plant Polyphenols. *Biochem J.* ***1997,*** *325*, 417-422.

[194] Van Zanden, J. J.; Geraets, L.; Wortelboer, H. M.; Van Bladeren, P. J.; Rietjens, I. M.; Cnubben, N. H. Structural Requirements for the Flavonoid-mediated Modulation of Glutathione *S*-transferase P1-1 and GS-X pump Activity in MCF-7 Breast Cancer Cells. *Biochem. Pharmacol.* **2004**, *67*, 8, 1607-1617.

[195] Hall, A.; Robson, C. N.; Hickson, I. D.; Harris, A. L.; Proctor, S. J.; Cattan, A. R. Possible Role of Inhibition of Glutathione *S*-Transferase in the Partial Reversal of Chlorambucil Resistance by Indomethacin in a Chinese Hamster Ovary Cell Line. *Cancer Res.* **1989**, *49*, 6265-6268.

[196] Ford, J. M.; Hait, W. N.; Matlin, S. A.; Benz, C. C. Modulation of Resistance to Alkylating Agents in Cancer Cell by Gossypol Enantiomers. *Cancer Lett.* **1991**, *56*, 85-94.

[197] Schultz, M.; Dutta, S.; Tew, K. D. Inhibitors of Glutathione *S*-transferases as Therapeutic Agents. *Adv. Drug Deliv. Rev.* **1997**, *26*, 91-104.

[198] Van Iersel, M. L. P. S.; Ploemen, J.-P. H. T. M.; Struik, I.; Van Amersfoort, C.; Keyzer, A. E.; Schefferlie, J. G.; Van Bladeren, P. J. Inhibition of Glutathione *S*-transferase Activity in Human Melanoma Cells by *α,β*-unsaturated Carbonyl Derivatives. Effect of Acroelin, Cinnamaldehyde, Citral, Crotonaldehyde, Curcumin, Ethacrynic Acid, and *Trans*-2-hexenal. *Chem. Biol. Interact.* **1996**, *102*, 117-132.

[199] Van Iersel, M. L. P. S.; Ploemen, J.-P. H. T. M.; Lo Bello, M.; Frederici, G.; Van Bladeren, P. J. Interaction of *α,β*-unsaturated Aldehydes and Ketones with Human Glutathione *S*-transferase P1-1. *Chem. Biol. Interact.* **1997**, *108*, 67-78.

[200] Awasthi, S.; Pandya, U.; Singhal, S: S:; Lin, J. T.; Thiviyanathan, V.; Seifert Jr.; W. E.; Awasthi, Y. C.; Ansari, G. A. S. Curcumin-glutathione Interactions and the Role of Human Glutathione *S*-transferase P1-1. *Chem. Biol. Interact.* **2000**, *128*, 19-38.

[201] Ahokas, J. T.; Davies, C.; Ravencrift, O. J. ; Emmerson, B. T. Inhibition of Soluble Glutathione *S*-Transferase by Diuretic Drugs. *Biochem. Pharmacol.* **1984**, *33*, 12, 1929-1932.

[202] Ahokas, J. T.; Nicholls, A.; Ravencroft, P. J.; Emmerson, B. T. Inhibition of Purified Rat Liver Glutathione *S*-Transferase Isoenzymes by Diuretic Drugs. *Biochem. Pharmacol.* **1985**, *34*, 12, 2157-2161.

[203] Burg, D.; Filippov, D. V.; Hermanns, R.; Van Der Marel, G. A.; Van Boom, J. H.; Mulder, G. J. Peptidomimetic Glutathione Analogues as Novel γGT Stable GST Inhibitors. *Bioorg. Med. Chem.* **2002**, *10*, 195-205.

[204] Burg, D.; Mulder, G. J. Glutathione Conjungates and Their Synthetic Derivatives as Inhibitors of Glutathione-Dependend Entymes Involved in Cancer and Drug Resistance. *Drug. Metab. Rev.* **2002**, *34*, 4, 821-863.

[205] Ploemen, J. H. T. M.; Van Ommen, B.; Van Bladeren, P. J. Inhibition of Rat and Human Glutathione *S*-Transferase Isoenzymes by Ethacrynic Acid and Its Glutathione Conjungate. *Biochem. Pharmacol.* **1990**, *40*, 7, 1631-1635.

[206] Ploemen, J. H. T. M.; Bogaards, J. J. P.; Veldink, G. A.; Van Ommen, B.; Jansen, D. H. M.; Van Bladeren, P. J. Isoenzyme Selective Irreversible Inhibition of Rat and Human Glutathione *S*-Transferases by Ethacrynic Acid and Two Brominated Derivatives. *Biochem. Pharmacol.* **1993**, *45*, 3, 633-639.

[207] Ploemen, J. H.; Van Ommen, B.; De Haan, A.; Schefferlie, J. G.; Van Bladren, P. J. *In Vitro* and *In Vivo* Reversible and Irreversible Inhibition of Rat Glutathione *S*-transferase Isoenzymes by Caffeic Acid and Its 2-S-glutathionyl Conjungate. *Food. Chem. Toxicol.* **1993**, *31*, 7, 475-482.

[208] Zaman, G. J. R.; Cnubben, N. H. P.; Van Bladeren, P. J.; Evers, R.; Borst, P. Transport of the Glutathione Conjungate of Ethacrynic Acid by the Human Multidrug Resistance Protein MRP. *FEBS Lett.* **1996**, *391*, 126-130.

[209] Burg, D.; Wielinga, P.; Zelcer, N.; Saeki, T.; Mulder, G. J.; Borst, P. Inhibition of the Multidrug Resistance Protein 1 (MRP1) by Peptidomimetic Glutathione-Conjungate Analogs. *Mol. Pharmacol.* **2002**, *62*, 1160-1166.

[210] O'Dwyer, P. J.; LaCreta, F.; Nash, S.; Tinsley, P. W.; Schilder, R.; Clapper, M. L.; Tew, K. D.; Panting, L.; Litwin, S.; Comis, R. L.; Ozols, R. F. Phase I Study of Thiotepa in Combination with the Glutathione Transferase Inhibitor Ethacrynic Acid. *Cancer Res.* **1991**, *51*, 6059-6065.

[211] Boyland, E.; Chasseaud, L. F. Enzymes Catalysing Conjungations of Glutathione with *α,β*-Unsaturated Carbonyl Compounds. *Biochem. J.* **1968**, *109*, 651-661.

[212] Wallin, J. D.; Clifton, G.; Kaplowitz, N. The Effect of Phenobarbital, Probenecid and Diethyl Maleate on the Pharmacolo-Kinetics and Biliary Excretion of Ethacrynic Acid in the Rat. *J. Pharmacol. Exp. Ther.* **1978**, *205*, 2, 471-479.

[213] Kaplowitz, N.; Clifton, G.; Kuhlenkamp, J.; Wallin, J. D. Comparison of Renal and Hepatic Glutathione *S*-Transferases in the Rat. *Biochem. J.* **1976**, *158*, 243-248.

[214] Foliot, A.; Touchard, D.; Celier, C. Impairment of Hepatic Glutathione *S*-Transferase Activity as a Cause of Reduced Biliary Sulfobromophthalein Excretion in Clofibrate-treated Rats. *Biochem. Pharmacol.* **1984**, *33*, 18, 2829-2834.

[215] Kumar, K. S.; Weiss, J. F. Inhibition of Glutathione Peroxidase and Glutathione Transferase in Mouse Liver by Misonidazole. *Biochem. Pharmacol.* **1986**, *35*, 18, 3143-3146.

[216] Tew, K. D.; Bomber, A. M.; Hoffman, S. J. Ethacrynic Acid and Piriprost as Enhancers of Cytotoxicity in Drug Resistant and Sensitive Cell Lines. *Cancer Res.* **1988**, *48*, 3622-3625.

[217] Van Ommen, B.; Den Besten, C.; Rutten, A. L. M.; Ploemen, J. H. T. M.; Vos, R. M. E.; Müller, F.; Van Bladeren, P. J.; Active Site-directed Irreversible Inhibition of Glutathione *S*-Transferases by the Glutathione Conjungate of Tetrachloro-1,4-benzoquinone. *J. Biol. Chem.* **1988**, *263*, 26, 12939-12942.

[218] Van Ommen, B.; Ploemen, J. H. T. M.; Bogaards, J. J. P.; Monks, T. J.; Gau, S. S.; Van Bladeren, P. J. Irreversible Inhibition of Rat Glutathione *S*-transferase 1-1 by Quinones and Their Glutathione Conjungates. *Biochem. J.* **1991**, *276*, 661-666.

[219] Awasthi, S.; Sharma, R.; Singhal, S. S.; Herzog, N. K.; Chaubey, M.; Awasthi, Y. C. Modulation of Cisplatin Cytotoxicity by Sulphasalazine. *Br. J. Cancer* **1994**, *70*, 190-194.

[220] Gupta, V.; Jani, J. P.; Jacobs, S.; Levitt, M.; Fields, L.; Awathi, S.; Xu, B. H.; Sreevardhan, M.; Awasthi, Y. C.; Singh, S. Activity of Melphalan in Combination with Glutathione Transferase Inhibitor Sulfasalazine. *Cancer Chemother. Pharmacol.* **1995**, *36*, 13-19.

[221] Morgan, A. S.; Sanderson, P. E.; Borch, R. F.; Tew, K. D.; Niitsu, Y.; Takayama, T.; Von Hoff, D. D.; Izbicka, E.; Mangold, G.; Paul, C.; Broberg, U.; Mannervik, B.; Henner, W. D.; Kauvar, L. M. Tumor Efficacy and Bone Marrow-sparing Properties of TER286, a Cytotoxin Activated by Glutathione *S*-Transferase. *Cancer Res.* **1998**, *58*, 2568-2575.

[222] Askelöf, P.; Guthenbergm C.; Jakobson, I.; Mannervik, B. Purification and Characterization of Two Glutathione *S*-Aryltransferase Activities from Rat Liver. *Biochem. J.* **1975**, *147*, 513-522.

[223] Flatgaard, J. E.; Bauer, K. E.; Kauvar, L. M. Isozyme Specifity of Novel Glutathione-*S*-transferase Inhibitors. *Cancer Chemother. Pharmacol.* **1993**, *33*, 63-70.

[224] Crook, T. R.; Souhami, R. L.; Whyman, G. D.; McLean, A. E. M. Glutathione Depletion as a Determinant of Sensitivity of Human Leukemia Cells to Cyclophosphamide. *Cancer Res.* **1986**, *46*, 5035-5038.

[225] Lind, M. J.; McGown, A. T.; Hadfield, J. A.; Thatcher, N.; Crowther, D.;Fox, B. W. The Effect of Ifosfamid and Its Metabolites on Intracellular Glutathione Levels *In Vitro* and *In Vivo*. *Biochem. Pharmacol.* **1989**, *38*, 11, 1835-1840.

[226] Manzano, R. G.; Wright, K. A.; Twentyman, P. R. Modulation by Acrolein and Chloroacetaldehyde of Multidrug Resistance Mediated by the Multidrug Resistance-associated Protein (MRP). *Clin. Cancer Res.* **1996**, *2*, 1321-1326.

[227] Kramer, R. A.; Zakher, J.; Kim, G. Role of the Glutathione Redox Cycle in Acquired and De Novo Multidrug Resistance. *Science* **1988**, *241*, 694-697.

[228] Yusa, K.; Hamada, H.; Tsuruo, T. Comparison of Glutathione *S*-transferase Activity between Drug-resististant and –sensitive Human Tumor Cells: Is Glutathione *S*-transferase Associated with Multidrug Resistance? *Cancer Chemother. Pharmacol.* **1988**, *22*, 17-20.

[229] Griffith, O. W.; Anderson, M. E.; Meister, A. Inhibition of Glutathione Biosynthesis by Prothionine Sulfoximine (*S-n*-Propyl Homocysteine Sulfoximine), a Selective Inhibitor of γ-Glutamycysteine Synthase. *J. Biol. Chem.* **1979**, *254*, 4, 1205-1210.

[230] Griffith, O. W.; Meister, A. Potent and Specific Inhibition of Glutathion of Glutathione Synthesis by Buthionine Sulfoximine (*S*-*n*-Butyl Homocysteine Sulfoximine). *J. Biol. Chem.* **1979**, *254*, 16, 7558-7560.

[231] Gekeler, V.; Ise, W.; Sanders, K. H.; Ulrich, W.-R.; Beck, J. The Leukotriene LTD4 Receptor Antagonist MK571 Specifically Modulates MRP Associated Multidrug Resistance. *Biochem. Biophys. Res. Comm.* **1995**, *208*, 1, 345-352.

[232] Nakano, R.; Oka, M.; Nakamura, T.; Fukuda, M.; Kawabata, S.; Terashi, K.; Tsukamato, K.; Noguchi, Y.; Soda, H.; Kohno, S. A Leukotriene Receptor Antagonist, ONO-1078, Modulates Drug Sensitivity and Leukotriene C4 Efflux in Lung Cancer Cells Expressing Multidrug Resistance Protein. *Biochem. Biophys. Res. Comm.* **1998**, *251*, 307-312.

[233] Csandl, M. A.; Conseil, G.; Cole, S. P. C. Cysteinyl Leukotriene Receptor 1/2 Antagonists Nonselectively Modulate Organic Anion Transport by Multidrug Resistance Proteins (MRP1-4). *Drug. Metab. Dispos.* **2016**, *44*, 857-866.

[234] Ketteler, B.; Coles, B.; Meyer, D. J. The Role of Glutathione in Detoxication. *Environ. Health Perspect.* **1983**, *49*, 59-69.

[235] Orrenius, S.; Moldeus, P. The Multiple Roles of Glutathione in Drug Metabolism. *Trends Pharmacol. Sci.* **1984**, *5*, 431-435.

[236] Morrow, C. S.; Diah, S.; Smitherman, P. K. S.; Schneider, E.; Townsend, A. J. Multidrug Resistance Protein and Glutathione *S*-transferase P1-1 Act in Synergy to Confer Protection from 4-nitroquinoline 1-oxide Toxicity. *Carcinogenesis* **1998**, *19*, 1, 109-115.

[237] Peklak-Scott, C.; Townsend, A. J.; Morrow, C. S. Dynamics of Glutathione Conjungation and Conjungate Efflux in Detoxification of the Carcinogen, 4-Nitroquinoline 1-Oxide: Contributions of Glutathione, Glutathione *S*-Transferase, and MRP1. *Biochemistry* **2005**, *44*, 4426-4433.

[238] Morgan, A. S.; Ciaccio, P. J.; Tew, K. D.; Kauvar, L. M. Isozyme-specific Glutathione *S*-transferase Inhibitors Potentiate Drug Sensitivity in Cultured Human Tumor Cell Lines. *Cancer Chemother. Pharmacol.* **1996**, *37*, 363-370.

[239] O'Brien, M. L.; Vulevic, B.; Freer, S.; Boyd, J.; Shen, H.; Tew, K. D. Glutathione Peptidomimetic Drug Modulator of Multidrug Resistance-associated Protein. *J. Pharmacol. Exp. Ther.* **1999**, *291*, 3, 1348-1355.

[240] Loe, D. W.; Almquist, K. C.; Deeley, R. C.; Cole, S. P. C. Multidrug Resistance (MRP)-mediated Transport of Leukotriene C4 and Chemotherapeutic Agents in Membrane Vesicles: Demonstration of Glutathione-Dependent Vincristine Transport. *J. Biol. Chem.* **1996**, *271*, 16, 9675-9682.

[241] Müller, M.; Meijer, C.; Zaman, G. J. R.; Borst, P.; Scheper, R. J.; Mulder, N. H.; De Vries, E. G. E.; Jansen, P. L. M. Overexpression of the Gene Encoding the Multidrug Resistance-associated Protein Results in Increased ATP-dependent Glutathione *S*-conjungate Transport. *Proc. Natl. Acad. Sci. U. S. A.* **1994**, *91*, 12033-13037.

[242] Ballator, N.; Truong, A. T. Multiple Canalicular Transport Mechanisms for Glutathione *S*-Conjungates. *J. Biol. Chem.* **1995**, *270*, 1, 3594-3601.

[243] Furuta, K.; Tomokiyo, M.; Kuo, M. T.; Ishikawa, T.; Suzuki, M. Molecular Design of Glutathione-derived Biochemical Probes targeting the *GS-X* Pump. *Tetrahedron* **1999**, *55*, 7529-7540.

[244] Leslie, E. M.; Bowers, R. J.; Deeley, R. G.; Cole, S. P. C. Structural Requirements for Functional Interaction of Glutathione Tripeptide Analogs with the Human Multidrug Resistance Protein 1 (MRP1). *J. Pharmacol. Exp. Ther.* **2003**.

[245] Stewart, A. J.; Canitrot, Y.; Barachini, E.; Dean, N. M.; Deley, R. G.; Cole, S. P. C. Reduction of Expression of the Multidrug Ressitance Protein (MRP) in Human Tumor Cells by Antisense Phosphothioate Oligonucleotides. *Biochem. Pharmacol.* **1996**, *51*, 461-469.

[246] Niewiarowski, W.; Gendaszewska, E.; Rebowski, G.; Wojcik, M.; Mikolajczyk, B.; Goss, W.; Soszynski, M.; Bartosz, G. Multidrug Resistance-associated Protein – Reduction of Expression in Human Leukemia Cells by Antisense Phosphothioate Oligonucleotides. *Acta Biochim. Pol.* **2000**, *47*, 4, 1183-1188.

[247] Matsumoto, Y.; Miyake, K.; Kunishio, K.; Tamiya, T.; Nagao, S. Reduction of Expression of the Multidrug Resistance Protein (MRP)1 in Glioma Cells by Antisense Phosphothioate Oligonulceotides. *J. Med. Invest.* **2004**, *51*, 194-201.

[248] Kuss, B. J.; Corbo, M.; Lau, W. M.; Fennell, D. A.; Dean, N. M.; Cotter, F. E. *In Vitro* and *In Vivo* Downregulation of MRP1 by Antisense Oligonucleotides: A Potential Role in Neuroblastoma Therapy. *Int. J. Cancer* **2002**, *98*, 128-133.

[249] Liang, Z.; Wu, H.; Xia, J.; Li, Y.; Zhang, Y.; Huang, K.; Wagar, N.; Yoon, Y.; Cho, H. T.; Scala, S.; Shim, H. Involvement of miR-326 in Chemotherapy Resistance of Breast Cancer Through Modulating Expression of Multidrug Resistance-associated Protein 1. *Biochem. Pharmacol.* **2010**, *79*, 6, 817-824.

[250] Liu, H.; Wu, X.; Huang, J.; Peng, J.; Guo, L. miR-7 Modulates Chemoresistance of Small Cell Lung Cancer by Repressing MRP1/ABCC1. *Int. J. Exp. Pathol.* **2015**, *96*, 240-247.

[251] Guo, L.; Liu, Y.; Bai, Y.; Sun, Y.; Xiao, F.; Guo, Y. Gene Expression Profiling of Drug-resistant Small Cell Lung Cancer Cells by Combining microRNA and cDNA Expression Analysis. *Eur. J. Cancer* **2010**, *46*, 1692-1702.

[252] Lu, L.; Ju, F.; Zhao, H.; Ma, X. MicroRNA-134 Modulates Resistance to Doxorubicin in Human Breast Cancer Cells by Downregulating *ABCC1*. *Biotechnol. Lett.* **2015**, *37*, 2387-2394.

[253] Zhang, M.; Zhao, X.; Wang, H.; Chen, W.; Xu, S.; Wang, W.; Shen, H.; Huang, S.; Wang, J. miR-145 Sensitizes Gallbladder Cancer to Cisplatin by Regulating Multidrug Resistance Associated protein 1. *Tumor Biol.* **2016**, *37*, 10553-10562.

[254] Gao, M.; Miao, L.; Liu, M.; Li, C.; Yu, C.; Yan, H.; Yin, Y.; Wang, Y.; Qi, X.; Ren, J. miR-145 Sensitizes Breast Cancer to Doxorubicin by Targeting Multidrug Resistance-associated Protein-1. *Oncotarget* **2016**, *7*, 37, 59714-59726.

[255] Borel, F.; van Logtenstein, R.; Koornneef, A.; Maczuga, P.; Ritsema, T.; Petry, H.; van Deventer, S. J. H.; Jansen, P. L. M.; Konstantinova, P. *In Vivo* Knock-down of Multidrug Resistance Transporters ABCC1 and ABCG2 by AAV-delivered shRNAs and by Artificial miRNAs. *J. RNAi Gene Silencing* **2011**, *7*, 434-442.

[256] Hipfner, D. R.; Gao, M.; Scheffer, G.; Scheper, R. J.; Deeley, R. G.; Cole, S. P. C. Epitope Mapping of Monoclonal Antibodies Specific for the 190-kDa Multidrug Resistance Protein (MRP). *Br. J. Cancer* **1998**, *78*, 9, 1134-1140.

[257] Connolly, L.; Moran, E.; Larkin, A.; Scheffer, G.; Scheper, R.; Sarkadi, B.; Kool, M.; Clynes, M. A New Monoclonal Antibody, P2A8(6), that Specifically Recognizes a Novel Epitope on the Multidrug Resistance-Associated Protein 1 (MRP1), but not on MRP2 nor MRP3. *Hybrid Hybridomics* **2001**, *20*, 5-6, 333-341.

[258] Häcker, H.-G.; Leyers, S.; Wiendlocha, J.; Gütschow, M.; Wiese, M. Aromatic 2-(Thio)ureidocarboxylic acids As a New Family of Modulators of Multidrug Resistance-Associated Protein 1: Synthesis, Biological Evaluation, and Structure-Activity Relationships. *J. Med. Chem.* **2009**, *52*, 4586-4595.

[259] Breitfeld, J. Lead Optimization of a *p*-Aminobenzoid Acid Derivative as Novel Inhibitor for Multidrug Resistance-Associated Proteins. *Master Thesis* **2012**.

[260] Leyers, S.; Häcker, H.-G.; Wiendlocha, J.; Gütschow, M.; Wiese, M. A 4-aminobenzoic Acid Derivative as Novel Lead for Selective Inhibitors of Multidrug Resistance-associated Proteins. *Bioorg. Med. Chem. Lett.* **2008**, *18*, 4761-4763.

[261] Ebert, S: P.; Wetzel, B.; Myette, R. L.; Conseil, G.; Cole, S. P. C.; Sawada, G. A.; Loo, T. W.; Bartlett, M. C.; Clarke, D. M.; Detty, M. R. Chalcogenpyrylium Compounds of the ATP-Binding Cassette Transporters P-Glycoprotein (P-gp/*ABCB1*) and Multidrug Resistance Protein 1 (MRP1/*ABCC1*). *J. Med. Chem.* **2012**, *55*, 4683-4699.

[262] Myette, R. L.; Conseil, G.; Ebert, S. P.; Wetzel, B.; Detty, M. R.; Cole, S. P. C. Chalcogenpyrylium Dyes as Differential Modulators of Organic Anion Transport by Multidrug Resistance Protein 1 (MRP1), MRP2, and MRP4. *Drug. Metab. Dispos.* **2013**, *41*, 1231-1239.

[263] Pellicani, R. Z.; Stefanachi, A.; Niso, M.; Carotti, A.; Leonetti, F.; Nicolotti, O.; Perrone, R.; Berardi, F.; Cellamare, S.; Colabufo, N. A. Potent Galloyl-Based Selective Modulators Targeting Multidrug Resistance Associated Protein 1 and P-glycoprotein. *J. Med. Chem.* **2011**, *55*, 424-436.

[264] Norman, B. H.; Dantzig, A. H.; Kroin, J. S.; Law, K. L.; Tabas, L. B.; Shepard, R. L.; Palkowitz, A. P.; Hauser, K. L.; Winter, M. A.; Sluka, J. P.; Starling, J. J. Reversal of Resistance in Multidrug Resistance Protein (MRP1)-Overexpressing Cells by LY329146. *Bioorg. Med. Chem. Lett.* **1999**, *9*, 3381-3386.

[265] Abdul-Ghani, A.; Györffy, B.; Jürchott, K.; Solf, A.; Dietel, M.; Schäfer, R. The PI3K Inhibitor LY294002 Blocks Drug Export from Resistant Colon Carcinoma Cells Overexpressing MRP1. *Oncogene* **2006**, *25*, 1743-1752.

[266] Mao, Q.; Qiu, W.; Weigl, K. E.; Lander, P. A.; Tabas, L. B.; Shepard, R. L.; Dantzig, A. H.; Deeley, R. G.; Cole, S. P. C. GSH-dependent Photolabelling of Multidrug Resistance Protein MRP1 (ABCC1) by [125I]475776. *J. Biol. Chem.* **2002**, *277*, 32, 28690-28699.

[267] Norman, B. H.; Gruber, J. M.; Hollinshead, S. P.; Wilson, J. W.; Starling, J. J.; Law, K. L.; Self, T. D.; Tabas, L. B.; Williams, D. C.; Paul, D. C.; Wagner, M. M.; Dantzig, A. H. Tricyclic Isoxazoles are Novel Inhibitors of the Multidrug Resistance Protein (MRP1). *Bioorg. Med. Chem. Lett.* **2002**, *12*, 883-886.

[268] Dantzig, A. H.; Shepard, R. L.; Pratt, S. E.; Tabas, L. B.; Lander, P. A.; Ma, L.; Paul, D. C.; Williams, D. C.; Peng, S.-B.; Slapak, C. A.; Godinot, N.; Perry III.; W. L. Evaluation of the Binding of the Tricyclic Isoxazole Photoaffinity Label LY475776 to Multidrug Resistance Associated Protein 1 (MRP1) Orthologs and Several ATP-binding Cassette (ABC) Drug Transporters. *Biochem. Pharmacol.* **2004**, *67*, 1111-1121.

[269] Norman, B. H.; Lander, P. A.; Gruber, J. M.; Kroin, J. S.; Cohen, J. D.; Jungheim, L. N.; Starling, J. J.; Law, Kevin L.; Self, Tracy D.; Tabas, L. B.; Williams, D. C.; Paul, D. C.; Dantzig, A. H. Cyclohexyl-linked Tricyclic Isoxazoles are Potent and Selective Modulators of the Multidrug Resistance Protein (MRP1). *Bioorg. Med. Chem. Lett.* **2005**, *15*, 5526-5530.

[270] Wang, S.; Ryder, H.; Pretswell, I.; Depledge, P.; Milton, J.; Hancox, T. C.; Dale, I.; Dangerfield, W.; Charlton, P.; Faint, R.; Dodd, R.; Hassan, S. Studies on Quinazolinones as Dual Inhibitors of P-gp and MRP1 in Multidrug Resistance. *Bioorg. Med. Chem. Lett.* **2002**, *12*, 571-574.

[271] Wang, S.; Folkes, A.; Chuckowree, I.; Cockroft, X.; Sohal, S.; Miller, W.; Milton, J.; Wren, S. P.; Vicker, M.; Depledge, P.; Scott, J.; Smith, L.; Jones, H.; Mistry, P., Faint, R.; Thompson, D.; Cocks, S. Studies on Pyrrolopyrimidines as Selective Inhibitors of Mutlidrug-Resistance-Associated Protein in Multidrug Resistance. *J. Med. Chem.* **2004**, *47*, 1329-1338.

[272] Wang, S.; Wan, N. C.; Harrison, J.; Miller, W.; Chuckowree, I.; Sohal, S.; Hancox, T. C.; Baker, S.; Folkes, A.; Wilson, F.; Thomson, D.; Cocks, S.; Farmer, H.;Boyce, A.; Freathy, C.; Broadbridge, J.; Scott, J.; Depledge, P.; Faint, R.; Mistry, P.; Charlton, P. Design and Synthesis of New Templates Derived from Pyrrolopyrimidines as Selective Multidrug-Resistance-Associated Protein Inhibitors in Multidrug Resistance. *J. Med. Chem.* **2004**, *47*, 1339-1350.

[273] Shapiro, A. B.; Ling, V. Positively Cooperative Sites for Drug Transport by P-glycoprotein with Distinct Drug Specifities. *Eur. J. Biochem.* **1997**, *250*, 130-137.

[274] Shapiro, A. B.; Fox, K.; Lam, P.; Ling, V. Stimulation of P-glycoprotein-mediated Drug Transport by Prazosin and Progesterone. Evidence for a third drug-binding site. *Eur. J. Biochem.* **1999**, *259*, 841-850.

[275] Wang, E.-J.; Barecki-Roach, M.; Johnson, W.W. Evaluation of P-glycoprotein Function by a Catechin in Green Tea. Biochem. *Biophys. Res. Com.* **2002**, *297*, 412-418.

[276] Berginc, K.; Zakelj, S.; Ursic, D.; Kristl, A. Aged Garlic Extracts Stimulates P-Glycoprotein and Multidrug Resistance Associated Protein 2 Mediated Efflux. *Biol. Pharm. Bull.* **2009**, *32*, 694-699.

[277] Nogushi, K.; Kawahara, H.; Kaji, A.; Katayama, K.; Mitsuhashi, J.; Sugimoto, Y. Substrate-dependent Bidirectional Modulation of P-glycoprotein-mediated Drug Resistance by Erlotinib. *Cancer Sci.* **2009**, *9*, 1701-1707.

[278] Kondratov, R.V.; Komarov, P.G.; Becker, Y.; Ewenson, A.; Gudkov, A.V. Small Molecules That Dramatically Alter Multidrug Resistance Phonotype by Modulating the Substrate Specificity of P-glycoprotein. *Proc. Natl. Acad. Sci.* **2001**, *98*, 14078-14083.

[279] Sterz, K.; Möllmann, L.; Jacobs, A.; Baumert, D.; Wiese, M. Activators of P-glycoprotein: Structure-Activity Relationships and Investigation of their Mode of Action. *Chem. Med. Chem.* **2009**, *11*, 1897-1911.

[280] Möllmann, L. Benzimidazol-Analoga als Modulatoren von ABC-Transportern. *PhD Thesis* **2011**.

[281] Sterz, K. Characterisierung neuer MDR-Modulatoren und Entwicklung von Methoden zur Bestimmung der ATPase-Aktivität von P-Glycoprotein. *Diploma Thesis* **2006**.

[282] Sterz, K. Funktionelle Untersuchungen von Benzimidazolen und Acridonsäureamiden als Modulatoren des ABC-Transporters ABCB1. *PhD Thesis* **2012**.

[283] Häcker, H.-G.; de la Haye, A.; Sterz, K. ; Schnakenburg, G. ; Wiese, M.; Gütschow, M. Analogs of a 4-aminothieno[3,2-*d*]pyrimidine Lead (QB13) as Modulators of P-glycoprotein Substrate Specifity. *Bioorg. Med. Chem. Lett.* **2009**, *19*, 6102-6105.

[284] De la Haye, A. Charakterisierung von P-Glykoprotein Aktivatoren mittels funktioneller FACS-basierter Assays. *Dimploma Thesis* **2007**.

[285] Phang, J. M.; Poore, C. M.; Lopacxnska, J.; Yeh, G. C.; Flavonol-stimulated Efflux of 7,14-Dimethylbenz(a)anthracene in Multidrug-resistant Breast Cancer Cells. *Cancer Res.* **1993**, *53*, 5977-5981.

[286] Critchfield, J. W.; Welsh, C. J.; Phang, J. M. Yeh, G. C. Modulation of Adriamycin Accumulation and Efflux by Flavonoids in HCT-15 Colon Cells. Activation of P-glycoprotein as Putative Mechanism. *Biochem. Pharmacol.* **1994**, *48*, 7, 1437-1445.

[287] Shapiro, A. B., Ling, V. Effect of Quercetin on Hoechst 33342 Transport by Purified and Reconstituted P-Glycoprotein. *Biochem- Pharmacol.* **1997**, *53*, 587-596.

[288] Jodoin, J.; Demeule, M.; Béliveau, R. Inhibition of the Multidrug Resistance P-glycoprotein by Green Tee Polyphenols. *Biochim. Biophys. Acta* **2002**, *1542*, 149-159.

[289] Sharom, F. J.; Yu, X.; DiDiodato, G.; Chu, J. W. K. Synthetic Hydrophobic Peptides are Substrates for P-glycoprotein and Stimulate Drug Transport. *Biochem. J.* **1996**, *320*, 421-428.

[290] Leslie, E. M.; Mao, Q.; Oleschuk, C. J.; Deeley, R. G.; Cole, S. P. C. Modulation of Multidrug Resistance Protein 1 (MRP1/ABCC1) Transport and ATPase Activities by Interaction with Dietary Flavonoids. *Mol. Pharmacol.* **2001**, *59*, 1171-1180.

[291] Zhang, S.; Morris, M. E. Effects of the Flavonoids Biochanin A, Morin, Phloretin, and Silymarin on P-Glycoprotein-Mediated Transport. *J. Pharmacol. Exp. Ther.* **2003**, *304*, 1258-1267.

[292] W.T. Loo; D.M. Clarke. Defining the Drug-binding Site in the Human Multidrug Resistance P-glycoprotein Using a Methanethiosulfonate Analog of Verapamil, MTS-verapamil. *J. Biol. Chem.* **2001**, *18*, 14972-14979.

[293] Leyers, S. Funktionelle Untersuchungen der Multidrug-Resistance-Associated Proteins (MRP) 1 und 2. *PhD Thesis* **2009**.

[294] Loe, D. W.; Deeley, R. G.; Cole, S. P. C. Verapamil Stimulates Glutathione Transport by the 190-kDa Multidrug Resistance Protein 1 (MRP1). *J. Pharm. Exp. Ther.* **2000**, *293*, 530-538.

[295] Chearwae, W.; Wu, C. P.; Chu, H. Y.; Lee, T. R.; Abudkar, S. V.; Limtrakul, P. Curcuminoids Purified from Turmeric Powder Modulate the Function of Human Multidrug Resistance Protein 1 (ABCC1). *Cancer Chemother. Pharmacol.* **2006**, *57*, 3, 376-388.

[296] Hooijberg, J. H.; Pinedo, H. M.; Vrasdonk, C.; Priebe, W.; Lankelma, J.; Broxterman, H. J. The effect of Glutathione on the ATPase Activity of MRP1 in Its Natural Membranes. *FEBS Lett.* **2000**, *469*, 47-51.

[297] Mao, Q.; Leslie, E. M.; Deeley, R. G. ; Cole, S. P. C. ATPase-activity of Purified and Reconstituted Multidrug Resistance Protein MRP1 from Drug-selected H69AR Cells. *Biochim. Biophys. Acta* **1999**, *1461*, 69-82.

[298] Leslie, E.M.; Deeley, R.G.; Cole, S.P.C. Bioflavonoid Stimulation of Glutathione Transport by the 190-kDa Multidrug Resistance Protein (MRP1). *Drug Metab. Dispos.* **2002**, *31*, 11-15.

[299] Hooijberg, J. H.; Broxterman, H. J.; Heijn, M.; Fles, D. L. A.; Lankelma, J.; Pinedo, H. M. Modulation by (Iso)flavonoids of the ATPase Activity of the Multidrug Resistance Protein. *FEBS Lett.* **1997**, *413*, 344-348.

[300] Perloff, M. D.; Von Moltke, L. L., Marchand, J. E.; Greenblatt, D. J. Ritonavir Induces P-Glycoprotein Expression, Multidrug Resistance-Associated Protein (MRP1) Expression, and Drug Transporter-Mediated Activity in a Human Intestinal Cell Line. *J. Pharm. Sci.* **2001**, *99*, 11, 1829-1837.

[301] Park, H.-A.; Kubicki, N.; Gnyawali, S.; Chan, C.; Roy, S.; Khanna, S.; Sen, C. Natural Vitamin E α-Tocotrienol Protects Against Ischemic Stroke by Induction of Multidrug Resistance-Associated Protein 1. *Stroke* **2011**, *42*, 8, 2308-2314.

[302] El Azreq, M.-A.; Naci, D.; Aoudjit, F. Collagen/β-1-integrin Signalling Up-regulates the ABCC1/MRP1 Transporter in an ERK/MAPK-dependent Manner. *Mol. Biol. Cell.* **2012**, *23*, 3473-3484.

[303] Wesolowska, O.; Molnar, J.; Motohashi, N.; Michalak, K. Inhibition of P-glycoprotein Transport Function by N-acetylphenothiazines. *Anticancer Res.* **2002**, *22*, 2863-2867.

[304] Wesolowska, O.; Mosiadz, D.; Motohashi, N.; Kawase, M.; Michalak, K. Phenothiazine Maleates Stimulate MRP1 Transport Activity in Human Erythrocytes. *Biochim. Biophys. Acta*, **2005**, *1720*, 52-58.

[305] Wesolowska, O.; Molnar, J.; Ocsovszki, I.; Michalak, K. Differential Effect of Phenothiazines on MRP1 and P-Glycoprotein Activity. *In Vivo* **2009**, *23*, 293-948.

[306] Hummel, I.; Klappe, K.; Ercan, C.; Kok, J. W. Multidrug Resistance-Related Protein 1 (MRP1) Function and Localization Depend on Cortical Actin. *Mol. Pharmacol.* **2011**, *79*, 229-240.

[307] Li, D.-Q.; Wang, Z.-B.; Bai, J.; Zhao, J.; Wang, Y.; Hu, K.; Du, Y.-H. Reversal of Multidrug Resistance in Drug-resistant Human Gastric Cancer Cell Line SGC7901/VCR by Antiprogestin Drug Mifepriston. *World J. Gastroenerol.* **2004**, *10*, 12, 1722-1725.

[308] Cornwell, M. M.; Pastan, I.; Gottesmann, M. M. Certain Calcium Channel Blockers Bind Specifically to Multidrug-resistant Human KB Carcinoma Membrane Vesicles and Inhibit Drug Binding to P-glycoprotein. *J. Biol. Chem.* **1987**, *48*, 2793-2797.

[309] Tsuruo, T.; Iida, H.; Tsukagoshi, S. ; Sakurai, Y. Overcoming of Vincristine Resistance in P388 Leukemia *In Vivo* and *In Vitro* through Enhanced Cytotoxicity of Vincristine and Vinblastine by Verapamil. *Cancer Res.* **1981**, *41*, 1967-1972.

[310] Slovak, M. L.; Hoeltge, G. A.; Dalton, W. S.; Trent, J. M. Pharmacological and Biological Evidence for Differeing Mechanisms of Doxorubicin Resistance in Two Human Tumor Cell Lines. *Cancer Res.* **1988**, *48*, 2793-2797.

[311] Sun, M.; Xu, X.; Lu, Q.; Pan, Q.; Hu, X. Schisandrin B: A Dual Inhibitor of P-glycoprotein and Multidrug Resistance-associated Protein 1. *Cancer Lett.* **2007**, *246*, 300-307.

[312] Pan, Q.; Wang, T.; Lu, Q.; Hu, X. Schisandrin B – A Novel Inhibitor of P-glycoprotein. *Biochem. Biophys. Res. Comm.* **2005**, *335*, 406-411.

[313] Wiese, M. BCRP/ABCG2 Inhibitors: a Patent Review (2009 – Present). *Expert Opin.* **2015**, *25*, 1-9.

[314] Chow, L. M. C.; Chan, T. H.; Chan, K. F.; Wong, I. L. K.; Law, M. C. Alkyne-, Azide- and Triazole-containing Flavonoids as Modulators for Multidrug Resistance in Cancers. U.S. *Patent WO 2013/127361 A1*, September 6, **2013**.

[315] Maliepaard, M.; van Gastelen, M. A.; Tohgo, A.; Hausheer, F. H.; van Waardenburg, R. C. A. M.; de Jong, L. A.; Pluim, D.; Bijnen, J. H.; Schellens, J. H. M. Circumvention of Breast Cancer Resistance Protein (BCRP)-mediated Resistance to Camptothecins *In Vitro* Using Non-Substrate Drugs or the BCRP Inhibitor GF120918. *Clin. Cancer Res.* **2001**, *7*, 935-941.

[316] Robey, R. W.; Steadman, K.; Polgar, O.; Morisaki, K.; Blayney, M.; Mistry, P.; Bates, S. E. Pheophorbide a Is a Specific Probe for ABCG2 Function and Inhibition. *Cancer Res.* **2004**, *64*, 1242-1246.

[317] Pick, A.; Müller, H.; Wiese, M. Structure-activity Relationships of New Inhibitors of Breast Cancer Resistance Protein (ABCG2). *Bioorg. Med. Chem.* **2008**, *16*, 8224-8236.

[318] Jekerle, V.; Klinkhammer, W.; Reilly, R. M.; Piquette-Miller, M.; Wiese, M. Novel Tetrahydroisoquinolin-ethyl-phenylamine Based Multidrug Resistance Inhibitors with Broad-spectrum Modulating Properties. *Cancer Chemother. Pharmacol.* **2007**, *59*, 61-69.

[319] Köhler, S. C.; Wiese, M. HM30181 Derivatives as Novel Potent and Selective Inhibitors of the Breast Cancer Resistance Protein (BCRP/ABCG2). *J. Med. Chem.* **2015**, *58*, 3910-3921.

[320] Spindler, A.; Stefan, K.; Wiese, M. Synthesis and Investigation of Tetrahydro-*β*-carboline Derivatives as Inhibitors of the Breast Cancer Resistance Protein (ABCG2). *J. Med. Chem.* **2016**, *59*, 6121-6135.

[321] Pick, A.; Müller, H.; Mayer, R.; Haensch, B.; Pajeva, I. K.; Weigt, M.; Boenisch, H.; Müller, C. E.; Wiese, M. Structure-activity Relashionships of Flavonoids as Inhibitors of Breast Cancer Resistance Protein (BCRP). *Bioorg. Med. Chem.* **2011**, *19*, 2090-2102.

[322] Gu, X.; Ren, Z.; Tang, X.; Peng, H.; Ma, Y.; Lai, Y.; Peng, S.; Zhang, Y. Synthesis and Biological Evaluation of Bifendate-chalcone Hybrids as a New Class of Potential P-glycoprotein Inhibitors. *Bioorg. Med. Chem.* **2012**, *20*, 2540-2548.

[323] Juvale, K.; Pape, V. F. S.; Wiese, M. Investigation of Chalcones and Benzochalcones as Inhibitors of Breast Cancer Resistance Protein. *Bioorg. Med. Chem.* ***2012,*** 20*, 346-355.*

[324] Gu, X.; Ren, Z.; Peng, H.; Peng, S.; Zhang, Y. Bifendate-chalcone Hybrids: A New Class of Potential Dual Inhibitors of P-glycoprotein and Breast Cancer Resistance Protein. *Biochem. Biophys. Res. Comm.* **2014**, *455*, 318-322.

[325] Gu, X.; Tang, X.; Zhao, Q. ; Peng, H. ; Peng, S.; Zhang, Y. Discovery of Alkoxyl Biphenyl Derivatives Bearing Dibenzo[*c,e*]azepine Scaffold as Potential Dual Inhibitors of P-glycoprotein and Breast Cancer Resistance Protein. *Bioorg. Med. Chem. Lett.* **2014**, *24*, 3419-3421.

[326] Kraege, S.; Stefan, K.; Juvale, K.; Ross, T.; Willmes, T.; Wiese, M. The Combination of Quinazoline and Chalcone Moieties Leads to Novel Potent Heterodimeric Modulators of Breast Cancer Resistance Protein (BCRP/ABCG2). *Eur. J. Med. Chem.* **2016**, *117*, 212-229.

[327] Singh, M. S.; Juvale, K.; Wiese, M.; Lamprecht, A. Evaluation of Dual P-gp-BCRP Inhibitors as Nanoparticle Formulation. *Eur. J. Pharm. Sci.* **2015**, *77*, 1-8.

[328] Juvale, K.; Wiese, M. 4-Substituted-2-phenylquinazolines as Inhibitors of BCRP. *Bioorg. Med. Chem. Lett.* **2012**, *22*, 6766-6769.

[329] Krapf, M. K.; Gallus, J.; Wiese, M. Synthesis and Biological Evaluation of 4-Anilino-2-pyridylquinazolines and –pyrimidines as Inhibitors of Breast Cancer Resistance Protein (ABCG2). **2017**, [in preperation].

[330] Schwarz, T.; Montanari, F.; Cseke, A.; WIcek, K.; Visvader, L.; Palme, S.; Chiba, P.; Kuchler, K.; Urban, E.; Ecker, G. F. Subtle Structureal Differences Trigger Inhibitory Activity of Propafenone Analogues at the Two Polyspecific ABC Transporters: P-Glycoprotein (P-gp) and Breast Cancer Resistance Protein (BCRP). *Chem. Med. Chem.* **2016**, *11*, 1380-1394.

[331] Kraege, S.; Köhler, S. C.; Wiese, M. Acryloylphenylcarboxamides: A New Class of Breast Cancer Resistance Protein (ABCG2) Modulators. *Chem. Med. Chem.* **2016**, *11*, 21, 2422-2435.

[332] Kraege, S.; Stefan, K.; Köhler, S. C.; Wiese, M. Optimization of Acryloylphenylcarboxamides as Inhibitors of ABCG2 and Comparison with Acryloylphenylcarboxylates. *Chem. Med. Chem.* **2016**, *11*, 22, 2547-2558.

[333] Li, S.; Lei, Y.; Jia, Y.; Li, N.; Wink, M.; Ma, Y. Piperine, a Piperidine Alkaloid from *Piper nigrum* Re-sensitizes P-gp, MRP1 and BCRP Dependent Multidrug Resistant Cancer Cells. *Phytomedicine* **2011**, *19*, 83-87.

[334] Minderman, H.; O'Loughlin, K. L.; Pendyala, L.; Baer, M. R. VX-710 (biricodar) Increases Drug Retention and Enhances Chemosensitivity in Resistant Cells Overexpressing P-glycoprotein, Multidrug Resistance Protein, and Breast Cancer Resistance Protein. *Clin. Cancer Res.* **2004**, *10*, 1826-1834.

[335] Weidner, L. D.; Zoghbi, S. S.; Lu, S.; Shukla, S.; Ambudkar, S. V.; Pike, V. W.; Mulder, J.; Gottesmann, M. M.; Innis, R. B.; Hall, M. D. The Inhibitor Ko143 Is Not Specific for ABCG2. *J. Pharmacol. Exp. Ther.* **2015**, *354*, 384-393.

[336] Pick, A.; Klinkhammer, W.; Wiese, M. Specific Inhibitors of the Breast Cancer Resistance Protein (BCRP). *Chem. Med. Chem.* **2010**, *5*, 1498-1505.

[337] Juvale, K.; Gallus, J.; Wiese, M. Investigation of Quinazolines as Inhibitors of Breast Cancer Resistance Protein (ABCG2). *Bioorg. Med. Chem.* **2013**, *21*, 7858-7873.

[338] Krapf, M.; Wiese, M. Synthesis and Biological Evaluation of 4-Anilino-quinazolines and -quinolines as Inhibitors of Breast Cancer Resistance Protein (ABCG2). *J. Med. Chem.* **2016**, *59*, 5449-5461.

[339] Zhou, Y.; Hopper-Borge, E.; Shen, T.; Huang, X.-C.; Shi, Z.; Kuang, Y.-H.; Furukawa, T.; Akiyama, S.-I.; Peng, X.-X.; Ashby Jr., C. R.; Chen, X.; Kruh, G. D.; Chen, Z.-S. Cepharanthine is a Potent Reversal Agent for MRP7(ABCC10)-mediated Multidrug Resistance. *Biochem. Pharmacol.* **2009**, *77*, 993-1001.

[340] Wang, E.-J.; Casciano, C. N.; Clement, R. P.; Johnson, W. W. *In Vitro* Flow Cytometry Method to Quantitatively Assess Inhibitors of P-glycoprotein. *Drug Metab. Dispos.* **2000**, *28*, 522-528.

[341] Wang, E.J.; Casciano, C. N.; Clement, R. P.; Johnson, W. W. Cooperativity in the Inhibition of P-Glycoprotein-Mediated Daunorubicin Transport: Evidence for Half-of-the-Sites Reactivity. *Arch. Biochem. Biophys.* **2000**, *383*, 1, 91-98.

[342] Köhler, S. C.; Silbermann, K.; Wiese, M. Phenyltetrazolyl-phenylamides: Substitutent Impact on Modulation Capability and Selectivity toward the Efflux Protein ABCG2 and Investigation of Interaction with the Transporter. *Eur. J. Med. Chem.* **2016**, *124*, 881-895.

[343] Kühnle, M.; Egger, M.; Müller, C.; Mahringer, A.; Bernhardt, G.; Fricker, G.; König, B.; Buschauer, A. Potent and Selective Inhibitors of Breast Cancer Resistance Protein (ABCG2) Derived from the *p*-Glycoprotein (ABCB1) Modulator Tariquidar. *J. Med. Chem.* **2009**, *52*, 1190-1197.

[344] Barnes, B.; Berzt, J.; Bittmann-Schweiger, N.; Fiebig, J.; Jordan, S.; Kraywinkel, K.; Niemann, H.; Nowossadeck, E.; Poethko-Müller, C.;Prütz, F.;Rattay, R.; Schönefeld, I.; Starker, A.; Wienecke, A.; Wolf, U. Bericht zum Krebsgeschehen in Deutschland 2016. *Robert Koch Institut*, **2016**, 22-77.

[345] Ozols, R. F. Cunnion, R. E.; Klecker, W. R.; Hamilton, T. C.; Ostecha, Y.; Parrillo, J. E.; Young, R. C. Verapamil and Adriamycin in the Treatment of Drug-Resistant Ovarian Cancer Patients. *J. Clin. Oncol.* **1987**, *5,* 4, 641-647

[346] Ozols, R. F. Pharmacologic Reversal of Drug Resistance in Ovarian Cancer. *Semin. Oncol.* **1985**, *12*, 7-11.

[347] Kloke, O.; Osieka, R. Interaction of Cyclosporin A with Antineoplastic Agents. *Klin. Wochenschr.* **1985**, *63*, 1081-1082.

[348] Milton, J.; Wren, S.; Wang, S.; Folkes, A.; Chuckowree, I.; Hancox, T.; Miller, W.; Sohal, S. Pyrrolopyrimidine Derivatives Useful as Modulators of Multidrug Resistance. U.S. *Patent WO 2004/065389 A1*, August 5, **2004**.

[349] Schmitt, S. M.; Stefan, K. Pyrrolopyrimidine Derivatives as Novel Inhibitors of Multidrug Resistance-Associated Protein 1 (MRP1/ABCC1). *J. Med. Chem.* **2016**, *59*, 3018-3033.

[350] Schmitt, S. M.; Stefan, K. Pyrrolopyrimidine Derivatives and Purine Analogs as Novel Activators of Multidrug Resistance-associated Protein 1 (MRP1, ABCC1). *Biochim. Biophys. Acta* **2017**, *1*, 69-79.

[351] Moore, J. L.; Taylor, S. M.; Solohonok, V. A. An Efficient and Operationally Convenient General Synthesis of Tertiary Amines by Direct Alkylation of Secondary Amines with Alkyl Halides in the Presence of Huenig's Base. *ARKIVOC* **2005**, *6*, 287-292.

[352] Wiendlocha, J. Identification and Characterization of Novel MRP1 Inhibitors. *Diploma Thesis* **2008**.

[353] Bobrowska-Hägerstrand, M.; Wróbel, A.; Rychlik, B.; Öhman, I.; Hägerstrand, H. Flow Cytometric Monitoring of Multidrug Drug Resistnace Protein 1 (MRP1/ABCC1) – mediated Transport of 2',7'-bis-(3-carboxypropyl)-5-(and-6)- Carboxyfluorescein (BCPCF) into Human Erythrocyte Membrane Inside-out Vesicles. *Molec. Membrane Biol.* **2007**, *24*, 5-6, 485-495.

[354] Versantvoort, C. H. M.; Broxterman, H. J.; Lankelma, J.; Feller, N.; Pinedo, H. M Competitive Inhibition by Genistein and ATP Dependence of Daunorubicin Transport in Intact *MRP* Overexpressing Human Small Cell Lung Cancer Cells. *Biochem. Pharmacol.* **1994**, *48*, 6, 1129-1136.

[355] Segel, I. H. Enzyme Kinetics. *John Wiley Sons, Inc.* **1975**.

[356] Stefan, K.; Schmitt, S. M.; Wiese, M. 9-Deazapurines as Broad-spectrum Inhibitors of the ABC Transport Proteins P-glycoprotein, Multidrug Resistance-associated Protein 1, and Breast Cancer Resistance Protein. *J. Med. Chem.* **2017**, *accepted 10th of October, 2017).*

[357] Essodaigui, M.; Broxterman, H. J.; Garnier-Suillerot, A. Kinetic Analysis of Calcein and Calcein-acetoxymethylester Efflux Mediated by Multidrug Resistance Protein and P-glycoprotein. *Biochemistry* **1998**, *37*, 2243–2250.

[358] Olson, D. P.; Taylor, B. J.; Ivy, S. P. Detection of MRP Functional Activity: Calcein AM but not BCECF AM as a Multidrug Resistance-related Protein (MRP1) Substrate. *Cytometry* **2001**, *46*, 105–113.

[359] Müller, H.; Kassack, M.U.; Wiese, M. Comparison of the Usefulness of the MTT, ATP, and Calcein AM Assays to Predict the Potency of Cytotoxic Agents in Various Human Cancer Cell Lines. *J. Biomol. Screen.* **2004**, *9*, 506–515.

[360] Tiberghien, F.; Loor, F. Ranking of P-glycoprotein Substrates and Inhibtors by Calcein-AM Fluorometry Screening Assay. *Anti-Cancer Drugs* **1996**, *7*, 568–578.

[361] Eneroth, A.; Astroem, E.; Hoogstraate, J.; Schrenk, D.; Conrad, S.; Kauffmann, H.-M.; Gjellan, K. Evaluation of a Vincristine Resistance Caco-2- cell Line for Use in a Calcein AM Extrusion Screening Assay for P-glycoprotein Interaction. *Eur. J. Pharm. Sci.* **2001**, *12*, 205–214.

[362] Müller, H.; Pajeva, I. K.; Globisch, C.; Wiese, M. Functional Assay and Structure-activity Relationships of New Third-generation Pglycoprotein Inhibitors. Bioorg. Med. Chem. 2008, 16, 2448–2462.

[363] Müller H. Funktionelle Untersuchungen des ABC-Transporters P-Glykoprotein. *PhD Thesis* **2007**.

[364] Mattews, J. C. Fundamentals of Receptor, Enzyme, and Transport Kinetics. *CRC Press* **1993**.

[365] Jekerle, V.; Klinkhammer, W.; Scollard, D. A.; Breitbach, K.; Reilly, R. M.; Piquette-Miller, M.; Wiese, M. *In Vitro* and *In Vivo* Evaluation of WK-X-34, a Novel Inhibitor of P-glycoprotein and BCRP, Using Radio Imaging Techniques. *Int. J. Cancer* **2006**, *119*, 414-422.

[366] Jekerle, V. Investigations of Combined Strategies to Reserve P-glycoprotein and BCRP-mediated Multidrug Resistance in Human Ovarian Cancer Cells and Xenograft Tumors. *PhD Thesis* **2006**.

[367] Pick, A.; Müller, H.; Wiese, M. Novel Lead for Potent Inhibitors of Breast Cancer Resistance Protein (BCRP). Bioorg. Med. Chem. Lett. 2010, 20, 180–183.

[368] Pick, A.; Wiese, M. Tyrosine Kinase Inhibitors Influence ABCG2 Expression in EGFR-positive MDCK BCRP Cells via the PI3K/Akt Signaling Pathway. *Chem. Med. Chem.* **2012**, *7*, 650–662.

[369] Mosmann, T. Rapid Colorimetric Assay for Cellular Growth and Survival: Application to Proliferation and Cytotoxicity Assays. *J. Immunoln. Methods* **1983**, *65*, 55-63.

[370] Müller, H.; Klinkhammer, W.; Globisch, C.; Kassack, M. U.; Pajeva, I. K.; Wiese, M. New Functional Assay of P-glycoprotein Using Hoechst 33342. *Bioorg. Med. Chem.* **2007**, *15*, 7470-7479.

[371] Garnier-Suillerot, A.; Marbeuf-Gueye, C.; Salerno, M.; Loetchutinat, C.; Fokt, I.; Krawczyk, T.; Krowalczyk, W.; Priebe, W. Analysis of Drug Transport Kinetics in Multidrug-resistant Cells: Implications for Drug Action. *Curr. Med. Chem.* **2001**, *8*, 51-64.

Pubications

Research Articles:

Almeida, C.; Hemberger, Y.; **Schmitt**, **S**. **M**.; Bouhired, S.; Natesan, L.; Kehraus, S.; Dimas, K.; Gütschow, M.; Bringmann, G.; König, G. M. Marilines A-C: Novel Phthalimidines from the Sponge-Derived Fungus *Stachylidium* sp. *Chem. Eur. J.* **2012**, *18*, 8827-8834.

Schmitt, **S**. **M**.; Stefan, K.; Wiese, M. Pyrrolopyrimidine Derivatives as Novel Inhibitors of Multidrug Resistance-associated Protein 1 (MRP1, ABCC1). *J. Med. Chem.* **2016**, *59*, 3018-3033.

Schmitt, **S**. **M**.; Stefan, K.; Wiese, M. Pyrrolopyrimidine Derivatives and Purine Analogs as Novel Activators of Multidrug Resistance-associated Protein 1 (MRP1, ABCC1). *Biochim. Biophys. Acta* **2017**, *1859*, 69-79.

Stefan, K; **Schmitt**, **S**. **M**.; Wiese, M. 9-Deazapurines as Broad-spectrum Inhibitors of the ABC Transport Proteins P-glycoprotein, Multidrug Resistance-associated Protein 1, and Breast Cancer Resistance Protein. *J. Med. Chem.* **2017**, *accepted 10th of October, 2017*.

Poster Presentations:

Schmitt, **S**. **M**.; Köhler, S. C.; Wiese, M. Pyrrolopyrimidines as Novel Inhibitors for Multidrug Resistance-associated Protein 1 (MRP1 / ABCC1). *5th FEBS Special Meeting: ATP-Binding Cassette (ABC) Proteins: From Multidrug Resistance to Genetic Diseases*, Innsbruck (Austria), March **2014**.

Schmitt, **S**. **M**.; Wiese, M. *N*-substituted Pyrrolopyrimidines as Partial Inhibitors for Multidrug Resistance-associated Protein-1 (MRP1 / ABCC1). *7th SFB35 Symposium: Transmembrane Transporters in Health and Disease*, Vienna (Austria), September **2014**.

Stefan, K.; **Schmitt**, **S**. **M**. Characterization of Inhibitors of Multidrug Resistance-associated Protein 1 (MRP1) for Their Influence on ATP-dependent Transport of Glutathione (GSH/GSSG). *Gordon Research Conference (GRC): Multi-Drug Efflux Systems – A Paradigm Shift from Fundamental Mechanisms to Practical Applications*, Lucca (Italy), April/May **2015**.

Schmitt, **S**. **M**.; Stefan, K.; Wiese, M. Pyrrolopyrimidine-derivatives and Analogues as Novel Modulators of Multidrug Resistance-associated Protein 1 (MRP1). *AAPS Annual Meeting and Exposition*, Orlando (Florida, United States of America), October **2015**.

Schmitt, **S**. **M**.; Stefan, K.; Wiese, M. Pyrrolopyrimidine Derivatives and Analogs as Activators of Multidrug Resistance-associated Protein 1 (MRP1, ABCC1). *6th Special Meeting: ATP-Binding Cassette (ABC) Proteins: From Multidrug Resistance to Genetic Diseases*, Innsbruck (Austria), March **2016**.

Stefan, K.; **Schmitt**, **S**. **M**.; Wiese, M. Pyrrolopyrimidine Derivatives as Novel Inhibitors of Multidrug Resistance-associated Protein 1 (MRP1, ABCC1). *6th Special Meeting: ATP-Binding Cassette (ABC) Proteins: From Multidrug Resistance to Genetic Diseases*, Innsbruck (Austria), March **2016**.

Invited Speaker:

Schmitt, **S**. **M**. Modulators of ABCC1: A Summary of Three Decades of Research. *TransportDEMENTIA3*, Svolvær (Norway), September **2017**.

Verfassererklärung

Hiermit erkläre ich, dass ich die vorliegende Arbeit selbstständig verfasst habe. Ich habe keine anderen als die angegebenen Quellen und Hilfsmittel benutzt und die den verwendeten Werken wörtlich oder inhaltlich entnommenen Stellen als solche gekennzeichnet.

Bonn, den .....

Unterschrift .....